# The potential role of bacterial metabolic toxins in the development of diabetes

**Nasrin Vassel**

A thesis submitted to Cardiff University in accordance with the requirements for the degree of Doctor of Philosophy

October 2012

Cardiff University

Welsh School of Pharmacy and Pharmacological Sciences

Redwood Building

King Edward VII Avenue

Cardiff CF10 3NB

## Summary

Irritable bowel syndrome is one of the most common problems reported to general practitioners and gastroenterologists. It has been shown that many of the gut and systemic symptoms are due to lactose sensitivity, the sugar found mainly in milk. Undigested carbohydrates and other foods absorbed by the small intestine reach the bacteria in the large intestine. There is little oxygen here, the bacteria metabolise these to produce gases such as hydrogen and methane, and a variety of small organic metabolites such as methylglyoxal. These metabolites are absorbed into the bloodstream and can affect tissues around the body.

The overall aim of this thesis was to investigate the potential role of the bacterial metabolic toxin hypothesis in the development of diabetes. To specifically investigate the ability of these toxins to covalently modify proteins and to investigate the biological activity of these modified proteins on glucose uptake and cell differentiation. Albumin and insulin have been shown to exhibit mono-oxygenase activity demonstrated by coelenterazine chemiluminescence. It was heat denaturable, demonstrated saturable substrate characteristics, was inhibited or activated by cations ($Fe^{2+}$, $Fe^{3+}$, $Zn^{2+}$ and $Ca^{2+}$) known to bind to these proteins and was inhibited by drugs that are known to bind to Sudlow's site I on albumin. The inhibition of albumin catalysed coelenterazine chemiluminescence observed in the presence of drugs that are known to bind to Sudlow's site I on albumin proposes that this is also the coelenterazine binding site. Molecular 3D modelling confirmed that coelenterazine binds to this site. Methylglyoxal covalently modified these proteins resulting in reduced biological activity. Tetraethylammonium significantly inhibited 3T3-L1 cell differentiation in the presence of insulin. However, methylglyoxal and tetrandrine did not significantly inhibit 3T3-L1 cell differentiation. The results in this thesis support the hypothesis that bacterial metabolic toxins can covalently modify proteins and alter their biological activity.

## List of contents

**Acknowledgements**

It is a pleasure to acknowledge all of those who have provided me with the support and assistance throughout the course of this thesis. First, I would like to thank my supervisors Dr Ken Wann and Professor Anthony Campbell for their continuous support, guidance and patience. I would like to thank Dr Andrea Brancale who gave his time and expertise with regards to molecular 3D modelling. I would also like to thank Dr Neil Henney, who taught me some of the techniques required to carry out this project. I must thank my fellow PhD students as the years would not have been quite the same without them. I would like to thank my parents and my brother, who have provided me with an endless amount of encouragement and support in everything I have done to date. Without them I would not be where I am today. Finally, I would like to thank both The Darwin Centre and The Waterloo Foundation, who with their financial support made this thesis possible.

**List of figures**

**List of tables**

## Abbreviations

| | |
|---|---|
| $[Ca^{2+}]_i$ | intracellular calcium |
| [S] | substrate concentration |
| 4E-BP1 | eIF-4E binding protein |
| ADAMTS9 | ADAM metallopeptidase with thrombospondin type 1 motif 9 |
| ADP | adenosine diphosphate |
| AGEs | advanced glycation endproducts |
| AKT | serine/threonine protein kinase (also known as PKB) |
| Al | aluminium |
| Ala | alanine |
| AMP | adenosine monophosphate |
| ANOVA | analysis of variance |
| APS | SIRP family member |
| ARAP1 | ArfGAP with RhoGAP domain, ankyrin repeat and PH domain 1 |
| Arg | arginine |
| Asn | asparagine |
| ATP | adenosine triphosphate |
| Au | gold |
| B | basic |
| BCL11A | B-cell CLL/lymphoma 11A (zinc finger protein) |
| BCM | beta-casomorphin |
| BFP | blue fluorescent protein |
| BK | big potassium |
| bp | base pairs |
| BSA | bovine serum albumin |
| C/EBP | CCAAT/enhancer binding protein |
| C3G | Rho-family guanine nucleotide exchange factor |

| | |
|---|---|
| Ca | calcium |
| $CaCl_2$ | calcium chloride |
| cAMP | cyclic adenosine monophosphate |
| CAP | CbI associated protein |
| CAPN10 | calpain 10 |
| $Ca_v3.1$ | voltage dependent T-type calcium channel |
| Cb1 | SIRP family member |
| CDC123-CAMK1D | cell division cycle 123 homolog-calcium/calmodulin-dependent protein kinase 1D |
| CDK | cyclin-dependent kinase |
| CDKAL1 | CDK5 regulatory subunit associated protein 1-like 1 |
| cDNA | complementary DNA |
| CEL | carboxyethyl-lysine |
| $CH_3$ | methane |
| CHCHD9 | coiled-coil-helix-coiled-coil-helix domain containing 9 |
| $CHCl_3$ | chloroform |
| cm | centimetres |
| CML | carboxymethyl-lysine |
| $CO_2$ | carbon dioxide |
| CoA | coenzyme A |
| C-peptide | connecting peptide |
| Crk | adapter protein |
| CTLA4 | cytotoxic T-lymphocyte-associated protein-4 |
| Cu | copper |
| CVB | Coxsackie B virus |
| Cys | cysteine |
| Da | Dalton |
| DAG | diacylglycerol |
| DEX | dexamethasone |
| DGI | Diabetes Genetics Initiative |
| DHAP | dihydroxyacetone phosphate |

| | |
|---|---|
| DIAGRAM | Diabetes Genetics, Replication and Meta-Analysis |
| DMEM | Dulbecco's Modified Eagle Medium |
| DMF | dimethylformamide |
| DMSO | dimethyl sulphoxide |
| DNA | deoxyribonucleic acid |
| dNTP | deoxyribonucleotide triphosphate |
| DUSP9 | dual specificity phosphatase 9 |
| D-PBS | Dulbecco's phosphate buffered saline |
| E | expanded |
| EDTA | ethylenediaminetetraacetic acid |
| eIF2B | guanine nucleotide exchange factor |
| ELISA | enzyme-linked immunosorbant assay |
| ER | endoplasmic reticulum |
| ESRD | end-stage renal disease |
| F | fast |
| FA | fatty acid |
| FAD | flavin adenine dinucleotide |
| FBS | foetal bovine serum |
| FCS | foetal calf serum |
| Fe | iron |
| $FeCl_3$ | iron III chloride |
| $FeSO_4$ | iron II sulphate |
| FFA | free fatty acid |
| FUSION | Finland-United States Investigation of NIDDM |
| g | grams |
| G | gravity |
| Gab1 | SIRP family member |
| GAD | glutamic acid decarboylase |
| GAD-65 | glutamic acid decarboxylase-65 |
| GADA | antibody to GAD |

| | |
|---|---|
| GAP | glyceraldehyde-3-phosphate |
| GAPDH | glyceraldehydes 3-phosphate dehydrogenase |
| GDH | glycerophosphate dehydrogenase |
| GFP | green fluorescent protein |
| Gln | glutamine |
| Glu | glutamic acid |
| GLUT2 | glucose transporter 2 |
| GLUT4 | glucose transporter 4 |
| Gly | glycine |
| Grb2 | adapter protein containing SH3 domains |
| GSH | glutathione |
| GSIS | glucose stimulated insulin secretion |
| GSK3 | glycogen synthase kinase 3 |
| GTP | guanosine triphosphate |
| GWA | genome wide association |
| GWAS | genome wide association studies |
| $H_2$ | hydrogen |
| $H_2O$ | water |
| $H_2O_2$ | hydrogen peroxide |
| $H_2SO_4$ | sulphuric acid |
| HCl | hydrochloric acid |
| HEPES | 4-(2-hydroxyethyl)-1-piperazineethanesulfonic acid |
| HHEX | hematopoietically expressed homeobox |
| His | histidine |
| HLA | non-human leukocyte antigen |
| HMGA2 | high mobility group AT-hook 2 |
| HMIT | $H^+$-coupled myo-inositol transporter |
| HNF1A | HNF homeobox A |
| HNF1B | HNF homeobox B |
| HSA | human serum albumin |

| | |
|---|---|
| IA2 | islet-cell antigen-2 |
| IAA | insulin autoantibody |
| IBMX | isobutylmethylxanthine |
| IBS | irritable bowel syndrome |
| $IC_{50}$ | the half maximal inhibitory concentration |
| ICA | islet cell autoantibody |
| IDDM | insulin-dependent diabetes mellitus |
| IFIH1 | interferon induced with helicase C domain 1 |
| IGF | insulin-like growth factor |
| IGF2BP2 | insulin-like growth factor 2 mRNA binding protein 2 |
| IKKβ | TNF-induced insulin resistance mediator |
| IL | interleukin |
| IL2RA | interleukin 2 receptor, alpha |
| Ile | isoleucine |
| INF | interferon |
| *INS* | insulin gene |
| $IP_3$ | inositol-1,4,5-triphosphate |
| IR | infra red |
| IR | insulin receptor |
| IRS | insulin receptor substrate |
| JAZF1 | JAZF zinc finger 1 |
| JNK1 | JUN kinase-1 |
| K | potassium |
| K+-ATP | ATP-dependent potassium channel |
| $K_a$ | association constant |
| $k_{cat}$ | turnover number |
| KCNJ11 | potassium inwardly-rectifying channel, subfamily J, member 11 |
| KCNQ1 | potassium voltage-gated channel, KQT-like subfamily, member 1 |
| $K_d$ | dissociation constant |

| | |
|---|---|
| kDa | kilodalton |
| kg | kilogram |
| $K_i$ | inhibition constant |
| KLF14 | Kruppel-like factor 14 |
| $K_m$ | Michaelis constant |
| Leu | leucine |
| LPH | lactase-phloritzin hydrolase |
| Lys | lysine |
| M | molar |
| m/z | mass-to-charge ratio |
| mA | milliamps |
| MAPK | mitogen-activated protein kinase |
| MeG | methylglyoxal |
| MEM-α | Alpha Minimum Essential Medium |
| Mg | magnesium |
| mg | milligrams |
| MG-H | MeG-derived hydroimidazolones |
| MG-H1 | $N_\delta$-(5-hydro-5-methylimidazol-4-on-2-yl)ornithine |
| MG-H2 | 2-amino-5-(2-amino-5-hydro-5-methyl-4-imidazolon-1-yl)pentanoic acid |
| MG-H3 | 2-amino-5-(2-amino-4-hydro-4-methyl-5-imidazolon-1-yl)pentanoic acid |
| MHC | major histocompatibility complex |
| min | minutes |
| ml | millilitres |
| mm | millimetres |
| mM | millimolar |
| MOE | Molecular Operating Environment |
| MOLD | MeG-lysine dimer |
| mRNA | messenger ribonucleic acid |
| mTOR | mammalian target of rapamycin |

| | |
|---|---|
| mV | millivolts |
| N | native |
| Na | sodium |
| $Na_2HPO_4$ | sodium phosphate dibasic |
| NAC | *N*-acetyl-cysteine |
| NAD | nicotinamide adenine dinucleotide |
| $NaH_2PO_4$ | sodium dihydrogen phosphate |
| NaOH | sodium hydroxide |
| Nck | small adapter protein |
| NEFA | non-esterified fatty acid |
| NHS | national health service |
| NIDDM | non-insulin-dependent diabetes mellitus |
| NK | natural killer |
| nm | nanometres |
| nmol | nanomoles |
| NOTCH2 | notch 2 |
| $O_2$ | oxygen |
| p110 | catalytic subunit of PI 3-kinase |
| p70s6k | p70 ribosomal S6 kinase |
| PARP | poly(ADP-ribose) polymerase |
| PBS | phosphate buffered saline |
| PC1 | prohormone convertase 1 |
| PC2 | prohormone convertase 2 |
| PDB | Protein Data Bank |
| PDK-1 | protein kinase 3-phosphoinositide-dependent protein kinase-1 |
| PDX-1 | pancreatic and duodenal homeobox 1 |
| Phe | phenylalanine |
| PI 3-kinase | phosphatidylinositol 3-kinase |
| PI3K | phosphoinositide 2-kinase |
| $PIP_2$ | phosphatidylinositol-4,5-bisphosphate |

| | |
|---|---|
| pKa | acid dissociation constant |
| PKB | protein kinase B |
| PKC | protein kinase C |
| PMT | photomultiplier tube |
| PP | pancreatic polypeptide |
| PPAR | peroxisome proliferator activated receptor |
| PPARG | peroxisome proliferator-activated receptor gamma |
| ppm | parts per million |
| PRC1 | protein regulator of cytokinesis 1 |
| Pro | proline |
| PTP | protein tyrosine phosphatase |
| PTPN22 | protein tyrosine phosphatase, non-receptor type 22 |
| PTPRD | protein tyrosine phosphatase, receptor type D |
| rER | rough endoplasmic reticulum |
| RNA | ribonucleic acid |
| ROS | reactive oxygen species |
| rpm | rotations per minute |
| SE | standard error |
| SEM | standard error of the mean |
| Ser | serine |
| SGLT | sodium-dependent glucose transporter |
| SH2 | src-homology 2 |
| shc | src homology 2 domain |
| SHP2 | tyrosine-specific protein phosphatase |
| SLC30A8 | solute carrier family 30 (zinc transporter), member 8 |
| SOCS | suppressor of cytokine signalling |
| sos | son-of-sevenless |
| SREBP-1c | steroid regulatory element binding protein |
| SRR | serine racemase |
| SUMO4 | small ubiquitin-like modifier 4 |

| | |
|---|---|
| TAE | Tris acetate-EDTA |
| TC10 | small signalling G-protein |
| TCA | tricarboxylic acid |
| TCF7L2 | transcription factor 7-like 2 |
| TEA | tetraethylammonium |
| THADA | thyroid adenoma associated |
| Thr | threonine |
| TP53INP1 | tumour protein p53 inducible nuclear protein 1 |
| Trp | tryptophan |
| TSPAN8-LGR5 | tetraspanin 8-leucine-rich repeat-containing G protein coupled receptor 5 |
| Tyr | tyrosine |
| UK | United Kingdom |
| UV | ultraviolet |
| v | reaction rate |
| Val | valine |
| $V_{max}$ | maximum rate |
| VNTR | variable number of tandem nucleotide repeats |
| WAT | white adipose tissue |
| WFS1 | Wolfram syndrome 1 (wolframin) |
| WHO | World Health Organisation |
| WTCCC | The Wellcome Trust Case Control Consortium |
| ZBED3 | zinc finger, BED-type containing 3 |
| ZFAND6 | zinc finger, AN1 type domain 6 |
| Zn | zinc |
| $ZnCl_2$ | zinc chloride |
| α-cells | alpha cells |
| α-GAL | α-galactosidease |
| β-cells | beta cells |
| β-galactose-1,4-glucose | lactose |
| δ-cells | delta cells |

| | |
|---|---|
| µl | microlitres |
| µm | micrometres |
| µM | micromolar |

# Chapter 1:

# Introduction

## 1. Introduction

The most common condition observed by gastroenterologists is irritable bowel syndrome (IBS). This condition accounts for approximately 50 % of all referrals (Campbell *et al.,* 2010). IBS is characterised by a diverse range of gut and systemic symptoms such as gut pain, gas, diarrhoea or constipation as well as severe headaches, severe fatigue, muscle and joint pain and heart palpitations. The success rates at treating this condition are poor leading to a reduced quality of life for the affected individual as well as costing the NHS a significant amount for consultations with doctors and for the relevant drug therapy for the management of the symptoms. So that this condition can be controlled effectively, it is important to understand the mechanism involved in the production of the symptoms that characterise it. It has been shown that lactose and food intolerance are the major causes of IBS (Campbell and Matthews, 2005, Campbell *et al.,* 2005, Waud *et al.,* 2008). The symptoms of IBS occur due to the production of "toxic" metabolites by the bacteria found in the large intestine as a result of the anaerobic breakdown of food such as carbohydrates that were unable to be absorbed by the small intestine. The "toxic" metabolites produced by the bacteria can include alcohols, diols (e.g. butan-2,3-diol), ketones, acids and aldehydes (e.g. methylglyoxal). The production of these bacterial toxins can have a significant effect on the signalling mechanisms of cells around the body and this explains why individuals with IBS, lactose and food intolerance experience these symptoms (Campbell *et al.,* 2005).

Charles Darwin (1809 – 1882) was unwell for the majority of his life. In December 1831, he was in Plymouth waiting to board a ship called the "Beagle", when he developed chest pain and palpitations. However, once on the ship these symptoms improved and he seemed to be healthy apart from the occasional fever and some sea-sickness (Campbell and Matthews, 2005). These symptoms were thought to be due to Darwin contracting typhoid (Campbell *et al.,* 2005). After returning home and marrying in 1837 he developed the same symptoms and was ill again. At times, Darwin felt so unwell he had to stop working for a number of weeks at a time. He began a diary recording his symptoms (Table 1.1) and the worst symptoms he experienced were constant nausea and vomiting, stomach pain, flatulence as well as headaches and some dizziness.

Some other symptoms he also had included eczema (mainly on his face), boils and chronic fatigue. He saw a number of doctors – one of these included his father and tried a diverse range of medications and some home remedies, however these were all unsuccessful in treating his symptoms. The only time Darwin's condition improved was when he reduced his milk and cream intake (Campbell and Matthews, 2005, Campbell *et al.,* 2005).

| **Symptoms recorded by Charles Darwin** |
| --- |
| • Severe gastrointestinal problems, such as gut pain<br>• Nausea and vomiting<br>• Severe headaches and dizziness<br>• Joint pain<br>• Chronic fatigue<br>• Trembling<br>• Insomnia<br>• Allergies, such as eczema<br>• Mouth ulcers<br>• Boils<br>• Heart palpitations<br>• Depression<br>• Poor resistance to infections |

**Table 1.1. The symptoms recorded by Charles Darwin** (Campbell and Matthews, 2005)**.**

The regular occurrence of these symptoms began to have a significant impact on Darwin's life. His work began to slow down and he turned down invites to parties as well as preventing him from attending the Oxford debate in 1860 (Campbell and Matthews, 2005). Many proposals have been put forward in an attempt to diagnose Darwin and these include: arsenic poisoning, Chagas' disease and psychosomatic disorders, such as bereavement syndrome and more recently Crohn's disease, but none of these conditions match with the symptoms he experienced (Orrego and Quintana, 2007, Sheehan *et al.,* 2008, Hayman, 2009, Greene and Greene, 2009). However, the symptoms do match exactly those seen in patients with systemic lactose intolerance and there is a substantial amount of evidence to suggest that Darwin had this condition:

- The symptoms Darwin had matched those seen in patients suffering with systemic lactose intolerance

- He began to develop gut pain and vomiting 2-3 hours after eating and this is consistent with the time that it takes for lactose to reach the large intestine
- His diet consisted mainly of milk, cream and other dairy containing products
- He had a family history of illness
- He did not have his illness whilst on board the Beagle between 1831 and 1836 as there was no fresh milk or dairy products on board the ship
- He displayed significant improvement when he reduced his milk and cream intake

It is therefore predicted that Charles Darwin suffered for most of his life with lactose intolerance and had this been known, simply reducing the amount of lactose intake in his diet would have considerably improved his way of life.

## 1.1. Lactose, lactase and lactose sensitivity

### 1.1.1. Lactose and lactase

Lactose (β-galactose-1,4-glucose) is the disaccharide sugar found in the milk of all mammals. The only mammals that do not have lactose are *Pinnepedia* (sea lions and walruses). Lactose is made up of the two sugars galactose and glucose linked together by a 1,4-linkage. On average, human milk contains 7.0 g of lactose in 100 ml whereas cow's milk contains approximately 4.7 g of lactose in 100 ml (Arola and Tamm, 1994).

When lactose is ingested, it must be broken down into galactose and glucose (Arola and Tamm, 1994). So that lactose can be absorbed it is hydrolysed in the small intestine by lactase-phloritzin hydrolase (LPH) also known as lactase in short (Matthews *et al.,* 2005, Vesa *et al.,* 2000, Escher *et al.,* 1992). Lactase is found at high levels in the jejunum at the start of the small intestine and its only purpose is to hydrolyse lactose (Vesa *et al.,* 2000). Lactase is a protein consisting of 1059 amino acids and has a molecular weight of 320 kDa. It is an unusual protein in that it contains two active sites in its polypeptide chain. One active site is responsible for hydrolysing lactose and the other is responsible for hydrolysing aryl and aliphatic glycosides e.g. phloritzin into glucose and phloretin. Phloretin can be found in apple tree leaves and is a potent diabetic

agent (Matthews *et al.,* 2005). Once lactose has been broken down by lactase into its constituent monosaccharides, they are absorbed from the intestine.

The sodium-dependent glucose transporter 1 (SGLT1) is found on the apical surfaces of the intestinal absorptive cells (enterocytes) of the small intestine. The presence of this type of transporter enables the uptake of these monosaccharides into the cells against the concentration gradient, using the $Na^+$ gradient as the energy source. The presence of another glucose transporter, glucose transporter 2 (GLUT2), which is located on the opposite side of the cells, then allows the release of glucose and galactose into the bloodstream. Galactose is harmful to the eyes as well as other cells of the body and therefore once in the bloodstream it is rapidly metabolised by the liver to remove it from the body. Some compounds found in foods can lead to the inhibition of glucose and galactose uptake by the SGLT1 transporter. For example, raffinose and stachyose, a tri- and tetra-saccharide, respectively can inhibit the uptake of glucose and galactose by the SGLT1 transporter. Raffinose is a trisaccharide consisting of galactose, glucose and fructose, whereas stachyose is a tetrasaccharide composed of two galactose units, glucose and fructose (or stachyose = raffinose + galactose). These sugars are found in beans, chick peas, pulses and root vegetables, such as parsnips. They can be hydrolysed by the enzyme α-galactosidease (α-GAL). However, the human digestive tract does not contain the enzyme α-GAL, that is required to breakdown these sugars. Therefore, these sugars pass undigested through the small intestine and stomach. When they reach the large intestine, the bacteria here which do contain the α-GAL enzyme can breakdown these sugars resulting in the production of gases such as $CO_2$, methane and hydrogen, leading to the flatulence that is commonly associated with the consumption of beans and some vegetables (Matthews *et al.,* 2005, Campbell *et al.,* 2005).

### 1.1.2. Hypolactasia and lactose sensitivity

Depending on the ethnic background of an individual, normal lactase activity (normolactasia) can continue into adulthood and it is this that allows humans to be able to consume large quantities of milk without developing any symptoms (Arola and Tamm, 1994). However, after weaning, the lactase levels can significantly decrease. Hypolactasia is a medical term for the loss of lactase in the small intestine therefore leaving the unhydrolysed lactose in the

jejunum where it can then be metabolised by the intestinal bacteria (Arola and Tamm, 1994). If there is little or no lactase in the small intestine, lactose is either partially digested or undigested and remains in the small intestine where it can cause the wide range of symptoms seen in lactose intolerance.

It is due to these low levels of lactase that has resulted in a significant proportion of the world's population becoming hypolactasic. There are three mechanisms that can cause this:

**Primary adult hypolactasia** – this is the most common type and is the loss of the enzyme on weaning (Campbell *et al.,* 2005). The activity of the enzyme, lactase, will have decreased to approximately 10 % of normal levels found in children. At which age the amount of lactase declines varies from less than two years to 10 - 20 years (Arola and Tamm, 1994).

**Secondary hypolactasia** – this type is also known as acquired hypolactasia and usually occurs following any gastrointestinal illness that results in brush border damage or can be due to significant increases in transit time in the jejunum border. This type has the potential to be reversed and is therefore able to be treated (Campbell *et al.,* 2005).

**Congenital alactasia** – this type is rare and therefore only a small number of people suffer with congenital alactasia however, it is common amongst the Finnish population. This is the absence of lactase, even from birth. Babies that are born with this type cannot digest lactose that is present in breast milk and standard infant milk formulas. This absence of lactase is due to mutations in the lactase gene (Campbell *et al.,* 2005).

Most adults have a normal lactase level at birth however; this level significantly decreases following weaning (Swagerty *et al.,* 2002). Humans lose between 90 and 95 % of birth lactase levels by the time they reach early childhood and the level of lactase continues to decrease throughout life. The prevalence of hypolactasia can vary between different ethnic groups (fig. 1.1 and Table 1.2). Asians are predicted to have a very low tolerance to lactose due to losing between 95 and 100 % of lactase.

| Ethnic group | Prevalence (%) |
|---|---|
| • Northern Europeans | 2 – 15 |
| • White Americans | 6 – 22 |
| • Central Europeans | 9 – 23 |
| • Northern Indians | 20 – 30 |
| • Southern Indians | 60 – 70 |
| • Hispanics | 50 – 80 |
| • Ashkenazi Jews | 60 – 80 |
| • Blacks | 60 – 80 |
| • American Indians | 80 – 100 |
| • Asians | 95 – 100 |

**Table 1.2. The prevalence of primary lactose hypolactasia in various ethnic groups** (Swagerty *et al.,* 2002).

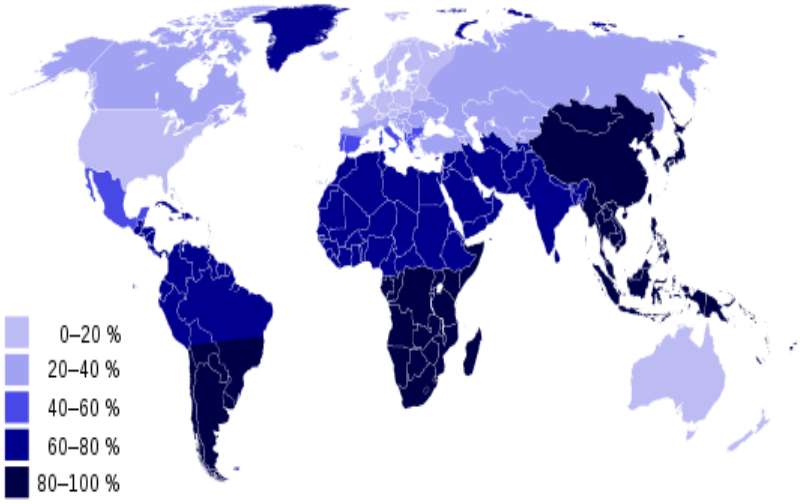


**Figure 1.1. The global incidence of lactose sensitivity**

Lactose malabsorption is caused when lactose is metabolised into its two sugar constituents, glucose and galactose, by lactase, but these are not fully absorbed by the small intestine. As a result of these not being fully absorbed, patients experience symptoms similar to those seen in patients who suffer with lactose intolerance e.g. abdominal pain, flatulence and diarrhoea. Patients with lactose malabsorption are able to consume a moderate amount of milk without experiencing significant symptoms (Johnson *et al.,* 1993). Lactose malabsorption does not always lead to lactose intolerance (Ferguson, 1981).

Lactose sensitivity is due to the lack of the enzyme, lactase, on the brush border (microvilli) of the small intestine (Matthews and Campbell, 2000, Campbell *et al.,* 2004).

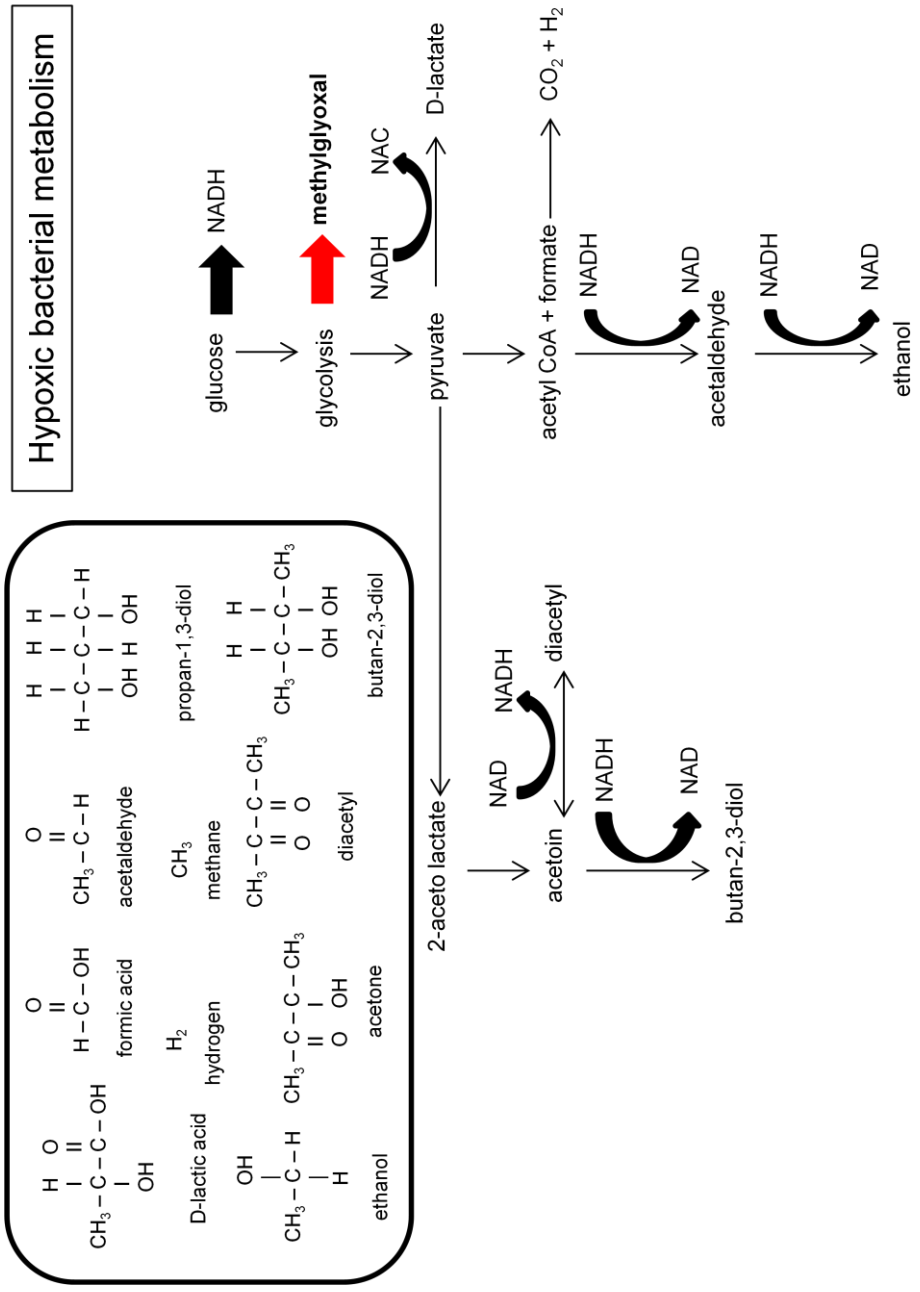


**Figure 1.2. The pathways through which anaerobic bacteria in the large intestine generate gases and bacterial metabolic toxins.** The structures of the fermentation products and putative bacterial metabolic toxins are shown in the box (Campbell *et al.,* 2005, Campbell *et al.,* 2010).

So that it can be absorbed, the milk sugar lactose must be hydrolysed at the intestinal brush border by the enzyme lactase. Following weaning, there is a decrease in lactase activity and this reduction in lactase activity leads to the development of lactose intolerance (Suarez *et al.,* 1995). When undigested lactose remains and is not absorbed in the small intestine, it is passed to the large intestine. In the large intestine there are $10^{14}$ individual bacteria representing over 1000 different species and weighing approximately 1 kg. There is very little oxygen in the large intestine, approximately < 1 μM. The bacteria here anaerobically metabolise lactose resulting in the production of gases and metabolic toxins (fig. 1.2) (Campbell *et al.,* 2010). The gases (hydrogen and methane) produced cause gut distension, resulting in pain and flatulence, whereas, the metabolic toxins can be reabsorbed into the bloodstream and can travel around the body and can be harmful to a range of tissues throughout the body, such as neurones, cardiac cells, other muscles, endocrine cells and cells making up the immune system (Campbell *et al.,* 2005). It is predicted that these putative metabolic toxins can lead to the development of diabetes. Lactose sensitivity produces gastrointestinal symptoms such as abdominal pain and distension but there are also systemic symptoms (Table 1.3). Some of the systemic symptoms are missed by clinicians due to their intermittent appearance.

| **Symptoms** | |
|---|---|
| ***Gut related:*** | ***Systemic related:*** |
| • Abdominal pain<br>• Gut distension<br>• Borborygmi<br>• Flatulence<br>• Diarrhoea<br>• Constipation<br>• Nausea and vomiting | • Headache and light headedness<br>• Loss of concentration<br>• Poor short term memory<br>• Severe fatigue<br>• Muscle pain<br>• Joint pain (+/- swelling and stiffness)<br>• Allergy (eczema, asthma, rhinitis, sinusitis, pruritis<br>• Mouth ulcers<br>• Heart palpitations and arrhythmias<br>• Sore throat<br>• Increased micturition |

**Table 1.3. The gut and systemic symptoms of lactose sensitivity** (Matthews *et al.,* 2005).

These symptoms can vary between individuals and depends on the amount of lactase a person has in the small intestine and how much lactose has been consumed. For example, if there is a significant amount of lactose compared to the amount of lactase present the symptoms of lactose intolerance can be quite severe.

To determine if a patient is lactose sensitive the patient is required to consume 50 g of lactose orally. The consumption of 50 g of lactose is the equivalent to the same patient drinking 1 litre of cow's milk. Once the lactose has been consumed breath hydrogen is measured every half an hour over a time course of 3 hours. The development of symptoms after the consumption of this 50 g lactose does not necessarily mean that individuals cannot tolerate a small amount of milk, as some people who did not have a history of any gut problems prior to ingestion did however, display some symptoms after taking the 50 g lactose. A person is considered to be lactose sensitive if they have a breath hydrogen measurement above 20 parts per million (ppm). The consumption of 50 g lactose is significantly high and will over whelm the remaining lactase available in those individuals that have already lost the enzyme after weaning, resulting in the symptoms shown in Table 1.3 (Matthews *et al.,* 2005, Waud *et al.,* 2008).

Lactose sensitivity can often be misdiagnosed and after years of discomfort and a poor quality of life, the right diagnosis and by simply removing lactose from the diet can considerably improve the quality of life of someone with this condition (Matthews *et al.,* 2005).

### 1.2. Lactose sensitivity and irritable bowel syndrome

Irritable bowel syndrome (IBS) is a chronic gastrointestinal problem that is characterised by abdominal discomfort, bloating and diarrhoea. It is a common condition and is the most common reason for visiting a gastroenterologist, where there are approximately 2.4 – 3.5 million visits each year (Waud *et al.,* 2008, Cash and Chey, 2004). The symptoms of IBS are the same as those seen in individuals with lactose sensitivity (Gupta *et al.,* 2007) and the prevalence of lactose sensitive patients with IBS ranges from 17 to 86 % (Frissora and Koch, 2005). Therefore, patients who have been diagnosed with IBS are often advised to undergo a lactose sensitivity test or breath hydrogen test to see if they are also lactose sensitive (Waud *et al.,* 2008). Sometimes, if the lactose sensitivity test does not suggest that the patient is lactose

sensitive, the patients are advised to remove lactose containing products from their diet and this has helped to considerably reduce their symptoms and improved their overall quality of life.

### 1.3. Gas and metabolite release as a result of carbohydrate metabolism

It is known that when undigested carbohydrates remain in the small intestine rather than being broken down into monosaccharides so that they can be absorbed they get passed into the large intestine where the bacteria can anaerobically metabolise them. As a result of carbohydrate metabolism by the bacteria, gases and a range of metabolites are produced. The metabolites produced will depend on the species of bacteria (Campbell *et al.,* 2007). Table 1.4 shows the gases and metabolites that can be released by the different bacteria in the large intestine.

| **Substances that are released:** | **Examples:** |
|---|---|
| Gases | Carbon dioxide, hydrogen, methane, hydrogen sulphide, oxygen, nitrogen and ammonia |
| Metabolites | Alcohols (e.g. ethanol), diols (e.g. butan-2,3-diol), aldehydes (acetaldehyde), short chain fatty acids, dimethyl hydrazine, amino acid degradation products and cyclic AMP |

**Table 1.4. The gases and metabolites that are released by the different bacteria in the gut following carbohydrate metabolism** (Campbell *et al.,* 2005).

Of these substances that are released, the metabolites are of particular interest. These metabolites include compounds such as methylglyoxal, diacetyl, propan-1,3-diol, butan-2,3-diol, acetaldehyde, formic acid, D-lactic acid and ethanol (Campbell *et al.,* 2005, Campbell *et al.,* 2010). It is proposed that these bacterial metabolic toxins are responsible for the development of diseases such as diabetes. This thesis will focus on the putative toxin, methylglyoxal.

### 1.3.1. Methylglyoxal and its pathway

Methylglyoxal (MeG) (fig. 1.3) is also known as pyruvaldehyde or 2-oxopropanal (CH3-CO-CH=O or $C_3H_4O_2$). It is a dicarbonyl compound as it consists of two carbonyl groups. Of these two carbonyl groups, one is aldehydic and the other is ketonic and this therefore makes MeG a ketal.

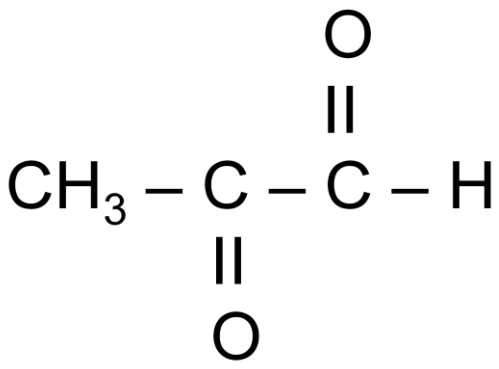

**Figure 1.3. The chemical structure of methylglyoxal (MeG).**

MeG is present at low concentrations in the body (Jan *et al.,* 2005) but it can also be produced by bacteria in the gut and by mammalian cells. Many bacteria in the gut contain the enzyme MeG synthase (*E.C. 4.2.99.11*) and it is this enzyme that is responsible for the conversion of dihydroxyacetone phosphate (DHAP) into MeG *via* the removal of a phosphate group. From this, it has been predicted that the bacteria found in the intestine may be one of the most important sources of MeG production (Baskaran *et al.,* 1989, Ferguson *et al.,* 1998).

MeG can also be produced intracellularly *via* enzymatic or non-enzymatic pathways in nearly all mammalian cells (Cook *et al.,* 1998, Turk, 2010). The primary source of MeG in mammalian cells is by the fragmentation and removal of a phosphate group from the enediol intermediate, triose 1,2-enediol-3-phosphate in the interconversion of DHAP and glyceraldehyde-3-phosphate (GAP) (fig. 1.4). The removal of this phosphate group may occur enzymatically. The enzymatic removal of the phosphate group from DHAP is carried out by the enzyme, MeG synthase (Thornalley, 1996, Best and Thornalley, 1999, Mukohda *et al.,* 2009, Chaplen, 1998).

The generation of MeG is controlled by the amount of DHAP and phosphate that is present. During times where there are increased concentrations of DHAP, MeG synthase is stimulated and is responsible for the production of MeG (Booth *et al.,* 2003). High phosphate concentrations inhibit the enzyme, MeG synthase thus preventing further production of MeG. The enzyme, triosephosphate isomerase, can affect the levels of DHAP present as the enzyme is responsible for the interconversion of GAP to DHAP when there are low concentrations of phosphate (Booth *et al.,* 2003). The increased production of DHAP leads to the stimulation of MeG synthase and results in MeG production. MeG can also be produced as a result of lipid and/or L-threonine and L-lysine catabolism (Chaplen, 1998).

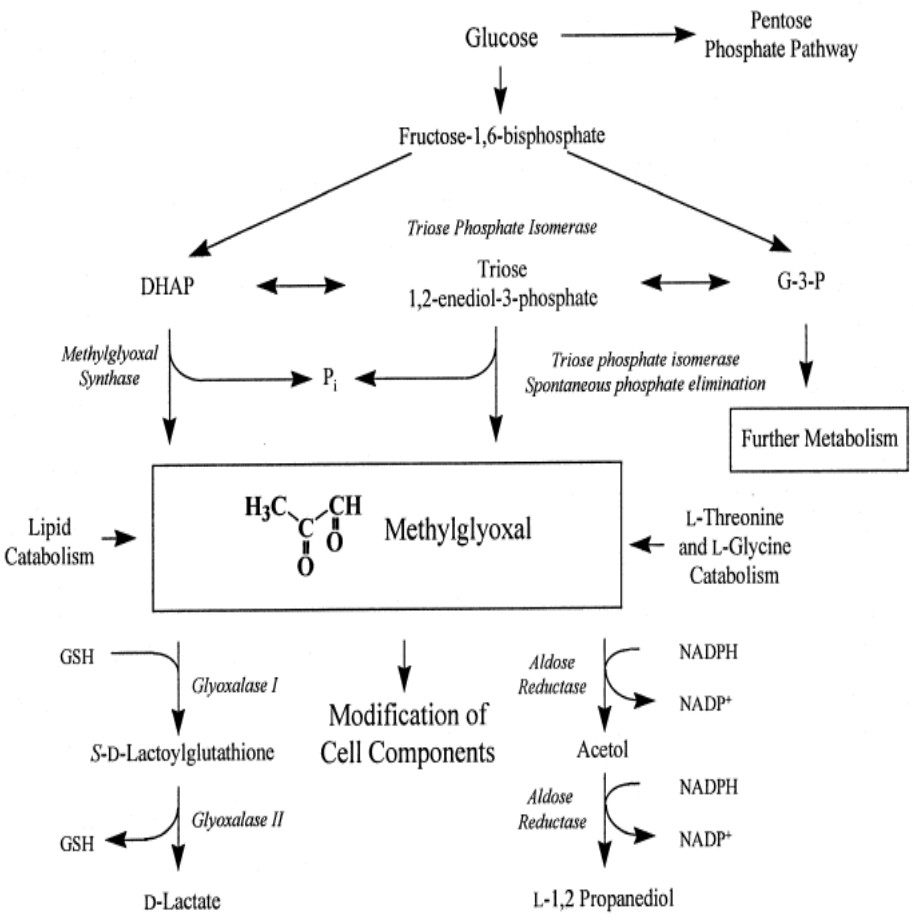


**Figure 1.4. The metabolism of methylglyoxal (MeG) in mammalian systems** (Chaplen, 1998).

Therefore, from this it can be seen that both bacterial cells and mammalian cells produce MeG *via* the removal of a phosphate group from DHAP by the enzyme MeG synthase.

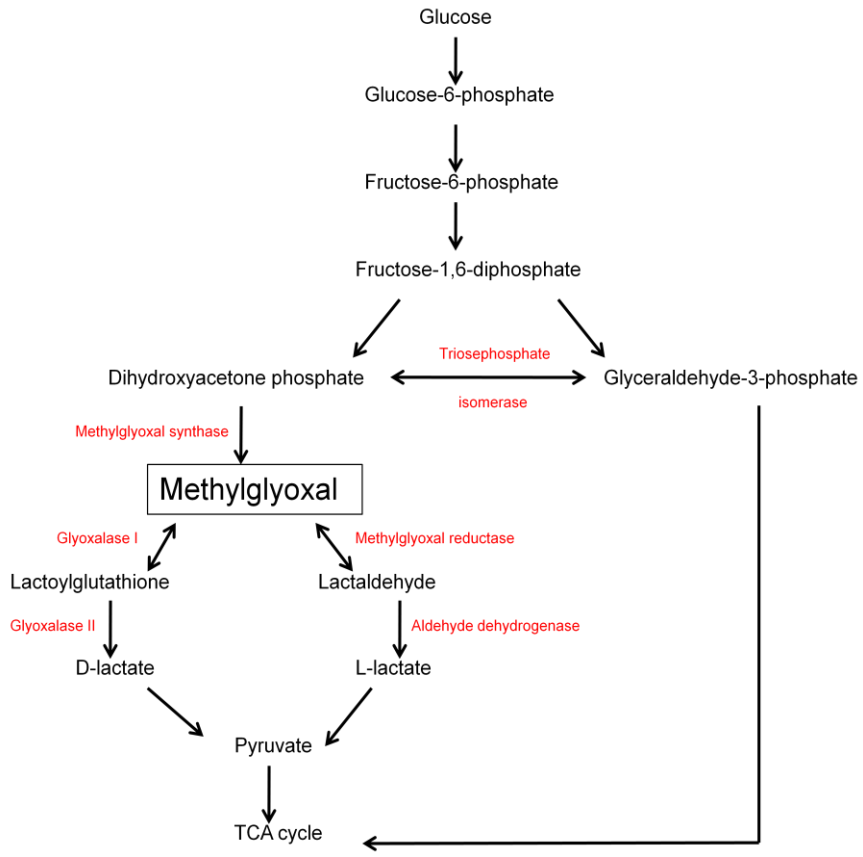


**Figure 1.5. The methylglyoxal pathway** (Ackerman *et al.,* 1974).

The excessive intake of carbon containing compounds (e.g. glucose) by a cell stimulates the MeG pathway (fig. 1.5) and therefore causes increased MeG production. MeG is toxic to cells, therefore there are number of mechanisms in place to convert it into non-toxic metabolites. Once MeG has been produced, the enzyme MeG reductase is responsible for the conversion of MeG to lactaldehyde and then the enzyme aldehyde dehydrogenase converts lactaldehyde into L-lactate. MeG is also the physiological substrate for the glyoxalase system. The glyoxalase system can be found in the cytosol of all mammalian cells and is comprised of the two enzymes, glyoxalase I (*E.C. 4.4.1.5*) and glyoxalase II (*E.C. 3.1.2.6*) (Chaplen, 1998).

The enzymes of this system are responsible for maintaining low levels of MeG by converting it into non-toxic metabolites (Best and Thornalley, 1999, Jan *et al.,* 2005). Glyoxalase I is the enzyme that converts MeG into lactoylglutathione and glyoxalase II is the enzyme that converts lactoylglutathione into D-lactate. Both L- and D-lactate are then converted into pyruvate which can then go on to enter the TCA cycle.

MeG has a concentration of 1.4 μM in healthy subjects. Elevated concentrations have been noticed in diabetic patients. Patients with type 1 diabetes have a 5- to 6-fold increase whereas patients with type 2 diabetes have a 2- to 3-fold increase in MeG concentration. Therefore a strong association has been formed between increased MeG concentration and hyperglycaemia. Increased MeG concentrations at times of hyperglycaemia can affect cellular function due to the toxin reacting with the amino groups of proteins thus resulting in impaired cell function and diabetic complications. For example, the modification of the insulin receptor substrate by MeG has been proposed to be involved in impaired insulin signalling (Queisser *et al.,* 2010, Rabbani and Thornalley, 2011, Lee *et al.,* 2009).

Not only is MeG produced as a result of carbohydrate metabolism by the bacteria in the large intestine, but it can also be obtained from the diet and is found at high levels in some products. High levels of MeG can be found in processed food and coffee. Individuals that do not consume a diet rich in carbohydrates but in fact have a diet rich in vegetables, beans and pulses can still have elevated concentrations of these bacterial metabolic toxins. The production of MeG can alter the balance of gut microflora and will eventually get absorbed into the blood where it can have damaging effects on tissues in the body. Diet is an easy factor to modify and a simple change in diet may help to rebalance the gut microflora and reduce MeG production.

The glyoxlase system is found in the cytosol of all mammalian cells and is responsible for the detoxification of MeG. Any alterations in the expression of the genes involved in this process can affect MeG production. For example, the inhibition of the gene *glyoxalase I* can prevent the detoxification of MeG thus allowing it to damage target tissues.

Variations in the production of bacterial toxins like MeG may help to explain why only a small minority of individuals develop diabetes. It can be concluded that diet has an important role in the production of MeG as the toxin can be

produced as a result of metabolism or can be found at high levels in some food products. This may help to explain why non-obese individuals are just as likely as obese individuals to develop diabetes as a consequence of elevated MeG production.

### 1.4. The structure of the pancreas

The pancreas (fig. 1.6) is a gland organ in the digestive and endocrine systems of invertebrates that has an unusual structure. It can be found slightly below and behind the stomach. It is soft, pinkish-grey in colour, measuring 15-25 cm in length and has a mass of approximately 70 – 150 g (Carola *et al.,* 1990, Slack, 1995).

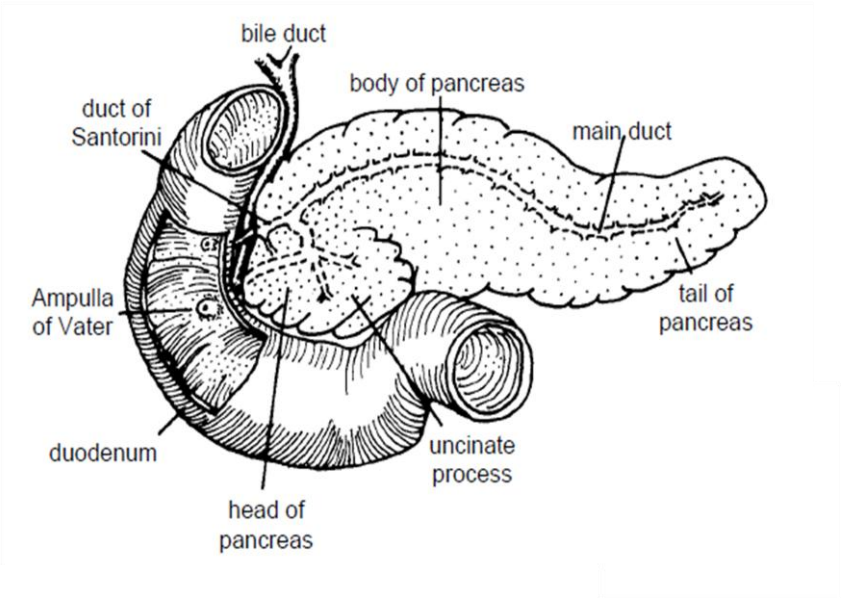


**Figure 1.6. The structure of the pancreas** (Slack, 1995).

The pancreas consists of three regions:

- The head
- The body
- The tail

The pancreas has an exocrine and endocrine function. Therefore, the pancreas is made of both exocrine and endocrine cells (Pocock and Richards, 2004, Slack, 1995).

### 1.4.1. The exocrine pancreas

The exocrine cells are grouped in acini. They are shaped like a pyramid and contain basal nuclei, rough endoplasmic reticulum (rER), golgi complex and a number of secretory granules containing the digestive enzymes. There are at least 22 digestive enzymes and these include proteases, amylases, lipases and nucleases. The majority of these enzymes are secreted as inactive precursors, however, when the reach the duodenum they become activated. At the junction where the acini and ducts meet, there are centroacinar cells which are rich in mitochondria. These centroacinar cells are responsible for the secretion of non-enzymatic components of the pancreatic juice, such as bicarbonate.

The ducts are lined with columnar epithelial cells. A small number of goblet and brush cells similar to those found in the intestine are also found in larger ducts. The release of pancreatic juice is controlled by hormonal stimulation by secretin, cholecystokinin and gastrin as well as by neural stimuli (Slack, 1995).

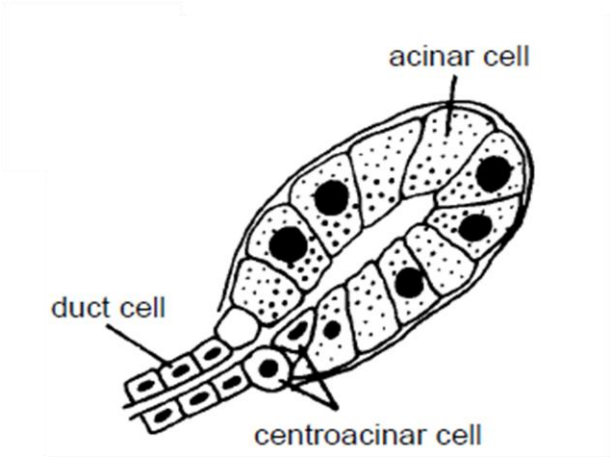


**Figure 1.7. The histology of a pancreatic acinus** (Slack, 1995).

The exocrine acinar cells (fig 1.7) secrete digestive enzymes such as:

- **Pancreatic amylase** – starch is a major dietary carbohydrate. This enzyme is responsible for converting polysaccharides into smaller molecules such as monosaccharides and disaccharides. It is a powerful enzyme that will act on cooked and uncooked starches

- **Pancreatic lipase** – triglyceride molecules are too large to be readily absorbed across the intestinal mucosa so they are broken down into a 2-monosaccharide and two free fatty acids by the enzyme pancreatic lipase. For the triglyceride to be digested and for the products of this digestion to be absorbed, there must be a sufficient amount of bile salts present in the intestinal lumen, therefore suggesting that normal absorption and digestion of fat relies on secretions from the pancreas and the liver
- **Pancreatic proteolytic enzymes (proteases)** – this category consists of trypsinogen, chymotrypsinogen and procarboxypeptidase. This enzyme is responsible for the breakdown of proteins. Proteases are harmful enzymes to have in cells, however, the synthesis and storage of the inactive precursors, trypsinogen, chymotrypsinogen and procarboxypeptidase in secretory vesicles is the way in which the cells can deal with these enzymes safely. The secretory vesicles also contain a trypsin antagonist just in case some of the trypsinogen becomes activated resulting in the formation of trypsin. Following exocytosis, the trypsin antagonist is diluted out and is ineffective. When trypsinogen is secreted into the lumen of the duodenum it is converted by enterokinase that is found in the intestinal mucosa into its active from trypsin. Trypsin then goes on to convert chymotrypsinogen and procarboxypeptidase into their active forms, chymotrypsin and carboxypeptidase. These enzymes are responsible for the breaking of different peptide linkages forming a mixture of amino acids and small peptides (Carola *et al.,* 1990).

The centroacinar cells are responsible for the secretion of bicarbonate. Bicarbonate is alkaline and its function is to neutralise the acid that enters the small intestine from the stomach.

### 1.4.2. The endocrine pancreas

The endocrine portion of the pancreas makes up approximately 1 % of the total mass of the gland. The endocrine cells are mainly grouped into the islets of Langerhans. The islets of Langerhans are microscopic organelles that are widely distributed throughout the pancreas and are clusters of cells that are found embedded in the endocrine tissue (Slack, 1995). The adult pancreas contains between 200,000 and 2,000,000 islets throughout the gland (Carola

*et al.,* 1990) and each individual islet contains approximately 2,000 cells (Robertson and Harmon, 2006).

The islets of Langerhans are neuroendocrine organs that are responsible for the control of blood glucose homeostasis (Soria *et al.,* 2000) and they are highly vascular, being supplied by arterioles that reach the islet core where they branch out into capillaries (Pickup and Williams, 2003). Four types of endocrine cell can be found in the pancreas:

- **Alpha cells (α-cells)** – these cells synthesize, store and secrete the hormone glucagon in response to a decrease in blood glucose levels (hypoglycaemia). Glucagon is responsible for the stimulation of glycogenolysis in the liver where glycogen is converted to glucose resulting in increased blood glucose levels (Robertson and Harmon, 2006).
- **Beta cells (β-cells)** – these cells are the most common type of cell located in the islets of Langerhans (Besser and Thorner, 2002) and can be found near the centre of the islet surrounded by the other cell types (Carola *et al.,* 1990). Elevated plasma glucose levels stimulate the release of insulin into the bloodstream from the secretory granules (Besser and Thorner, 2002). The β-cell is sensitive to changes (within the physiological range 1 – 10 ng/ml) in plasma glucose and is able to rapidly release insulin as a result of elevated glucose concentrations.
- **Delta cells (δ-cells)** – these cells secrete somatostatin. Somatostatin is required for the inhibition of many hormones (e.g. insulin and glucagon) that are released. These cells can potentially behave as an intraislet regulator of α-cells and β-cells (Robertson and Harmon, 2006).
- **Pancreatic polypeptide cells (PP cells)** – these cells secrete pancreatic polypeptide in response to a decrease in blood glucose levels (Carola *et al.,* 1990, Slack, 1995, Robertson and Harmon, 2006).

The secretion of glucagon by α-cells and insulin by β-cells occurs simultaneously and both of these hormones help regulate metabolism (Carola *et al.,* 1990). Islets rich in pancreatic polypeptide are found in the posterior part of the head (Slack, 1995).

### 1.5. Insulin synthesis, storage and secretion

Insulin is a peptide hormone that is required for tissue development, growth as well as maintaining glucose homeostasis and acts on the liver, muscle and fat (Kahn and White, 1988). It does this by accelerating glucose uptake while at the time inhibits glucose production and lipolysis (Rorsman *et al.,* 2000).

After a meal, the levels of circulating levels of glucose are elevated. In response to the elevated concentrations of glucose in the blood, the β-cells of the islets of Langerhans secrete insulin. The secretion of insulin controls glucose homeostasis at a number of different sites. Insulin can decrease hepatic glucose output by decreasing gluconeogenesis and glycogenolysis. It can also enhance glucose uptake into striated muscle and adipose tissue. Insulin can also have an effect on lipid metabolism resulting in the increased production of lipids by liver and adipose cells as well as increasing the secretion of fatty acids from triglycerides in fat and muscle (Pessin and Saltiel, 2000).

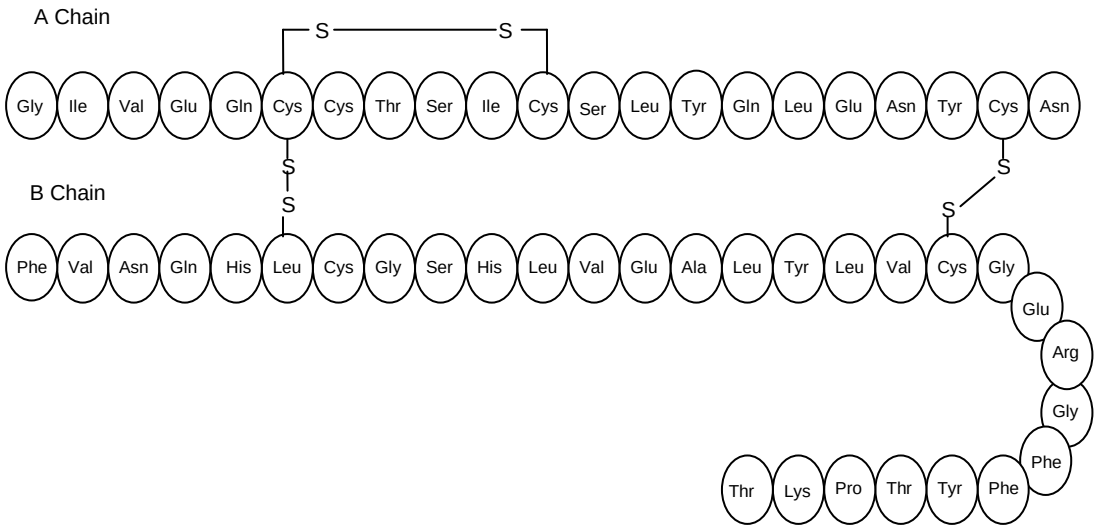


**Figure 1.8. The amino acid sequence of human insulin** (Pickup and Williams, 2003).

Insulin is made up of 51 amino acid residues (fig 1.8) and has a molecular weight of 5808 Da. The insulin molecule consists of two polypeptide chains that are joined by two disulphide bonds. The two polypeptide chains are

known as the A and B chain. The A chain consists of 21 amino acids as well as a intrachain disulphide bridge linking amino acids residues 6 and 11 whereas the B chain contains 30 amino acid residues (Derewenda *et al.,* 1989).

### 1.5.1. Insulin synthesis

Preproinsulin is rapidly secreted into the cisternal space of the rER. When in the rER, proteolytic enzymes cleave preproinsulin into proinsulin by removing the signal peptides. Proinsulin is made up of 86 amino acids and is a single polypeptide chain with a molecular weight of 9000 kDa. Proinsulin is further cleaved into insulin containing both the A and B chains that are linked together by a connecting peptide. This connecting peptide is known as C-peptide. This C-peptide is responsible for aligning the disulphide bridges that link the A and B chains so that the molecule can be folded correctly for cleavage. Microvesicles transport proinsulin to the Golgi apparatus. When it reaches the Golgi apparatus, proinsulin is then packed in the storage vesicles that are surrounded by a membrane containing an ATP-dependent proton pump. The conversion of proinsulin into insulin takes place in the Golgi apparatus and the conversion continues whilst in the secretory vesicles. The conversion of proinsulin into insulin is carried out by the proteolytic enzymes – prohormone convertases 1 and 2 (PC1 and PC2) as well as the enzyme exoprotease carboxypeptidase E (Besser and Thorner, 2002). These proteolytic enzymes are responsible for the rapid and specific cleavage of proinsulin (preventing the further breakdown of insulin) resulting in the removal of the C-peptide chain and the production of two cleavage dipeptide, finally yielding insulin (Pickup and Williams, 2003). Both insulin and C-peptide are then released on a one-to-one basis (Jia *et al.,* 2006).

### 1.5.2. Insulin storage

Insulin has a low solubility and once it has been processed by PC1 and PC2 it can along with zinc ions, form the water-insoluble microcrystals of hexamer ($Zn_2insulin_6$) in the slightly acidic (pH 5.5) environment of the secretory granules where it is stored (Noormagi *et al.,* 2010).

### 1.5.3. Insulin secretion

Glucose is the most important fuel for the body, and its plasma concentration is tightly controlled by a number of mechanisms.

The pancreatic β-cells are able to tell when there is a change in the plasma glucose concentration and in response they secrete insulin. The release of insulin from the pancreatic β-cell occurs in two stages. During the first stage, insulin is rapidly secreted due to elevated blood glucose concentrations.

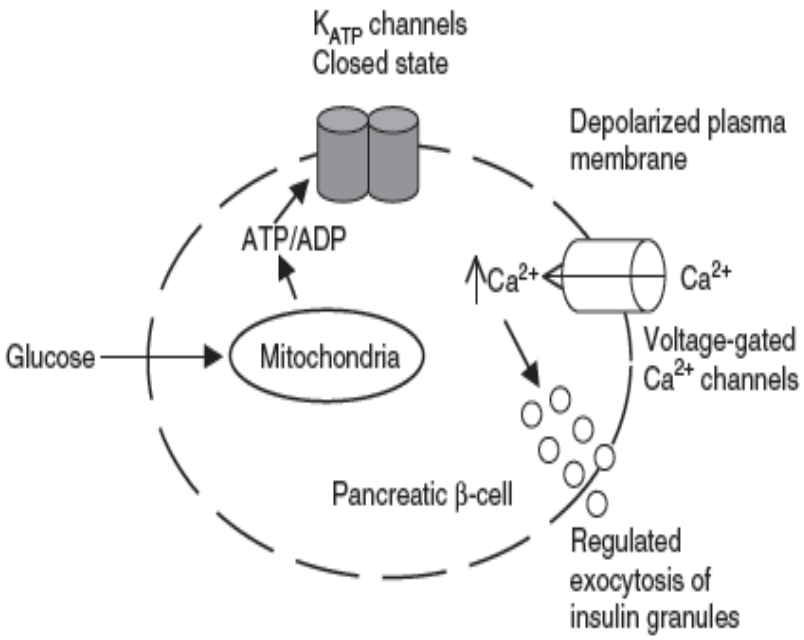


**Figure 1.9. A diagram showing the processes involved in glucose-stimulated insulin secretion (GSIS)** (Hussain and Cosgrove, 2005).

The most common pathway where glucose stimulates insulin secretion (fig. 1.9) starts with the transport of glucose into the β-cell through the GLUT2 glucose transporter. Glucose can be phosphorylated by the β-cell specific glucokinase enzyme (*EC 2.7.1.2)* to form glucose-6-phosphate. This is the rate-limiting metabolic step which acts as a glucose sensor. The metabolism involving mitochondrial FAD- glycerophosphate dehydrogenase (GDH) leads to the production of ATP. An increase in glucose levels leads to increases in the cytoplasm ATP/ADP ratio. The ATP/ADP ratio controls the ATP-dependent potassium channel ($K^+$-ATP channel) in the cell membrane of the β-cells. The presence of glucose increases the ATP/ADP ratio and this causes the $K^+$-ATP channel to close.

Once these channels are closed the cell membrane becomes depolarised and this causes the voltage-dependent calcium ($Ca^{2+}$) channels to open. Once the voltage-dependent $Ca^{2+}$ channels have opened there is an influx of calcium into the cytoplasm of the cell. Increases in intracellular calcium $[Ca^{2+}]_i$ leads to the activation of phospholipase C (*EC 3.1.4.3*). The enzyme phospholipase C, is then responsible for the breakdown of the membrane phospholipid, phosphatidylinositol-4,5-bisphosphate ($PIP_2$) into inositol-1,4,5-triphosphate ($IP_3$) and diacylglycerol (DAG). Once formed, $IP_3$ can then bind to the receptor proteins found on the membrane of the endoplasmic reticulum (ER) and causes the release of calcium through $IP_3$-gated channels into the cell and further increases the calcium concentration. The significant increases in calcium levels within the cell results in the release of insulin that was already stored in the secretory vesicles. Although this is the main mechanism for insulin release it may also be released after food consumption (Grill and Bjorklund, 2000, Koster *et al.,* 2005, Flatt *et al.,* 1997, Soria *et al.,* 2000, Aizawa *et al.,* 1994, Best, 2002).

### 1.6. The insulin receptor and the mechanism of insulin action

#### 1.6.1. The insulin receptor

The insulin receptor can be found embedded in the plasma membrane. It is a heterotetrametric glycoprotein that has two ligand binding α-subunits with a molecular weight of 135,000 Da as well as two tyrosine-specific protein kinase β-subunits with a molecular weight of 95,000 Da (fig. 1.10) (Kahn, 1985, Virkamaki *et al.,* 1999). The subunits are linked by disulphide bonds resulting in the formation of a β-α-α-β structure (Siddle *et al.,* 2001). This oligomeric structure divides the receptor into two functional domains (Gammeltoft and Van Obberghen, 1986) such that the α-subunits contain the high affinity insulin binding site. Even though there are two equivalent binding sites prior to the binding of the protein, only a single insulin molecule will bind to the site with high affinity.

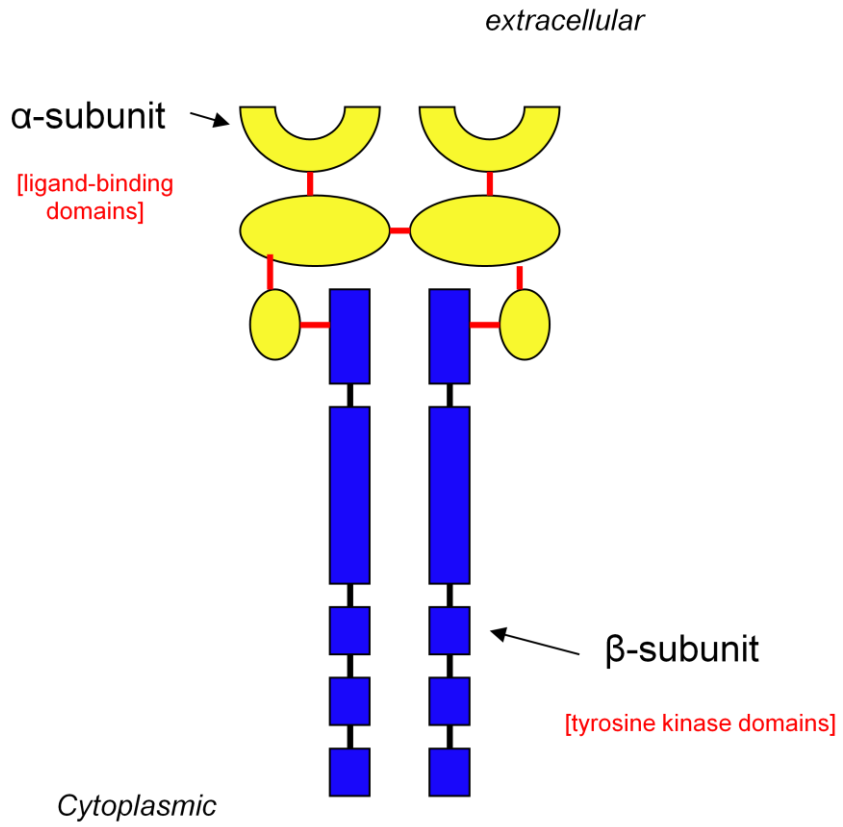


**Figure 1.10. The structure of the insulin receptor (IR) (Rosen, 1987)**.

The β-subunits are transmembrane proteins and are therefore the subunits involved in intracellular signalling (Kahn and White, 1988). The α-subunit is hydrophilic, disulphide bonded, glycosylated and can be found extracellularly whereas, the β-subunit has a short extracellular region that links the α-subunit by a disulphide bridge, a hydrophobic transmembrane domain and a long cytoplasmic region (Gammeltoft and Van Obberghen, 1986).

When insulin binds to the extracellular α-subunits a signal is transmitted across the plasma membrane resulting in the activation of the intracellular tyrosine kinase of one of the two β-subunits (Virkamaki *et al.,* 1999). The insulin receptor then undergoes a series of intracellular transphosphorylation reactions where one of the β-subunits can phosphorylate the specific tyrosine residues of its adjacent partner. Each tyrosine residue is responsible for a different function. For example, when the COOH-terminal tyrosine residue is phosphorylated this stimulates the mitogenic actions of insulin.

The phosphorylation of the tyrosine residue found in the juxtamembrane domain results in substrate binding, however, the phosphorylation of the tyrosine residues found in the kinase domain controls the catalytic activity of the β-subunit (Pessin and Saltiel, 2000).

### 1.6.2. The mechanism of insulin action

Insulin has an important role in the regulation of pathways that result in energy storage as well as cell proliferation and cell differentiation. The pathway (fig. 1.11) is initiated when insulin in the bloodstream binds to the extracellular α-subunits and a signal is transmitted across the plasma membrane. This signal results in the activation of the intracellular tyrosine kinase domain belonging to the β-subunit of the same insulin receptor.

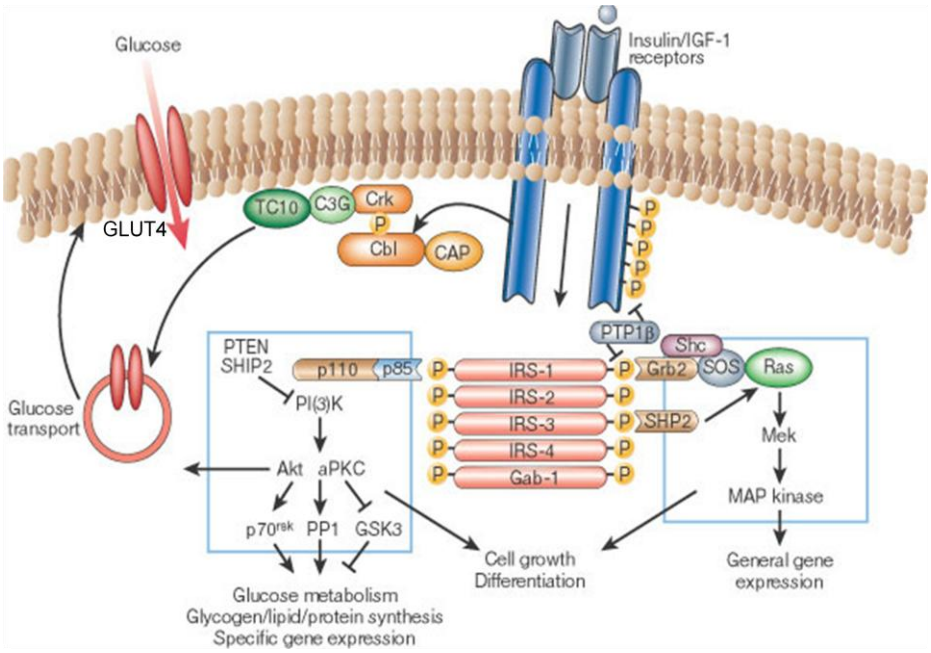


**Figure 1.11. The mechanism of insulin action** (Saltiel and Kahn, 2001).

The receptor then undergoes a number of intramolecular transphosphorylation reactions whereby one of the β-subunits can phosphorylate certain tyrosine residues of the adjacent partner. As well as tyrosine autophosphorylation, the β-subunit of the insulin receptor can also undergo serine/threonine phosphorylation. When the insulin receptor is activated *via* insulin binding, it

can phosphorylate a wide range of proximal substrates on tyrosine such as members of the insulin receptor substrate family (IRS 1/2/3/4), isoforms of the shc family, Gab1, Cb1 and APS. The phosphorylation of the IRS proteins results in the formation of recognition sites for additional effector molecules that have src-homology 2 (SH2) domains. The most important of these additional effector molecules with SH2 domains is the regulatory subunit belonging to the type 1A phosphatidylinositol 3-kinase (PI 3-kinase). However, others include small adapter proteins (e.g. Grb2 and Nck) as well as the SHP2 protein tyrosine phosphatase (Pessin and Saltiel, 2000).

Then p110 (a catalytic subunit of PI 3-kinase) phosphorylates $PIP_2$ and this leads to the formation of $PIP_3$. An important downstream effector of $PIP_3$ is AKT (also known as PKB). So that AKT/PKB can be phosphorylated and thus activated, there is a need for the protein kinase 3-phosphoinositide-dependent protein kinase-1 (PDK-1). When AKT/PKB is activated it will enter the cytoplasm of the cell and it is here where AKT/PKB phosphorylates and thus inactivates the enzyme glycogen synthase kinase 3 (GSK3). The enzyme glycogen synthase is a substrate of GSK3 and is responsible for catalysing the final stages of glycogen synthesis. The phosphorylation of glycogen synthase by GSK3 leads to the inhibition of glycogen synthesis and therefore leads to the activation of GSK3 by AKT/PKB thus promoting glucose storage as glycogen (Pessin and Saltiel, 2000).

A crucial function of insulin is to stimulate the uptake of glucose into cells *via* the glucose transporter, GLUT4. For glucose uptake to occur, insulin stimulates the translocation of the GLUT4 transporter from the intracellular storage vesicles to the plasma membrane. PI 3-kinase and AKT/PKB are known to be involved in GLUT4 translocation. GLUT4 translocation from the intracellular storage vesicles to the plasma membrane can also occur *via* a PI 3-kinase independent pathway. During the PI 3-kinase independent pathway, Cb1 is phosphorylated. Cb1 is linked with the CAP adapter protein when the receptor is activated. Once phosphorylated, Cb1 will then interact with the Crk adapter protein which is linked with C3G. C3G is a Rho-family guanine nucleotide exchange factor and is responsible for the activation of TC10 which is a member of the GTP-binding protein family. The activation of TC10 promotes the translocation of the GLUT4 transporter to the plasma membrane (Pessin and Saltiel, 2000, Siddle *et al.,* 2005).

Insulin is also involved in amino acid uptake into cells as well as promoting protein synthesis and inhibiting protein degradation. Under normal conditions, the activation of GSK3 will lead to the phosphorylation and inhibition of eIF2B which is a guanine nucleotide exchange factor that is responsible for controlling protein translation. Once an insulin signal has been detected, AKT/PKB renders GSK3 inactive. The inactivation of GSK3 leads to the dephosphorylation of eIF2B and therefore promotes protein synthesis as well as encouraging amino acid storage. AKT/PKB will activate mammalian target of rapamycin (mTOR) and therefore promotes protein synthesis *via* p70 ribosomal S6 kinase (p70s6k) and the inhibition of the eIF-4E binding protein (4E-BP1) (Pessin and Saltiel, 2000).

Insulin also stimulates fatty acid uptake as well as lipid synthesis, however, insulin inhibits lipolysis. For lipid synthesis to occur there must be enhanced expression of the steroid regulatory element binding protein (SREBP)-1c transcription factor. Insulin inhibits lipid metabolism *via* reducing cAMP levels and by activating a cAMP specific phosphodiesterase in adipocytes (Pessin and Saltiel, 2000).

Other signal transduction proteins such as GRB2 (an adapter protein containing SH3 domains) can interact with IRS and can then associate with the son-of-sevenless (sos) which is a guanine nucleotide exchange factor. This then results in the activation of the MAPK pathway resulting in the production of mitogenic signals. Another substrate for the insulin receptor is SHC. Once phosphorylated, SHC will link with GRB2 and this linkage will lead to the activation of the MAPK pathway independently of IRS (Pessin and Saltiel, 2000).

### 1.7. Diabetes, its complications and the involvement of methylglyoxal

Glucose is an important fuel for the body and the hydrolysis of carbohydrates (e.g. starch or sucrose) in the small intestine results in the production of glucose. Glucose can be absorbed into the bloodstream. Increased levels of glucose circulating in the blood results in the stimulation of insulin release from the pancreatic β-cells.

Depending on the target tissue, insulin can have different effects on glucose metabolism. Insulin has two effects on glucose metabolism:

- Cells can take up glucose through a family of hexose transporters *via* facilitated diffusion. The most common glucose transporter, glucose transporter 4 (GLUT4) is located on the plasma membrane and is responsible for glucose uptake in the presence of insulin. The advantage of having this low-affinity, high-capacity glucose transporter on the plasma membrane of cells is that there is an instantaneous equilibrium between extracellular and intracellular glucose at the β-cell (Aizawa *et al.,* 1994). However, if insulin is not present, GLUT4 transporters remain in the cytoplasmic storage vesicles (Das, 1999) rather than being relocated to the plasma membrane and cannot therefore aid with the transport of glucose. When the levels of glucose in the blood fall and the insulin receptors are no longer occupied by the protein, then the GLUT4 transporters are recycled back into the cytoplasm of the cells (Das, 1999).
- When blood glucose levels rise, insulin is secreted from the pancreas. Glucose then enters the hepatocytes of the liver where insulin stimulates enzymes (e.g. glycogen synthase) resulting in the production of glycogen. When insulin is not present in the liver, glycogen synthesis no longer takes place and the enzymes that are important for the breakdown of glycogen are activated. However, when the glucose levels decrease below normal levels (hypoglycaemia), glucagon is released. Glucagon can also stimulate the breakdown of glycogen.

The inability of the body to control the blood glucose concentration causes hyperglycaemia and results in the development of diabetes.

Diabetes has reached epidemic properties and the World Health Organisation (WHO) have quantified the prevalence and the number of people that are affected by diabetes throughout the world. Table 1.5 shows the number of people who were affected by diabetes at the start of the new millennium as well as the number of people this disease is likely to affect in the future.

| Countries | Year 2000 | Year 2030 |
|---|---|---|
| Worldwide | 171,000,000 | 366,000,000 |
| UK | 1,765,000 | 2,668,000 |
| Europe | 33,332,000 | 47,973,000 |
| Africa | 7,020,000 | 18,234,000 |
| America | 33,016,000 | 66,812,000 |
| Eastern Mediterranean | 15,188,000 | 42,600,000 |
| South East Asia | 46,903,000 | 119,541,000 |
| Western Pacific | 35,771,000 | 71,050,100 |

**Table 1.5. The number of people potentially affected by diabetes in the future compared to those affected by the disease in the year 2000** (Wild *et al.,* 2004).

Table 1.5 shows that there were 171 million people diagnosed with diabetes worldwide in the year 2000 and it is thought that this number will rise to approximately 366 million by 2030 (Wild *et al.,* 2004).

Diabetes mellitus, simply known as diabetes, is fast becoming a common condition that is characterised by increased blood glucose concentrations (hyperglycaemia). Hyperglycaemia arises because the pancreatic β-cells are no longer producing insulin (type 1 diabetes) or they do not produce sufficient amounts of insulin to help glucose enter the cells (muscle, fat and liver cells) or that the insulin being produced by these cells does not work efficiently (insulin resistance) (type 2 diabetes) (Watkins, 1998). Elevated levels of glucose have been linked to the formation of the potentially toxic α-oxoaldehydes, such as MeG. Patients with diabetes often experience a number of symptoms and the following are just a few examples:

- Excessive urine production (polyuria)
- Increased thirst and increased fluid intake (polydipsia)
- Blurred vision
- Extreme fatigue
- Weight loss
- Slow wound healing

However, if the symptoms of diabetes are not well controlled, patients can go on to develop more serious conditions that are associated with the diabetes. These patients have an increased risk of developing serious microvascular

complications (e.g. retinopathy, nephropathy and neuropathy) and macrovascular damage (e.g. ischemic heart disease) (WHO, 2006).

The risk of cardiovascular morbidity in patients with type 2 diabetes is between 2- to 4-fold higher than the risk in non-diabetic individuals.

### 1.7.1. Type 1 diabetes

Type 1 diabetes is also known as insulin-dependent diabetes mellitus (IDDM). Approximately 5 - 15 % of all people with diabetes are diagnosed as having type 1 diabetes and it is therefore the least common of the two types. The onset of this type is usually rapid and appears before the age of 40. Type 1 diabetes is characterised by the loss of functioning β-cells resulting in insulin deficiency or simply due to the body being unable to produce insulin. The β-cells of the pancreas that are responsible for the production of insulin to control the glucose levels in the blood can be destroyed by the immune system through a process known as autoimmune attack.

Therefore, the destruction of the β-cells prevents the removal of glucose from the blood and results in elevated glucose concentrations (hyperglycaemia) and leads to the symptoms associated with diabetes (e.g. excessive thirst). Increased thirst occurs when the elevated concentrations of glucose in the blood cause an osmotic imbalance leading to reduced reabsorption of water by the kidneys and results in the frequent passing of urine. This can then lead to severe dehydration and hence increased thirst. When there is an elevated concentration of glucose in the blood, glucose will filter into the renal tubes; this then enters the urine and is the reason behind why the urine smells sweet. For energy, the cells are then made to burn fat causing the patient to lose weight and leaves ketones (the byproducts of fat metabolism) in the urine and on the breath. In the absence of insulin, proteins can also be metabolised for energy. Decreases in stored protein causes muscle wasting, weakness and weight loss. This autoimmune attack also leaves antibodies in the blood (Turkoski, 2006).

#### 1.7.1.1. The causes of type 1 diabetes

The destruction of the β-cells as a result of an autoimmune attack is the major factor considered to be involved in the development of type 1 diabetes. however, a number of other factors can also contribute to its pathogenesis (e.g. genetic predisposition, environmental factors and toxins).

***The genetic predisposition***

IDDM occurs in a genetically predisposed population. In individuals with this type of the disease, the main genetic susceptibility factor is the major histocompatibility complex (MHC) which is located on chromosome 6. There are two combinations of genes (haplotypes) that are thought to be important: $DR_4$-$DQ_8$ and $DR_3$-$DQ_2$. These combinations can be found in 90 % of children that have been diagnosed with this type. There is a third haplotype, $DR_{15}$-$DQ_6$ and this can be found in a small population (>1%) of children and it is therefore predicted that this haplotype is protective against the disease. The genotype that combines the two susceptibility haplotypes ($DR_4$-$DQ_8$-$DR_3$-$DQ_2$) is predicted to increase the probability of developing the disease. Children who develop this disease early in their lives have been shown to contain the $DR_4$-$DQ_8$-$DR_3$-$DQ_2$ genotype (Gillespie, 2006, Atkinson and Eisenbarth, 2001, Bresson and Von Herrath, 2004).

There are also more than 40 non-human leukocyte antigen (HLA) susceptibility loci that are considered to participate in the genetic predisposition of type 1 diabetes. These non-HLA susceptibility loci include: the insulin gene (*INS*); the polymorphic, cytotoxic T-lymphocyte-associated protein 4 (*CTLA4*) gene and the protein tyrosine phosphatase, non-receptor type 22 (lymphoid) (*PTPN22*) located on chromosomes 11p15, 2q33, 1p13, respectively. Of these 3 genes, the strongest link can be found on chromosome 11p15 where there are a variable number of tandem nucleotide repeats (VNTR) 5' of *INS*. The insulin promoter contains shorter forms of VNTR and these have been linked to the development of the disease, whilst longer forms of VNTR are associated with protection against the disease (Gillespie, 2006, Steck and Rewers, 2011). The *PTPN22* and *CTLA4* genes are responsible for preventing the spontaneous activation of T-cells and the modulation of the immune response, respectively (Steck and Rewers, 2011, Atkinson and Eisenbarth, 2001).

Following this, other genes have also been identified that are thought to contribute to the predisposition of the disease such as: interleukin 2 receptor, alpha (*IL2RA*); small ubiquitin-like modifier 4 (*SUMO4*) and interferon induced with helicase C domain 1 (*IFIH1*). Of these 3 genes, the *IL2RA* gene, located on chromosome 10p15, has been predicted to have a strong association with type 1 diabetes (Steck and Rewers, 2011).

More recently, a number of genome wide association studies (GWAS) have been carried out and the results have been published. The Wellcome Trust Case Control Consortium (WTCCC) carried out a GWAS in 2007 and as a result of this study were able to confirm the identification of those previously identified genes (MHC region, *INS*, *PTPN22*, *CTLA4*, *IL2RA* and *IFIH1*) as well as six novel type 1 diabetes susceptibility loci: 12q13, 12q24, 16p13, 4q27, 12p13 and 18p11. These type 1 diabetes susceptibility loci were also identified and confirmed in several other independent studies (Steck and Rewers, 2011).

***Environmental factors***

A number of environmental factors have been suggested to be involved in the pathogenesis of type 1 diabetes. These factors can behave as triggers as well as stimulators of β-cell destruction (Knip *et al.,* 2005). In genetically predisposed individuals these environmental factors can trigger or enhance the development of the autoimmune disease (Bresson and Von Herrath, 2004). Environmental factors that contribute to this type of diabetes can be separated into three groups:

*Viral infections*

Human enteroviruses like the Coxsackie B viruses (CVBs) are environmental factors that may trigger and/or enhance this autoimmune disease. The virus-mediated cell damage (fig. 1.12) of target organs results in a local immune response that leads to the generation of cytokines like type 1 (IFN-α and IFN-β) and type 2 (IFN-γ) interferons (IFNs). The production of these IFNs prevents the virus from replicating and encourages removal of the virus. Therefore, these IFNs and other proinflammatory cytokines are responsible for stimulating an immune response against the virus, however in genetically susceptible individuals, they can also initiate an autoimmune response *via* an immunological cross reactivity (molecular mimicry) or by the mobilisation of endogenous antigens. Both of these can lead to immune-mediated cell damage and the eventual development of the autoimmune disease in these individuals (Fairweather and Rose, 2002).

The damage of pancreatic β-cells or cardiac myocytes due to the presence of CVB (fig. 1.12) results in a local immune response with the production of the IFN-α and IFN-γ cytokines. The generation of these IFNs inhibits the

replication of the virus as well as facilitating the removal of the virus in those individuals that are resistant to the virus. However, in genetically susceptible individuals, these IFNs and along with other proinflammatory cytokines can also stimulate an autoimmune response against self-antigens specific to those cell types (e.g. pancreatic β-cells or cardiac myocytes) again causing immune-mediated cell damage resulting in the development of diabetes (Fairweather and Rose, 2002).

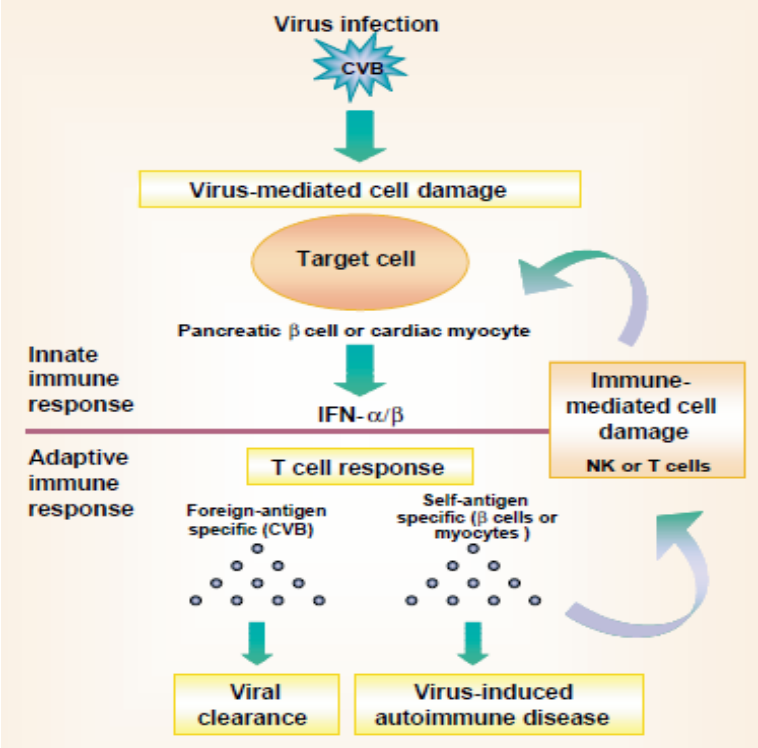


**Figure 1.12. Virus-induced autoimmune disease** (Fairweather and Rose, 2002).

The acute infection by CVB4 results in the development of diabetes. The direct effects of acute CVB4 on the insulin signalling pancreatic β-cells have been studied. It is known that the cytokines IFN-α and IFN-γ are responsible for preventing the β-cells from becoming infected by the virus. However, the production of these IFNs can be inhibited by the expression of suppressor of cytokine signalling 1 (SOCS-1). Due to the inhibition of the IFNs by SOCS-1, the pancreatic β-cells are exposed to virus. Once the cells have been infected by the virus, the cells are then exposed to the attack by natural killer (NK)

cells. NK cells are responsible for the destruction of these cells once they have become infected. The destruction of the pancreatic β-cells results in hyperglycaemia and diabetes. The β-cells are damaged through apoptosis occurring during the innate response as opposed to the T- and B-cells of the adaptive immune system. This suggests that the early innate immune response to CVB4 may be directly responsible for the development of diabetes (Fairweather and Rose, 2002).

*Early infant diet*

Milk is the most important food for young mammals and is a source of protein for adults. Towards the end of the 1990s, it was predicted that the consumption of the A1 variant found in some milk types could increase the risk of the development of type 1 diabetes. It is predicted that the early introduction of dairy products containing cow's milk into an infant's diet could potentially increase the probability of the infant developing type 1 diabetes later in their life (Wasmuth and Kolb, 2000, Kaminski *et al.,* 2007).

Milk is approximately 88% water and the remaining 12% is solid. The solids include milk fat, protein, lactose and minerals (Wasmuth and Kolb, 2000). Milk contains two major protein groups: casein and whey protein. Here we will be focusing on the casein protein group and will be paying close attention to beta-casein. Bovine milk consists of four caseins: alpha s1, alpha s2, beta and kappa (Kaminski *et al.,* 2007).

Both the A1 and A2 variants are the most common forms found in dairy cattle around the world. Holstein-Friesian dairy cattle are the most common cattle throughout the world. It is predicted that it is the A1 variant in the milk that contributes to the development of diabetes. Both the A1 and A2 variants are made up of 209 amino acids. The A1 variant has a histidine (His) amino acid residue at position 67 on the beta-casein chain, whereas the A2 variant has contains a proline (Pro) amino acid residue at the same position on the beta-casein chain (fig. 1.13) (Kaminski *et al.,* 2007).

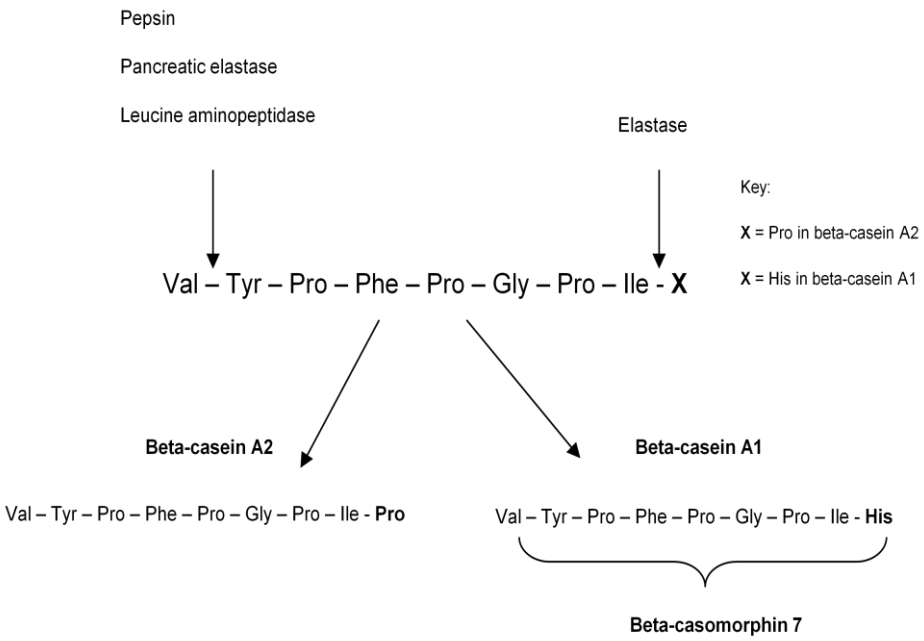


**Figure 1.13. A diagram showing the release of beta-casomorphin-7 (BCM-7) from the beta-casein variant A1 but not from the A2 variant** (Kaminski *et al.,* 2007).

It is predicted that by changing the amino acid residue at position 67 of the beta-casein chain from proline in the A2 variant to histidine in the A1 variant will facilitate the release of the bioactive peptide known as β-casemorphin-7 (BCM-7). The substitution of proline with histidine is due to a natural mutation occurring as a result of a single nucleotide polymorphism at codon 67 of the β-casein gene: CCT (A2, proline) → CAT (A1, histidine). Differences observed in the amino acid sequence predict that there is a conformational change in the secondary structure of the expressed protein (Kaminski *et al.,* 2007).

Beta-casomorphins are proteins that originate from the beta-casein protein. They consist of 4 – 11 amino acids in length and they all start with a tyrosine residue at position 60 of the amino acid chain.

| Beta-casomorphin (BCM) | Amino acid composition |
|---|---|
| | |
| Bovine BCM-4 | Tyr-Pro-Phe-Pro |
| Bovine BCM-5 | Tyr-Pro-Phe-Pro-Gly |
| Bovine BCM-6 | Tyr-Pro-Phe-Pro-Gly-Pro |
| Bovine BCM-7 | Tyr-Pro-Phe-Pro-Gly-Pro-Ile |
| Bovine BCM-8 | Tyr-Pro-Phe-Pro-Gly-Pro-Ile-Pro |
| Bovine BCM-11 | Tyr-Pro-Phe-Pro-Gly-Pro-Ile-Pro-Asn-Ser-Leu |
| | |
| Human BCM-7 | Tyr-Pro-Phe-Val-Glu-Pro-Ile |
| Human BCM-8 | Tyr-Pro-Phe-Val-Glu-Pro-Ile-Pro |

**Table 1.6. Groups of peptides that have been isolated from both bovine and human beta-casein** (Kaminski *et al.,* 2007).

Of these BCMs, bovine BCM-7 is of particular interest as it is predicted to have a role in the development of diabetes. In 1979, BCM-7 was first isolated as a peptide with an opioid function (i.e. a morphine-like activity) in the body. It is a bioactive peptide and *in vitro* it stimulates human lymphocyte T cell proliferation. BCM-7 corresponds for position 60 to position 67 of the bovine beta-casein amino acid sequence. However, human BCM-7 corresponds for positions 51 to position 57 of human beta-casein. Both bovine and human BCM-7 peptides are made up of 7 amino acids (Kaminski *et al.,* 2007).

They both have a Tyr-Pro-Phe sequence at the N-terminus as well as having opiate properties within or close to the BCM-7 amino acid sequence (Kaminski *et al.,* 2007). Bovine BCM-7 is considered to be fairly stable due to it containing three proline residues in its amino acid sequence.

It has been shown *in vitro* that BCM-7 is produced as a result of the gastrointestinal proteolytic digestion of β-casein A1 (but not the A2 variant) by pepsin, pancreatic elastase and leucine amino peptidase. Elastase is responsible for breaking the peptide bond between the Ile and His residues thus releasing the carboxyl-terminus of BCM-7. On the other hand, pepsin and leucine amino peptidase are responsible for the release of the amino acid terminus of the peptide.

A number of mechanisms have been proposed to help explain the potential risk of developing type 1 diabetes due to milk intake. However, these mechanisms are based on BCM-7. BCM-7 is released from the A1 variant *in vitro* and it is known to inhibit the proliferation of human intestinal lymphocytes. The behaviour of BCM-7 as an immune-suppressant can influence the development of gut-associated immune tolerance or inhibits defence mechanisms against enteroviruses (such as CVB), both of which are said to be involved in the development of type 1 diabetes (Kaminski *et al.,* 2007).

Another mechanism for the association of the exposure of cow's milk and autoimmune diabetes could be due to immunological cross reactivity between the proteins found in cow's milk and autoantigens of the β-cell. An alternative concept of cross reactivity between the proteins and β-cells has been developed, and proposes that infants who have been exposed to cow's milk formula early in their lives have elevated antibody titres to bovine insulin, a normal constituent of cow's milk. Therefore, this exposure to cow's milk at a young age can lead to immunisation rather than a normal tolerance to insulin, the only identified β-cell-specific autoantigen in type 1 diabetes (Wasmuth and Kolb, 2000).

***Toxins (e.g. N-nitroso derivatives)***

Nitrites (and indirectly nitrates) are commonly found in some foods. Nitrates are found in vegetables and both nitrates and nitrites are found in meat products (e.g. sausages). They are capable of reacting with amines and amides resulting in the formation of nitrosamines and nitrosamides. Nitrate can be reduced in the gut to nitrite and this is then converted into the *N*-nitroso compounds. There is a possible link between the consumption of nitrate containing compounds and the development of type 1 diabetes however, this is undergoing further investigation. If this is the case, the consumption of antioxidants (e.g. vitamin C and vitamin E) may protect the β-cells against damage caused by the *N*-nitroso compounds (Akerbolm and Knip, 1998).

### 1.7.1.2. The pathogenesis of type 1 diabetes

#### *Islet cell autoantibodies*

Type 1 diabetes is associated with a chronic autoimmune response against islet β-cell antigens. This autoimmunity begins in early life and the development of diabetes can occur several years later. There are three islet β-cell autoantigens and these are glutamic acid decarboxylase (GAD-65), insulin and the protein tyrosine phosphatase related molecules (islet-cell antigen-2, IA2) (Achenbach *et al.,* 2005). It has been predicted that GAD-65 is an important islet cell autoantigen and is localised to the synaptic-like microvesicles in the β-cells, but it is also expressed in all the other cells found in the islets of Langerhans as well as the testes, ovaries, thymus, stomach and the brain of mammals.

Insulin is also an autoantigen and it is the only known β-cell specific antigen that has been directly associated with this particular type of diabetes. IA-2 belongs to the protein tyrosine phosphatase (PTP) family and it is predicted to be another important autoantigen (Yoon and Jun, 2001). Autoantibodies to these islet β-cell antigens are important markers of preclinical type 1 diabetes (Naserke *et al.,* 1998). Autoantibodies are generated by the immune system where it cannot distinguish between “self” and “nonself” antigens. The immune system can normally recognise and ignore the cells of the body as well as being able to recognise and ignore substances in the environment that pose no threat to the body. However, the immune system must simultaneously be able to generate antibodies that are able to fight certain foreign substances that have been detected as a potential threat to the body. A problem arises when the immune system is switched on to self-antigens and as a consequence damages target tissues (Pihoker *et al.,* 2005).

There are several different types of autoantibodies and these are known as islet cell autoantibodies (ICAs). The relevant islet autoantibodies that have been identified so far are the GADA (the autoantibody to GAD-65), IAAs (insulin autoantibodies) and IA-2A (IA-2 autoantibodies). These autoantibodies are present prior to the development of diabetes and can be used as markers of the pre-clinical disease. After a series of enterovirus infections, islet cell associated antibodies are generated however; the diagnosis of diabetes may not be identified for a number of weeks, months or even years (Cabrera-Rode

*et al.,* 2005). The autoantibodies against the autoantigens GAD-65 and IA-2 have been identified as the main constituents of ICAs.

Early studies primarily carried out over a period of time in first-degree relatives demonstrated that ICAs can predict the likelihood of an individual developing type 1 diabetes prior to any hyperglycaemia arising (Pihoker *et al.,* 2005). Around 70 – 80 % of all newly diagnosed individuals with type 1 diabetes already have autoantibodies to GAD-65 and approximately the same number have autoantibodies to IA-2 (Notkins and Lernmark, 2001). Children that develop type 1 diabetes early in their lives (under the age of 10 years) usually demonstrate the initial signs of islet autoimmunity by the time they reach the age of 2 and they also have a high number of insulin autoantibodies. These children are then more likely to develop numerous islet autoantibodies eventually leading to the development of type 1 diabetes (Achenbach *et al.,* 2005). Some patients carry autoantibodies for only one of the major autoantigens, but others can react to all three autoantigens. A number of assays that have been carried out have shown that these autoantigen-specific antibodies can predict the likelihood of a person developing type 1 diabetes. However, these assays so far have been unsuccessful at identifying which of these autoantibodies is a better predictor of type 1 diabetes.

***T-cell mediated destruction of β-cells***

Type 1 diabetes is mainly a T-cell mediated autoimmune disease which is characterised by the destruction of the insulin-producing pancreatic β-cells by T-cells (Gillespie, 2006, Paronen *et al.,* 2000).

Studies have been carried out on samples taken from the pancreatic biopsies obtained from pre-diabetic individuals and patients diagnosed with recent-onset type 1 diabetes and it has shown that there are several reducing stages in β-cell volume in all individuals. Half of these patients studied were also diagnosed with an inflamed pancreas (insulitis). The samples taken from the patients diagnosed with insulitis showed that the infiltrate contained $CD8^+$ (cytotoxic) and $CD4^+$ (helper) T-cells, B-lymphocytes and macrophages. Even though the infiltrate contained all these, the majority was made up of $CD8^+$ T-cells. This therefore suggests a possible mechanism in which the β-cells are destroyed.

Fas was found on the β-cells located within the inflamed islets whilst the infiltrating mononuclear cells in the islets express Fas ligand. This suggests that there is an interaction between the Fas located on the β-cells and the Fas ligand in the infiltrating cells that may result in β-cell destruction by apoptosis leading to the development of type 1 diabetes (Atkinson and Eisenbarth, 2001). Studies carried out on the pancreas of animals that have died as a result of recent-onset type 1 diabetes have identified auto-aggressive T-cells. Aggressive β-cell destruction can result in the development of the disease within a few months in children, however in other patients the process can continue for many years before the disease presents itself (Knip *et al.,* 2005). It is not known how these auto-aggressive T-cells enter the pancreas and the islets, but blocking this process and thus avoiding the destruction of the β-cells could be important for the development of future therapies for the treatment of this disease (Bresson and Von Herrath, 2004).

#### 1.7.1.3. The treatment and prevention of type 1 diabetes

If left untreated, chronic exposure of bodily tissue for long periods of time can result in the severe tissue damage. This results in reduced blood supply to vital organs leading to the increased risk of heart attack, kidney failure, stroke and blindness. Reduced blood supply can also result in impaired wound healing, infections and even gangrene (Turkoski, 2006). Although this is happening, the body is still able to respond to insulin, so with the daily intravenous administration of insulin, the symptoms disappear (Whelan, 2007). As well as injecting insulin, oral hyperglycaemic drugs can also be added for maintaining constant blood glucose concentrations.

Individuals whose parents are diabetic can undergo tests to measure the amount of autoantibodies in their body and this will predict the likelihood of them developing the disease and thus if it is caught in time the future development of the disease can be prevented.

### 1.7.2. Type 2 diabetes

Type 2 diabetes is also known as non-insulin dependent diabetes mellitus (NIDDM). Approximately 85 – 95 % of diabetic patients have been diagnosed with this type and it is therefore the most prevalent type of the disease. This type of diabetes usually appears in individuals over the age of 40 and is associated with obesity, however more and more children are being

diagnosed with this type of the disease. The onset of type 2 diabetes is gradual and the diagnosis can often be missed (Turkoski, 2006, Rignell-Hydbom *et al.,* 2007, Whelan, 2007).

#### 1.7.2.1. The causes of type 2 diabetes

Type 2 diabetes is a heterogenous disorder that is caused by a combination of genetic and environmental factors and the result is an effect on glucose metabolism (Gerich, 1999).

***The genetic predisposition***

Like type 1 diabetes, genetic factors can also contribute to the pathogenesis of type 2 diabetes. The inherited defects result in the more common forms of insulin resistance (Fujimoto, 2000), for example, if one parent suffers with this type of diabetes, the likelihood of this person's offspring developing the disease has been calculated to be approximately 38 – 40 %. Whereas, if both parents suffer with the disease, the prevalence of the offspring developing the disease is approximately 60 – 70 % by the time they reach the age of 60 (Stumvoll *et al.,* 2005, Ahlqvist *et al.,* 2011).

The search for diabetes susceptibility genes began many years ago. During this time, many linkage scans and candidate gene studies for type 2 diabetes have been carried out (McCarthy and Zeggini, 2009). Although a large number of linkage studies of type 2 diabetes have been carried, only 2 genes have been identified: calpain 10 (*CAPN10*) and transcription factor 7-like 2 (*TCF7L2*). Of these two genes, the *TCF7L2* gene is thought to have a strong association with this type of the disease. However, the mechanism through which these genes affect diabetes remains unknown (Ahlqvist *et al.,* 2011, McCarthy and Zeggini, 2009). Candidate gene studies have identified 6 genes that are predicted to be associated with the development of type 2 diabetes: peroxisome proliferator-activated receptor gamma (*PPARG*), insulin receptor substrate I (*IRS1*), potassium inwardly-rectifying channel, subfamily J, member 11 (*KCNJ11*), Wolfram syndrome I (wolframin) (*WFS1*), HNF1 homeobox A (*HNF1A*) and HNF1 homeobox B (*HNF1B*) (Ahlqvist *et al.,* 2011, McCarthy and Zeggini, 2009).

More recently, GWAS have been proven more successful at identifying type 2 diabetes susceptibility genes. In 2007, the results of several GWAS were published and this led to a greater understanding of the genetics underlying

the development of type 2 diabetes. In these studies the DNA of patients diagnosed with this type of the disease (cases) was compared with the DNA of healthy individuals (controls). The first GWAS of type 2 diabetes was carried out in France and consisted of 661 cases and 614 controls. The results of this study identified two new diabetes susceptibility genes: hematopoietically expressed homeobox (*HHEX*) and solute carrier family 30 (zinc transporter), member 8 (*SLC30A8*). Following the results of this study, a further four studies were carried out in European populations with similar case-control setups.

The WTCCC carried out a study in the UK and it consisted of 1924 cases and 2938 controls; the Diabetes Genetics Initiative (DGI) study consisted of 1464 cases and 1467 controls from Sweden and Finland; Finland-United States Investigation of NIDDM (FUSION) genetics study was carried out in Finland and consisted of 1161 cases and 1174 control and finally, a study carried out by Steinthorsdottir et al was carried out in Iceland and consisted of 1399 cases and 5275 controls (Ahlqvist *et al.,* 2011, McCarthy and Zeggini, 2009, Wheeler and Barroso, 2011, Steinthorsdottir *et al.,* 2007). Before the results were released for publication, the WTCCC, DGI and FUSION shared their results. As a result of these studies, two new loci were identified – cyclin-dependent kinase inhibitor 2A (melanoma, p16, inhibits CDK4)/cyclin-dependent kinase inhibitor 2B (p15, inhibits CDK4) (*CDKN2A/CDKN2B*) and insulin-like growth factor 2 mRNA binding protein 2 (*IGF2BP2*) as well as confirming the identity of the previously identified loci.

Also, each of the four studies identified a new type 2 diabetes locus: CDK5 regulatory subunit associated protein 1-like 1 (*CDKAL1*) (Ahlqvist *et al.,* 2011, McCarthy and Zeggini, 2009, Wheeler and Barroso, 2011). GWAS have also been carried out in non-European populations and have identified the potassium voltage-gated channel, KQT-like subfamily, member 1 (*KCNQ1*) as a new type 2 diabetes susceptibility gene and have also shown that this gene is expressed in the pancreas. Studies carried out within an Asian population have identified a further 2 diabetes loci: protein tyrosine phosphatase, receptor type D (*PTPRD*) and serine racemase (*SRR*) (Ahlqvist *et al.,* 2011).

Although these GWAS have been able to identify some type 2 susceptibility genes, there are still some limitations. Therefore, to overcome these limitations, genome wide association (GWA) meta-analyses have been carried out. GWA meta-analyses have been carried out to improve the ability to

identify genuine type 2 diabetes susceptibility genes (McCarthy and Zeggini, 2009). Researchers from the WTCCC, DGI and FUSION came together and formed the Diabetes Genetics, Replication and Meta-Analysis (DIAGRAM) Consortium to carry out the first GWA meta-analysis. This GWA meta-analysis was carried out within a European population and consisted of 4549 cases and 5579 controls. As a result of this, six novel type 2 diabetes susceptibility genes were identified: JAZF zinc finger 1 (*JAZF1*), cell division cycle 123 homolog-calcium/calmodulin-dependent protein kinase ID (*CDC123-CAMK1D*), tetraspanin 8-leucine-rich repeat-containing G protein-coupled receptor 5 (*TSPAN8-LGR5*), thyroid adenoma associated (*THADA*), ADAM metallopeptidase with thrombospondin type 1 motif 9 (*ADAMTS9*) and notch 2 (*NOTCH2*) (Ahlqvist *et al.,* 2011, McCarthy and Zeggini, 2009, Wheeler and Barroso, 2011).

In June 2010, a number of other GWAS were added to the DIAGRAM consortium thus leading to the formation of DIAGRAM plus. As a result of the formation of DIAGRAM plus, a further 12 novel loci were identified: B-cell CLL/lymphoma 11A (zinc finger protein) (*BCL11A*); zinc finger, BED-type containing 3 (*ZBED3*); Kruppel-like factor 14 (*KLF14*); dual specificity phosphatase 9 (*DUSP9*); high mobility group AT-hook 2 (*HMGA2*); tumour protein p53 inducible muclear protein 1 (*TP53INP1*); *KCNQ1*; transducin-like enhancer of split 4 (*TLE4*); protein regulator of cytokinesis 1 (*PRC1*); coiled-coil-helix-coiled-coil-helix domain containing 9 (*CHCHD9*); zinc finger, AN1-type domain 6 (*ZFAND6*) and ArfGAP with RhoGAP domain, ankyrin repeat and PH domain 1 (*ARAP1*) (Ahlqvist *et al.,* 2011).

Therefore it can be concluded that most of the individual type 2 diabetes susceptibility genes have been indentified recently as a result of GWAS and GWA meta-analyses. The majority of the genes identified code for proteins that are involved in β-cell function (Petrie *et al.,* 2011). However, a few genes have been implicated in impaired β-cell function (*IGF2BP2, SLC30A8* and *CDKN2A/CDKN2B*), and impaired glucose-stimulated insulin release (*JAZF1, CDC123-CAMK1D* and *TSPAN8*) (Ahlqvist *et al.,* 2011).

***Environmental factors***

There are a number of environmental factors that can affect cells found within the islet of Langerhans in the pancreas either directly or indirectly. These

factors can then potentially lead to the development and/or progression of type 2 diabetes (Marchetti *et al.,* 2006).

Many lifestyle factors are known to be important in the development of this type of diabetes. These factors include reduced physical activity and excessive food consumption both of which result in obesity, as well as other factors such as ageing, high levels of free fatty acids (FFAs) and some factors that individuals are exposed to during foetal and neonatal life.

Excessive food consumption along with reduced physical activity throughout the world has resulted in increased prevalence of obesity and diabetes. Approximately between 60 and 90% of patients with type 2 diabetes are also suffering with obesity (Kasuga, 2006). The development of obesity due to reduced physical activity is the most important factor that is involved in the development of insulin resistance (Stumvoll *et al.,* 2005).

Obese patients have increased β-cell mass as a result of increased insulin resistance (Sweene, 1992). If insulin resistance is present along with β-cell dysfunction then glucose intolerance will result.

Obese patients have elevated levels of FFAs circulating in the blood. These high levels of FFAs result in the inhibition of insulin-stimulated glucose uptake therefore leading to hyperglycaemia and eventually diabetes. By reducing the levels of FFAs that are circulating in the bloodstream of obese subjects, will in turn reduce insulin resistance (Boden *et al.,* 1994, Qatanani and Lazar, 2007).

Obesity is also linked with a systemic chronic inflammatory response and not just as a result of lipid accumulation in the liver and muscle of some individuals. This inflammatory response is characterised by the release of cytokines from the adipose tissue as well as the activation of the inflammatory signalling pathways. As these cytokines are released from the adipose tissue, they are also known as “adipokines”. The adipokines that are produced include – leptin, adiponectin, resistin, tumor necrosis factor-α (TNFα) and interleukin-6 (IL-6) (Savage *et al.,* 2007). Of these adipokines, TNFα and IL-6 are the most widely studied. They are biomarkers of inflammation and can be found at increased concentrations in individuals that are obese and resistant to insulin. As they are biomarkers, they can be used to predict the risk of obese and insulin resistant people going on to develop type 2 diabetes in the future. Obesity can also be characterised by the accumulation of

macrophages in adipose tissue and these macrophages can produce some of the previously described adipokines (Savage *et al.,* 2007).

During this inflammatory response, a number of serine/threonine kinases become activated. Of these serine/threonine kinases, JUN kinase-1 (JNK1) is considered to be important and is activated by the adipokine, TNFα. Once activated by TNFα, JNK1 can phosphorylate IRS-1 resulting in impaired insulin signalling. This may help to explain why obese individuals have demonstrated increased JNK1 activity. If this is the case, the removal of the *JNK1* gene would result in increased insulin sensitivity in these obese and insulin resistant individuals. The TNF-induced insulin resistance mediator, IKKβ can reduce insulin signalling, however treatment with high doses of aspirin can counteract this and improve insulin signalling. IKKβ can affect insulin signalling either directly or indirectly. This mediator can directly affect insulin signalling *via* the phosphorylation of IRS-1 located on the inhibitory serine residues but it can also indirectly affect insulin signalling by activating NK-κB *via* the phosphorylation of its inhibitor IκB. NK-κB is a transcription factor that is responsible for the stimulation of TNFα and IL-6. Other inflammatory mediators, known as suppressor of cytokine signalling (SOCS) are considered to be involved in obesity-induced insulin resistance. Of this family of proteins, SOCS-3 has an important role in the association between obesity, inflammation and insulin resistance (Savage *et al.,* 2007, Nandi *et al.,* 2004, Qatanani and Lazar, 2007).

Along with obesity, ageing can also contribute to the development of insulin resistance. Ageing is also characterised by the build of lipid in the cells of the liver and muscle of elderly subjects (Savage *et al.,* 2007, Qatanani and Lazar, 2007).

There is a strong association between individuals that were born at a low birth weight and the risk of developing type 2 diabetes later in life (Ozanne and Hales, 2002). This association has been observed in a diverse range of ethnic populations throughout the world (Warner and Ozanne, 2010).

The environmental factors a foetus is exposed to during the early stages of life can play a crucial role in the health and quality of life of individuals in adulthood. Changes in nutrition or a disturbed oxygen supply will be dangerous for the foetus in terms of it will not only alter the growth pattern but they may also contribute to the development of metabolic syndrome later in

life (Warner and Ozanne, 2010). A significant amount of work has been carried out using animal models to study and understand the mechanisms that contribute to the pathogenesis of disease as a result of these factors but not many have been carried out in humans. The mechanisms indentified as a result of the animal studies have shown some similarities to those that may also occur in humans. These mechanisms include permanent structural changes, permanent changes in gene expression and mitochondrial dysfunction (Warner and Ozanne, 2010).

*Permanent structural changes*

The early stages of life are vital for the development of the pancreas because by the time an individual reaches the age of 1, they will have already formed approximately half of their adult pancreas. Once adulthood has been reached, pancreatic development decreases dramatically. Therefore any changes that occur during the early stages can inhibit progenitor cell proliferation and/or differentiation as well as affecting the development of the pancreas (Warner and Ozanne, 2010).

*Permanent changes in gene expression*

Insulin is an important component that is required during early life development. Therefore any changes in protein expression that occur downstream of the insulin receptor can alter insulin signalling. The inhibition of insulin stimulated glucose uptake by adipose tissue of rats may be a result of reduced association between the catalytic subunit, p110β with the regulatory subunit p85 and this was linked with the inhibition of PI3K activity. Individuals that were born with a low birth weight have showed reduced expression of GLUT4, IRS-1, p110β and p85 and all of these may contribute to reduced foetal development. The inhibition of insulin-stimulated glucose uptake by the skeletal muscle of rats may be due to the inhibition of PKCζ expression. Healthy subjects that were born with a low birth weight have reduced expression of GLUT4, PKCζ as well as low expression of the two subunits of PI3K, p110β and p85 in their skeletal muscle. These healthy individuals with low birth weights were able to tolerate glucose, they had similar weights and their insulin concentrations were similar when compared to healthy individuals born with a normal birth weight. It can therefore be concluded that the reduced expression of the insulin signalling proteins mentioned above can occur prior to the development of the disease (Warner and Ozanne, 2010).

*Mitochondrial dysfunction*

Mitochondria play a significant role in both normal and disease processes. The mitochondria are not only responsible for ATP production but they also generate reactive oxygen species (ROS) which can be detrimental for the cells. Mitochondrial dysfunction is associated with oxidative stress and an early exposure to oxidative stress can have an effect on many of the tissues in the body, particularly the pancreas. So that the pancreas can maintain glucose-stimulated insulin secretion, the cells require a lot of energy in the form of ATP. The β-cells contain low levels of antioxidant enzymes and as a result, when there is mitochondrial dysfunction or increased oxidative stress there will be a severe impact on the cells due to the lack of protection. Mitochondrial dysfunction can also occur in the liver and skeletal muscle. In the liver, the oxidation of pyruvate is decreased and this can result in increased glucose release whereas in skeletal muscle, the generation of ATP is significantly reduced thus resulting in decreased GLUT4 translocation and therefore inhibition of glucose uptake into the tissue. Both of these will result in elevated glucose concentrations that are typically associated with type 2 diabetes (Warner and Ozanne, 2010).

### 1.7.2.2. The pathogenesis of type 2 diabetes

The pathogenesis of type 2 diabetes is complex and in the majority of cases is due to β-cell dysfunction and insulin sensitivity. Both β-cell dysfunction and insulin sensitivity result in increased glucose release from the liver and the kidney as well as inhibiting the removal of glucose from the bloodstream and therefore leading to hyperglycaemia.

Type 2 diabetes develops when the β-cells in the islets of Langerhans are unable to produce enough insulin to keep up with the metabolic demand (hyperglycaemia). Type 2 diabetes can arise due to insulin resistance with slight β-cell dysfunction or due to β-cell dysfunction with slight insulin resistance (Fujimoto, 2000). Obesity has been predicted to cause insulin resistance and can therefore be considered as a factor that can lead to the pathogenesis of this type of diabetes. Randle et al (1963) were the first to suggest a relationship between the build up of triglycerides and insulin resistance when he described the glucose-fatty acid cycle (Randle *et al.,* 1963, Gordon, 1964, Frayn, 2003).

### *Insulin resistance*

Insulin resistance is how type 2 diabetes develops and can be present for many years and therefore precedes the development of diabetes (Fujimoto, 2000). It is predicted that the blood glucose and insulin levels are within their normal ranges for many years. However, the presence of genetic (inherited) and environmental (e.g. obesity) factors can lead to the development of insulin resistance. A large proportion of patients who are known to be insulin resistant are still able to produce enough insulin to maintain normal blood glucose concentrations and are therefore not considered to be hyperglycaemic (Goldstein, 2002). Insulin is necessary for the uptake of glucose by both muscle and adipose tissue to maintain normoglycaemia. As insulin resistance develops, these cells can no longer take up glucose from the bloodstream as efficiently and the pancreatic β-cells compensate by secreting more insulin. This then leads to high levels of insulin in the blood and this is known as hyperinsulinemia. As long as there is enough insulin to overcome this resistance then the blood glucose concentrations remain normal. Over time the pancreatic β-cells become “exhausted” and will eventually tire. Once tired, the β-cells are no longer able to keep up with the demand of insulin secretion that is required for the maintenance of normal blood glucose concentrations. Therefore, blood glucose levels rise, initially after meals and then eventually leading to impaired glucose tolerance resulting in diabetes (Goldstein, 2002, Turkoski, 2006, Kasuga, 2006, Renstrom *et al.,* 2007).

### *Impaired β-cell function*

The development of β-cell function that is associated with the development of type 2 diabetes occurs well in advance of the symptoms of hyperglycaemia. Therefore, β-cell dysfunction may occur several years before the individual is diagnosed with the disease. As the development of type 2 diabetes progresses, there is a gradual loss of β-cell function.

By the time an individual is diagnosed with this type of diabetes, approximately only 50% of β-cells are functioning efficiently (Goldstein, 2002).

Numerous mechanisms have been suggested to be involved in the development of β-cell dysfunction associated with type 2 diabetes:

- β-cell exhaustion due to the increased release of insulin as a result of insulin resistance
    - Under normal conditions, the secretory function of the β-cell increases due to insulin resistance. The increased requirement for the production and secretion of insulin suggests that over a long periods of time, the β-cells will tire and are more likely to fail (Kahn, 2001)
- Increases in glucose leads to the desensitisation of the β-cells
    - Hyperglycaemia can lead to the generation of high levels of reactive oxygen species (ROS) in the β-cells. The generation of these ROS can damage the cellular components and can therefore impair insulin secretion. ROS can stimulate NFκB activity and it is the stimulation of this that can cause β-cell apoptosis (Stumvoll *et al.,* 2005, Bonora, 2008). As a result of impaired insulin secretion, increased glucose concentrations remain in the blood, and it is this high glucose concentration that leads to a decrease in the expression of the insulin and PDX-1 genes. The PDX-1 gene is responsible for β-cell replication.
- Lipotoxicity
    - Excessive central fat is usually a predictor of type 2 diabetes. Both obese and non-diabetic and diabetic patients usually have increased non-esterified fatty acids (NEFA) concentrations due to enhanced adipocyte lipolysis. Fatty acids cause increased insulin secretion; however, after 24 hours these fatty acids can inhibit insulin secretion. When glucose is present, there is a build up of long chain acyl coenzyme A and fatty acid oxidation is inhibited in the β-cell. Long chain acyl coenzyme A can inhibit the insulin secretion process by opening the potassium channels of the β-cells. Another possible mechanism involves the enhanced expression of the uncoupling protein-2 which causes decreased ATP formation and therefore inhibits insulin secretion (Stumvoll *et al.,* 2005). Also, fatty acids may cause β-cell dysfunction through altering the $[Ca^{2+}]_i$ signal and

generating ceramide which induces apoptosis (Chakravarthy and Semenkovich, 2007).

- Reduced β-cell mass
    - Decreases in β-cell mass might be as a result of apoptosis due to changes in metabolic state where there are increases in the levels of glucose and NEFAs. Another possibility could be due to the accumulation of islet amyloid resulting in the progressive decline in insulin secretion and glucose tolerance (Kahn, 2001).

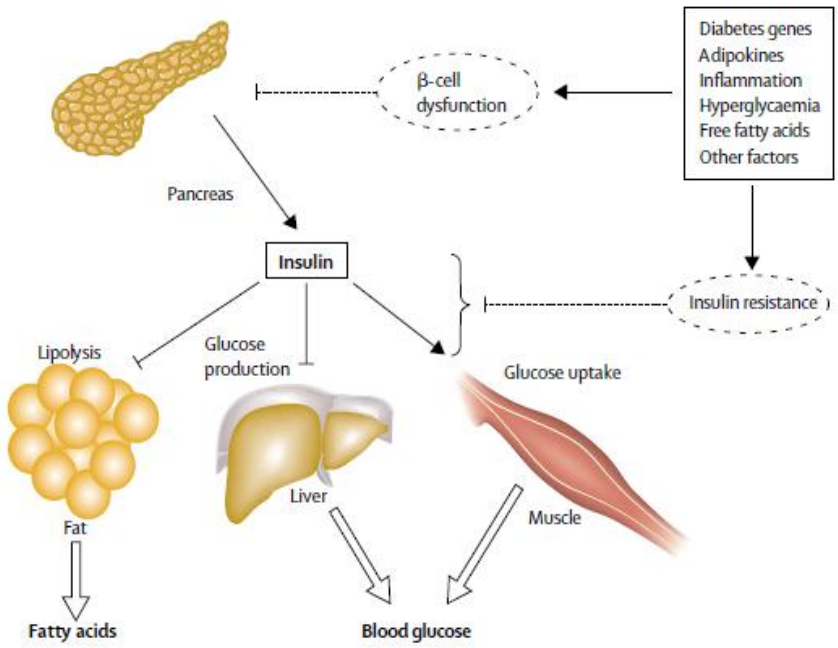


**Figure 1.14. The pathophysiology of hyperglycaemia in type 2 diabetes** (Stumvoll *et al.,* 2005).

Figure 1.14 shows the pathophysiology of hyperglycaemia in type 2 diabetes. The secretion of insulin from the pancreas usually results in the inhibition of glucose production by the liver and therefore enhances glucose uptake from the bloodstream by skeletal muscle. The release of insulin from the β-cell can act to suppress fatty acid release from adipose tissue.

The inhibition of insulin secretion will lead to the inhibition of insulin signalling in the target tissues. Insulin resistance pathways can affect insulin action in each of the major target tissues resulting in hyperglycaemia and increased circulation of fatty acids (Stumvoll *et al.,* 2005). There is a substantial amount of evidence suggesting that these abnormalities exist in most individuals prior to the development of diabetes (Weyer *et al.,* 1999). If left untreated, type 2 diabetes can causes similar problems to those observed if type 1 diabetes remains untreated (e.g. retinopathy, neuropathy, end-stage renal disease and cardiovascular problems) (Barnett, 2006). The likelihood of developing these conditions is particularly high in individuals with this type of diabetes because insulin resistance can develop over a number of years and can often go undiagnosed until it is too late and extensive damage has already occurred.

#### 1.7.2.3. The treatment and prevention of type 2 diabetes

If this type of diabetes is diagnosed in the early stages, it can be controlled by diet, exercise and weight loss, but more people are requiring the need for insulin-sensitising drugs, such as metformin, when the lifestyle changes no longer control the symptoms. However, the disease can progress and many people then go on to require intravenous insulin administration due to β-cell failure (Turkoski, 2006, Rignell-Hydbom *et al.,* 2007, Frayn, 2003, Whelan, 2007).

### 1.7.3. Type 1.5 diabetes

Some people with diabetes have symptoms that are characteristic of type 1, thus suggesting the need for the injection of insulin as well as having the symptoms that are characteristic of type 2 diabetes suggesting that a change in diet along with regular exercise would be sufficient to maintain normal blood glucose concentrations. More and more people are visiting their doctors exhibiting symptoms that are somewhere between type 1 and type 2 diabetes. Individuals that have symptoms of both types of diabetes are said to have type 1.5 diabetes (Donath and Ehses, 2006).

Some patients are being diagnosed with type 1 and type 2 diabetes simultaneously and this helps to explain why type 1.5 diabetes is also known as “double diabetes”. In the majority of cases of people with double diabetes, they are initially diagnosed with type 1 diabetes but then go on to develop the symptoms associated with type 2 diabetes. It has been proposed that both

type 1 and type 2 diabetes are the same disease and the only difference being the rates in which the disease progresses. It has also been suggested that all cases of diabetes are triggered with weight gain.

It is this gaining of weight that causes the body to develop a resistance to insulin and therefore the pancreatic β-cells are required to work harder to increase insulin release (hyperinsulinemia) and therefore the β-cells are more exposed to autoimmune attack. The exposure of β-cells to autoimmune attack can result in the destruction of the insulin producing cells thus preventing insulin from being released and eventually leading to the need for the intravenous administration of insulin. Patients who suffer with double diabetes are likely to have some of the complications that are linked with both types of diabetes. For example, an individual diagnosed with double diabetes can have small blood vessel damage (retina and kidney) which is associated with type 1 diabetes as well as the cardiovascular disease and elevated levels of lipids in the blood which are associated with type 2 diabetes. However, the progression from type 1 to type 2 diabetes occurs at different rates and this is probably due to the difference in immune response (Whelan, 2007).

### 1.7.4. Advanced glycation end-products and the pathogenesis of diabetes

Alterations in insulin action can lead to the development of diabetes (Jia et al., 2006). All types of diabetes are primarily characterised by chronic hyperglycaemia and the development of microvascular conditions, such as blindness, end-stage renal disease (ESRD), retinopathy and neuropathy as well as potentially fatal macrovascular complications, such as myocardial infarction and stroke (Brownlee, 2001, Peppa *et al.,* 2003). These complications arise due to protein alterations that result in the irreversible damage of tissues (Vinson and Howard, 1996).

The condensation reaction that occurs between a reducing sugar and the amino acids of a protein is not enzymatically catalysed, therefore this reaction is known as non-enzymatic glycosylation. The French chemist, Louis Camille Maillard studied this condensation reaction extensively hence why this reaction is also known as the Maillard reaction (Vinson and Howard, 1996, Turk, 2010). This process begins with the covalent interaction between the carbonyl groups (aldehyde or ketone) of a reducing sugar (e.g. glucose) with the free amino group of a protein resulting in the formation of an unstable

Schiff base (aldimine) (Singh *et al.,* 2001, Riboulet-Chavey *et al.,* 2006, Ahmed and Thornalley, 2007, Tan *et al.,* 2008). During Schiff base formation, the aldehydic double bond (C=O) of the reducing sugar is converted to a C=N double bond with the free amino group of the protein. The formation of the Schiff base is fast and reversible.

The Schiff bases then either dissociate (Garlick and Mazer, 1983) or undergo spontaneous rearrangements (Amadori products) *via* an intermediate, open chain enol form (Ulrich and Cerami, 2001) leading to the formation of a more stable 1-amino-2-deoxy-2-ketose (ketoamine) compound known as Amadori products (Thornalley *et al.,* 1999, Singh *et al.,* 2001, Riboulet-Chavey *et al.,* 2006, Ahmed and Thornalley, 2007). For example, when the reducing sugar is glucose, the Amadori product is commonly known as fructosamines (Zhang *et al.,* 2009).

There is an intermediate stage during the Maillard reaction which is characterised by the generation of a number of secondary products. The sugar part of an early glycation product undergoes a number of chemical reactions leading to the production of reactive α-dicarbonyl compounds, such as MeG (Yim *et al.,* 2001, Saraiva *et al.,* 2006). The production of these reactive α-dicarbonyl compounds can damage target cells throughout the body thus contributing to the complications associated with diabetes.

The reactive α-dicarbonyl compound is of particular interest as it can be found in all biological systems and healthy individuals have a MeG plasma concentration of 1.4 μM. Interestingly, the MeG plasma concentration in individuals that have been diagnosed with type 1 diabetes is 5- to 6-fold higher whereas, the MeG plasma concentration in individuals with type 2 diabetes is 2- to 3-fold higher than the concentrations observed in healthy subjects (Jia *et al.,* 2006, Wang *et al.,* 2007, Han *et al.,* 2009). Therefore both hyperglycaemia and elevated MeG plasma concentrations as a result of changes in glucose metabolism are considered to be associated with the microvascular and macrovascular symptoms of diabetes (Han *et al.,* 2007, Hsieh and Chan, 2009).

MeG is a potent glycating agent because it is able to modify proteins. MeG can modify proteins within the cells, especially those that are involved in the regulation of gene transcription. However, it can also react with the free amino groups of proteins circulating in the blood (e.g. albumin) resulting in the

formation of irreversible AGEs (Mostafa *et al.,* 2007, Thornalley, 2005, Brownlee, 2005, Brownlee, 2001).

Of all the amino acid residues that can be found in proteins, MeG favours and reacts readily with the arginine, lysine (and cysteine) residues of circulating proteins.

When MeG reacts with free arginine residues of the protein, hydroimidazolone adducts are formed, whereas when it reacts with free lysine residues of the protein, carboxyethyl-lysine (CEL) and the MeG-lysine dimer (MOLD) are formed. The most common AGEs that are found in the plasma are hydroimidazolones (Turk, 2010). The protein insulin contains an arginine and lysine residue on its B-chain at positions 22 and 29, respectively. In the presence of elevated concentrations of glucose again MeG will react with both of these residues resulting in the formation of irreversible AGEs at these sites. The glycation of these two residues on the B-chain of insulin can significantly alter the biological function of the protein by inhibiting insulin signalling thus indicating a potential role for the involvement of MeG in the development of insulin resistance and eventually diabetes (Jia *et al.,* 2006). The extent of modification of the protein increases as the concentration of MeG in the blood increases.

Modified proteins that are circulating in the blood can bind to and activate the AGE receptors on endothelial cells and macrophages resulting in the release of inflammatory cytokines, growth factors as well as ROS. The production of these may be implicated in the development of macrovascular complications (Brownlee, 2005). MeG can also irreversible modify lipids and genes over a period of time as has been implicated in cellular mutagenesis, a number of cancers, ageing, damage to blood vessels as well as some of the complications associated with diabetes.

The formation of irreversible AGEs as a consequence of the reaction between MeG reacting and the free amino groups of proteins is only one of the many possible mechanisms that can lead to the complications associated with diabetes. Brownlee (2005) predicted that the activation of a combination of four pathways including the polyol pathway, increased intracellular AGE formation, PKC and the hexosamine pathway can result in the tissue damage associated with elevated intracellular concentrations of glucose. He predicted that when the concentration of glucose increases inside the cells of target

tissues, the production of ROS by the mitochondria increases. The increased production of ROS can then cause strand breaks in the DNA thus resulting in the activation of poly(ADP-ribose) polymerase (PARP). Glyceraldehyde 3-phosphate dehydrogenase (GAPDH) is modified once PARP becomes activated and therefore reduces its activity. Finally, this inhibition of GAPDH activity causes the activation of the polyol pathway, increases intracellular production of AGEs, activates PKC and NF-κB as well as activating the hexosamine pathway (Brownlee, 2005).

### 1.8. Hypothesis, aims and experimental strategy

#### 1.8.1. The bacterial metabolic toxin hypothesis

Lactose sensitivity and IBS are common reasons for referrals to gastroenterologists. Symptoms associated with these conditions include: flatulence, abdominal pain, diarrhoea or constipation, fatigue, muscle and joint pain, severe headaches, and heart palpitations just to name a few (Matthews and Campbell, 2000, Campbell and Matthews, 2005, Matthews *et al.,* 2005, Waud *et al.,* 2008, Campbell *et al.,* 2005).

Carbohydrates (e.g. lactose and glucose) that are not broken down and absorbed by the small intestine are passed to the large intestine. The large intestine contains approximately $10^{14}$ individual bacteria representing over 1000 different species (Qin *et al.,* 2010). There is very little oxygen in the large intestine (< 1 μM) and because of this more than 90% of the bacteria found here are anaerobes (approximately 25% are *Bifidobacter* and 75% are other anaerobes). So that ATP can be made *via* glycolysis, the bacteria need to remove hydrogen from the carbohydrates in the form of hydrogen gas and through a wide range of small organic metabolites such as MeG, diols, alcholols, aldehydes, ketones and acids. Once produced these get absorbed into the blood and can go on to effect ion channels in skeletal and cardiac muscle, nerves, cells of the immune system, the liver and pancreas. It is proposed that the production of these gases and metabolites are what produce the symptoms that are associated with lactose sensitivity and IBS. It is also thought that this mechanism may play a significant role in the development of diabetes.

The metabolite MeG produced by both bacterial and mammalian cells from the glycolytic intermediate DHAP (fig. 1.2, 1.4 and 1.5) is of particular interest. It has previously been shown to inhibit bacterial cell growth (Freedberg *et al.,* 1971, Ackerman *et al.,* 1974) as well as causing impaired cell function, e.g. inhibiting insulin secretion and insulin action (Cook *et al.,* 1998, Guo *et al.,* 2009, Jia *et al.,* 2006, Riboulet-Chavey *et al.,* 2006). It is also proposed that MeG will react non-enzymatically with specific amino groups of proteins (e.g. albumin and insulin) resulting in the covalent modification of these proteins thus altering their biological function.

### 1.8.2. Overall aim and specific aims

#### 1.8.2.1. Overall aim

The overall aim of this thesis was to investigate the potential role of the bacterial metabolic toxin hypothesis in the development of diabetes.

#### 1.8.2.2. Specific aims

The specific aims of this thesis were:

- To establish a new approach to investigate the interaction between bacterial metabolic toxins and insulin
- To investigate the biological activity of insulin
- To investigate the biological activity of these toxins on cells

### 1.8.3. Experimental strategy

- To develop the coelenterazine chemiluminescence method to investigate the enzymatic activity of albumin and insulin
- To develop a tissue culture system to investigate the biological activity of insulin.

# Chapter 2:

# Materials & Methods

## 2.1. Materials

All proteins used to catalyse the coelenterazine chemiluminescence reaction were obtained from Sigma-Aldrich, Dorset, UK. Coelenterazine was a kind gift from Bruce Bryan, Prolume Inc. All cell culture media ingredients, unless otherwise stated, were obtained from Gibco®, Invitrogen Ltd, Paisley, UK.

## 2.2. Protein catalysed coelenterazine chemiluminescence

### 2.2.1. The chemiluminometer

Chemiluminescence can be measured using a chemiluminometer (fig. 2.1).

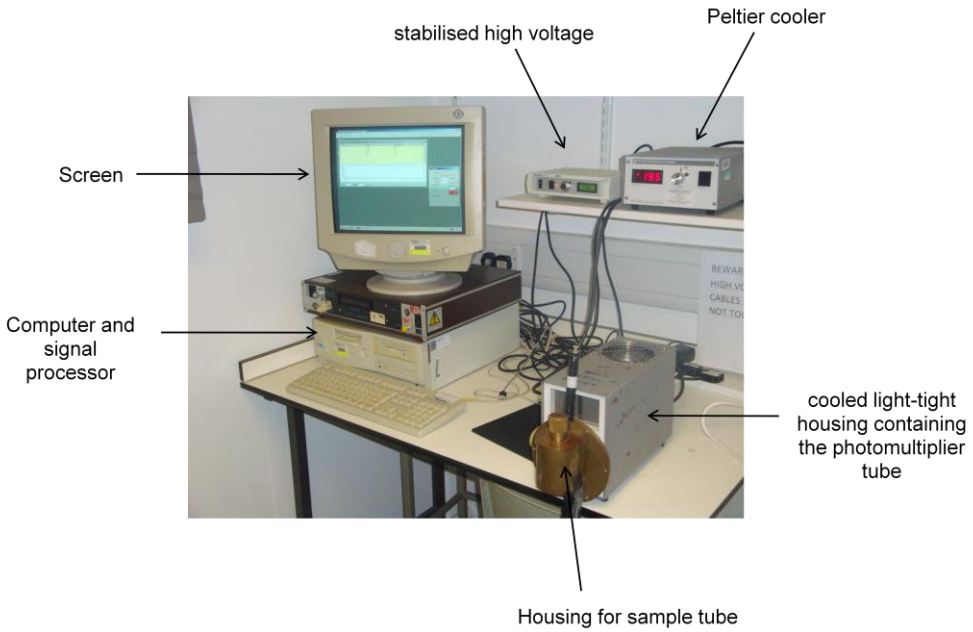


**Figure 2.1. The set of the chemiluminometer used.**

The chemiluminometer is made up of five important components:

1. The sample housing
2. The photomultiplier tube (PMT)
3. The light detector
4. The signal processor
5. The recorder and data processor

The following section will look at the five important components in more detail.

#### 2.2.1.1. The sample housing

The volume of a sample for chemiluminescence analysis can vary from a few microlitres to hundreds of millilitres. For all chemiluminescence analysis in this thesis, the volume of a sample was 100 µl as measurements in solution are normally carried out in a few microlitres to 2 ml volumes. The sample holders used were small test tubes. Although, spherical containers allow almost all the light to escape, cylinders, such as the test tubes used in the experiments were considered to be adequate. The main function of the test tube is to maintain the sample in a temperature and pressure controlled environment, as well as in a dark environment, to which substances can be added. Another function of the housing is to ensure all the light produced during the chemiluminescence reaction reaches the light detector. The chosen housing must take the following into account (Campbell, 1988):

- It must be light-tight so that no light can escape
- The sample volume should be adjustable, without affecting the amount of light reaching the detector
- It must be possible to add to the sample
- It must have temperature regulation
- There must be efficient reflection of light from the chamber to the detector
- It must handle the frequency of samples and analysis as well as being suitable for automation

The sample housing contained a Peltier cooler. This device is a heat pump that when a direct current passes through it, it can transfer heat from one side to another (from cold to hot) against the temperature gradient as well as consuming electrical energy. Therefore, this device can be used for heating or cooling, although its main use is for cooling. This device can also be used as a temperature control.

#### 2.2.1.2. The photomultiplier tube

A photomultiplier tube is a photosensitive device that produces electrons at the photocathode. These electrons are focused and multiplied by an electrode chain and are then collected at the anode (Campbell, 1988).

### 2.2.1.3. The detector

This is the most important component in any chemiluminometer. In the majority of chemiluminometers, the light source is placed a short distance (only a few centimetres) away from the detector. The closer the light source is to the detector, the better.

Choosing the right detector is important as using the wrong detector can restrict experiments and analysis. There are four requirements for choosing the right detector (Campbell, 1988):

- The detector must be able to detect a light signal over several orders of magnitude of intensity, whether it be a few photons per second to tens of millions of photons per second
- It must be sensitive over the spectral range 400 – 600 nm, but ideally it must be sensitive over the complete visible spectrum range including UV and IR, 380 – 750 nm
- The signal output produced by the detector should be directly related to the light intensity hitting the detector. The signal output should be generated in a form that can be displayed, recorded and easily analysed
- The response of the detector must be quicker than the rate of the coelenterazine chemiluminescence reaction. The detector in the chemiluminometer used was a photomultiplier tube. The coelenterazine chemiluminescence generates blue light and the photomultiplier tube was chosen because it is better at detecting light in the blue region of the spectrum

A photomultiplier tube is a photosensitive device that produces electrons at the photocathode, which are focused and multiplied by an electrode chain. These electrons are then collected at the anode. The photomultiplier tube contains four important components (Campbell, 1988):

- The glass envelope is important for maintaining a vacuum within it as well as having a glass window which allows the photons (light) to enter
- The photocathode receives light and is responsible for the generation of the primary electrons
- The dynode chain is the device that is responsible for the focusing and multiplication of the electrons, resulting in the production of secondary

electrons. The chemiluminometer used contained a 13-dynode chain, therefore the multiplication of electrons was repeated 13 times

- The anode is positively charged and its function is to collect the electrons

When the photomultiplier tube receives a photon at the photocathode, an electron is emitted due to the photoelectric effect. This is known as primary emission. The electron is then electrostatically accelerated and focused so that it will hit the first dynode. This causes the emission of several electrons and is known as secondary emission. Each of these electrons produced through secondary emission is then accelerated and focused so that they will hit the second dynode. At the second dynode further multiplication of electrons occurs. The multiplication of electrons can be repeated up to 13 times as the chemiluminometer used contained a 13-dynode chain. After the multiplication process has been completed, the resulting electrons are collected as a pulse of charge at the anode. The anode then passes the pulse of charge through a preamplifier to the discriminator. Once at the discriminator it is decided if it is big enough to be considered as a count (Campbell, 1988).

#### 2.2.1.4. Signal processing

The signal processor amplifies the output from the detector and then shows this to the recording device. To be able to detect a signal from any instrument it must be possible to be able to distinguish it from the “noise” produced by the detector and the processor. An easy way to compare devices is to measure the background from the instrument (“noise”) and then to measure the signal produced by the light standard. However, the chemiluminometer can be optimised by minimising the “noise” and producing the highest signal to noise ratio (fig. 2.2) (Campbell, 1988).

### 2.2.2. The optimisation of conditions

To be able to measure the amount of light emission accurately it was important to ensure that there were no external sources of light that could alter the results. To prevent this from happening experiments were carried out in a dark room. Before experimentation could begin, the room temperature was left to reach 20 $^{o}$C, the voltage was set to 1700 volts and the photomultiplier tube was left to reach at least -20 $^{o}$C.

To optimise the chemiluminometer for signal to noise it was necessary to determine the optimum temperature of the photomultiplier tube required for maximum sensitivity.

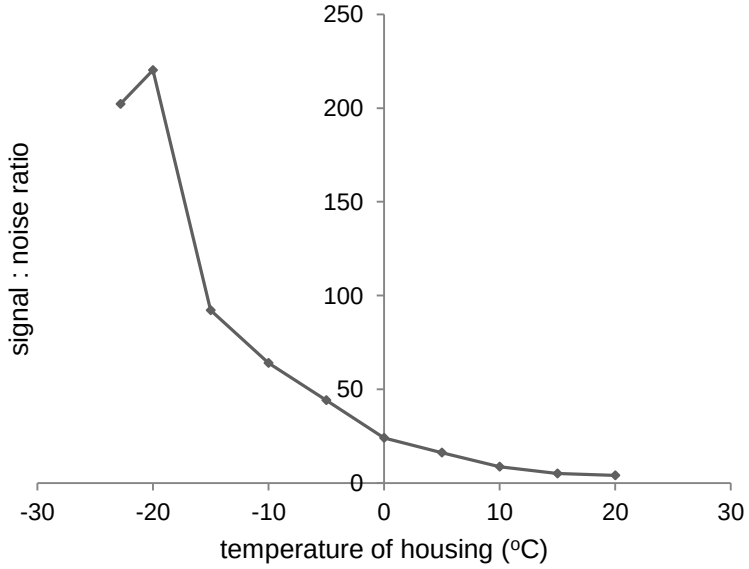


**Figure 2.2. The optimisation of the photomultiplier tube.** The optimum temperature was shown to be approximately -20 $^{o}$C. The machine background ("noise") and the protein readings ("signal") were measured over a temperature range of +20 to -20 $^{o}$C. The signal to noise ratio was determined by dividing the results for the albumin catalysed coelenterazine chemiluminescence by the corresponding results for coelenterazine chemiluminescence in the absence of the protein.

The "noise" is the background of the instrument, which in this case was the coelenterazine chemiluminescence in the absence of the protein (machine background) and the signal was the albumin catalysed coelenterazine chemiluminescence over the temperature range of +20 to -20 $^{o}$C. Therefore, the signal produced by the instrument was determined by the addition of 10 µl HSA (1 % (w/v) final concentration) to buffer containing 50 mM HEPES, pH 7.4 and 10 µM coelenterazine. The signal:noise ratio was determined by dividing the machine background measurements by the corresponding albumin catalysed coelenterazine chemiluminescence measurements.

The albumin catalysed coelenterazine chemiluminescence increased dramatically when the photomultiplier tube was cooled reaching a maximum at -20 $^{o}$C, however, further decreasing the temperature to -23 $^{o}$C the chemiluminescence decreased. Therefore, -20 $^{o}$C was considered to be the optimum temperature required for maximum sensitivity and was the temperature used in all chemiluminescence experiments.

### 2.2.3. The preparation of reagents

#### 2.2.3.1. The preparation of 50 mM HEPES buffer, pH 7.4

0.48 g of HEPES (4-(2-hydroxyethyl)-1-piperazineethanesulfonic acid) was added to 40 ml of distilled water. The pH was adjusted to 7.4 using 0.1 M NaOH. The buffer was stored at 4.5 $^{o}$C.

#### 2.2.3.2. The preparation of proteins

A 1 % (w/v) solution of HSA and BSA was made by adding 500 mg of the protein to 50 ml of distilled water. A 1 % (w/v) solution of human insulin was also made by adding 10 mg of the protein to 1 ml of 10 mM HCl. The proteins were stored at -20 $^{o}$C. For a 1 % (w/v) gelatin solution, 50 mg of the protein was added to 5 ml of 50 mM HEPES buffer, pH 7.4. The gelatin solution was heated in a microwave for a few seconds to dissolve and stored in a water bath at 37 $^{o}$C throughout the experiment to prevent it from solidifying. For a 5 % (w/v) solution of haemoglobin, 250 mg of haemoglobin was dissolved in 50 mM HEPES buffer, pH 7.4. Both gelatin and haemoglobin were discarded after use.

#### 2.2.3.3. The preparation of coelenterazine

Eppendorfs containing 20 nmol and 200 nmol coelenterazine were stored at -20 $^{o}$C. Coelenterazine is very unstable when dry. It reacts with the oxygen in water and other solvents and therefore degrades. Stock amounts of coelenterazine were stored dry and then dissolved. 20 nmol coelenterazine was dissolved in 100 µl methanol and the volume was topped up to 200 µl by adding 100 µl of 50 mM HEPES buffer, pH 7.4.

### 2.2.4. The determination of protein catalysed coelenterazine chemiluminescence

In aqueous solution, coelenterazine is capable of emitting efficient chemiluminescence in the presence of a luciferase e.g. HSA. Figure 2.3 shows the coelenterazine chemiluminescence reaction in the presence of a luciferase that can catalyse the reaction.

In the reaction, coelenterazine reacts with oxygen resulting in the production of an organic dioxetanone intermediate and therefore generates enough energy to produce the excited-state products. The end products of this reaction are coelenteramide and $CO_2$ *via* the breakdown of the dioxetanone intermediate.

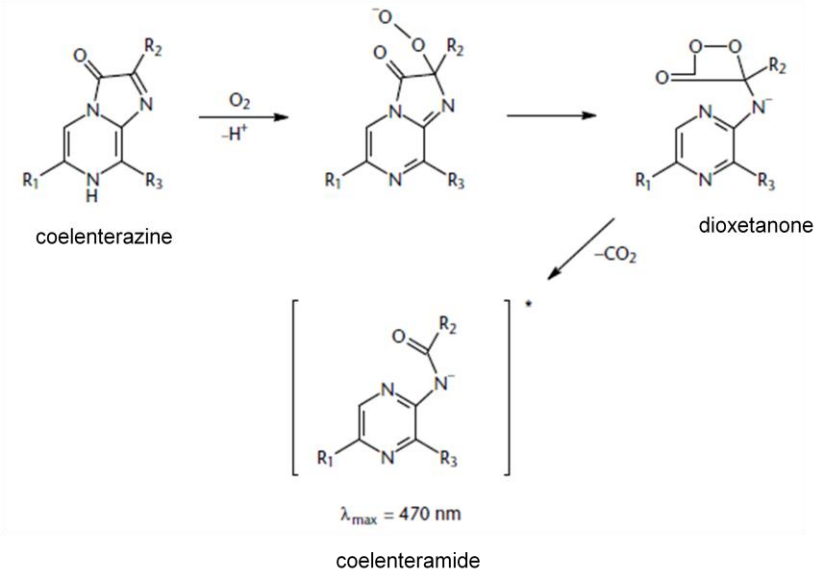


**Figure 2.3. The pathway showing the chemiluminescence reaction of coelenterazine.** R groups represent either a benzyl or phenyl group: $R_1$ = phenyl group ($C_6H_4OH$); $R_2$ = phenyl group ($CH_2C_6H_4OH$) and $R_3$ = benzyl group ($CH_2C_6H_5$) (Lee, 2001).

The measurement of protein catalysed coelenterazine chemiluminescence was carried out in a dark room to minimise light exposure thus preventing the degradation of coelenterazine as it is light sensitive. The voltage was set to

1700 volts. This was the optimum voltage that resulted in the lowest signal to noise ratio.

The photomultiplier tube was allowed to reach its optimum temperature of at least -20 $^{o}$C and the room temperature was allowed to reach 20 $^{o}$C.

First, the machine background was measured by inserting an empty test tube into the photomultiplier tube. Secondly, the coelenterazine chemiluminescence was measured by adding 10 µM coelenterazine to 80 µl of buffer containing 50 mM HEPES, pH 7.4. Thirdly, an additional stage can be added to determine the effect of a cation/drug on coelenterazine chemiluminescence, whereby 10 µl of the cation/drug is added to 80 µl of 50 mM HEPES buffer, pH 7.4, containing 10 µM coelenterazine. Finally, the protein chemiluminescence was measured by adding 10 µl HSA (0.1 % (w/v) final concentration) to 90 µl of buffer containing 50 mM HEPES, pH 7.4 and 10 µM coelenterazine. The chemiluminescence was recorded as 6 x 10 second counts.

When the data was recorded, the results were calculated as follows: coelenterazine chemiluminescence minus the machine background, coelenterazine chemiluminescence in the presence of the cation/drug minus the coelenterazine chemiluminescence and protein catalysed coelenterazine chemiluminescence minus the coelenterazine chemiluminescence.

### 2.3. Cell culture

7F2 (mouse osteoblast progenitor cell line) cells and 3T3-L1 (mouse embryonic fibroblast-adipose like cell line) cells were donated from Dr Bronwen Evans, Department of Child Health, University Hospital of Wales, Heath Park Campus, Cardiff.

#### 2.3.1. Cell culture medium

Specific culture media were selected for each cell-type according to instructions from the respective suppliers. Prepared culture media were kept refrigerated at 4.5 $^{o}$C and warmed to room temperature or 37 $^{o}$C prior to use. Generally, media were used within 14 days of preparation or discarded.

##### 2.3.1.1. DMEM for 3T3-L1 cell culture and maintenance

Dulbecco's Modified Eagle Medium (DMEM) containing L-glutamine, pyruvate and 4.5 $gL^{-1}$ glucose was supplemented with 10 % foetal bovine serum (FBS)

and with 100 µg $ml^{-1}$ streptomycin and 100 U $ml^{-1}$ penicillin (penicillin-streptomycin 10,000:10,000, Invitrogen) (Tafuri, 1996).

#### 2.3.1.2. MEM-α for 7F2 cell culture and maintenance

Alpha Minimum Essential Medium (MEM-α) containing Earl's salts, 1 mM sodium pyruvate and 2 mM L-glutamine, but without ribonucleosides or deoxyribonucleosides, was supplemented with 10 % FBS, 100 µg $ml^{-1}$ streptomycin and 100 U $ml^{-1}$ penicillin.

### 2.3.2. Cell husbandry

7F2 and 3T3-L1 cells were kindly supplied by Dr Bronwen Evans, Department of Child Health, University Hospital of Wales, Heath Park Campus, Cardiff. The 7F2 cells are a mouse osteoblast progenitor cell line whereas the 3T3-L1 cells are a mouse embryonic fibroblast-adipose like cell line. All cells were cultured in 25 $cm^2$ or 75 $cm^2$ flasks and incubated at 37 $^oC$ (5 % $CO_2$ and 95 % air), with a working volume of 3 ml or 9 ml cell culture medium, respectively.

Confluent cultures were divided weekly and the cell culture medium was aspirated and replaced every 2-3 days. To detach cells, cultures were washed with 1x D-PBS (calcium- and magnesium-free, Gibco®, Invitrogen Ltd.) and then 500 µl of trypsin solution (trypsin 0.025 %, EDTA 0.2 %) (trypsin from bovine pancreas and EDTA both purchased from Sigma) per 25 $cm^2$ was added and left for up to 10 minutes. Once the trypsin solution had been added, the culture was closely monitored so that when all the cells had become detached, trypsinisation was stopped. If the trypsin solution is left on the cells for too long it causes the cell membranes to break down resulting in the destruction of the cells. Once the cells had detached, 2-3 ml of the respective cell culture medium was added to stop trypsinisation and the cells were evenly suspended by gentle pipetting. The cell suspension was centrifuged at 500 x G for 3 minutes at room temperature to pellet the cells, the supernatant was aspirated and replaced with cell culture medium. The pellet was resuspended by gentle pipetting resulting in an even distribution of cells throughout the suspension. The cells were pipetted accordingly into new sterile flasks.

## 2.4. Cell counting

### 2.4.1. Haemocytometry

Haemocytometry is a process in which cells are counted in order to determine the density of a cell suspension. The Neubauer haemocytometer is a slide that consists of two flat chambers and each is engraved with a microscopic grid containing 1 mm squares, and when fixed with a coverslip, the chambers have a depth of 0.1 mm.

Therefore, each 1 mm x 1 mm square of depth 0.1 mm has a volume of 0.1 µl. The coverslip is considered to be attached when the interference patterns known as Newton's rings can be seen.

Cells were detached and pelleted as previously described in section 2.3.2. The pellet was then evenly resuspended in a known volume of cell culture medium by gentle pipetting. Then 8 µl of the cell suspension was added to each of the chambers on the haemocytometer and allowed to be drawn in by capillary action between the coverslip and the chamber. At 10x magnification under a microscope, the central 1 $mm^2$ square of one chamber was found and all the cells within the boundaries were counted, including the cells that lay on the top and left-hand boundary lines. However, those that lay on the bottom and right-hand boundary lines were not included. This ensured that only 1 $mm^2$ was counted. If the central square contained less than 100 cells, one or more additional squares found in the same chamber were also counted to improve accuracy. The same was done for the second chamber on the haemocytometer. The average of the cells was calculated and the density of the cell suspension was determined using the following equation:

$$\textit{number of cells per ml} = \frac{\textit{total number of cells counted}}{\textit{number of squares counted}} \times 10^4$$

# Chapter 3:

# Chemiluminescence activity of albumin and insulin

## 3.1. Introduction

The bacterial metabolic toxin hypothesis predicts that putative toxins will react with proteins resulting in the covalent modification of these proteins (Campbell *et al.,* 2010, Lo *et al.,* 1994). This covalent modification should affect the biological activity of these proteins. In order to test the hypothesis, the strategy was to use the ability of proteins to catalyse coelenterazine chemiluminescence and then to investigate if the putative bacterial metabolic toxins affected the activity of the proteins. Bovine serum albumin (BSA) has been previously shown to catalyse coelenterazine chemiluminescence (Campbell *et al.,* 1989). From this, the initial aim of this chapter was to investigate the ability of HSA to catalyse coelenterazine chemiluminescence and to compare it with that of three other proteins – human insulin, gelatin and haemoglobin. Then if these proteins were able to catalyse coelenterazine chemiluminescence it would then be important to determine if this was consistent with an enzymatic activity.

### 3.1.1. Types of luminescence

Luminescence is light emission from an electronically-excited state. Each type of luminescence is designated by a prefix. The prefix states the source of energy, for example: **photo**luminescence is produced when light is absorbed, **thermo**luminescence is a result of slight heating and **chemi**luminescence is the production of light as a result of a chemical reaction (Campbell, 1988). Table 3.1 that follows contains more types of luminescence and their basis of light emission.

| Type of luminescence | Prefix | Basis of light emission |
|---|---|---|
| Candoluminescence | Cando- | Certain materials that have been heated to incandescence and emit at shorter wavelength than expected |
| Pyroluminescence | Pyro- | Luminescence of metal atoms in flames |
| Thermoluminescence | Thermo- | The slight heating of solids and crystals resulting in light emission |
| Photoluminescence | Photo- | Irradiation by UV or visible light |
| Cathodoluminescence | Cathodo- | Irradiation by electrons |
| Anodoluminescence | Anodo- | Irradiation by nuclei |
| Radioluminescence | Radio- | Irradiation by γ or x-rays |
| Electroluminescence and piezoluminescence | Electro- and piezo- | Light emission associated with electric discharges and fields |
| Galvanoluminescence | Galvano- | Light emission during electrolysis |
| Triboluminescence | Tribo- | Light emission from intense sound waves in a solution |
| Crystalloluminescence | Crystallo- | Light emission on crystallisation |
| Lyoluminescence | Lyo- | Light emission on dissolving crystals |
| Chemiluminescence | Chemi- | Light emission as a result of a chemical reaction |
| Bioluminescence | Bio- | Light emission as a result of a chemical reaction in a biological system |

**Table 3.1. Types of luminescence and the basis of light emission** (Campbell, 1988).

### 3.1.1.1. Chemiluminescence and its discovery

In the 17$^{th}$ century, Robert Boyle invented the air pump and later demonstrated that by removing the air surrounding what he called “shining wood” or “shining flesh” would result in a significant decrease in the intensity of light emission and in some cases extinguished the luminescence altogether. He then showed that if he exposed these materials to air again they both glowed brightly. However, it was unknown what important component in the air made these materials glow. It was not until 100 years later that the important component in the air was identified as molecular oxygen by Scheele and Priestly. Therefore, this experiment by Boyle was the first demonstration showing that oxygen or one of its derivatives is required in all bioluminescent reactions (Campbell, 1988, Lee, 2001).

Since this discovery by Boyle, many more experiments have been carried out to further study bioluminescence. At the end of the 19th century (between 1885 and 1887) Raphael Dubois carried out experiments on the "click beetle," *Pyrophorus*. It is the results of these experiments that have had a significant impact on the study of bioluminescence.

He extracted the light organ and placed it in cold water and this produced a suspension that glowed, however, this glow diminished with time. He then placed a luminous organ in hot water but this time no light emission was observed. It was the results of these studies that led to the discovery of the enzyme-substrate property of many bioluminescence reactions. The enzyme that is stable in the cold is now known as the "luciferase" and the substrate that is heat stable is known as the "luciferin". Dubois argued that the luminescence observed in cold water was due to a chemical reaction occurring, hence the term chemiluminescence (Campbell, 1988, Lee, 2001).

It is as a result of these discoveries that chemiluminescence and bioluminescence have since been defined. Chemiluminescence is the light produced as a result of a chemical reaction whereas bioluminescence is the light produced as a result of a chemical reaction in a biological system with the help of an enzyme (Campbell and Herring, 1990, Shimomura and Teranishi, 2000). Therefore all known bioluminescence is due to chemiluminescence (Campbell and Herring, 1990).

#### 3.1.1.2. Bioluminescence

Bioluminescence is the light emitted as a result of a chemical reaction in a biological system. It is also known as living light. Living light can be found on land, in the air, but is most commonly found in deep-sea waters where approximately 97 % of the species found there are bioluminescent (Rees *et al.,* 1998, Thomson *et al.,* 1997).

Luminous species include bacteria, fungi, dinoflagellates, jellyfish, shrimps, worms, insects, some squid and fish. These living organisms use the ability to produce light for a number of purposes:

- *Attraction and hunting* – many deep-sea creatures use the light generated to attract their mates, whereas others can use the light they produce to attract or lure prey (e.g. anglerfish) (Lee, 2001)

- *Repulsion and warning* – some species of squid can produce light to warn their predators. Squids can also release a cloud of ink to repel the predator, this ink is also luminescent as it contains bioluminescent bacteria (Lee, 2001)
- *Communication and illumination* – many species of bacteria can use bioluminescence for communication (Lee, 2001)

### 3.1.2. Light emission due to these reactions

#### 3.1.2.1. Light emission as a result of a chemical reaction (chemiluminescence)

If a chemical reaction is to generate light, molecules must be generated in an electronically-excited state and must be capable of releasing its energy either as a photon or by transferring its energy to another molecule thus making this second molecule the light emitter (Campbell, 1988).

When two molecules chemically react there is a release of energy (exothermic). Rather than heat, this energy can show itself in the form of light, hence why the light emitted due to a chemiluminescent reaction is sometimes called “cold light”. The energy that is produced leads to the production of an electronically-excited product. If this excited product is allowed to relax to the ground state, light is generated and this is known as type I chemiluminescence. However, if the electronically-excited product is not allowed to relax to the ground state, the excited product transfers its energy to a second molecule and it is then this second molecule that becomes the light emitter. This process of energy transfer is known as type II chemiluminescence or energy transfer chemiluminescence (Campbell, 1988).

Reactant + $O_2$ → dioxetanone intermediate → excited products →products + hv

**Figure 3.1. The equation for a chemiluminescence reaction** (Campbell, 1988).

From this information there are three main features for a chemiluminescence reaction:

- The reaction must produce enough energy to generate a molecule in an electronically-excited state
- There must be a pathway through which the energy can pass leading to the production of an electronically-excited state
- The electronically-excited product must be able to lose its energy as a photon or be capable of transferring its energy to a fluorescent protein (Campbell, 1988).

### 3.1.2.2. Light emission as a result of a chemical reaction in a biological system (bioluminescence)

Even though bioluminescence can vary between species the general mechanism is similar. For a bioluminescence reaction to occur it requires the presence of oxygen or one of its metabolites to oxidise a small organic molecule (the luciferin) and a protein to catalyse the reaction (the luciferase) (Campbell and Herring, 1990).

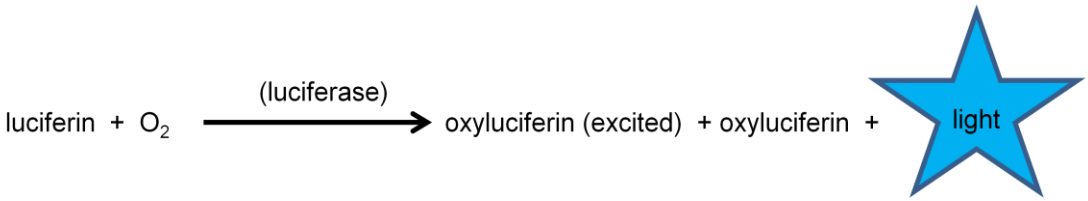


**Figure 3.2. The equation for a bioluminescence reaction** (Campbell, 1988).

The oxidation of the luciferin by oxygen or one of its metabolites is catalysed by the presence of a luciferase. In the absence of the protein catalyst, oxidation of the luciferin is usually slow, resulting in poor chemiluminescence and the production of the wrong colour light. The oxidation of the luciferin produces the electronically-excited state oxyluciferin. The excited oxyluciferin then relaxes to the ground state, oxyluciferin and then blue light is emitted (Campbell, 1988).

As well as oxygen (or one of its metabolites), the luciferin and the luciferase other components such as cofactor(s), cation(s) and fluorescent proteins may be necessary for the bioluminescence reaction:

*Oxygen, or one of its metabolites (e.g. hydrogen peroxide, $H_2O_2$)*

All chemiluminescent and thus all bioluminescent reactions require oxygen whether it is molecular oxygen or a metabolite. However, aequorin, a photoprotein extracted from the jellyfish, *Aequorea victoria* can generate light with or without the presence of oxygen (Shimomura, 1986).

*Luciferin (e.g. coelenterazine)*

For light to be generated the oxidation of a small organic molecule, such as coelenterazine is required for the production of the electronically-excited product. The excited product may be fluorescent and is therefore the emitter (Cormier *et al.,* 1975). The luciferin usually has a molecular weight of less than 1000. Many luciferins are unstable and can oxidise spontaneously in a weak chemiluminescent reaction. For example, if a solution of coelenterazine is left on a work surface in sunlight, more than 80 % can be destroyed within an hour (Campbell, 1988).

*Luciferase*

All bioluminescence reactions require a protein and the protein is known as a luciferase. The luciferase catalyses the reaction, therefore, making it go fast enough to generate efficient light for it to be visible. Proteins can be found in any biological reaction but the oxidation of these proteins by either oxygen or one of its metabolites would not generate visible light unless a luciferin is present (Cormier *et al.,* 1975).

*Cofactor(s)*

If the chemiluminescent components are isolated as a photoprotein another component is required to trigger the bioluminescence reaction. Cofactors can include ATP and the calcium ion ($Ca^{2+}$) (Campbell, 1988).

*Cation(s)*

Cations such as the alkaline earth metals ($Mg^{2+}$ or $Ca^{2+}$) or transition metals ($Fe^{2+}$, $Fe^{3+}$, $Cu^{+}$ or $Cu^{2+}$) are sometimes required. Transition metals are

involved in oxidant processing resulting in a change in the valency state during chemiluminescence (Campbell, 1988).

*Fluorescent protein*

A fluorescent protein can interact directly or indirectly with a chemiluminescent reaction. When fluors interact directly with the chemiluminescence reaction they enhance the rate of reaction and yield. When fluors interact indirectly their role is to act as a passive acceptor of the energy from the excited state reaction product through a non-radiative process, therefore making the fluor the light emitter. This then changes the spectrum of light and yield from that of the initial chemiluminescence reaction (Campbell, 1988).

### 3.1.3. The jellyfish, *Aequorea victoria* and the discovery of coelenterazine

*Aequorea victoria* is also known as the crystal jellyfish. It is a bioluminescent hydrozoan jellyfish. The active extract, the photoprotein aequorin, was isolated by Shimomura et al (Adamczyk *et al.,* 2001, Shimomura *et al.,* 1962). Aequorin is a protein with a molecular weight of 22 kDa and is a charged complex that is very stable as well as having a high energy (Ohmiya and Hirano, 1996). The luciferin, coelenterazine and oxygen are bound to aequorin (Adamczyk *et al.,* 2001, Lee, 2001). Photoproteins like aequorin can hold on to the bound oxygen, either as molecular oxygen or in the form of $H_2O_2$ (Campbell, 1988) whereas coelenterazine is bound to the protein through a peroxidic bond (Teranishi *et al.,* 1994). The addition of calcium ($Ca^{2+}$) ions to the non-luminous photoprotein results in the protein undergoing a conformational change thus triggering the bioluminescence reaction and results in the emission of blue light (465 nm) either in the presence or absence of oxygen (Adamczyk *et al.,* 2001, Shimomura and Johnson, 1978).Therefore, the intensity of light emitted by the jellyfish, *Aequorea victoria*, does not directly depend on oxygen (Lee, 2001).

**Figure 3.3. *Aequorea victoria*** (Ohmiya and Hirano, 1996).

Therefore, as a result of this discovery, coelenterazine is now known as the luciferin responsible for the “blue glow” emitted by the jellyfish. The isolation and extraction of coelenterazine from marine organisms is not only laborious but is also low yielding. Nowadays, coelenterazine is commercially available but is very expensive where 1 mg costs approximately $1240 (Adamczyk *et al.,* 2001).

### 3.1.4. Coelenterazine and its role in bioluminescence

#### 3.1.4.1. Coelenterazine

Coelenterazine is a well characterised luciferin (Oba *et al.,* 2004) for a number of luciferases. It is also known to be the light emitter of photoproteins in a number of jellyfish and ctenophores (Shimomura and Teranishi, 2000). It is known as 3,7-dihydro-2-(p-hydroxybenzyl)-6-(p-hydroxyphenyl)-8-benzylimidazo-[1,2-a]pyrazin-3-one (De Wergifosse *et al.,* 2004).

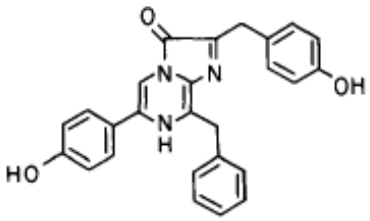


**Figure 3.4. The structure of coelenterazine** (Shimomura, 1987).

Coelenterazine has an imidazopyrazine skeleton (Hastings and Krause, 2005) with three lateral groups (Dubuisson *et al.,* 2005). These lateral groups are either phenyl or benzyl groups. It is widely distributed in bioluminescent organisms such as *Renilla*, *Oplophorus*, *Periphylla* and *Gaussia* and can be found within the light organs of these animals (Dubuisson *et al.,* 2005, Shimomura and Johnson, 1978). This imidazolopyrazine has been reported so far in 18 phyla and approximately 92 genera of both luminous and non-luminous marine species (Thomson *et al.,* 1997, Vassel *et al.,* 2012).

It is also found in various non-luminescent organisms (Shimomura, 1987, Campbell and Herring, 1990). Coelenterazine is present in the liver of a number of species (e.g. some fish and squid) (Thomson *et al.,* 1997), however, as there is such a widespread distribution among distantly related marine organisms it is possible that these organisms can obtain coelenterazine through their diet *via* the food chain (Mallefet and Shimomura, 1995, Shimomura, 1987).

When coelenterazine is dissolved in a suitable aprotic organic solvent (e.g. dimethylformamide, DMF or dimethyl sulphoxide, DMSO) it spontaneously oxidises and emits blue chemiluminescence (465 nm) (Shimomura and Teranishi, 2000).

### 3.1.4.2. The bioluminescence reaction of coelenterazine

The luciferin, coelenterazine is part of the photoprotein and is involved in bioluminescence. Bioluminescence can occur either in a living organism and this is known as *in vivo* bioluminescence or in aqueous medium and this is known as *in vitro* bioluminescence (Lee, 2001). *In vitro* bioluminescence requires the presence of a protein, i.e. luciferase such as albumin or the presence of an apoprotein to catalyse the oxidation reaction as well as providing a sufficient environment for light emission. The need for a luciferase makes this reaction more complex than that of chemiluminescence, especially when the protein undergoes a significant conformational change as that seen in aequorin (Shimomura and Teranishi, 2000).

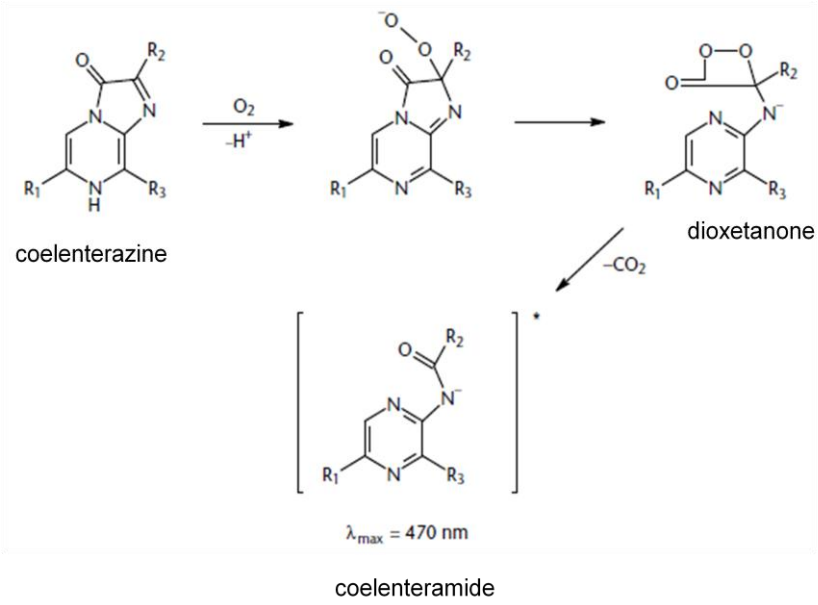


**Figure 3.5. The pathway of the chemiluminescence reaction of coelenterazine.** R groups represent either a benzyl or phenyl group: $R_1$ = a phenyl group ($C_6H_4OH$); $R_2$ = a phenyl group ($CH_2C_6H_4OH$) and $R_3$ = a benzyl group ($CH_2C_6H_5$) (Lee, 2001).

In an aqueous solution, coelenterazine is capable of emitting sufficient light emission providing a luciferase (e.g. *Renilla* luciferase or albumin) is present. In the reaction, coelenterazine reacts with oxygen producing an organic dioxetanone intermediate and therefore generates enough energy to produce an excited-state product. The dioxetanone intermediate is broken down and leads to the production of the endproducts, coelenteramide and $CO_2$. Coelenteramide only emits faint fluorescence in aqueous solution, however, it does fluoresce bright blue ($\lambda_{max}$ 465 nm) in organic solvents. This wavelength does not suggest that coelenteramide is responsible for the blue light emission but it is now known that the amide ion is the light emitter (Shimomura and Teranishi, 2000).

For aequorin to emit blue light of wavelength 460 nm it must bind calcium ions. When calcium binds to the photoprotein it causes an intermolecular reaction where coelenterazine is oxidised to coelenteramide resulting in the production of blue light (465 nm), $CO_2$ and blue fluorescent protein (BFP). Light emission occurs when the bound coelenteramide relaxes from the excited state to the ground state (Shimomura and Teranishi, 2000).

However, *in vivo* bioluminescence of *Aequorea victoria* is green. It was proposed that there was another component involved in the bioluminescence reaction that emits light with a wavelength that is consistent with the green bioluminescence observed. It was then proposed that a mechanism of energy transfer was involved as this second compound accepts the energy. This second compound was discovered by Shimomura in 1979 and is now known as “green fluorescent protein (GFP)” (Lee, 2001, Shimomura, 1979).

### 3.1.5. Overall aim, specific aims and experimental strategy

#### 3.1.5.1. Overall aim

The overall aim of this chapter was to confirm that HSA displays enzymatic activity and to also determine if insulin also displays this property.

#### 3.1.5.2. Specific aims

- To investigate if HSA and insulin were able to catalyse coelenterazine chemiluminescence
- If so to demonstrate if this was consistent with enzymatic activity
- To use coelenterazine chemiluminescence to test if bacterial metabolic toxins can alter the activity of key proteins in the blood, specifically HSA and insulin
- To demonstrate whether the covalent modification of proteins altered coelenterazine chemiluminescence

Four criteria were used to determine if protein catalysed coelenterazine chemiluminescence was enzymatic: (1) heat denaturable; (2) saturable by the substrate (coelenterazine); (3) inhibition or activation by specific cations that are known to bind to the proteins and (4) inhibition by drugs that are known to bind to the proteins (Chapter 4).

#### 3.1.5.3. Experimental strategy

Coelenterazine chemiluminescence was selected as the model to characterise the enzymatic activity of albumin and to determine if human insulin also has enzymatic activity.

## 3.2. Materials and methods

### 3.2.1. Materials

Coelenterazine was a generous gift from Bruce Bryan, Prolume Inc. All other compounds were purchased from Sigma-Aldrich unless otherwise stated.

### 3.2.2. Preparation of reagents

All reagents such as proteins and coelenterazine were made as previously described in Chapter 2.

### 3.2.3. The determination of protein enzymatic activity

The photomultiplier tube was allowed to reach its optimum temperature and all reagents required were prepared prior to the start of experimentation as described previously in Chapter 2.

The addition of 10 µM coelenterazine to 90 µl of HEPES buffer, pH 7.4 containing 10 µl HSA demonstrated that the activity decreased by < 10 % over the time course of 6 x 10s counts. From this it can be concluded that the reaction rates were linear across the time course chosen. The ability of a protein to act as an enzyme was determined using the method described in 2.2.4. However, at this stage the aim was to determine which proteins demonstrated enzymatic activity and there was no need for the addition of a test compound (e.g. cation or drug).

### 3.2.4. The effect of thermal denaturation on protein enzymatic activity

Albumin and human insulin were prepared as previously described in 2.2.3.2. Half the protein suspension was then denatured using a thermocycler for 15 minutes at a temperature of 95 $^{o}$C. Experimentation was then carried out as previously described in section 2.2.4.

### 3.2.5. The effect of increasing substrate concentration on chemiluminescence

The photomultiplier tube was allowed to reach its optimum temperature and all reagents required were prepared prior to the start of experimentation as described previously in Chapter 2. Experimentation was then carried out as previously described in section 2.2.4 using coelenterazine over a concentration range (0.5 – 50 µM).

### 3.2.6. The effect of increasing pH on protein enzymatic activity

The method used to determine the effect of increasing pH on protein catalysed coelenterazine chemiluminescence was similar to that described in section 2.2.4 but here it was the pH of the buffer that changed.

### 3.2.7. The effect of divalent cations on protein enzymatic activity

The method used to determine the effect of divalent cations on protein catalysed coelenterazine chemiluminescence was the same as that described in section 2.2.4 with the additional testing compound (e.g. iron (III) chloride) step to determine if the addition of the cation would modulate the coelenterazine chemiluminescence catalysed by a protein.

### 3.2.8. Statistical analysis

Statistical analysis was carried out on the means using a t-test and the results were considered to be statistically different when $p < 0.05$.

## 3.3. Results

In order to establish albumin chemiluminescence it was necessary to compare albumin chemiluminescence with that of three other proteins: human insulin, gelatin and haemoglobin. Four criteria were used to determine if protein catalysed coelenterazine chemiluminescence was enzymatic: (1) heat denaturable; (2) saturable by the substrate (coelenterazine); (3) inhibition or activation by specific cations that are known to bind to the proteins and (4) inhibition by specific drugs that bind to the proteins. The inhibition by specific drugs that bind to proteins (4) is investigated in Chapter 4 that follows.

### 3.3.1. The effect of HSA and other proteins on coelenterazine chemiluminescence

An important feature of bioluminescent enzymes is to form a solvent cage around the luciferin with the ability to catalyse a light-emitting reaction. In order to test this it was important to demonstrate the ability of both bovine (BSA) and human (HSA) serum albumin to catalyse coelenterazine chemiluminescence. With increasing concentrations of coelenterazine, the chemiluminescence increased linearly.

BSA and HSA, over the concentration range 0.01 – 0.5 % (w/v) which was equivalent to 0.15 to 7.5 μM, caused a 100- to 3000-fold increase in light emission (fig. 3.6). The addition of 0.5 % (w/v) (or 7.5 μM) BSA resulted in a 5-fold increase in light emission when compared to the light emission produced with the same concentration of HSA suggesting that BSA was better than HSA at catalysing coelenterazine chemiluminescence.

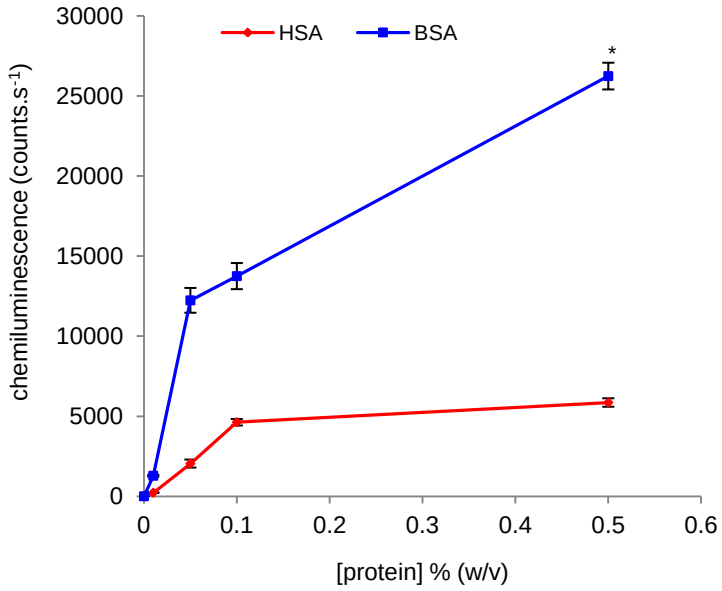


**Figure 3.6. The stimulation of coelenterazine chemiluminescence catalysed by human (HSA) and bovine (BSA) albumin.** The machine background produced an average of 36 counts.$s^{-1}$. The coelenterazine chemiluminescences prior to the addition of the proteins were between 71 and 74 counts.$s^{-1}$ for HSA and 63 and 65 counts.$s^{-1}$ for BSA. Protein catalysed coelenterazine chemiluminescence was measured by adding 10 μl of albumin (0.01 – 0.5 % (w/v); 0.1 – 5 g.$l^{-1}$ final concentration) to 90 μl of 50 mM HEPES buffer pH 7.4, containing 10 μM coelenterazine. The results represent the mean +/- SEM of three experiments. Asterisk indicates significant difference where $p < 0.01$ when compared to 0.5 % (w/v) HSA.

In order to test the ability of three other proteins: human insulin, gelatin and haemoglobin at catalysing coelenterazine chemiluminescence the light emission produced by these three proteins was compared with HSA chemiluminescence.

Human insulin, another important protein found in mammalian plasma, over the concentration range 0.01 - 0.5 % (w/v) which was equivalent to 1.7 to 86 µM caused a 20- to 100-fold increase in chemiluminescence (fig. 3.7). In contrast, the addition of gelatin and haemoglobin (fig. 3.7) also over a concentration range of 0.01 – 0.5 % (w/v) (equivalent to 0.2 to 10 µM for gelatin and 0.6 to 29 µM for haemoglobin) only produced very small light emission and was approximately 1,000 to 10,000 times less than the light emission produced with albumin.

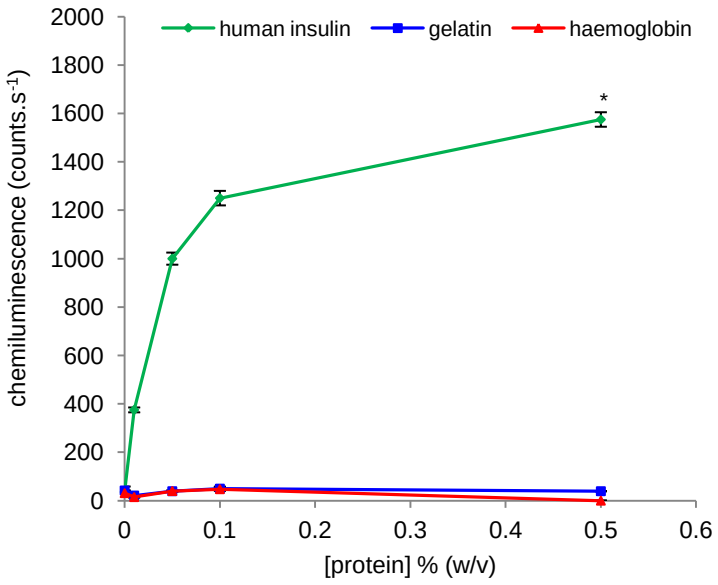


**Figure 3.7. The stimulation of coelenterazine chemiluminescence by human insulin, compared with that of gelatin and haemoglobin.** The machine background produced an average of 32 counts.$s^{-1}$. The coelenterazine chemiluminescences prior to the addition of the proteins were between 80 and 115 counts.$s^{-1}$ for insulin, 66 and 70 counts.$s^{-1}$ for gelatin and 67 and 70 counts.$s^{-1}$ for haemoglobin. Protein catalysed coelenterazine chemiluminescence was measured by adding 10 µl of human insulin, gelatin or haemoglobin (0.01 – 0.5 % (w/v); 0.1 – 5 g.$l^{-1}$ final concentration) to 90 µl of 50 mM HEPES pH 7.4, containing 10 µM coelenterazine. The results represent the mean +/- SEM of three experiments. Asterisk indicates significant difference where $p < 0.01$ when compared to 0.5 % (w/v) HSA.

After comparing the abilities of these 5 proteins at catalysing coelenterazine chemiluminescence, they can be ranked in order starting with the protein that

was best at catalysing coelenterazine chemiluminescence: BSA > HSA > human insulin > gelatin > haemoglobin.

### 3.3.2. Investigating the enzymatic activity of HSA and insulin

It was shown that albumin catalysed coelenterazine chemiluminescence and the next aim was to determine if this was consistent with the protein having an enzymatic activity. Therefore to test if the coelenterazine chemiluminescence produced by albumin was enzymatic it was necessary to investigate protein denaturation, if it could be saturated by the substrate (coelenterazine) and if certain cations would result in either the inhibition or activation of the protein.

#### 3.3.2.1. The effect of denatured HSA and insulin on coelenterazine chemiluminescence

In order to determine the enzymatic activity of HSA it was important to investigate if the protein was heat denaturable. HSA was denatured as described in section 3.2.4. Once the protein had been denatured its ability at catalysing coelenterazine chemiluminescence was determined and compared with the coelenterazine chemiluminescence catalysed by normal HSA. Heating HSA inhibited coelenterazine chemiluminescence by approximately 50 % (fig. 3.8).

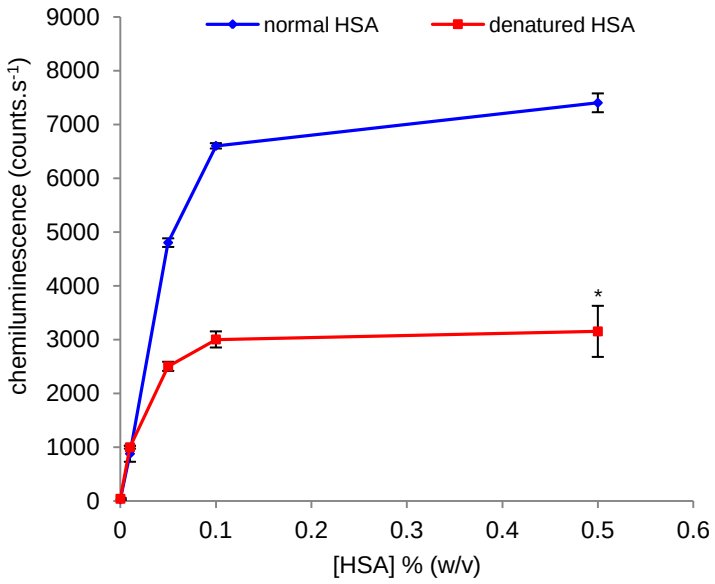


**Figure 3.8. The inhibition of human serum albumin (HSA) catalysed coelenterazine chemiluminescence by thermal denaturation.** The coelenterazine chemiluminescence prior to the addition of normal HSA produced between 84 and 105 counts.$s^{-1}$ whereas the coelenterazine chemiluminescence prior to the addition of denatured HSA produced between 86 and 127 counts.$s^{-1}$. To determine the effect of thermal denaturation on HSA catalysed coelenterazine chemiluminescence, 1 % (w/v) albumin was heated in a thermocycler at 95 $^{o}$C for 15 minutes. Protein catalysed coelenterazine chemiluminescence was measured by adding 10 µl of normal or denatured albumin (0.01 – 0.5 % (w/v); 0.1 – 5 g.$l^{-1}$ final concentration) to 90 µl of 50 mM HEPES buffer pH 7.4, containing 10 µM coelenterazine. The results represent the mean +/- SEM of three experiments. Asterisk indicates significant difference where $p < 0.01$ when compared to 0.5 % (w/v) normal HSA.

In order to investigate the enzymatic activity of human insulin it was necessary to determine if this protein was also heat denaturable. Human insulin was denatured as described in section 3.2.4. The coelenterazine chemiluminescence catalysed by denatured human insulin was compared with the coelenterazine chemiluminescence catalysed by normal human insulin. Heating human insulin under these conditions had no significant effect on the light emission produced (fig. 3.9).

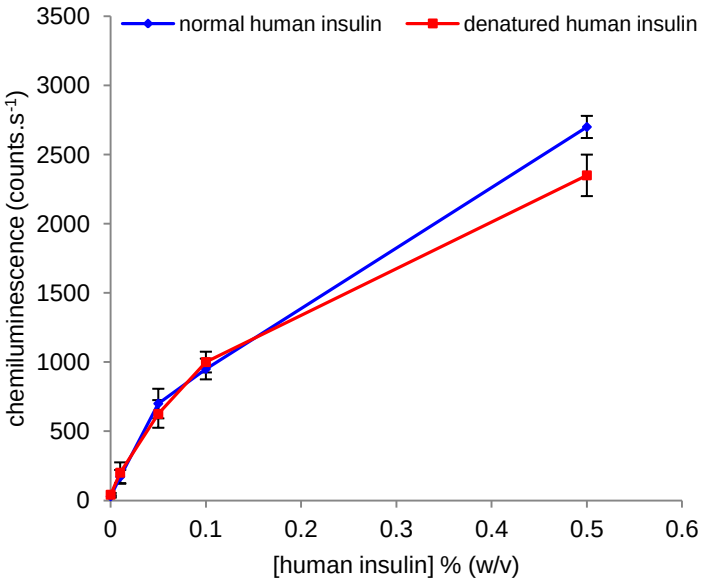


**Figure 3.9. The effect of thermal denaturation on human insulin catalysed coelenterazine chemiluminescence.** The coelenterazine chemiluminescence prior to the addition of normal insulin produced between 86 and 121 counts.$s^{-1}$ whereas the coelenterazine chemiluminescence prior to the addition of denatured insulin produced between 95 and 119 counts.$s^{-1}$. To determine the effect of thermal denaturation on human insulin catalysed coelenterazine chemiluminescence, 1 % (w/v) human insulin was heated in a thermocycler at 95 $^{o}$C for 15 minutes. Protein catalysed coelenterazine chemiluminescence was measured by adding 10 µl of normal and denatured human insulin (0.01 – 0.5 % (w/v); 0.1 – 5 g.$l^{-1}$ final concentration) to 90 µl of 50 mM HEPES buffer pH 7.4, containing 10 µM coelenterazine. The results represent the mean +/- SEM of three experiments.

### 3.3.2.2. The effect of increasing coelenterazine concentration on HSA catalysed coelenterazine chemiluminescence

In order to test the enzymatic activity of albumin the ability of the protein to become saturated by the substrate (coelenterazine) was also investigated. As the concentration of coelenterazine increased the chemiluminescence increased plateauing with the addition of 40 µM coelenterazine. This suggested that at a concentration of 40 µM coelenterazine the protein was saturated by the substrate. Therefore, it can be said that the light emission was saturable by the substrate, coelenterazine (fig. 3.10; half maximum ~ 20 µM).

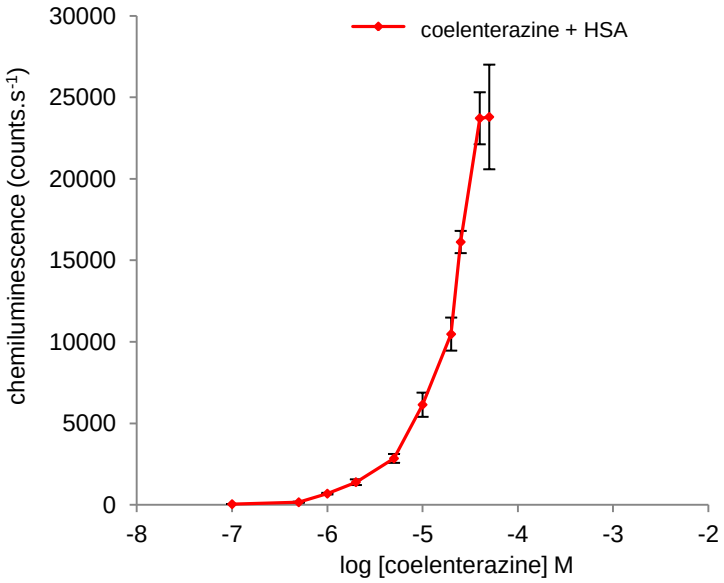


**Figure 3.10. The effect of varying coelenterazine concentration on human serum albumin (HSA) catalysed chemiluminescence.** The coelenterazine chemiluminescence produced between 42 and 195 counts.$s^{-1}$. To determine the effect of varying coelenterazine concentration on HSA catalysed coelenterazine chemiluminescence 10 µl of HSA (0.1 % (w/v); 1 g.$l^{-1}$ final concentration) was added to 90 µl of 50 mM HEPES buffer pH 7.4, containing 0.1 – 50 µM coelenterazine. The results represent the mean +/- SEM of three experiments.

### 3.3.2.3. The effect of increasing pH on protein catalysed coelenterazine chemiluminescence

In order to further investigate the enzymatic activity of albumin, the effect of increasing pH on HSA catalysed coelenterazine chemiluminescence was determined. The coelenterazine chemiluminescence catalysed by HSA increased with alkaline pH (fig. 3.11). The half maximum for HSA was pH 8.2 and plateaued at approximately pH 9.0 (fig. 3.11). The large increase in HSA catalysed coelenterazine chemiluminescence with increasing alkaline pH suggested that at least one basic amino acid was involved in catalysis.

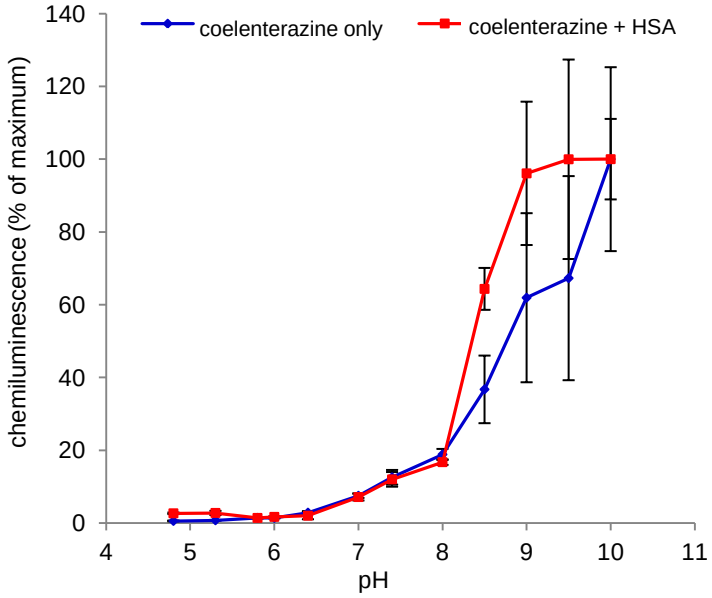


**Figure 3.11. The effect of pH on human serum albumin (HSA) catalysed coelenterazine chemiluminescence.** The effect of increasing pH on HSA catalysed coelenterazine chemiluminescence was determined by adding 10 µl of HSA (0.1 % (w/v); 1 $g.l^{-1}$ final concentration) to 90 µl of 50 mM phosphate buffer pH 4 – 10, containing 10 µM coelenterazine. The results represent the mean +/- SEM of three experiments. Coelenterazine chemiluminescence increased from 40 $counts.s^{-1}$ at pH 4.8 to 2,677 $counts.s^{-1}$ at pH 10 in the absence of albumin, whereas coelenterazine chemiluminescence increased from 1,852 $counts.s^{-1}$ at pH 4.8 to 100,189 $counts.s^{-1}$ at pH 10 in the presence of albumin.

In order to investigate the enzymatic activity of human insulin, the effect of increasing pH on protein catalysed coelenterazine chemiluminescence was determined. The coelenterazine chemiluminescence catalysed by human insulin increased with alkaline pH (fig. 3.12). The half maximum for human insulin was pH 7.8. Again the large increase in human insulin catalysed coelenterazine chemiluminescence with increasing alkaline pH suggested that at least one basic amino acid was involved in catalysis.

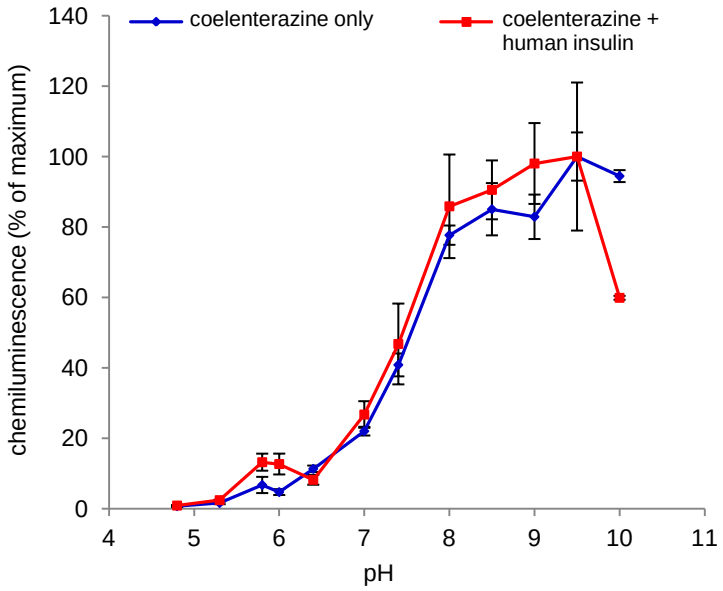


**Figure 3.12. The effect of pH on human insulin catalysed coelenterazine chemiluminescence.** The effect of increasing pH on human insulin catalysed coelenterazine chemiluminescence was determined by adding 10 µl of human insulin (0.1 % (w/v); 1 $g.l^{-1}$ final concentration) to 90 µl of buffer containing 50 mM sodium phosphate pH 4 – 10, containing 10 µM coelenterazine. The results represent the mean +/- SEM of three experiments. Coelenterazine chemiluminescence increased from 38 $counts.s^{-1}$ at pH 4.8 reaching a maximum of 145 $counts.s^{-1}$ at pH 9.5 in the absence of insulin, whereas coelenterazine chemiluminescence increased from 623 $counts.s^{-1}$ at pH 4.8 to reaching a maximum of 6,562 $counts.s^{-1}$ at pH 9.5 in the presence of insulin.

### 3.3.2.4. The effect of divalent cations on HSA (and insulin) catalysed coelenterazine chemiluminescence

In order to test the enzymatic activity of HSA, cations that are known to bind to the protein were added and the effect on coelenterazine chemiluminescence was investigated. HSA catalysed coelenterazine chemiluminescence was inhibited by all the cations tested. The inhibition observed ranged from 50 – 100 % (fig. 3.13 – fig. 3.17). The HSA catalysed coelenterazine chemiluminescence was significantly inhibited by $FeCl_3$ ($p < 0.001$; fig. 3.13). The results show that $FeCl_3$ alone (fig. 3.13A) over the concentration range $10^{-7}$ to $10^{-3}$ M did not significantly affect chemiluminescence when compared to the control in the absence of the cation. However, $10^{-2}$ M $FeCl_3$ alone did

significantly inhibit chemiluminescence ($p < 0.001$; fig. 3.13A). The maximum inhibition of HSA catalysed coelenterazine chemiluminescence by $FeCl_3$ over the concentration range $10^{-7}$ to $10^{-3}$ M was approximately 40 %, however the addition on $10^{-2}$ M $FeCl_3$ inhibited HSA catalysed coelenterazine chemiluminescence by 100 % (fig. 3.13B).

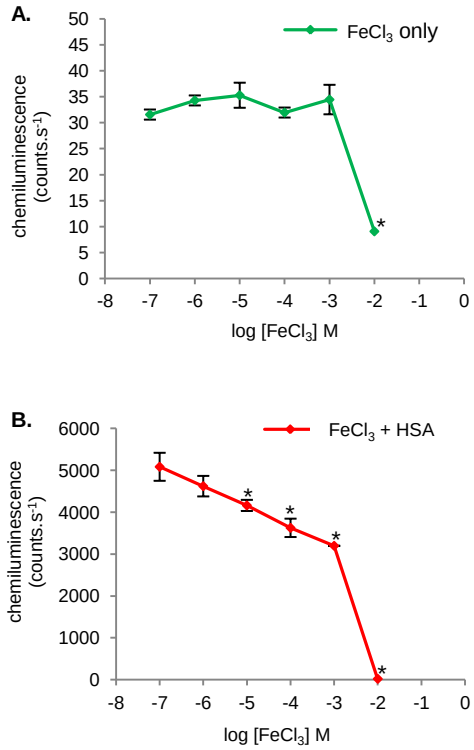


**Figure 3.13. The inhibition of human serum albumin (HSA) catalysed coelenterazine chemiluminescence by $Fe^{3+}$.** The machine background produced an average of 35 counts.$s^{-1}$ whereas the coelenterazine chemiluminescence produced averages of between 51 and 58 counts.$s^{-1}$. The effect of $Fe^{3+}$ on HSA catalysed coelenterazine chemiluminescence was measured by adding 10 µl of HSA (0.1 % (w/v); 1 g.$l^{-1}$ final concentration) to 90 µl of 50 mM HEPES buffer pH 7.4, containing 10 µM coelenterazine and $FeCl_3$ (0.0001 – 10 mM final concentration). The results represent the mean +/- SEM of three experiments. Asterisks indicate a significant difference where $p < 0.001$ when compared with the control in the absence of the $FeCl_3$.

$FeSO_4$ alone, over a concentration range of $10^{-6}$ – $10^{-5}$ M had no significant effect on chemiluminescence. However, the addition of $FeSO_4$ over the concentration range $10^{-4}$ – $10^{-2}$ M significantly inhibited chemiluminescence

between 30 - 100 % ($p < 0.001$; fig. 3.14A). The addition of increasing concentrations of $FeSO_4$ significantly inhibited HSA catalysed coelenterazine chemiluminescence reaching maximum inhibition in the presence of $10^{-2}$ M $FeSO_4$ ($p < 0.001$; fig. 3.14B).

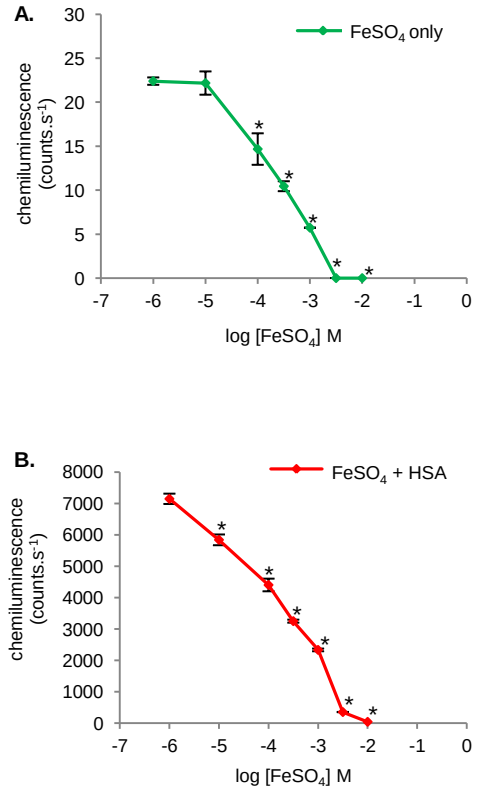


**Figure 3.14. The inhibition of human serum albumin (HSA) catalysed coelenterazine chemiluminescence by $Fe^{2+}$.** The machine background produced an average of 24 counts.$s^{-1}$ whereas the coelenterazine chemiluminescence produced averages of between 49 and 56 counts.$s^{-1}$. The effect of $Fe^{2+}$ on HSA catalysed coelenterazine chemiluminescence was measured by adding 10 µl of HSA (0.1 % (w/v); 1 g.$l^{-1}$ final concentration) to 90 µl of 50 mM HEPES buffer pH 7.4, containing 10 µM coelenterazine and $FeSO_4$ (0.001 – 10 mM final concentration). The results represent the mean +/- SEM of three experiments. Asterisks indicate a significant difference where $p < 0.001$ when compared with the control in the absence of the $FeSO_4$.

In order to determine which of the iron containing compounds were better at inhibiting HSA catalysed coelenterazine chemiluminescence, the inhibition by both $FeCl_3$ and $FeSO_4$ were compared (fig 3.15). $FeSO_4$ over the

concentration range $10^{-6}$ – $10^{-3}$ M decreased HSA catalysed coelenterazine chemiluminescence linearly, and a concentration of $10^{-2}$ M $FeSO_4$ resulted in maximum inhibition. The addition of $FeCl_3$ over the same concentration range also inhibited protein catalysed chemiluminescence linearly. However, $FeCl_3$ at a concentration of $10^{-3}$ M resulted in maximum inhibition of chemiluminescence. It can be concluded that $FeCl_3$ was better at inhibiting HSA catalysed coelenterazine chemiluminescence as maximum inhibition was observed with a concentration of $10^{-3}$ M whereas $10^{-2}$ M $FeSO_4$ was required for maximum inhibition.

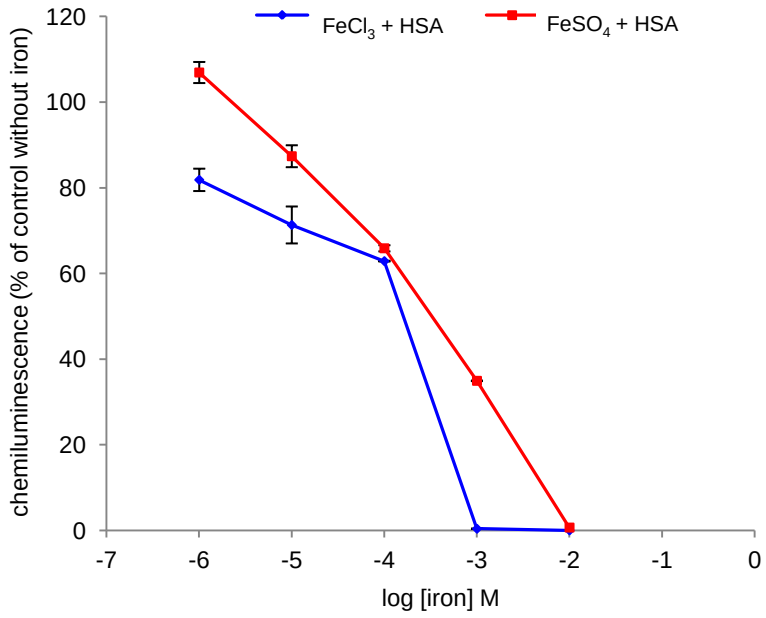


**Figure 3.15. The inhibition of human serum albumin (HSA) catalysed coelenterazine chemiluminescence by $Fe^{2+}$ and $Fe^{3+}$.** 10 µl of HSA (0.1 % (w/v); 1 $g.l^{-1}$ final concentration) was added to 90 µl of 50 mM HEPES buffer pH 7.4, containing 10 µM coelenterazine and $FeSO_4$ or $FeCl_3$ (0.001 – 10 mM final concentration). The results represent the mean +/- SEM of three experiments. $FeCl_3$ and $FeSO_4$ over the concentration range $10^{-6}$ – $10^{-2}$ M significantly inhibited HSA catalysed coelenterazine chemiluminescence. As the concentration of $FeCl_3$ and $FeSO_4$ increased the HSA catalysed coelenterazine chemiluminescence decreased from 4800 and 7100 $counts.s^{-1}$, respectively to 0 $counts.s^{-1}$.

$CaCl_2$ over the concentration range $10^{-3}$ – $10^{-1}$ M had no significant effect on chemiluminescence in the presence or absence of HSA (fig. 3.16).

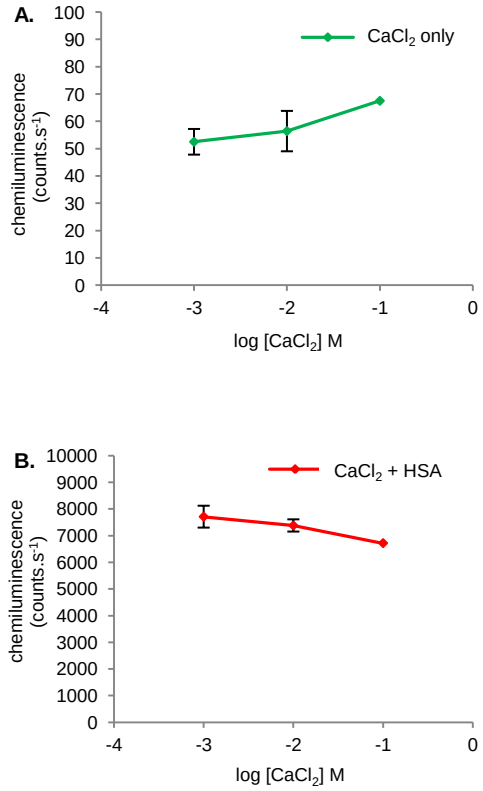


**Figure 3.16. The inhibition of human serum albumin (HSA) catalysed coelenterazine chemiluminescence by $Ca^{2+}$.** The machine background produced an average of 28 counts.$s^{-1}$ whereas the coelenterazine chemiluminescence produced averages of between 86 and 134 counts.$s^{-1}$. The effect of $Ca^{2+}$ on HSA catalysed coelenterazine chemiluminescence was measured by adding 10 µl of HSA (0.1 % (w/v); 1 g.$l^{-1}$ final concentration) to 90 µl of 50 mM HEPES buffer pH 7.4, containing 10 µM coelenterazine and $CaCl_2$ (1 – 100 mM final concentration). The results represent the mean +/- SEM of three experiments.

$ZnCl_2$ over the concentration range $10^{-7}$ – $10^{-3}$ M had no significant effect on the chemiluminescence in the absence of HSA (fig.3.17A). However, $ZnCl_2$ at a concentration of $10^{-2}$ M increased chemiluminescence, but this increase was not significant. The addition of $ZnCl_2$ at a concentration of $10^{-5}$ M or higher significantly inhibited HSA catalysed coelenterazine chemiluminescence and

maximum inhibition was observed in the presence of $10^{-2}$ M $ZnCl_2$ ($p < 0.001$; fig. 3.17B).

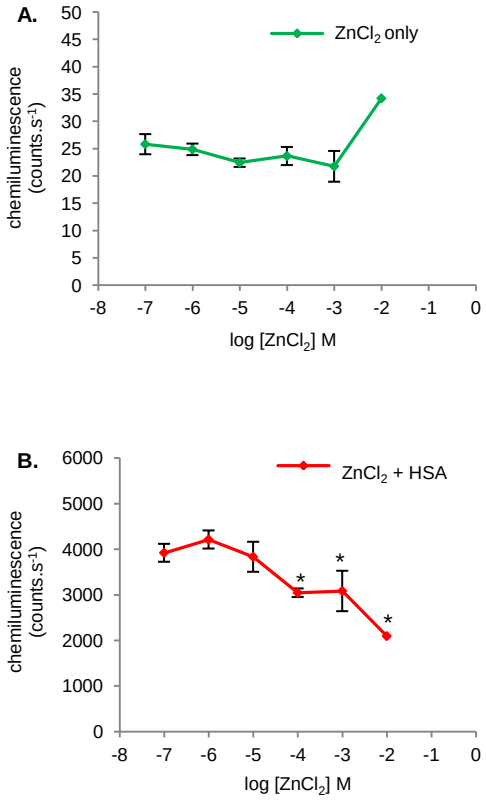


**Figure 3.17. The inhibition of human serum albumin (HSA) catalysed coelenterazine chemiluminescence by $Zn^{2+}$.** The machine background produced an average of 27 counts.$s^{-1}$ whereas the coelenterazine chemiluminescence produced averages of between 49 and 57 counts.$s^{-1}$. The effect of $Zn^{2+}$ on HSA catalysed coelenterazine chemiluminescence was measured by adding 10 µl of HSA (0.1 % (w/v); 1 g.$l^{-1}$ final concentration) to 90 µl of 50 mM HEPES buffer pH 7.4 containing 10 µM coelenterazine and $ZnCl_2$ (0.0001 – 10 mM final concentration). The results represent the mean +/- SEM of three experiments. Asterisks indicate a significant difference where $p < 0.001$ when compared with the control in the absence of $ZnCl_2$.

$ZnCl_2$ over the concentration range $10^{-5}$ – $10^{-2}$ M significantly increased chemiluminescence in the absence of human insulin ($p < 0.001$; fig. 3.18A). The addition of $ZnCl_2$ over the concentration range $10^{-5}$ – $10^{-2}$ M significantly increased insulin catalysed coelenterazine chemiluminescence between 100 and 250 % ($p < 0.0001$; fig. 3.18B).

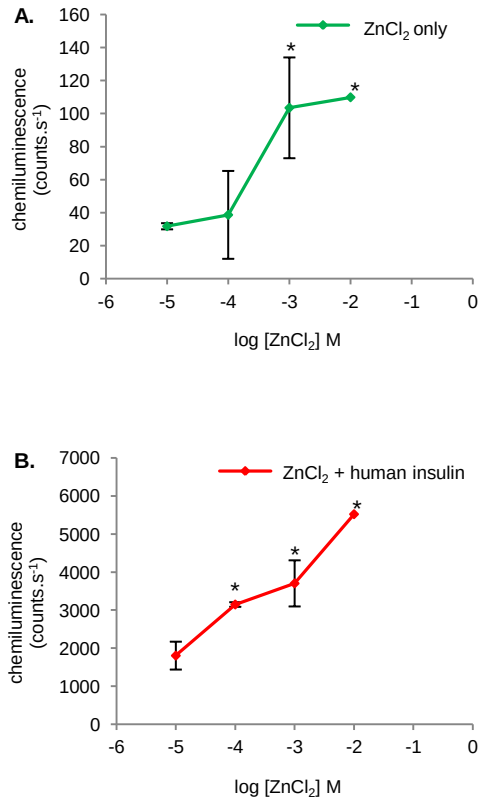


**Figure 3.18. The stimulation of human insulin catalysed coelenterazine chemiluminescence by $Zn^{2+}$.** The machine background produced an average of 24 counts.$s^{-1}$ whereas the coelenterazine chemiluminescence produced averages of between 85 and 100 counts.$s^{-1}$. The effect of $Zn^{2+}$ on human insulin catalysed coelenterazine chemiluminescence was measured by adding 10 µl of human insulin (0.1 % (w/v); 1 g.$l^{-1}$ final concentration) to 90 µl of 50 mM HEPES buffer pH 7.4 containing 10 µM coelenterazine and $ZnCl_2$ (0.01 – 10 mM final concentration). The results represent the mean +/- SEM of three experiments. Asterisks indicate a significant difference where $p < 0.0001$ when compared with the control in the absence of $ZnCl_2$.

Interestingly $ZnCl_2$ over the concentration range $10^{-5}$ – $10^{-2}$ M inhibited HSA catalysed chemiluminescence but it activated human insulin catalysed coelenterazine chemiluminescence. $ZnCl_2$ over the concentration range $10^{-5}$ – $10^{-2}$ M inhibited HSA catalysed coelenterazine chemiluminescence between 20 – 50 % whereas $ZnCl_2$ over the same concentration range significantly enhanced human insulin catalysed coelenterazine chemiluminescence between 100 – 250 % (fig. 3.19).

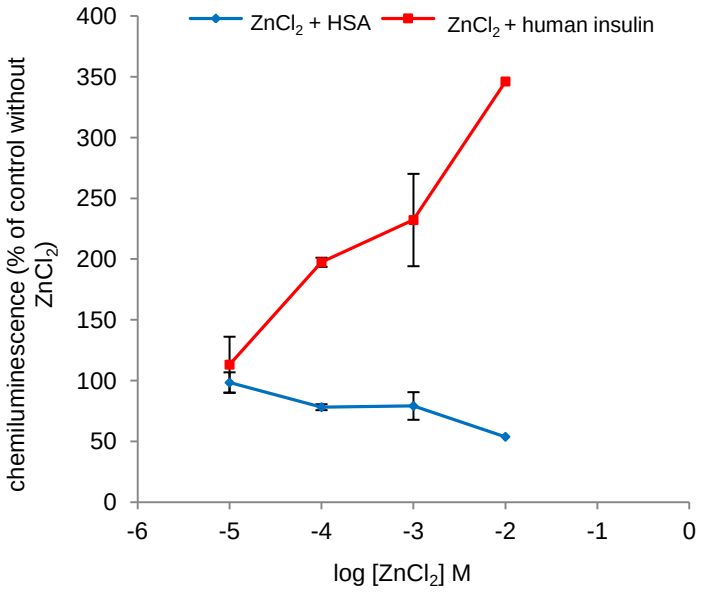


**Figure 3.19. The effect of $Zn^{2+}$ on human serum albumin (HSA) and human insulin catalysed coelenterazine chemiluminescence.** 10 µl of HSA or human insulin (0.1 % (w/v); 1 $g.l^{-1}$ final concentration) was added to 90 µl of 50 mM HEPES pH 7.4 containing 10 µM coelenterazine and $ZnCl_2$ (0.01 – 10 mM final concentration). The coelenterazine chemiluminescence prior to the addition of the protein was subtracted from the chemiluminescence catalysed by the protein. The results represent the mean +/- SEM of three experiments. As the concentration of $ZnCl_2$ increased, albumin catalysed coelenterazine chemiluminescence decreased from 3800 to 2100 $counts.s^{-1}$ however, insulin catalysed coelenterazine chemiluminescence increased from 1600 to 5400 $counts.s^{-1}$.

It can be concluded that all the cations tested inhibited HSA catalysed coelenterazine chemiluminescence by 50 – 100 %. The cations can be ranked in order starting with the best at inhibiting HSA catalysed protein coelenterazine chemiluminescence: $Fe^{2+}/Fe^{3+} > Zn^{2+}$.

### 3.4. Discussion and conclusions

The results in this chapter show that the two main plasma proteins, albumin and insulin can catalyse coelenterazine chemiluminescence (fig. 3.6 and fig. 3.7). Surprisingly, haemoglobin, an oxygen carrier, produced very small chemiluminescence and was approximately 1000 times lower than the chemiluminescence observed with albumin. The ability of albumin to catalyse coelenterazine chemiluminescence was consistent with the protein having a mono-oxygenase activity in which one atom of oxygen is transferred to coelenterazine and the other to carbon dioxide, $CO_2$. Albumin was considered to have a mono-oxygenase activity because it was heat denaturable (fig. 3.8), it exhibited saturable substrate characteristics (fig. 3.10) and was inhibited or stimulated by cations that are known to bind to the protein (fig. 3.12 to fig. 3.15).

The increase in chemiluminescence observed with alkaline pH was consistent with the presence of at least one basic amino acid residue being involved in the binding of coelenterazine. Only a few important amino acids in the coelenterazine binding site are required for the binding of coelenterazine and/or to catalyse chemiluminescence. The pH at the half maximum, pH 8.2 and pH 7.8 for albumin and human insulin, respectively, represent the pKa of the group in the protein that is important for catalysis. The chemiluminescence from both albumin and human insulin increased with alkaline pH. The albumin catalysed coelenterazine chemiluminescence curve was different to the coelenterazine chemiluminescence curve before the addition of the protein, this implicates that there is a direct effect on the protein taking place. However, with human insulin, the human insulin catalysed coelenterazine chemiluminescence curve was not significantly different from the coelenterazine chemiluminescence curve prior to the addition of the protein, this may be due to coelenterazine possessing different ionic forms or that insulin is not actually binding coelenterazine but is in fact producing superoxide instead.

The addition of the cations, $Fe^{2+}$, $Fe^{3+}$ and $Zn^{2+}$ inhibited albumin catalysed coelenterazine chemiluminescence. The addition of $FeCl_3$ (0.0001 – 1 mM final concentration) did not affect chemiluminescence and this suggested that there was a direct effect on the protein; however the addition of 10 mM $FeCl_3$ completely abolished chemiluminescence.

The complete inhibition observed with the addition of 10 mM $FeCl_3$ could be due to the removal of oxygen from the solution. The addition of 3 mM $FeSO_4$ also completely abolished chemiluminescence and again this could be due to the complete removal of oxygen from the solution. HSA plays an essential role in the transport and metabolism of $Zn^{2+}$ (Masuoka *et al.,* 1993). Interestingly, $Zn^{2+}$ that is known to bind to insulin and form crystals in pancreatic β-cells produced opposite effects on HSA and human insulin catalysed coelenterazine chemiluminescence. The addition of $Zn^{2+}$ significantly enhanced human insulin catalysed coelenterazine chemiluminescence, increasing light emission by 4-fold.

HSA has enzymatic activity or coelenterazine-luciferase activity, and is responsible for catalysing the conversion of the luciferin, coelenterazine, to coelenteramide in the presence of oxygen *via* an intermediate, resulting in the generation of light. Although BSA and HSA have a 78 % sequence similarity, BSA exhibited a higher luciferase activity and was significantly better at catalysing the coelenterazine chemiluminescence reaction.

As well as its ligand binding properties, it is known that the interaction between a small molecule and albumin can result in the protein displaying enzymatic activity. Albumin can also act as a thioesterase due to the presence of a free sulphydryl (free-SH) group at Cys34 (Varshney *et al.,* 2010). The enzymatic properties displayed by HSA can be stereospecific. Molecular dynamic simulation studies have shown the presence of both a deprotonated Lys199 and a protonated Lys195, and it is predicted that these residues are what facilitate the enzymatic activity of the protein. The short distance of 6.73 Å between these two residues determined by x-ray crystallography supports this (Kragh-Hansen *et al.,* 2002).

The HSA subdomain IIIA has a well known esterase-like activity towards substrates. The esterase-like activity of this particular domain is due to the close proximity and protrusion of two residues, Arg410 and Tyr411 into the centre of site II. The distance between the reactive group of the tyrosine residue and the nitrogen atoms of the arginine residue in the crystal structure is short, measuring approximately 2.7 Å. This may explain the unusual reactivity of this residue towards nucleophilic substitution.

These residues are important for the different functions of HSA and this is emphasised by the finding of both these residues in other mammalian albumins (Kragh-Hansen *et al.,* 2002, Yang *et al.,* 2007).

Watanabe et al (2000) have shown that Arg410 is closely involved in the esterase-like activity of HSA. They replaced the Tyr411 residue that is predicted to be the nucleophile involved in the hydrolytic reaction of HSA with alanine or phenylalanine and they found that the hydrolytic activity towards *p*-nitrophenyl acetate was completely abolished. However, the addition of serine at position 411 produced about 21 % activity, suggesting it is the presence of a hydroxyl group at this position as well as the nature of its surroundings that are crucial for the enzymatic activity of HSA (Varshney *et al.,* 2010, Watanabe *et al.,* 2000).

For proteins that have been confirmed to have enzymatic activity, denaturation is defined as the loss of enough structure leading to the inactivation of the enzyme. Increasing temperature is a factor that is known to denature proteins. When proteins become exposed to increasing temperature, they lose their enzymatic activity. This change in the protein may be reversible or irreversible but that depends on the protein and the severity of the heating, for example, a temperature of 95 $^{o}$C would be sufficient enough to cause irreversible denaturation of HSA. Depending on the conditions to which the protein has been exposed, HSA can undergo reversible and irreversible thermal unfolding and refolding (Mitra *et al.,* 2007).

It has been shown that the thermal denaturation of HSA produces two transitions, A and B. Transition A is a minor transition that corresponds to temperatures below 65 $^{o}$C. This transition is due to the reversible conformational changes that take place before protein unfolding. Transition A, also has 3 sub-transitions known as sub-transitions i, ii and iii. These sub-transitions occur one after another and are said to be related to the links between the three structural domains of HSA. Sub-transitions i, ii and iii occur at temperatures 27, 35 and 42 $^{o}$C, respectively. A mild conformational change in protein structure and thus reversible denaturation without the exposure of the pockets, leads to HSA aggregation during the first sub-transition. However, transition B is a major transition that corresponds to the thermal unfolding of the protein through an irreversible process (Rezaei Tavirani *et al.,* 2006).

Therefore, it can be said that HSA is denatured through this multi-step unfolding pathway:

$$N \leftrightarrow E \rightarrow I \rightarrow U$$

Where N is the native form of HSA, E is the expanded form, I is an intermediate in which domain II of the protein is unfolded but domain I is intact and U is the unfolded protein.

When the temperature is below 50 $^{o}$C HSA domain separation occurs, resulting in the irreversible separation of domains I and II generating a conformational change in the protein structure.

Further increasing the temperature above 50 $^{o}$C but still keeping it below 70 $^{o}$C causes irreversible unfolding of domain II and when the temperature is increased above 70 $^{o}$C it leads to the irreversible unfolding of domain I. Domain II of HSA needs to be completely unfolded before domain I can unfold. The U state is partially unfolded and is therefore not a completely unfolded random coil. This is due to the unfolding of the pocket containing the free-SH group of Cys34 enabling disulphide bonds to be formed within various domains, and/or the presence of some intramolecular cooperation in the thermal denaturation that act to maintain some degree of the structure (Rezaei Tavirani *et al.,* 2006).

From this it can therefore be concluded that when the protein was exposed to a temperature of 95 $^{o}$C for 15 minutes HSA was irreversibly denatured thus preventing it from refolding when cooled, resulting in its reduced enzymatic activity, hence the significant decrease in HSA catalysed coelenterazine chemiluminescence that was observed. However, it has since been shown that under more extreme circumstances HSA activity was inhibited by > 90 % by heat denaturation (Vassel *et al.,* 2012). Surprisingly, human insulin was not denatured under the same conditions as those used with HSA. This may be due to human insulin being a much smaller protein than HSA, thus making it more difficult to denature. Therefore, further work needs to be carried out to determine the conditions required for the denaturation of human insulin, for example, heating the protein at 95 $^{o}$C for a longer period of time.

To determine the maximum speed of the coelenterazine chemiluminescence reaction (fig. 3.8), the coelenterazine concentration was increased until a constant rate of product formation was seen. From this the substrate

concentration ($K_m$) at which the rate is half of the $V_{max}$ can be determined. It can be seen that at a coelenterazine concentration of 40 µM the protein became saturated. Saturation occurs because as the coelenterazine concentration increased, more of the free-HSA is converted to the coelenterazine-HSA form. Therefore, the apparent $K_m$ was shown to be approximately 20 µM.

It was not possible to determine the $K_m$ for insulin as an experiment to determine the chemiluminescence in the presence of increasing coelenterazine concentrations was not carried out. Further work can be carried out to demonstrate whether the effect of insulin on coelenterazine chemiluminescence is saturable and to test if it is binding or generating superoxide which is an established oxidant for coelenterazine. The maximum number of substrate molecules that an enzyme can convert into product for each catalytic site in a unit of time is known as the turnover number or $k_{cat}$. Turnover numbers ($k_{cat}$) can vary quite dramatically from 6 $x10^5$ $s^{-1}$ for the enzyme carbonic anhydrase to 4, 1 and 1 $s^{-1}$ for the bioluminescent enzymes *Obelin*, *Renilla luciferase* and *Aequorea*, respectively (Vassel *et al.,* 2012). The $k_{cat}$ of HSA has been calculated to be approximately 1 x $10^{-3}$ $s^{-1}$ which is significantly slower than those mentioned above.

In a solution of neutral pH the amino acids of a protein exist as zwitterions (dipolar ions). When in the dipolar form, the amino group of the amino acid is protonated ($+NH_3^+$) whereas the carboxyl group of the amino acid is deprotonated ($-COO^-$). Under acidic conditions, the amino group of the amino acid is protonated whereas the carboxyl group is not dissociated (-COOH). As the pH rises and the solution becomes more alkaline, the carboxylic acid is the first to lose a proton. The amino acids maintain the dipolar form until pH 9 has been reached and it is then the turn of the amino group to lose a proton (Berg *et al.,* 2002).

HSA undergoes pH-dependent reversible conformational isomerisation. At neutral pH, HSA presents itself in the neutral or native (N) form which is characterised by its heart-shaped structure (Fasano *et al.,* 2005). In acidic conditions, the protein undergoes a conformational transition, resulting in the production of two isomeric forms, the fast (F) and the expanded (E) form (Muzammil *et al.,* 1999). When the native albumin is exposed to a solution of pH 6.0 to 3.0 it forms the N-F transition. This N-F transition results in reduced

α-helical content but an increase in β-sheet content. However, when the protein is exposed to a more acidic solution, pH 3.0 and below, it forms the F-E transition and it is here where the protein further unfolds. It is called the expanded form because it expands as much as the disulphide bonds will allow it. The F-E transition leads to a further decrease in α-helical content as well as an increase in β-sheet content (Dockal *et al.,* 2000).

Under slightly alkaline conditions, from neutral pH to pH 9.0, albumin can undergo a further conformational change producing the basic (B) form and this change is known as the N-B transition. However, this N-B transition is more subtle as well as having a gradual onset.

Within this pH range, HSA displays a small decrease in α-helical content and a slight increase in β-sheet content (Dockal *et al.,* 2000). Also when in this pH range, HSA has an increased affinity for some ligands (e.g. warfarin).

As previously mentioned, when the pH rises above 9.0 it becomes the turn of the amino group to lose a proton (Berg *et al.,* 2002). Therefore, as the pH rises, only the imidazole groups of the histidines and the terminal amino group of the protein are able to lose protons (Bos *et al.,* 1989).

Albumin is negatively charged but cations can bind weakly and reversibly to the protein (Varshney *et al.,* 2010). Several cations are known to bind to both albumin and insulin. Of the cations tested, $Fe^{2+}$, $Fe^{3+}$ and $Zn^{2+}$ ($p < 0.001$; fig. 3.13 – fig. 3.15 and fig. 3.17) significantly inhibited coelenterazine chemiluminescence catalysed by HSA, however, this was dependent on the concentration and had a potency of $Fe^{2+}/Fe^{3+} > Zn^{2+}$. The addition of $Ca^{2+}$ (fig. 3.16) did not affect the coelenterazine chemiluminescence catalysed by HSA. The cation binding site is unknown and it is possible that the effect produced by these cations was due to an allosteric effect. Interestingly, zinc produced opposite effects on coelenterazine chemiluminescence modulated by HSA and human insulin. The addition of zinc significantly inhibited coelenterazine chemiluminescence catalysed by HSA (fig. 3.17) whereas the addition of zinc significantly enhanced the coelenterazine chemiluminescence catalysed by human insulin (fig. 3.18).

Albumin is the main zinc transporter in the plasma and can bind approximately 80 % of all zinc found in the plasma. As well as zinc, albumin has been shown to bind many other metal ions (e.g. Ca(II)). Zinc can bind with a high affinity to

albumin and this site is the primary binding site for Zn(II). The zinc binding site is located at the boundary between domain I and domain II (Lu *et al.,* 2008). This high affinity of zinc for albumin explains why when the concentration of zinc increased the light emission decreased. As the concentration of zinc increased, these ions are more likely to become bound to the protein, due to their high affinity for albumin, thus inhibiting the binding of coelenterazine leading to decreased light emission.

The biologically active insulin that circulates in the bloodstream is a monomer consisting of an A and a B chain made up of 21 and 30 amino acids, respectively. Insulin can pair with itself at micromolar concentrations resulting in the formation of a dimer. Dimerisation occurs when hydrogen bonds are formed between the ends of the two B-chains of the two insulin monomers (De Meyts, 2004). Still at micromolar concentrations but also in the presence of zinc ions, three dimers (6 monomers) can join together resulting in the formation of a hexamer (De Meyts, 2004). The 3D structure of insulin is composed of three helices and 3 disulphide bridges. The hydrophobic amino acid residues are clustered on the inner surface of the molecule whereas the polar amino acid residues are on the outside of the molecule. This arrangement of hydrophobic and polar amino acid residues results in the stabilisation of the molecule. The three disulphide bridges are formed between the –SH groups on cysteine residues. There are six cysteine residues found on the structure explaining why three disulphide bridges are formed.

Two of the disulphide bridges are formed between the A and B chains of the structure and the third disulphide bridge is formed within the A chain. These also contribute to stability to the molecule.

Insulin is synthesised by the pancreatic β-cells in the islets of Langerhans *via* the two insulin precursors – preproinsulin and proinsulin. In the Golgi apparatus of the cells, proinsulin is gathered in the storage vesicles that are rich in zinc. Here proteolytic enzymes remove the C-peptide from proinsulin resulting in insulin. In the secretory vesicles zinc will then interact with the insulin resulting in the formation of stable water-insoluble crystals of the zinc-insulin hexamer ($Zn_2Insulin_6$) (Dunn, 2005, Noormagi *et al.,* 2010). The addition of zinc to insulin causes the protein to undergo a conformational change. This conformational change enhances the binding of insulin to the insulin receptor (Faure *et al.,* 1992).

Aggregation usually occurs at high concentrations where there are increased numbers of the insulin monomers (Hua and Weiss, 2004). It is known that the formation of the $Zn_2Insulin_6$ hexamer prevents insulin aggregation. For example, insulin concentrations in the storage vesicles are high (~ 21 mM) but no aggregation occurs due to the presence of zinc ions (~ 11 mM) which stabilise the high insulin concentrations by forming water-insoluble crystals of $Zn_2Insulin_6$ (Noormagi *et al.,* 2010).

However, when no zinc ions are present, it is possible for insulin to still form hexamers and prevent insulin aggregation at high concentrations. Insulin aggregation at high concentrations is slower than aggregation at low concentrations, suggesting that oligomerization prevents insulin aggregation (Noormagi *et al.,* 2010).

Enhanced coelenterazine chemiluminescence in the presence of human insulin may be due to zinc causing the protein to undergo a conformational change and it is this change that allows the coelenterazine to bind more effectively thus resulting in increased light emission. It is possible that at the high concentration used for the catalysis of coelenterazine chemiluminescence that insulin was in the hexameric form and was not subjected to aggregation even in the absence of zinc ions.

At neutral pH and in the presence of zinc, dimeric insulin can further assemble to form a relatively stable hexamer that consists of three dimeric units. Conformational changes in tertiary structure of the hexamer may alter the biological activity of the protein. The hexamer can take one of three conformations but the importance of each of these individual conformations still remains unknown. However, what is known is that these conformational changes will affect receptor binding (Chausmer, 1998). When zinc ions were added along with human insulin, coelenterazine chemiluminescence was enhanced. This suggested that the presence of zinc caused the protein to undergo a conformational change and it is potentially this change that allows coelenterazine to bind more effectively, thus resulting in the increased light emission observed.

The plasma is rich in HSA and it is this protein that plays a significant role in the transport and metabolism of drugs (Yang *et al.,* 2007). It was necessary to use the coelenterazine chemiluminescence model to investigate if this model has the potential to be developed into a clinical test that can determine the

pharmacokinetics of new drugs before they are placed on the market for sale. To test this using this model, drugs that are already known to bind to insulin, such as warfarin, should affect the biological activity of the protein.

The results showed that albumin has mono-oxygenase activity, however, the mono-oxygenase activity of albumin in physiology and pathophysiology needs to be investigated. The results showed that cations can inhibit or stimulate protein catalysed coelenterazine chemiluminescence. A further prediction is that drugs that are known to bind to albumin should inhibit chemiluminescence if they bind to the same site as coelenterazine. In order to confirm this it would be necessary to do molecular 3D modelling. The next aim would be to investigate the covalent modification of proteins by MeG (and potentially other toxins) on protein catalysed coelenterazine chemiluminescence.

# Chapter 4:

# Testing the hypothesis that albumin and insulin chemiluminescence is enzymatic

## 4.1. Introduction

It has been shown in the previous chapter that both albumin and surprisingly insulin catalyse coelenterazine chemiluminescence. For a protein to be considered as an enzyme it must adhere to 4 criteria: denaturable, saturable by the substrate, cations and drugs that are known to bind to the protein should affect the biological activity of the protein. The previous chapter has shown that HSA is denaturable, saturable by the substrate and that cations can either inhibit or activate protein catalysed coelenterazine chemiluminescence. It is predicted that coelenterazine binds to a site on albumin and since albumin contains two major binding sites for pharmaceuticals it is possible to determine to which of these sites coelenterazine would bind. Molecular 3D modelling can also be used to either predict or confirm the coelenterazine binding site on albumin.

Proteins are macromolecules that are made up of amino acids arranged in different sequences of varying lengths, enabling them to form different 3D structures and to carry out a range of biological functions. Under natural conditions, the protein is flexible. Regulatory proteins have different binding sites and can undergo a conformational change when a ligand binds to one of these sites. Some monomeric proteins are able to bind more than one ligand at a time at different sites. This is one feature of human serum albumin (HSA) as it is able to bind a diverse range of biologically active molecules (Deeb *et al.,* 2009).

### 4.1.1. Human serum albumin

Human serum albumin (HSA) is synthesised in and secreted from liver cells (Fasano *et al.,* 2005). HSA is part of a multi-gene family of proteins. They are large globular proteins that have many domains and as it is the major soluble protein in the blood it has many physiological roles. HSA aids the transport, distribution, metabolism and excretion of many endogenous and exogenous ligands. Ligands can include molecules such as fatty acids, steroids, metals (e.g. calcium and zinc) (He and Carter, 1992), as well as a number of commonly used drugs with acidic or electronegative features, such as warfarin, diazepam and ibuprofen (Ghuman *et al.,* 2005).

### 4.1.2. The structure of HSA

HSA is a major extracellular protein and has a concentration of 0.6 mM (40 mg/ml) in blood plasma (Tajmir-Riahi, 2007), therefore approximately 50 – 60 % of the total plasma protein found in humans is HSA (Simard *et al.,* 2006). It is a single polypeptide chain made up of 585 amino acids and has a molecular weight of 66,500 Da. At neutral pH, the polypeptide forms a heart-shaped structure with the dimensions of 80 x 80 x 80 x 30 Å (Otagiri, 2005).

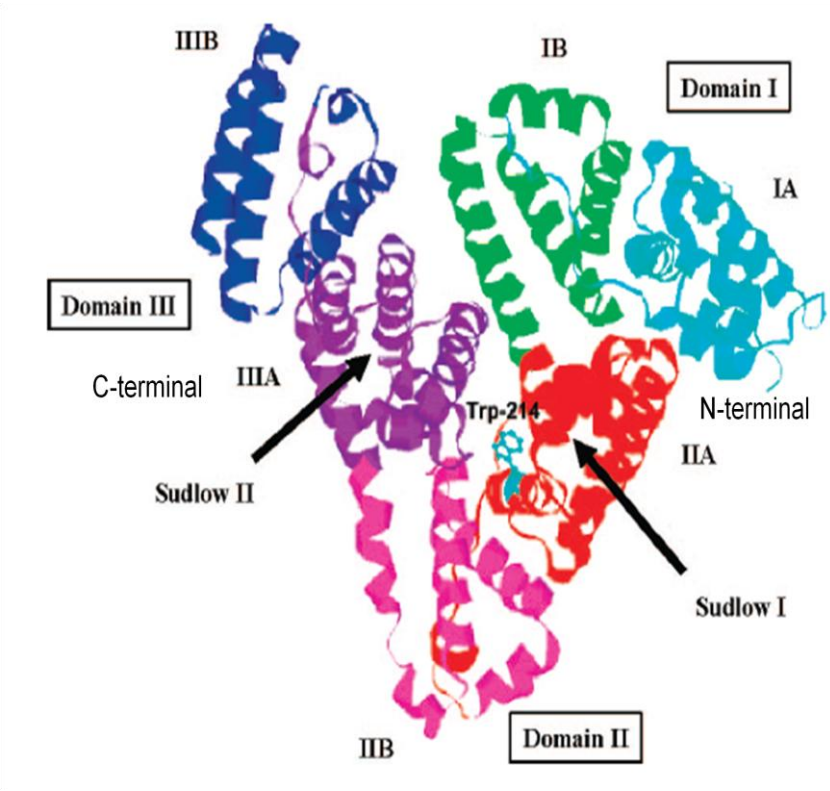


**Figure 4.1. Ribbon diagram of human serum albumin (HSA) showing the three major domains (domains I, II and III) and the six subdomains.** The six subdomains are coloured as follows**:** subdomain IA: light blue; subdomain IB: green; subdomain IIA: red; subdomain IIB: pink; subdomain IIIA: purple and subdomain IIIB: dark blue. The two primary binding sites, Sudlow's sites I and II, named after their founder are also shown. The lone tryptophan residue (Trp214) located in the middle of subdomain IIA is indicated (Abou-Zied and Al-Shihi, 2008).

HSA is formed from three topologically similar homologous domains (fig. 4.1). Domain I consists of residues 1 to 195, domain II consists of residues 196 to 383 and domain III consists of residues 384 to 585. Each of these domains is then made up of two separate helical subdomains known as subdomains A and B. Subdomain A consists of six α-helices flanked by two short α-helices whereas subdomain B consists of 4 α-helices (Sugio *et al.,* 1999). This shows that approximately 67 % of the HSA structure is made up of α-helices, however, no β-sheets exist in the structure (Otagiri, 2005). There are 35 cysteine residues throughout the structure and all but one of these residues (Cys34) are involved in the formation of 17 disulphide bridges to stabilise the subdomains (Fasano *et al.,* 2005, Tajmir-Riahi, 2007).The terminal regions of sequential domains can form interdomain helices. The N-terminal region was formed by linking subdomain IB to subdomain IIA, whereas, the C-terminal region was formed by linking subdomain IIB to subdomain IIIA (Fasano *et al.,* 2005). Crystallographic studies of HSA complexed with a diverse range of drugs and other biomolecules have revealed the binding sites as well as their locations on the protein. Until now, the binding sites for fatty acids, ions, thyroxine, bilirubin and a range of drugs have been identified (Varshney *et al.,* 2010).

### 4.1.3. HSA binding regions

Where the ligand will bind on HSA will largely depend on both the molecular and physical properties of the ligand and this helps to explain why all ligands do not bind to the same site on the protein (Sahoo *et al.,* 2008).

#### 4.1.3.1. The fatty acid binding regions

Many fatty acid (FA) binding sites are widely distributed throughout the protein across all six subdomains. High-resolution crystal structures of fatty acids bound to HSA have identified seven binding sites with different affinities distributed throughout the protein. FA binding sites can be found in subdomains IB, IIIA, IIIB as well as on the interfaces of the subdomains (Varshney *et al.,* 2010).

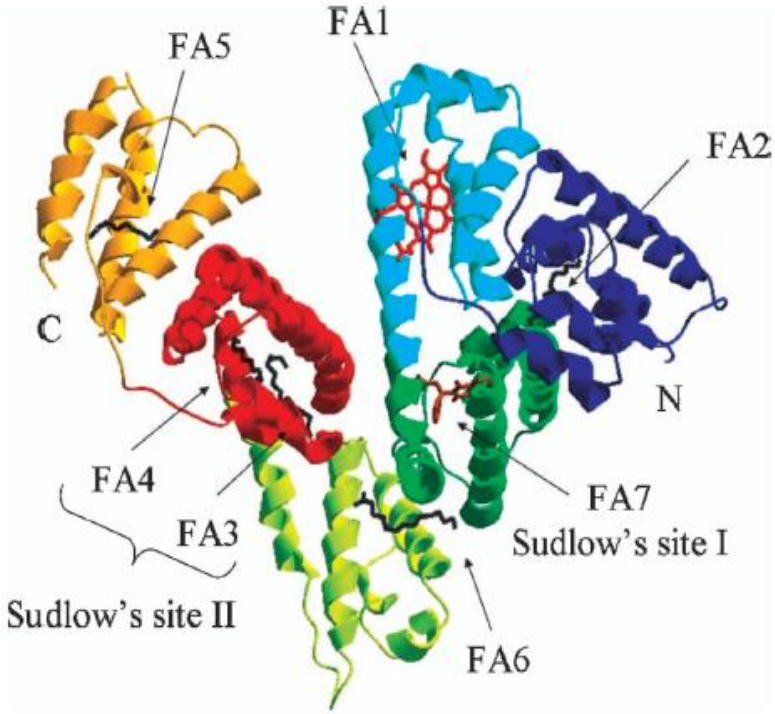


**Figure 4.2. Ribbon diagram of human serum albumin (HSA) showing the seven fatty acid binding sites distributed throughout the protein.** The subdomains are coloured as follows: subdomain IA: light blue; subdomain IB: dark blue; subdomain IIA: dark green; subdomain IIB: light green; subdomain IIIA: red and subdomain IIIB: orange (Fasano *et al.,* 2005).

If a compound is unable to bind to HSA, the compound can couple to a ligand, such as a FA and then bind to the protein (Varshney *et al.,* 2010). Therefore, the FA binding sites are also capable of binding other ligands as well as fatty acids. Sudlow et al (1975) identified and characterised two specific drug binding sites, now typically known as Sudlow's site I and site II after their founder. These two binding sites can overlap with some of the FA binding sites (fig. 4.2). Sudlow's site I which is located in subdomain IIA overlaps with FA site 7. FA site 7 is a low affinity binding site and at least two of its amino acid side-chains are shared with FA site 2. FA site 2 can be found at the interface between subdomains IA, IB and IIIA. A FA site found in subdomain IB also acts as a heme binding site. Sudlow's site II which is located in subdomain IIIA overlaps with both FA site 3 and FA site 4. FA site 1 not only binds fatty acids but it is also the primary binding site for haemin. FA site 5 is

located within subdomain IIIA and is also a secondary binding site for the drug propofol (a general anaesthetic) and thyroxine. Finally, FA site 6 is a low affinity binding site and is a secondary binding site for non-steroidal anti-inflammatory drugs (e.g. ibuprofen) (Simard *et al.,* 2006, Fasano *et al.,* 2005).

#### 4.1.3.2. The metal-binding regions

A number of studies have been carried out on the metal-binding properties of HSA and the results have shown that metal ions can bind to various sites on the protein (Chan *et al.,* 1995). The lone cysteine residue at position 34 (Cys34) is found at the base of a hydrophobic pocket and it favours the binding of hydrophobic complexes belonging to heavy metal ions (e.g. gold, $Au^{+}$). However, there are three other sites that are more versatile and easier to access. The best characterised metal-binding site is located on the N-terminal and it is made up of the first three amino acid residues of the HSA sequence (Sokolowska *et al.,* 2010). This metal-binding site and the N-terminal have a high affinity for copper and nickel (Tajmir-Riahi, 2007, Varshney *et al.,* 2010, Chan *et al.,* 1995).

#### 4.1.3.3. The two main drug binding regions

HSA can bind, either covalently or reversibly, a diverse range of endogenous and exogenous compounds. There are multiple drug binding sites that are distributed throughout the protein (fig. 4.3), however many drugs can bind to one or very few high-affinity sites that have association constants ($K_a$) within the range of $10^{-4}$ to $10^{-6}$ $M^{-1}$ (Table 4.1) (Kragh-Hansen *et al.,* 2002). The two main drug binding sites are known as Sudlow's site I and II and are named after their founder (Sudlow *et al.,* 1975, Varshney *et al.,* 2010). The *in vivo* concentration of a drug is significantly lower than the HSA concentration in the blood and therefore at therapeutic drug concentrations, only a small number of the available binding sites on HSA are occupied (Yamasaki *et al.,* 1996). The next section will focus on these two binding sites in detail.

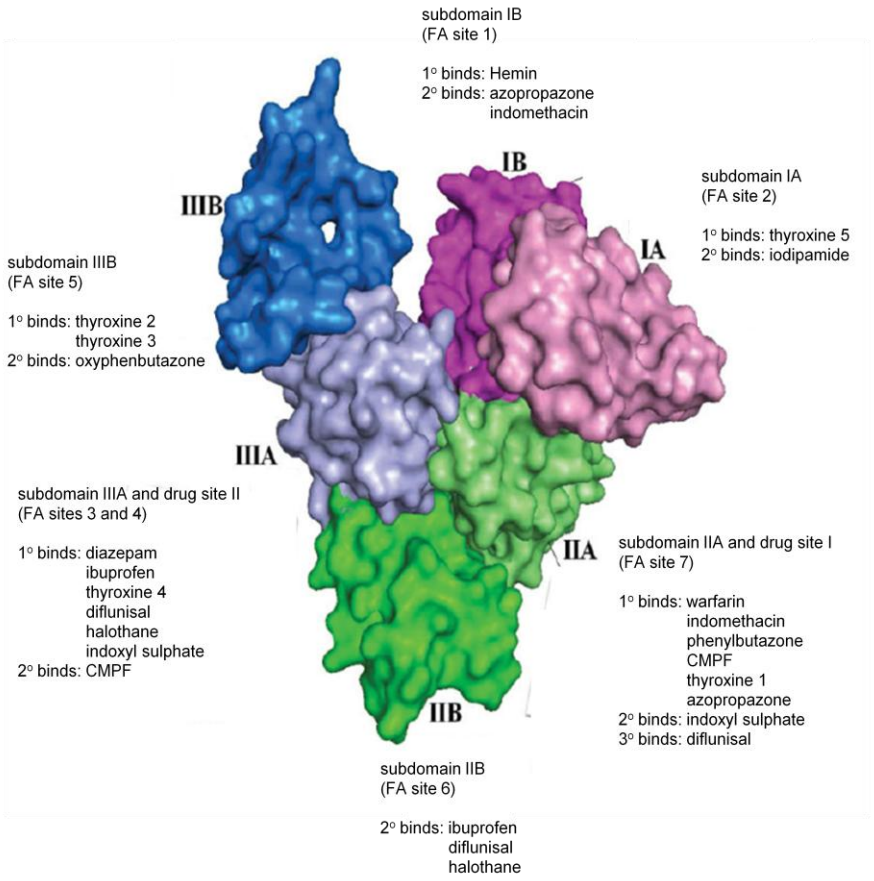


**Figure 4.3. The ligand binding capacity of human serum albumin (HSA).** The six subdomains are coloured as follows: subdomain IA: pink; subdomain IB: purple; subdomain IIA: light green; subdomain IIB: dark green; subdomain IIIA: light blue and subdomain IIIB: dark blue (Varshney *et al.,* 2010).

### 4.1.4. Ligand binding at Sudlow's site I

Sudlow's site I, also known as the warfarin binding site and can be found within subdomain IIA (Fujiwara and Amisaki, 2006). It is a pre-formed binding pocket (containing the FA site 7). It is composed of 6 α-helices and a loop helix (residues 148-154) that is donated from subdomain IB. The interior of the binding pocket is mostly apolar but does contain two groups of polar residues. One group of polar resides can be found on the base of the pocket and consists of residues Tyr150, His242 and Arg257 whereas the other polar group can be found at the entrance to the pocket and consists of residues Lys195, Arg218 and Arg222 (Otagiri, 2005, Sugio *et al.,* 1999).

This site is a large conformationally adaptable region (Varshney *et al.,* 2010) thus allowing large ligands (e.g. bilirubin; Mr ~ 585 Da) to bind. As well as being large, this site is flexible and adaptable as it is capable of binding ligands that have very different chemical structures with high-affinity (Table 4.1). This site contains a large number of ligand binding sites (Otagiri, 2005). Ligand-binding sites in this pocket are individual and are therefore independent of each other, but they are also capable of influencing one another. Compounds that favour this site are dicarboxylic acids and/or bulky heterocyclic anions that have a negative charge localised in the middle of the molecule (fig. 4.4) (Kragh-Hansen *et al.,* 2002, Baroni *et al.,* 2001). X-ray diffraction studies have identified 4 residues that contribute to binding, two of which contribute positively (Trp214 and Arg218) and two which contribute negatively (Lys199 and His242). The positive residue, the lone tryptophan at position 214 is found in the centre of the binding pocket and is thought to have a crucial role *(Bos et al.,* 1988, Kragh-Hansen *et al.,* 2002).

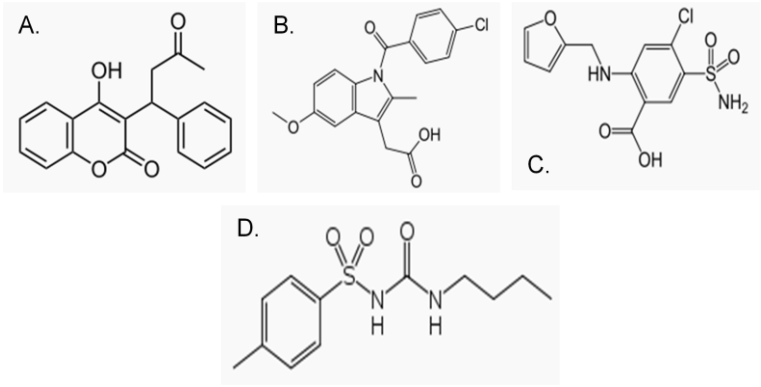


**Figure 4.4. The chemical structures of some of the drugs that bind to Sudlow's site I.** A) warfarin; B) indomethacin; C) furosemide and D) tolbutamide (Petitpas *et al.,* 2001).

Drugs such as warfarin cluster in the centre of the binding site. The planar group fits "snugly" between the apolar side-chains of the Leu238 and Ala291 residues. However, compounds can occupy the apolar compartments of this site to different extents. For example, warfarin can occupy the right-side and front sub-chambers.

All ligands that are able of binding at this site are positioned so that they form hydrogen bonds with the hydroxyl group of the Tyr150 residue. Therefore, the Tyr150 residue is important for drug interaction (Ascenzi and Fasano, 2010).

### 4.1.5. Ligand binding at Sudlow's site II

Sudlow's site II, also known as the indolebenzodiazepine or diazepam site can be found within subdomain IIIA (Fujiwara and Amisaki, 2006). It is composed of the six α-helices of subdomain IIIA. The inside of the pocket is lined with hydrophobic side-chains and the Arg210 side-chain is found at the entrance of the pocket whilst the hydroxyl group belonging to the Tyr411 residue faces towards the inside of the pocket (Sugio *et al.,* 1999). In comparison to binding site I, this site has one polar patch that can be found at one side of the entrance to the pocket and centred on the Tyr411 residue but does also include the Arg410, Lys414 and Ser489 residues. The Arg410 and Ser489 residues also take part in salt-bridge and hydrogen-bond formation.

This binding site only possesses one sub-compartment compared to site I. The hydrophobic sub-chamber is found towards the right rear side of the pocket. However, access to this sub-chamber is only possible after ligand-induced side-chain movements. This site is smaller and narrower than site I therefore explaining why no large ligands are able to bind to it. It is also less flexible because binding is significantly affected by stereoselectivity. If a large ligand is replaced by a small ligand this would significantly influence the binding, thus increasing the chances of the smaller ligand binding. Although this site can bind several ligands (Table 4.1) with high affinity, it is said to be more restricted than binding site I. The amino acids thought to be of importance for binding are Arg410 and Tyr411 (Kragh-Hansen *et al.,* 2002) and the hydroxyl group of the Tyr411 residue (Lejon et al., 2008).

Compounds that favour this site are aromatic carboxylic acids that have a negatively charged acidic group on one end of the molecule that is away from the hydrophobic centre (fig. 4.5) (Kragh-Hansen *et al.,* 2002, Baroni *et al.,* 2001).

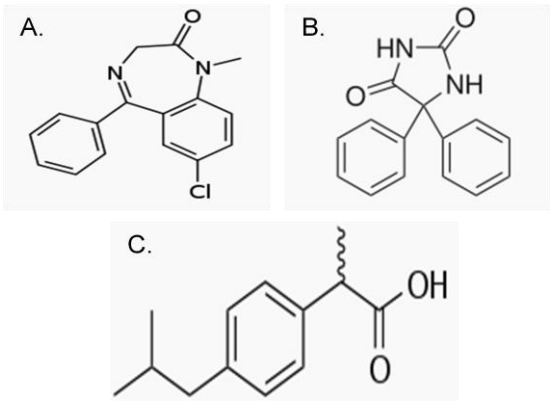


**Figure 4.5. The chemical structures of some of the drugs that bind to Sudlow's site II.** A). diazepam; B). phenytoin and C) ibuprofen (Chen *et al.,* 2006).

The binding of the benzodiazepine, diazepam, a compound with a large-branched structure and a molecular weight of 285 Da causes the Leu387 and Leu453 side-chains to rotate. This rotation allows the phenyl ring of the compound to gain access to the single sub-chamber of the pocket. Drugs such as ibuprofen can cluster in the centre of the drug binding site and form interactions with the hydroxyl group of the Tyr411 residue. However, the presence of a basic polar patch found at one end of the binding pocket is the preferred site of interaction for drugs that contain a peripheral electronegative group (Ascenzi and Fasano, 2010). Other compounds that are capable of binding to site II can also interact at additional sites out of this subdomain.

| Sudlow's site I | $K_a$ ($M^{-1}$) | Sudlow's site II | $K_a$ ($M^{-1}$) |
|---|---|---|---|
| **Warfarin** | **3.4 X $10^5$** | **Diazepam** | **3.8 X $10^5$** |
| Acenocoumarol | 2.2 X $10^5$ | Chlofibrate | 7.6 X $10^5$ |
| Azapropazone | 2.8 X $10^5$ | Chlorothiazide | 5.5 X $10^4$ |
| Benzylthiouracil | 4.1 X $10^4$ | Diclofenac | 3.3 X $10^6$ |
| Canrenoate | 2.0 X $10^5$ | Ethacrynate | 1.7 X $10^6$ |
| Chlorpropamide | 3.3 X $10^5$ | Ibuprofen | 2.7 X $10^6$ |
| Furosemide | 1.9 X $10^5$ | Iopanoate | 6.7 X $10^6$ |
| Indomethacin | 1.4 X $10^6$ | Ketoprofen | 2.5 X $10^6$ |
| Iodipamide | 9.9 X $10^6$ | Phenytoin | 1.7 x $10^4$ |
| Iophenoxate | 7.7 X $10^7$ | Pirprofen | 3.9 X $10^5$ |
| Oxyphenbutazone | 3.5 X $10^5$ | *S*(-)-Thiamylal | 8.7 X $10^4$ |
| Phenylbutazone | 1.5 X $10^6$ | *S*-Etodolac | 2.0 X $10^5$ |
| Piretanide | 9.5 X $10^4$ | *S*-Naproxen | 3.7 X $10^6$ |
| Quercetin | 2.7 X $10^5$ | | |
| *R*-Sulbenicillin | 5.2 X $10^3$ | | |
| Salicylate | 1.9 X $10^5$ | | |
| *S*-Carbenicillin | 2.4 X $10^3$ | | |
| Spironolactone | 3.0 X $10^3$ | | |
| Sulphadimethoxine | 9.0 X $10^4$ | | |
| Sulphathiazole | 2.5 X $10^4$ | | |
| Tenoxicam | 3.7 X $10^5$ | | |
| Tolbutamide | 4.0 X $10^4$ | | |
| Valproate | 2.8 X $10^5$ | | |

**Table 4.1. Drugs that bind to Sudlow's sites I and II on human serum albumin (HSA) with high affinities** (Kragh-Hansen *et al.,* 2002, Kober *et al.,* 1980).

### 4.1.6. The competitive binding properties of ligands

Many drug molecules are known to be enzyme inhibitors. An enzyme inhibitor is molecule that has the ability to bind to an enzyme and decrease its enzymatic activity. The binding of an enzyme inhibitor, such as a drug, can prevent a substrate, such as coelenterazine from entering the binding pocket as well as preventing the enzyme from catalysing the coelenterazine chemiluminescence reaction. Inhibitors can bind either reversibly or irreversibly. The irreversible binding of an inhibitor can induce changes in the enzyme, for example, inhibitors can modify the key amino acid residues required for enzymatic activity. However, the binding of reversible inhibitors

can produce different types of inhibition depending on where the inhibitors bind (i.e. enzyme, enzyme-substrate complex or both).

### 4.1.7. The covalent modification of proteins by methylglyoxal

It is known that the covalent modification of a protein has a significant influence on its conformational and functional properties (Otagiri, 2005). MeG is a potent glycating agent that at physiological concentrations can bind to and irreversibly modify plasma proteins such as HSA (Lo *et al.,* 1994). Glycation is a reaction that occurs between the free amino group of a protein and the carbonyl group belonging to a reducing sugar leading to the production of the stable advanced glycation end-products (AGEs) (Dhar *et al.,* 2009, Thornalley, 2008). The formation of these stable AGEs under physiological concentrations occurs directly and relatively rapidly. An example showed that when 1 μM MeG was added to human plasma *ex vivo* and incubated at 37 $^{o}$C it resulted in the complete and irreversible binding of MeG to the plasma protein within 24 hours. MeG is known to target and irreversibly modify arginine and lysine residues as well as amino-terminal amino groups however; MeG particularly favours arginine residues (Lo *et al.,* 1994, Thornalley, 1996, Ahmed *et al.,* 2005, Thornalley, 2008). The possible modification sites on HSA that play a role in glycation or AGE formation include the 59 lysine residues, the 23 arginine residues and the N-terminal amine (Wa *et al.,* 2007). When MeG irreversibly reacts with lysine residues, it results in the production of *Nε*-carboxymethyl-lysine (CML) and *Nε*-carboxyethyl-lysine (CEL). The most important AGEs quantitatively are the MeG-derived hydroimidazolones (MG-H) and these are formed when MeG modifies the arginine residues of the protein (Dhar *et al.,* 2009, Thornalley, 2008). There are three MG-H, they are structural isomers and are known as: $N_{\delta}$-(5-hydro-5-methylimidazol-4-on-2-yl)ornithine (MG-H1), 2-amino-5-(2-amino-5-hydro-5-methyl-4-imidazolon-1-yl)pentanoic acid (MG-H2), and 2-amino-5-(2-amino-4-hydro-4-methyl-5-imidazolon-1-yl)pentanoic acid (MG-H3) (Dhar *et al.,* 2009). Of these MG-H, MG-H1 residue formation has been noticed at Arg410 on HSA as a result of MeG modification. It is the formation of this MG-H at Arg410 that inhibits drug binding and function.

Interestingly, MG-H1 residue formation in albumin and other proteins has been found at increased levels in patients suffering with diabetes (Thornalley, 2008). Therefore, the formation of these hydroimidazolones at these sites can

cause distortion of the protein structure, loss of side-chain charge and reduced function (Thornalley, 2008). Hydroimidazolones have a moderate half-life of around 2 – 6 weeks as well as slow dynamic reversibility. Therefore, the protein content of these hydroimidazolones can be decreased if the concentration of MeG is also decreased. From this it can be concluded that the modification of proteins by MeG can be harmful when the amino acid residues that are modified are found at sites where protein-protein interactions, enzyme-substrate interactions and protein-DNA interactions take place (Ahmed *et al.,* 2005, Thornalley, 2008).

### 4.1.8. Hypothesis, aims and experimental strategy

#### 4.1.8.1. Hypothesis

The bacterial metabolic toxin hypothesis proposes that MeG and other metabolic toxins cause the covalent modification of proteins, such as albumin and insulin, thus leading to the pathogenesis of diseases such as diabetes. It is predicted that the covalent modification of both HSA and insulin by the bacterial metabolic toxin, MeG would reduce their enzymatic activity.

#### 4.1.8.2. Aims

The overall aim of this chapter was to investigate the effect of drugs that are known to bind to HSA on protein catalysed coelenterazine chemiluminescence and to determine the covalent modification of both HSA and human insulin by MeG and hydrogen peroxide ($H_2O_2$).

It has been shown in the previous chapter that both HSA and human insulin can catalyse the coelenterazine chemiluminescence reaction and the aims of this chapter were as follows:

- To investigate the effect of compounds, such as clinically used drugs on the activity of these proteins
- To determine the coelenterazine binding site using drugs that are known to bind to either Sudlow's site I (warfarin) and Sudlow's site II (diazepam) on HSA
- To demonstrate that both MeG and $H_2O_2$ covalently modify these proteins thus altering their activity

- To investigate if molecular 3D modelling can be used to confirm or predict the binding sites of compounds on these proteins

#### 4.1.8.3. Experimental strategy

To use the coelenterazine chemiluminescence model to investigate the effect of clinically used drugs on the activity of HSA and human insulin, to determine the coelenterazine binding site on HSA and to demonstrate the covalent modification of both HSA and human insulin. To investigate if molecular 3D modelling can be used to characterise the two main binding sites on HSA.

## 4.2. Materials and methods

### 4.2.1. Materials

Coelenterazine was a kind gift from Bruce Bryan, Prolume Inc. Snakeskin pleated dialysis tubing (pore size: 25 µm) was purchased from Fisher Scientific. All other compounds were purchased from Sigma-Aldrich unless otherwise stated.

### 4.2.2. Preparation of reagents

All reagents including proteins, coelenterazine and buffer were prepared as previously described in section 2.2.3. In this chapter there was also the need for 50 mM sodium-phosphate buffer, pH 8.3. 1 L of 50 mM basic $Na_2HPO_4$ was made and the pH was adjusted to 8.3 using the same concentration of acidic $NaH_2PO_4$. To make 1 L of 50 mM basic $Na_2HPO_4$, 7 g was dissolved in distilled water and to make 500 ml of 50 mM $NaH_2PO_4$, 3 g was dissolved in distilled water.

### 4.2.3. To investigate the effect of drugs on HSA catalysed coelenterazine chemiluminescence

All reagents were prepared as previously described in section 2.2.3 and the photomultiplier tube was allowed to reach its optimum temperature. The machine background was measured. The coelenterazine chemiluminescence (or chemical background) was measured by adding 10 µM coelenterazine to 70 µl of buffer containing 50 mM HEPES buffer, pH 7.4. Then the drug chemiluminescence was measured by adding 10 µl of the drug to 80 µl of

buffer containing 50 mM HEPES buffer, pH 7.4 and 10 µM coelenterazine. The protein chemiluminescence was measured by adding 10 µl HSA (0.1 % (w/v) final concentration) to 90 µl of buffer containing 50 mM HEPES buffer, pH 7.4, 10 µM coelenterazine and 10 µl of drug. The background or chemiluminescence was recorded as 6 x 10 second counts and the mean was taken.

### 4.2.4. The production of covalently modified proteins and their effect on protein catalysed coelenterazine chemiluminescence

Albumin and human insulin (1 % (w/v)) were incubated with MeG or hydrogen $H_2O_2$ (10 mM) for 1 week at room temperature. Also, albumin and human insulin (without toxins) were incubated under the same conditions so that any modifications could be determined. A week later sections of dialysis tubing were prepared by boiling in water containing EDTA. The tubing was rinsed with distilled water and one end tied securely. 1 ml of normal HSA was added to the tubing and the opposite end was tied securely. This was done for both normal and modified proteins. The tubing containing the solutions was placed into a beaker containing 50 mM sodium-phosphate buffer, pH 8.3 and placed on a stirrer in a cold room to dialyse for 24 hours. The buffer was replaced twice. Following dialysis, the solutions were removed from the tubing and transferred into universal tubes.

All reagents were prepared as previously described in section 2.2.3 and the photomultiplier tube was allowed to reach its optimum temperature. The machine background was measured. The coelenterazine chemiluminescence was measured by adding 10 µM coelenterazine to 80 µl of buffer containing 50 mM HEPES buffer, pH 7.4. The protein chemiluminescence was measured by adding 10 µl of HSA (0.1 % (w/v) final concentration) to 90 µl of buffer containing 50 mM HEPES buffer, pH 7.4 and 10 µM coelenterazine. The background or chemiluminescence was recorded as 6 x 10 second counts and the mean was taken.

### 4.2.5. To determine if molecular 3D modelling can be used to predict the coelenterazine binding site

All molecular modelling studies were performed on a MacPro dual 2.66 GHz Xeon running Ubuntu 8. The albumin structure was downloaded from the Protein Data Bank (PDB) (http://www.rcsb.org/ - PDB code: 2BXD) (Ghuman

*et al.,* 2005). Hydrogen atoms were added to the protein using Molecular Operating Environment (MOE), and minimised keeping all the heavy atoms fixed until a RMSD gradient of 0.05 kcal $mol^{-1}$ $Å^{-1}$ was reached. Ligand structures were built with MOE and minimised using the MMFF94X forcefield until a RMSD gradient of 0.05 kcal $mol^{-1}$ $Å^{-1}$ was reached. The docking simulations were performed using PLANTS with the default settings (Korb *et al.,* 2006).

### 4.2.6. Statistical analysis

Statistical analysis was carried out on the mean using a t-test and the results were considered to be statistically different when $p < 0.05$.

## 4.3. Results

The two well characterised drug binding sites on HSA, Sudlow's site I and Sudlow's site II can bind a diverse range of drugs. Drugs that bind to Sudlow's site I include warfarin, furosemide, indomethacin and tolbutamide, whereas drugs that bind to Sudlow's site II include diazepam, phenytoin and ibuprofen. The initial aim was to determine the coelenterazine binding site on HSA by using drugs that are known to bind to either Sudlow's site I or Sudlow's site II. The results that follow predict that coelenterazine binds to Sudlow's site I because only drugs that can bind to this site significantly inhibited HSA catalysed coelenterazine chemiluminescence ($p < 0.001$; fig. 4.6 – fig. 4.9).

### 4.3.1. The effect of drugs on HSA catalysed coelenterazine chemiluminescence

In order to determine the coelenterazine binding site, drugs that are known to bind to either Sudlow's site I or Sudlow's site II were used and their effects on HSA catalysed coelenterazine chemiluminescence were determined.

#### 4.3.1.1. The effect of drugs that are known to bind to Sudlow's site I on HSA catalysed coelenterazine chemiluminescence

In order to determine if Sudlow's site I was the coelenterazine binding site, drugs that are known to bind to this site – warfarin, furosemide, indomethacin and tolbutamide were used and their effect on HSA catalysed coelenterazine chemiluminescence was determined. The results that follow show that the addition of these four particular site I drugs significantly inhibited HSA catalysed coelenterazine chemiluminescence. However, the extent of the inhibition observed by each of these drugs varied.

From the results that follow, the drugs that bind to Sudlow's site I can now be ranked in order of producing maximum inhibition of HSA catalysed coelenterazine chemiluminescence: indomethacin > tolbutamide > furosemide > warfarin. The inhibition of HSA catalysed coelenterazine chemiluminescence was not consistent with the binding constants ($K_d$) for these drugs and this may be due to the high concentrations ($10^{-4}$ M) of the protein used. The $K_d$ values included in this chapter were obtained from published literature.

The HSA catalysed coelenterazine chemiluminescence was significantly inhibited by warfarin ($p < 0.001$; fig. 4.6). The results show that warfarin alone (fig. 4.6A) did not significantly affect chemiluminescence when compared to the control in the absence of the drug, and this suggested that there was a direct effect on the protein. In the presence of 10 μM coelenterazine (fig. 4.6B) the maximum inhibition of HSA catalysed coelenterazine chemiluminescence ($10^{-6}$ to $10^{-3}$; $K_d = 2.9 \times 10^{-6}$ M) was approximately 50 %.

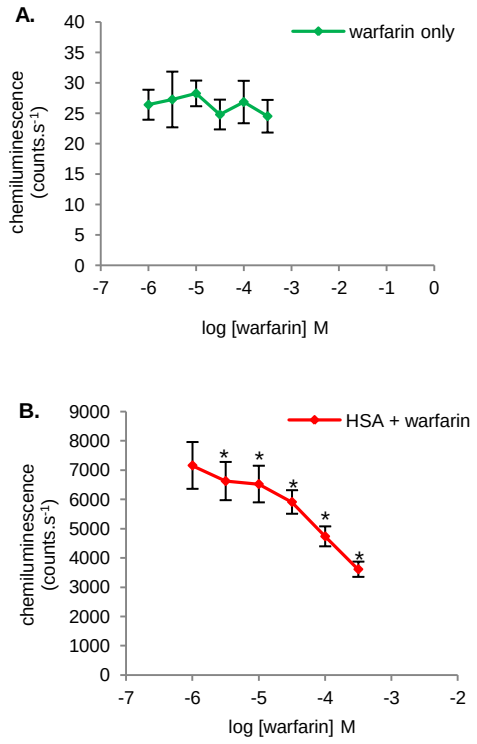


**Figure 4.6. The inhibition of human serum albumin (HSA) catalysed coelenterazine chemiluminescence by warfarin.** The machine background produced an average of 29 counts.s$^{-1}$ whereas the coelenterazine chemiluminescence produced averages of between 66 and 83 counts.s$^{-1}$. The effect of warfarin on HSA catalysed coelenterazine chemiluminescence was measured by adding 10 µl of HSA (0.1 % (w/v); 1 g.l$^{-1}$ final concentration) to 90 µl of buffer containing 50 mM HEPES buffer pH 7.4, 10 µM coelenterazine and $10^{-6}$ – $10^{-3}$ M warfarin. Results represent the mean +/- SEM of six determinations. Asterisks indicate a significant difference where $p < 0.001$ when compared with the control in the absence of warfarin.

The HSA catalysed coelenterazine chemiluminescence was significantly inhibited by furosemide ($p < 0.001$; fig. 4.7). The results show that furosemide alone (fig. 4.7A) did not significantly affect chemiluminescence when compared to the control in the absence of the drug and this suggested that there was a direct effect on the protein. In the presence of 10 µM coelenterazine (fig. 4.7B) the maximum inhibition of HSA catalysed coelenterazine chemiluminescence ($10^{-6}$ to $10^{-3}$ M; $K_d$ = 5.3 x $10^{-6}$ M) was approximately 60 %.

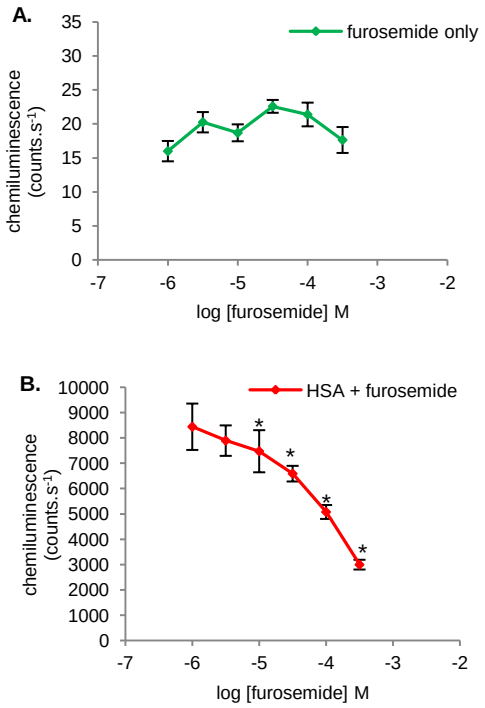


**Figure 4.7. The inhibition of human serum albumin (HSA) catalysed coelenterazine chemiluminescence by furosemide.** The machine background produced an average of 24 counts.s$^{-1}$ whereas the coelenterazine chemiluminescence produced averages of between 63 and 75 counts.s$^{-1}$. The effect of furosemide on HSA catalysed coelenterazine chemiluminescence was measured by adding 10 µl of albumin (0.1 % (w/v), 1 g.l$^{-1}$ final concentration) to 90 µl of buffer containing 50 mM HEPES buffer, pH 7.4, 10 µM coelenterazine and $10^{-6}$ – $10^{-3}$ M furosemide. Results represent the mean +/- SEM of six determinations. Asterisks indicate a significant difference where $p < 0.001$ when compared with the control in the absence of furosemide.

The HSA catalysed coelenterazine chemiluminescence was significantly inhibited by indomethacin ($p < 0.001$; fig. 4.8). The results show that indomethacin alone (fig. 4.8A) did not significantly affect chemiluminescence when compared to the control in the absence of the drug and this suggested that there was a direct effect on the protein. In the presence of 10 µM coelenterazine (fig. 4.8B) the maximum inhibition of HSA catalysed coelenterazine chemiluminescence ($10^{-6}$ to $10^{-2}$ M; $K_d$ = 7.1 x $10^{-7}$ M) was approximately >95 %.

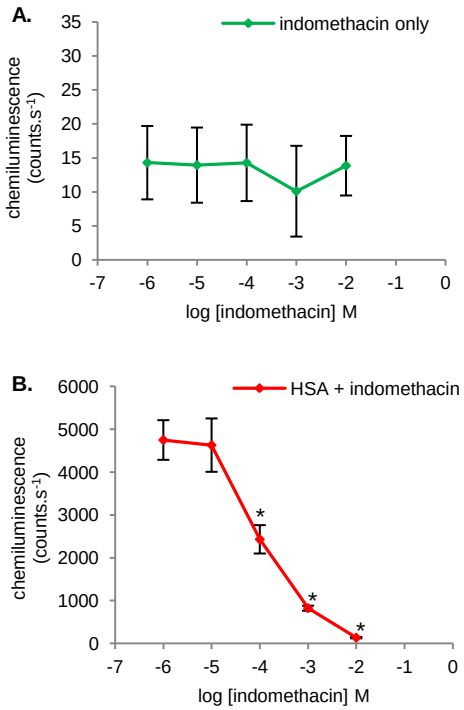


**Figure 4.8. The inhibition of human serum albumin (HSA) catalysed coelenterazine chemiluminescence by indomethacin.** The machine background produced an average of 29 counts.s$^{-1}$ whereas the coelenterazine chemiluminescence produced averages of between 48 and 58 counts.s$^{-1}$. The effect of indomethacin on HSA catalysed coelenterazine chemiluminescence was measured by adding 10 µl of albumin (0.1 % (w/v); 1 g.l$^{-1}$ final concentration) to 90 µl of buffer containing 50 mM HEPES buffer, pH 7.4, 10 µM coelenterazine and $10^{-6}$ – $10^{-2}$ M indomethacin. Results represent the mean +/- SEM of six determinations. Asterisks indicate a significant difference where $p < 0.001$ when compared with the control in the absence of indomethacin.

Tolbutamide significantly inhibited HSA catalysed coelenterazine chemiluminescence ($p < 0.001$; fig. 4.9). Tolbutamide alone (fig. 4.9A) at concentrations $10^{-6}$ to $10^{-3}$ M did not significantly affect chemiluminescence when compared to the control in the absence of the drug therefore suggesting that there was a direct effect on the protein. However, $10^{-2}$ M tolbutamide did significantly increase chemiluminescence ($p < 0.01$; fig. 4.9A) when compared to the control in the absence of the drug. In the presence of 10 µM coelenterazine (fig. 4.9B) the maximum inhibition of HSA catalysed coelenterazine chemiluminescence ($10^{-6}$ to $10^{-2}$ M; $K_d$ = 2.5 x $10^{-5}$ M) was approximately >90 %.

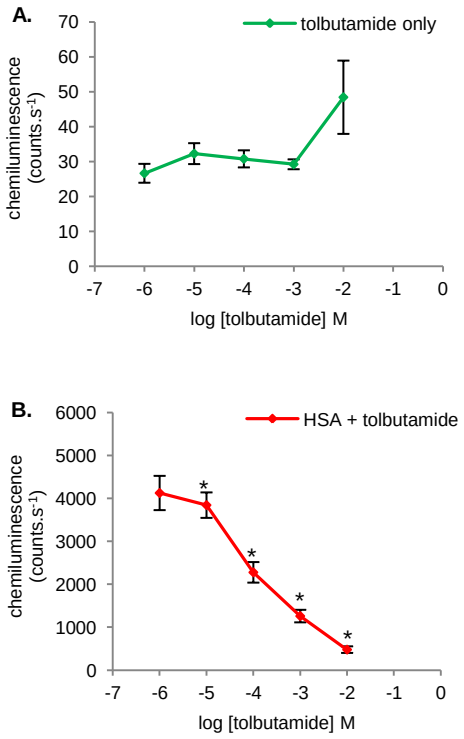


**Figure 4.9. The inhibition of human serum albumin (HSA) catalysed coelenterazine chemiluminescence by tolbutamide.** The machine background produced an average of 30 counts.s$^{-1}$ whereas the coelenterazine chemiluminescence produced averages of between 59 and 62 counts.s$^{-1}$. The effect of tolbutamide on HSA catalysed coelenterazine chemiluminescence was measured by adding 10 µl of albumin (0.1 % (w/v); 1 g.l$^{-1}$ final concentration) to 90 µl of buffer containing 50 mM HEPES buffers, pH 7.4, 10 µM coelenterazine and $10^{-6}$ – $10^{-2}$ M tolbutamide. Results represent the mean +/- SEM of six determinations. Asterisks indicate significant difference where $p < 0.001$ when compared to the control in the absence of tolbutamide.

### 4.3.1.2. The effect of drugs that are known to bind to Sudlow's site II on HSA catalysed coelenterazine chemiluminescence

In order to determine if Sudlow's site II was the coelenterazine binding site, drugs that are known to bind to this site – diazepam, phenytoin and ibuprofen were used and their effect on HSA catalysed coelenterazine chemiluminescence was determined. The HSA catalysed coelenterazine chemiluminescence was significantly inhibited by diazepam ($p < 0.001$; fig. 4.10). The results show that diazepam alone (fig. 4.10A) did not significantly

affect chemiluminescence when compared to the control in the absence of the drug and this suggested that there was a direct effect on the protein. In the presence of 10 μM coelenterazine (fig. 4.10B) the maximum inhibition of HSA catalysed coelenterazine chemiluminescence ($10^{-6}$ to $10^{-4}$ M; $K_d$ = 2.6 x $10^{-6}$ M) was approximately 20 %.

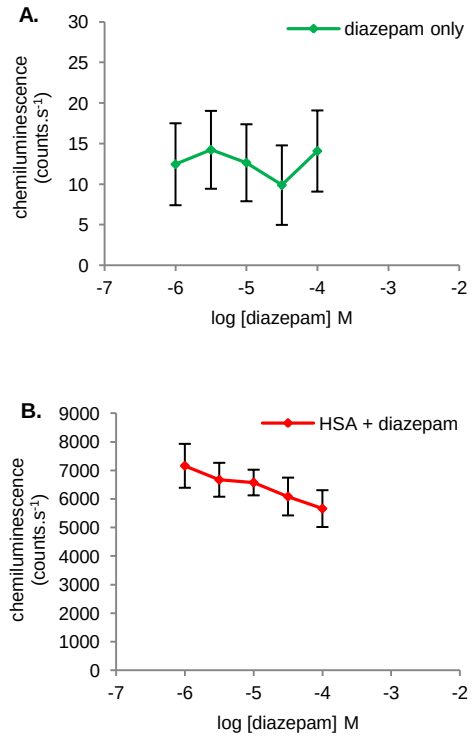


**Figure 4.10. The inhibition of human serum albumin (HSA) catalysed coelenterazine chemiluminescence by diazepam.** The machine background produced an average of 25 counts.$s^{-1}$ whereas the coelenterazine chemiluminescence produced between 67 and 78 counts.$s^{-1}$. The effect of diazepam on HSA catalysed coelenterazine chemiluminescence was measured by adding 10 μl of albumin (0.1 % (w/v); 1 g.$l^{-1}$ final concentration) to 90 μl of buffer containing 50 mM HEPES buffer, pH 7.4, 10 μM coelenterazine and $10^{-6}$ – $10^{-4}$ M diazepam. Results represent the mean +/- SEM of nine determinations.

Phenytoin ($10^{-6}$ to $10^{-4}$ M; $K_d$ = 5.9 x $10^{-5}$ M) had no significant effect on HSA catalysed coelenterazine chemiluminescence (fig. 4.11). The results show that phenytoin alone (fig. 4.11A) did not significantly affect chemiluminescence

when compared to the control in the absence of the drug and this suggested that there was a direct effect on the protein. In the presence of 10 μM coelenterazine (fig. 4.11B) there was no significant effect on HSA catalysed coelenterazine chemiluminescence.

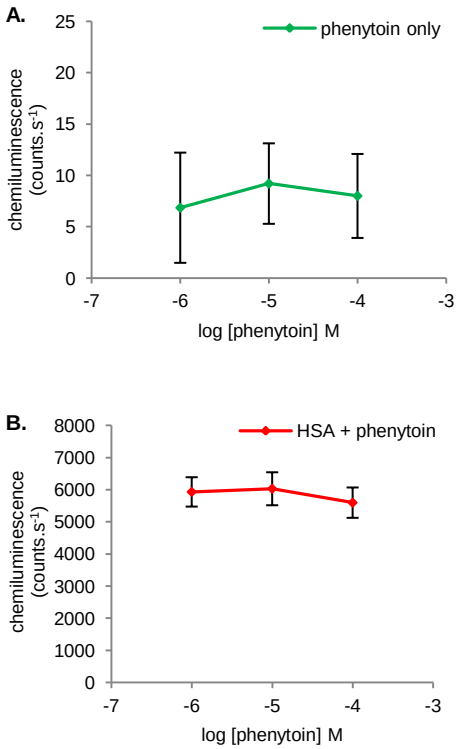


**Figure 4.11. The inhibition of human serum albumin (HSA) catalysed coelenterazine chemiluminescence by phenytoin.** The machine background produced an average of 25 counts.$s^{-1}$ whereas the coelenterazine chemiluminescence produced averages of between 65 and 75 counts.$s^{-1}$. The effect of phenytoin on HSA catalysed coelenterazine chemiluminescence was measured by adding 10 μl of albumin (0.1 % (w/v); 1 g.$l^{-1}$ final concentration) to 90 μl of buffer containing 50 mM HEPES buffer, pH 7.4, 10 μM coelenterazine and $10^{-6}$ – $10^{-4}$ M phenytoin. Results represent the mean +/- SEM of nine determinations.

Ibuprofen ($10^{-6}$ to $10^{-3}$ M; $K_d$ = 3.7 x $10^{-7}$ M) had no significant effect on HSA catalysed coelenterazine chemiluminescence (fig. 4.12). The results show that ibuprofen alone (fig. 4.12A) did not significantly affect chemiluminescence when compared to the control in the absence of the drug and this suggested

that there was a direct effect on the protein. In the presence of 10 µM coelenterazine (fig. 4.12B) there was no significant effect on HSA catalysed coelenterazine chemiluminescence.

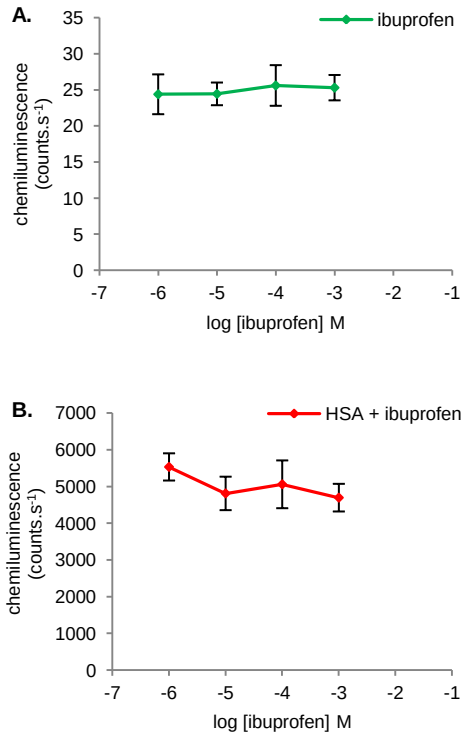


**Figure 4.12. The inhibition of human serum albumin (HSA) catalysed coelenterazine chemiluminescence by ibuprofen.** The machine background produced an average of 26 counts.s$^{-1}$ whereas the coelenterazine chemiluminescence produced averages of between 65 and 78 counts.s$^{-1}$. The effect of ibuprofen on HSA catalysed coelenterazine chemiluminescence was measured by adding 10 µl of albumin (0.1 % (w/v); 1 g.l$^{-1}$ final concentration) to 90 µl of buffer containing 50 mM HEPES buffer, pH 7.4, 10 µM coelenterazine and $10^{-6}$ – $10^{-3}$ M ibuprofen. Results represent the mean +/- SEM of six determinations.

From the data presented in sections 4.3.1.1 and 4.3.1.2 it can be concluded that the coelenterazine binding site is Sudlow's site I on HSA since only drugs that were able to bind to this site inhibited HSA catalysed coelenterazine chemiluminescence.

### 4.3.2. The mixed enzyme kinetics of albumin

Michaelis-Menten kinetics is the most common model used to demonstrate single substrate enzyme kinetics. The Michaelis-Menten equation describes the rate of an enzymatic reaction by linking the reaction rate (v) with the substrate concentration [S]. The maximum rate produced by the reaction in the presence of the maximum substrate concentration is known as $V_{max}$, whereas the Michaelis constant ($K_m$) is the substrate concentration when the reaction rate is half that of the $V_{max}$. The $K_m$ is an inverse measure of the substrates binding affinity for the enzyme.

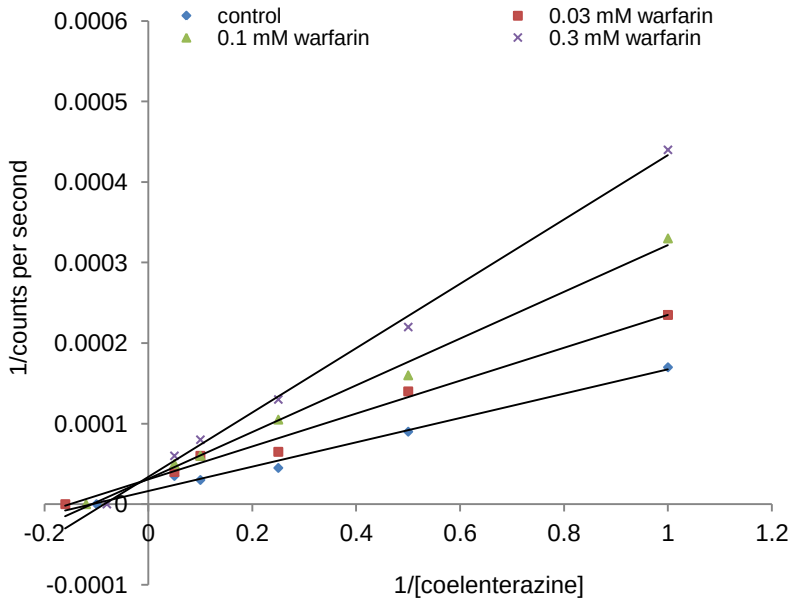


**Fig 4.13. The competitive binding properties of warfarin on human serum albumin (HSA) catalysed coelenterazine chemiluminescence.** 10 µl of albumin (0.1 % (w/v) final concentration) was added to buffer containing 50 mM HEPES buffer, pH 7.4, coelenterazine (1 – 20 µM final concentration) and warfarin (0.03, 0.1 or 0.3 mM). Results represent the mean +/- SEM of three determinations.

A small $K_m$ suggests that the substrate has a high affinity for the enzyme resulting in the rate reaching $V_{max}$ quickly whereas a high $K_m$ suggests that the substrate has a low affinity for the enzyme resulting in the rate reaching $V_{max}$ slowly.

As the rate of catalysis of an enzymatic reaction in the presence of increasing substrate concentration is not linear it is difficult to accurately estimate values for $K_m$ and $V_{max}$. A linearization of the Michaelis-Menten equation known as a Lineweaver-Burk plot has been developed and is commonly used for the illustration of kinetic data. Lineweaver-Burk plots can be used to estimate values for $K_m$ and $V_{max}$ as well as the type of enzyme inhibition. The x- and y-intercepts on these plots represent $-1/K_m$ and $1/V_{max}$, respectively. The inhibition observed in the presence of warfarin exhibited mixed enzyme kinetics because the inhibitors had different x- and y-intercepts (fig. 4.13). This inhibition was consistent with the warfarin reducing both the binding and catalytic activity of the HSA.

### 4.3.3. Molecular 3D modelling used to identify the coelenterazine binding site

Coelenterazine chemiluminescence predicted that Sudlow's site I on HSA is also the coelenterazine binding site. Molecular 3D modelling was carried out to confirm this prediction. Using this method, it was possible to identify both of Sudlow's drug binding sites on HSA (fig. 4.14). The images that follow show the binding of coelenterazine at Sudlow's site I (fig. 4.14A) and at Sudlow's site II (fig. 4.14B). Warfarin (green) and diazepam (red) were also included at their respective sites for comparison.

The results show that coelenterazine was able to fit "snugly" into Sudlow's site I (fig. 4.14A) but when it was inserted into Sudlow's site II it formed interactions with the surface of the protein (fig. 4.14B). Therefore molecular 3D modelling confirmed that Sudlow's site I as the preferred binding site for coelenterazine and identified five important amino acid residues - Tyr150, Lys195, Arg222, His242 and Arg257 (fig. 4.14A).

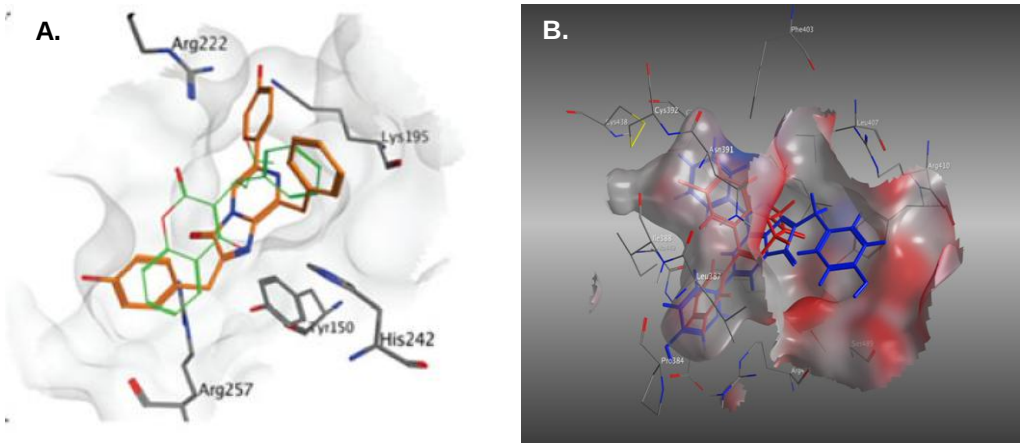


**Figure 4.14. Molecular 3D modelling showing coelenterazine binding to both Sudlow's site I and Sudlow's site II on human serum albumin (HSA).** A) shows Sudlow's site I and the important amino acid residues (Tyr150, Lys195, Arg222, His242 and Arg257) for the binding of coelenterazine (orange). Warfarin (green) was included for comparison. B) shows the binding of coelenterazine (blue) to Sudlow's site II. Diazepam (red) was included for comparison.

### 4.3.4. The inhibition of albumin and insulin catalysed coelenterazine chemiluminescence by methylglyoxal

In order to test the ability of covalently modified HSA and human insulin to catalyse coelenterazine chemiluminescence, the proteins were incubated with 10 mM MeG for 1 week. The normal and modified protein catalysed coelenterazine chemiluminescences were compared. The incubation of albumin and human insulin (fig. 4.15B) with MeG significantly inhibited chemiluminescence by approximately 50 %.

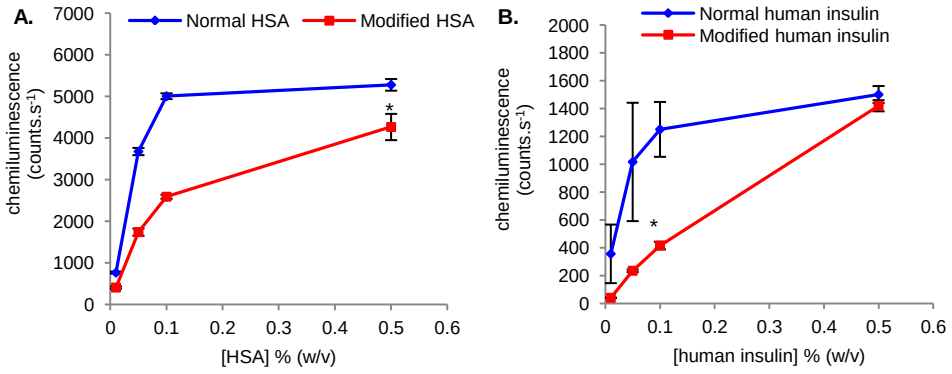


**Figure 4.15. The inhibition of protein catalysed coelenterazine chemiluminescence by methylglyoxal (MeG).** 1 ml of albumin and insulin (1 % (w/v)) were incubated with MeG (10 mM) and without MeG for 1 week at room temperature. Solutions were dialysed for 24 hours in 500 ml sodium-phosphate buffer, pH 8.3 to remove the toxin. A) Compares normal and modified HSA catalysed coelenterazine chemiluminescence. The machine background produced an average of 25 counts.$s^{-1}$. The coelenterazine chemiluminescence prior to the addition of the proteins averaged between 52 and 58 counts.$s^{-1}$ for normal HSA and 49 and 56 counts.$s^{-1}$ for modified HSA; B) Compares normal and modified human insulin catalysed coelenterazine chemiluminescence. The machine background produced an average of 28 counts.$s^{-1}$. The coelenterazine chemiluminescences prior to the addition of the proteins averaged between 80 and 115 counts.$s^{-1}$ for normal human insulin and 67 and 73 counts.$s^{-1}$ for modified human insulin. Results represent the mean +/- SEM of three determinations. Asterisks represent significant difference where $p < 0.01$ when compared with the same concentration of normal protein.

### 4.3.5. The increased albumin and insulin catalysed coelenterazine chemiluminescence by hydrogen peroxide

The proteins were also incubated with hydrogen peroxide, $H_2O_2$ (10 mM) for 1 week. The abilities of the normal and covalently modified proteins at catalysing coelenterazine chemiluminescence were investigated. Interestingly, the incubation of HSA and human insulin with $H_2O_2$ significantly enhanced chemiluminescence.

Following incubation with $H_2O_2$, the HSA catalysed coelenterazine chemiluminescence increased by 5-fold (fig. 4.16A) and human insulin catalysed coelenterazine chemiluminescence increased by approximately 2.5-fold (fig. 4.16B) with the addition of 0.5 % (w/v) protein.

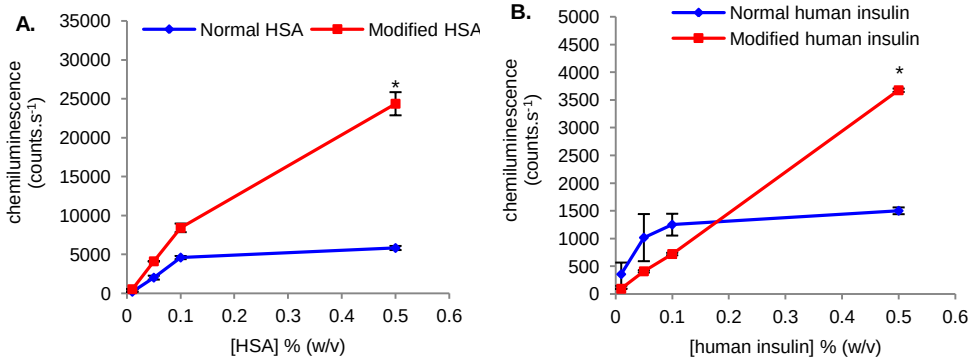


**Figure 4.16. The inhibition of protein catalysed coelenterazine chemiluminescence by hydrogen peroxide ($H_2O_2$).** 1 ml of albumin and insulin (1 % (w/v)) were incubated with $H_2O_2$ (10 mM) and without $H_2O_2$ for 1 week at room temperature. Solutions were dialysed for 24 hours in 500 ml sodium-phosphate buffer, pH 8.3 to remove the toxin. A) Compares normal and modified HSA catalysed coelenterazine chemiluminescence. The machine background produced an average of 22 counts.$s^{-1}$. The coelenterazine chemiluminescences prior to the addition of the proteins were between 52 and 58 counts.$s^{-1}$ for normal HSA and 65 and 79 counts.$s^{-1}$ for modified HSA; B) Compares normal and modified human insulin catalysed coelenterazine chemiluminescence. The machine background produced an average of 25 counts.$s^{-1}$. The coelenterazine chemiluminescences prior to the addition of the proteins were between 80 and 115 counts.$s^{-1}$ for normal human insulin and 68 and 77 counts.$s^{-1}$ for modified human insulin. Results represent the mean +/- SEM of three determinations. Asterisks indicates significant difference where $p < 0.01$ when compared to 0.5 % (w/v) normal HSA and human insulin.

## 4.4. Discussion and conclusions

This chapter has predicted that coelenterazine must bind to Sudlow's site I, since only drugs that were able to bind to this site significantly inhibited ($p < 0.001$) the HSA chemiluminescence (fig. 4.6 – fig. 4.9).

The inhibition demonstrated by warfarin suggested mixed inhibition enzyme kinetics (fig. 4.13) which was consistent with reduced ligand binding and reduced catalysis. Molecular 3D modelling was used and confirmed Sudlow's site I as the coelenterazine binding site (fig. 4.14). It was also demonstrated in this chapter that albumin and insulin were covalently modified after incubation with either MeG or $H_2O_2$. However, the covalent modification of albumin by MeG significantly inhibited protein catalysed chemiluminescence ($p < 0.01$; fig. 4.15A) whereas the covalent modification of these proteins by $H_2O_2$ significantly enhanced protein catalysed coelenterazine chemiluminescence ($p < 0.01$; fig. 4.16).

Drugs that are known to bind to Sudlow's site I (e.g. warfarin, furosemide, indomethacin and tolbutamide) significantly inhibited HSA catalysed coelenterazine chemiluminescence. The maximum inhibition of HSA catalysed coelenterazine chemiluminescence by warfarin ($10^{-6}$ to $10^{-3}$ M, $K_d = 2.9 \times 10^{-6}$ M), furosemide ($10^{-6}$ to $10^{-3}$ M, $K_d = 5.3 \times 10^{-6}$ M), indomethacin ($10^{-6}$ to $10^{-2}$ M, $K_d = 7.1 \times 10^{-7}$ M) and tolbutamide ($10^{-6}$ to $10^{-2}$ M, $K_d = 2.5 \times 10^{-5}$ M) was 50 %, 60 %, > 95 % and > 90 %, respectively, in the presence of 10 μM coelenterazine (fig. 4.6 – fig. 4.9). Thus, these drugs can now be ranked in order of maximum inhibition of HSA catalysed coelenterazine chemiluminescence: indomethacin > tolbutamide > furosemide > warfarin.

The data suggested that coelenterazine binds to Sudlow's site I and therefore competition is expected to exist between the drug and coelenterazine but the compound with the highest affinity will displace the other (Rahman *et al.,* 2005). The concentration of each of the compounds will determine which will become bound to HSA. If the concentration of the drug is lower than the coelenterazine concentration ($<10^{-5}$ M), more substrate is present and therefore coelenterazine will bind to HSA hence why there was no significant change in HSA catalysed coelenterazine chemiluminescence. When the concentration of the drug reached the same concentration as that of coelenterazine, the compound with the highest affinity for HSA will bind to the site. As the concentration of the drug increases above that of coelenterazine, more drug is present and able to bind, thus preventing coelenterazine from binding and hence why a decrease in chemiluminescence was observed. The addition of the site II drug, diazepam, significantly inhibited HSA catalysed coelenterazine chemiluminescence ($p < 0.001$; fig. 4.10).

The maximum inhibition of HSA catalysed coelenterazine chemiluminescence by diazepam was 20 %. However, the addition of increasing concentrations of the other site II drugs, phenytoin and ibuprofen (fig. 4.11 and fig. 4.12) did not affect HSA catalysed coelenterazine chemiluminescence. This helps to explain why Sudlow's site I was predicted to be the coelenterazine binding site.

Table 4.1 lists the $K_a$ values for drugs that are known to bind with high affinity to site I or site II on HSA. The $K_a$ of a drug describes the binding affinity between two molecules at equilibrium whereas the dissociation constant ($K_d$) is the inverse of the $K_a$ ($K_d = 1/K_a$) and can therefore be determined (Table 4.2). The $K_d$ describes the ability of a large compound to dissociate reversibly into smaller components at equilibrium. When a ligand (i.e. drug) binds to a protein, the $K_d$ is used to describe the binding affinity of the ligand to the protein. The binding affinities are influenced by non-covalent intermolecular interactions between the ligand and the protein, such as hydrogen bonding, electrostatic interactions, hydrophobic and Van der Waals.

| **Drug** | **Association constant** ($K_a$) ($M^{-1}$) | **Dissociation constant** ($K_d$) (M) |
|---|---|---|
| Warfarin | $3.4 \times 10^{5}$ | $2.9 \times 10^{-6}$ |
| Furosemide | $1.9 \times 10^{5}$ | $5.3 \times 10^{-6}$ |
| Indomethacin | $1.4 \times 10^{6}$ | $7.1 \times 10^{-7}$ |
| Tolbutamide | $4.0 \times 10^{4}$ | $2.5 \times 10^{-5}$ |
| Diazepam | $3.8 \times 10^{5}$ | $2.6 \times 10^{-6}$ |
| Phenytoin | $1.7 \times 10^{4}$ | $5.9 \times 10^{-5}$ |
| Ibuprofen | $2.7 \times 10^{6}$ | $3.7 \times 10^{-7}$ |
| Glibenclamide | $3.6 \times 10^{4}$ | $2.8 \times 10^{-5}$ |

**Table 4.2. The association ($K_a$) and dissociation ($K_d$) constants of drugs that are known to bind with high affinity to HSA** (Kragh-Hansen *et al.,* 2002, Kober *et al.,* 1980)**.**

The $K_d$ values of the drugs used in this chapter will determine how tightly each of the drugs will bind to the protein. If a drug has a low $K_d$, that particular drug is able to bind to the protein with high affinity and *vice versa*. Taking this into account, drugs that bind with a high affinity will require relatively low

concentrations for maximum occupancy of the protein binding site and drugs that bind with a low affinity will require higher concentrations for maximum occupancy of the protein binding site. Warfarin has a $K_d$ of 2.9 x $10^{-6}$ M and is known to have a high affinity for HSA. However, tolbutamide and furosemide have higher $K_d$ values of 2.5 x $10^{-5}$ M and 5.3 x $10^{-6}$ M, respectively, when compared to that of warfarin. Both tolbutamide and furosemide have lower binding affinities than warfarin for site I, thus for maximum occupancy of the binding site, higher concentrations of both of these drugs would be required. The $K_d$ for indomethacin, was lower than that of warfarin (7.1 x $10^{-7}$ M) and it has a higher affinity for the binding site thus requiring lower concentrations for maximum occupancy of the binding site.

The inhibition of HSA catalysed coelenterazine chemiluminescence observed in the presence of drugs that bind to Sudlow's site I was not consistent with the known $K_d$ values. The $IC_{50}$ values for the site I drugs used were much higher than the $K_d$ for the drugs (i.e. warfarin: $K_d$ = 2.9 x $10^{-6}$ M; $IC_{50}$ ~ $10^{-4}$ M (fig. 4.6)). The $IC_{50}$ values for all site I inhibitors were very similar and hence much higher (~ $10^{-4}$ M) than their respective $K_d$ values. The $IC_{50}$ values of these drugs may be high for all site I inhibitors due to the high concentrations of HSA used ($10^{-4}$ M). Drugs that bind to Sudlow's site II (e.g. diazepam, phenytoin and ibuprofen) did not have a significant effect on HSA catalysed coelenterazine chemiluminescence (fig. 4.10 – fig. 4.12). From this information, it can be concluded that coelenterazine must bind to Sudlow's site I, as site I and not site II drugs inhibited HSA catalysed coelenterazine chemiluminescence.

Ligand binding experiments were used to investigate the high affinity binding of drugs to the protein (Kragh-Hansen, 1991). Binding may occur competitively to one site (Brodersen *et al.,* 1977) and it was therefore necessary to investigate the binding properties of warfarin and coelenterazine on albumin catalysed coelenterazine chemiluminescence. Unbound warfarin has weak fluorescence, however when it binds to HSA, the fluorescence is enhanced. If a second ligand is present (i.e. coelenterazine), there is a decrease in fluorescence as both ligands will compete for the same site (Sahoo *et al.,* 2008).

In the experiment used to determine the type of enzyme inhibition, the concentration of HSA was similar to or higher than the coelenterazine concentration, thus a key condition for the Michaelis-Menten equation is that the enzyme does not significantly reduce the substrate concentration, therefore to a first approximation the equation may not hold. This is why the results state that the approximate $K_m$ was 20 μM as it was not possible to do a precise Lineweaver-Burk plot.

Molecular 3D modelling is widely used throughout the pharmaceutical industry to create new drugs and to help understand the molecular interactions that occur in protein-ligand binding. Molecular 3D modelling was used to confirm/predict the coelenterazine binding site. This method demonstrated the importance of Sudlow's site I as the major catalytic site on HSA (fig. 4.14A and fig. 4.14B) therefore confirming this site as the coelenterazine binding site. Figure 4.14A shows that coelenterazine fits "snugly" into site I, where warfarin is also capable of binding, but when it was placed in the pocket containing site II, it did not fit comfortably and resulted in interactions with the surface of the protein.

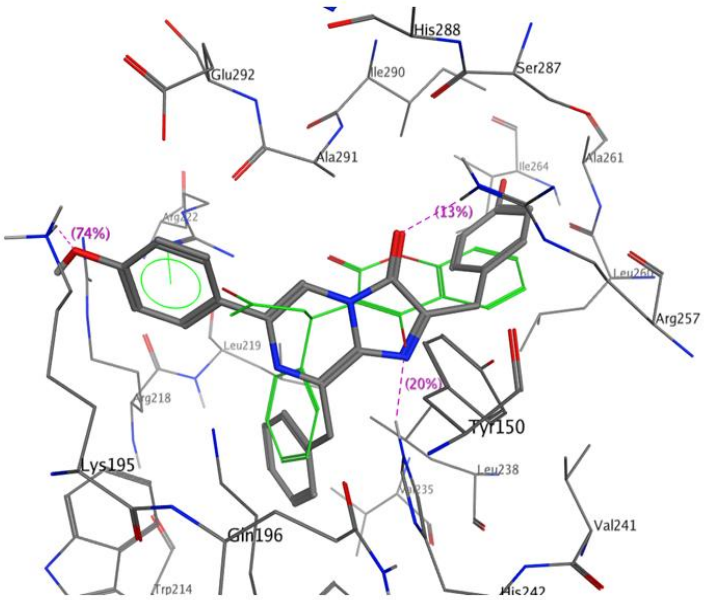


**Figure 4.17. The binding of coelenterazine and warfarin to Sudlow's site I on HSA demonstrated using molecular 3D modelling.** Structures: grey = coelenterazine and green = warfarin.

Warfarin and coelenterazine fit “snugly” between the apolar side-chains of Leu238 on the floor of the pocket and Ala291 on the roof of the pocket. The Trp214 residue is found in the hydrophobic part of the binding pocket and is an important part of the drug binding site. The Trp214 residue can interact hydrophobically with the non-polar part of the warfarin molecule (Petitpas *et al.,* 2001, Ascenzi and Fasano, 2010, Watanabe *et al.,* 2001).

It can be seen in figure 4.17 that a number of hydrogen bonds are formed between the protein and coelenterazine. A hydrogen bond was formed between the side chain of Arg257 and the carboxyl group of coelenterazine and another hydrogen bond was formed between the side chain of Lys195 and the hydroxyl group of coelenterazine. A hydrogen bond was also formed between the side chain of His242 and a nitrogen atom belonging to coelenterazine. The His242 side chain is known as a tautomer as it contains two nitrogen atoms on a benzyl ring that have the potential to readily interconvert *via* a process known as tautomerisation. This reaction causes the migration of the hydrogen atom that formed the hydrogen bond with the nitrogen atom of coelenterazine to the second nitrogen atom on the benzyl ring. The migration of the hydrogen atom to this position then has the potential of forming a hydrogen bond with the product of the coelenterazine chemiluminescence reaction, coelenteramide. This may be an important step in catalysing the coelenterazine chemiluminescence reaction. All compounds that bind to this site are positioned so that they form a hydrogen bond with the hydroxyl group of the Tyr150 residue thus this residue is considered to be important for drug binding (Ascenzi and Fasano, 2010). The drug binding site is split into two sub-chambers and these sub-chambers accommodate different portions of the drug structure. For example, the coumarin and benzyl parts of the warfarin structure fit into different but adjacent chambers in what is known as a “sock-shaped” pocket. The main chamber, located furthest away from the entrance of the pocket, holds the coumarin ring. The back end of the coumarin ring makes contact with Ile264, Ile290 as well as with the aliphatic portions of Arg257 and Ser287. The benzyl group of the warfarin structure binds to the sub-chamber that is made up of the Phe211, Trp214, Leu219 and Leu238 residues as well as making contact with the aliphatic portions of Arg218 and His242 (Petitpas *et al.,* 2001). Also, the acetonyl group that branches from the chrial carbon can be found at the entrance of the pocket.

Arg218 is located at the entrance of the binding pocket and it contributes positively to the binding of warfarin (Watanabe *et al.,* 2001).

Residues Lys199 and His242 are placed close to each other at the opening of the binding site. Mutations at either of these residues, increases drug binding significantly. However, when both of these residues are present, they can prevent warfarin from accessing the binding pocket (Watanabe *et al.,* 2001).

Molecular 3D modelling also highlighted five basic amino acid residues – Tyr150, Lys195, Arg222, His242 and Arg257 (fig. 4.14A). These residues fit with and support the pH profile of HSA shown in Chapter 3 (fig. 3.11) where an increase in chemiluminescence at alkaline pH was consistent with at least one basic amino acid being involved in coelenterazine binding and/or catalysis. Interestingly, similar basic amino acid residues have been found in the coelenterazine binding site of aequorin and obelin. Obelin is a calcium-regulated single subunit photoprotein with a molecular weight of approximately 22 kDa. Once calcium binds, the coelenterazine-oxygen complex undergoes oxidative decarboxylation resulting in light emission. Obelin is composed of 8 helices. These helices are known as helices A – H and each helix is composed of varying numbers of amino acid residues. The 8 helices are divided into two groups of 4. Helices A (residues 16-29), B (residues 39-54), C (residues 58 – 74) and D (residues 85-105) make up one group and are found in the N-terminal domain whereas helices E (residues 110-112), F (residues 132-142), G (residues 148-157) and H (residues 168-180) make up a second group and are found in the C-terminal domain. Both the N-terminal and the C-terminal can form a “cup” and the two can link together to form the overall structure of obelin. The inside of these “cups” are lined with hydrophobic residues. As with Sudlow’s site I on HSA, the coelenterazine-oxygen complex can fit comfortably in the pocket surrounded by the hydrophobic residues of the helices (Liu *et al.,* 2000). A number of residues from the 8 helices can contribute to the highly hydrophobic pocket in which the coelenterazine-oxygen complex fits. These residues include the Met25, Leu29, Ile42, Ala46, Ile50, Phe72, Phe88, Trp92, Ile111, Trp114, Val118, Phe199, Trp135, Ile144, Met171 and Trp179. This structure of the coelenterazine-oxygen binding pocket has not only been found in obelin, but other photoproteins such as aequorin are also thought to have the same binding pockets (Liu *et al.,* 2000).

It can be seen that obelin contains a number of Trp residues and these can interact closely with the coelenterazine-oxygen complex. For example, the side chains of the Trp92 and Trp179 residues are above and below the hydroxyphenyl ring of coelenterazine whereas the side chains of the Trp114 and Trp135 residues can be found near the hydroxyl-benzyl group of coelenterazine (Liu *et al.,* 2000). The presence of a Trp residue at position 86 in aequorin may play an important role in the production of the excited state product during the bioluminescence reaction.

Two His residues can be found at positions 22 and 175 in obelin and may play a role in the binding of oxygen to coelenterazine due to their close location to the coelenterazine-oxygen complex. Therefore any mutations at these two His residues may alter the bioluminescence. These photoproteins contain between 3 and 5 Cys residues and at least one of these may contribute to light emission. Obelin also contains two Tyr residues at positions 138 and 190 and these surround the coelenterazine-oxygen complex and can form strong hydrogen bonds with the complex. The Pro residue found at the C-terminal is crucial for light emission. This Pro residue acts as a “clip” to hold the coelenterazine in place and it has been shown that the removal of this particular residue will completely inhibit the ability of the photoprotein to emit light (Liu *et al.,* 2000, Vassel *et al.,* 2012).Therefore, of all the amino acid residues found in the photoproteins, the Trp, His, Cys as well as the C-terminal Pro are considered to be important for light emission. From this, it can be concluded that the active site located in the pocket of these photoproteins is highly hydrophobic and consists of a trio of amino acid residues including Trp, Tyr and His. Of these, one is responsible for the catalysis of the reaction and the other two are responsible for the binding of the coelenterazine-oxygen complex to the photoprotein (Woo *et al.,* 2008).

*Renilla* luciferase can also catalyse the bioluminescence reaction. This luciferase also has a large hydrophobic binding pocket to which coelenterazine can bind. The active site in this binding pocket also consists of a trio of amino acid residues and these include Asp120, Glu144 and His285. Of these three amino acid residues, His285 is responsible for the catalysis whereas both Asp120 and Glu144 are responsible for the binding of coelenterazine (Woo and Von Arnim, 2008).

The covalent modification of HSA by MeG significantly inhibited protein catalysed coelenterazine chemiluminescence by approximately 50 % (fig. 4.15A). The covalent modification of insulin also resulted in the inhibition of protein catalysed coelenterazine chemiluminescence but not to the same extent as that seen with albumin (fig. 4.15B). Interestingly, the covalent modification of 0.5 % (w/v) albumin (fig. 4.16A) and insulin (fig. 4.16B) by $H_2O_2$ significantly enhanced coelenterazine chemiluminescence by approximately 5- and 2.5-fold, respectively.

The conditions used to covalently modify both HSA and insulin *in vitro* varied significantly when compared to the conditions the same proteins are exposed to *in vivo*. The albumin concentration used *in vitro* (10 mg/ml) was approximately 5-fold lower than the concentration of albumin found *in vivo* (50 mg/ml). The concentration of insulin *in vitro* (10 mg/ml) exceeds both the normal and pathophysiological ranges *in vivo* (Jia *et al.,* 2006). The concentration of MeG (10 mM) used *in vitro* was significantly higher than the concentrations found in healthy individuals and was also higher than the reported elevated concentrations observed in patients with either type of diabetes. However, to determine the interaction of MeG with insulin *in vitro*, higher concentrations of MeG are required (Jia *et al.,* 2006). The proteins were incubated with MeG for one week but it has been shown by Jia et al (2006) that insulin appeared modified after 24 hours in the presence of much lower concentrations of the toxin.

The incubation of both albumin and insulin with MeG (fig. 4.15A and fig. 4.15B) for one week at room temperature resulted in the covalent modification of the proteins. It is know that arginine residues are the preferred target for MeG irreversible modification (Gao and Wang, 2006) and results in the formation of MG-H residues (Lo *et al.,* 1994, Thornalley, 2008). The modification of albumin by MeG resulted in high quantities of MG-H1 adduct formation at residues Arg114, Arg186, Arg218, Arg410 and Arg428. Both Arg114 and Arg186 have high surface exposure, whereas Arg218, Arg410 and Arg428 have low surface exposure and are also modified. There are also arginine residues at positions 81 and 209 with high surface exposure but these are not modified by MeG. Therefore, MeG modification only occurs at the residues that are exposed to the solvent (Gao and Wang, 2006). Depending on how accessible the arginine residues are on HSA to the toxin

will determine which of these residues will be modified. Residues Arg218 and Arg410 found in the binding pockets of drug sites I and II, respectively, are accessible to drugs and fatty acids, this indicates that these sites are also capable of binding other small molecules such as MeG and are therefore susceptible to modification. The modification of arginine residues by MeG leading to the formation of hydroimidazolones results in the subsequent loss of the positively charged arginine side chains as well as causing a change in the protein structure. These features are important for ligand binding, positioning of the substrate as well as stabilisation.

The majority of AGEs in the plasma of diabetic and non-diabetic patients are hydroimidazolones (Turk, 2010). The Tyr411 residues also located in the binding pocket containing Sudlow's site II can also be modified by MeG and forms an initial hemiacetal linkage that attaches this residue to the neighbouring Arg10 residues.

The B-chain of the insulin molecule also contains an arginine and lysine residue at positions 22 and 29, respectively. In the presence of elevated MeG concentrations as observed in diabetic patients, MeG will react with these residues resulting in the formation of irreversible AGEs (Turk, 2010).

The data in this chapter has identified Sudlow's site I as the coelenterazine binding site, and has also shown how the production of bacterial metabolic toxins as a result of carbohydrate metabolism can lead to the covalent modification of proteins such as insulin, thus altering their biological activity. Alterations in the biological activity of insulin can lead to insulin resistance and eventually type 2 diabetes (Lo *et al.,* 1994, Jia and Wu, 2007). Therefore, the coelenterazine chemiluminescence technique has the potential to be developed into a clinical test and can be used in the pharmaceutical industry to investigate the pharmacokinetics of new drugs prior to their release on to the market.

# Chapter 5:

# The effect of methylglyoxal on insulin action

## 5.1. Introduction

Insulin has a number of roles in the human body where it is responsible for regulating carbohydrate and fat metabolism. Methylglyoxal has been predicted to alter the structure and function of insulin. This aim of this chapter was to determine the effect of MeG on insulin action by investigating the effect of the toxin on glucose uptake and 3T3-L1 cell adipogenesis.

### 5.1.1. Glucose homeostasis

For cells to survive they need a stable environment. The process in which living organisms maintain this stable environment is known as homeostasis. This process ensures that the temperature, pH, ions and water balance of any living organism remains constant. If there are any environmental changes, cells are programmed to release molecules (e.g. hormones) so that the stable environment is maintained. This is known as negative feedback. For example, this negative feedback mechanism is the mechanism in which the body maintains normal glucose levels circulating in the blood *via* the release of hormones such as glucagon and insulin. This process is known as glucose homeostasis.

Cells use glucose as their main source of energy and levels of the sugar in the blood can vary due to a number of reasons. Elevated glucose concentrations occur after a meal and decreased glucose concentrations can occur as a result of glucose uptake by insulin-sensitive tissues. It is vital that the concentration of glucose in the blood stream is maintained well. If the blood glucose concentrations increase and are not controlled this can be toxic to the cells whereas if the blood glucose concentrations decrease and are not within the normal range this can result in starvation. Therefore, to ensure that blood glucose levels stay within the normal range the pancreas produces two important hormones:

- Glucagon is a catabolic hormone that is produced by the α-cells of the islets of Langerhans and is responsible for increasing blood glucose levels at times of starvation
- Insulin is an anabolic hormone that is produced by the β-cells of the islets of Langerhans and is responsible for decreasing blood glucose levels back within the normal range

### 5.1.2. Decreased blood glucose levels and the role of glucagon

Hypoglycaemia is the term used to describe reduced blood glucose concentrations. Blood glucose levels can fall below the normal range during exercise or during periods of fasting. Once this decrease in blood glucose concentration has been detected the α-cells of the islets of Langerhans release glucagon whilst inhibiting the release of insulin from the β-cells of the islets of Langerhans. The release of insulin is inhibited as any further release of the hormone would further reduce blood glucose levels. Both the liver and skeletal muscle store glucose in the form of glycogen. Glucagon stimulates the breakdown of glycogen in the hepatocytes of the liver *via* a process known as glycogenolysis. Once glycogen has been broken down, glucose is released into the blood stream through the GLUT2 transporter by facilitated diffusion ready for the uptake by other cells. Glucagon is also responsible for stimulating the breakdown of lipids stored in adipose tissue into fatty acids and glycerol. The fatty acids and glycerol are released into the bloodstream where other cells are able to use these for energy. The glycerol released into the blood as a result of lipolysis can be converted into glucose in the liver by glucagon. At times when glucose levels in the blood are low, glucose can be released into the blood from non-carbohydrate precursors such as amino acids *via* a process known as gluconeogenesis. These processes result in the release of glucose into the blood and help maintain normoglycaemia thus preventing hypoglycaemia.

### 5.1.3. Increased blood glucose and the role of insulin

Hyperglycaemia is the term used to describe elevated blood glucose concentrations. Blood glucose levels can increase above the normal range after a meal has been consumed. As a result of increased glucose levels, the glucose transporters, located on the surface on the β-cells of the islets of Langerhans detect this increase and as a result they release insulin. Insulin is important for reducing blood glucose levels by:

- Stimulating glucose uptake into insulin-sensitive tissues (e.g. adipose tissue and skeletal muscle)
- Stimulating the conversion of glucose to glycogen ready for storage in the liver until it is required
- Stimulating the conversion of glucose into lipids when the liver is no longer able to store glucose as glycogen

- Stimulating protein synthesis

### 5.1.3.1. Glucose transporters and glucose uptake by insulin-sensitive tissues

Glucose is mainly consumed through the diet. Once it reaches the small intestine it is ready to be transported in the blood until it reaches its target cell (Wood and Trayhurn, 2003). The majority of mammalian cells are able to transport glucose across the plasma membrane and occurs *via* specific transport proteins (Miki *et al.,* 2002). These specific transport proteins can be divided into two groups with different structures and functions (Wood and Trayhurn, 2003).

*The $Na^+$-dependent glucose cotransporters (SGLTs)*

This family of transporters transport glucose (as well as galactose) *via* a secondary active transport mechanism. The $Na^+$-$K^+$ ATPase pump generates a $Na^+$-electrochemical gradient, therefore for glucose transport into the cell, glucose must travel against the concentration gradient. This type of transport mainly occurs across the luminal membrane of cells that line the small intestine and in the cells found in the proximal tubules of the kidneys (Wood and Trayhurn, 2003).

*The facilitative glucose transporters (GLUTs)*

The facilitative glucose transporters are a large family of transporters that are found in mammals. These transporters form an aqueous pore across the plasma membrane therefore allowing glucose to flow freely into the cell. This family of transporters are proteins consisting of 12-transmembrane spanning domains (fig. 5.1). Individual transporters have different tissue distributions, different kinetic properties and different sugar specificities (Bryant *et al.,* 2002, Khan and Pessin, 2002).

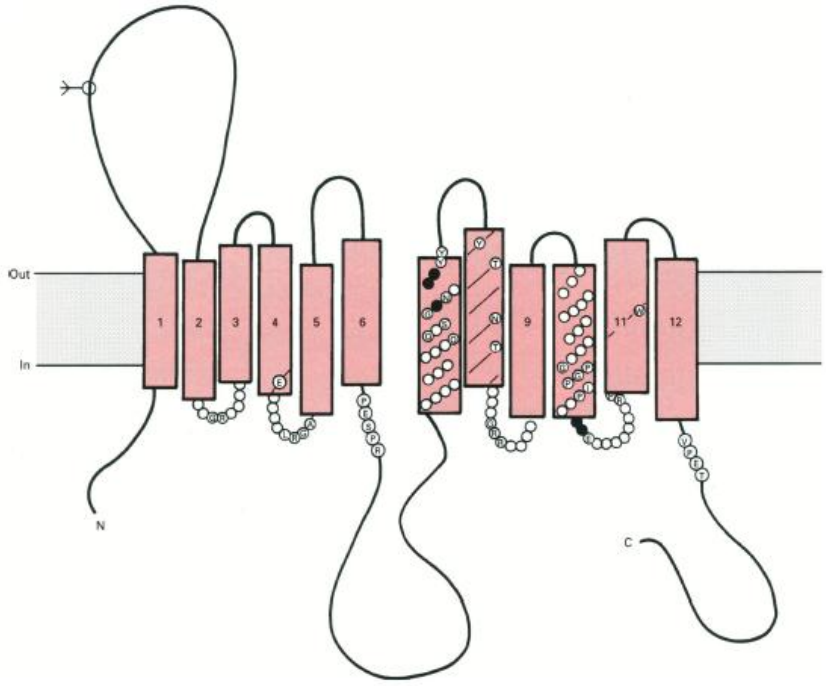


**Figure 5.1. The structure of the facilitative glucose transporters (GLUTs)** (Gould and Holman, 1993).

The 12-transmembrane spanning domains are arranged so that the N- and C-terminals are at the cytoplasmic surface. Two large loops can be found between helices 1 and 2 and helices 6 and 7, however, the large loop between helices 6 and 7 splits the structure in half. One half of the structure contains the N-terminal domain and the other contains the C-terminal domain. The loops linking the other helices are very short since they are made up of 8 residues and this is a common feature of this family (Gould and Holman, 1993).

Thirteen members of this family, GLUTs 1-12 and the $H^+$-coupled myo-inositol transporter (HMIT), have been identified. These transporters are responsible for the transport of glucose down its concentration gradient without the need for energy (Watson *et al.,* 2004). The identified members have been divided into three classes:

- **Class I facilitative glucose transporters**
    - This group of transporters is made up of GLUTs 1-4. These GLUTs are the most widely characterised in regards to their structure, function and tissue distribution (Wood and Trayhurn,

2003). The first member of this class to be identified was GLUT1, it is has a wide distribution and is found in the brain and erythrocytes as well as having moderate levels in adipocytes, myocytes and hepatocytes (Khan and Pessin, 2002, Olson and Pessin, 1996, Gould and Holman, 1993). The GLUT2 transporter is highly expressed in the β-cells of the pancreas as well as in the liver and kidneys. This transporter has a low affinity (high $K_m$) for glucose. In the α- and β-cells of the pancreas, GLUT2 has been predicted to have a role in the glucose sensing mechanism (Khan and Pessin, 2002, Wood and Trayhurn, 2003). GLUT2 transporters can also be found on the sinusoidal membrane of the liver cells and are responsible for the transport of glucose in and out of the cells. In contrast to GLUT2, GLUT3 has a high affinity (low $K_m$) for glucose and can be found in tissues where there is a need for glucose as a fuel (e.g. the brain) (Khan and Pessin, 2002). GLUT4 is also known as the insulin-sensitive glucose transporter and is found in cardiac myocytes, adipocytes and skeletal myocytes. GLUT4 transporters have also been identified in the brain (Wood and Trayhurn, 2003). The mechanism in which insulin stimulates glucose uptake into the insulin-sensitive tissues *via* this transporter follows below.

- **Class II facilitative glucose transporters**
    - This group of transporters comprises GLUT5, GLUT7, GLUT9 and GLUT11. GLUT5 is the fructose-specific transporter and can be located in the small intestine, testes and kidneys. However, GLUT7 and GLUT9 have not been functionally characterised. GLUT7 expression is unknown whereas GLUT9 is expressed in the liver and kidneys (Wood and Trayhurn, 2003, Watson *et al.,* 2004).
- **Class III facilitative glucose transporters**
    - This group of transporters comprises GLUT6, GLUT8, GLUT10, GLUT12 and HMIT (Wood and Trayhurn, 2003). The GLUT6 transporter is a pseudogene that is not expressed at the protein level (Mueckler, 1994). The GLUT8 transporter is expressed in the testes, brain as well as in adipocytes. GLUT10 can be found in insulin-sensitive tissues (e.g. skeletal and cardiac

myocytes) as well as being expressed in the liver and pancreas. GLUT12 can be found in the small intestine, prostate as well as in adipocytes and in cardiac and skeletal myocytes. The HMIT transporter can be found in the brain (Wood and Trayhurn, 2003, Watson *et al.,* 2004).

*The GLUT4 transporter and its role in insulin-stimulated glucose uptake*

Insulin enables glucose to pass through the insulin-sensitive glucose transporter, GLUT4, into the cells of muscle (striated and cardiac) and adipose tissue *via* facilitated diffusion. In the presence of low concentrations of insulin, GLUT4 transporters are found packed into storage vesicles in the cytoplasm of the cell. When in the storage vesicles, the GLUT4 transporters are not able to transport glucose. In contrast, when the glucose transporters on the surface of the pancreatic β-cells detect an increase in glucose levels, insulin is released. Insulin then binds to its receptor and the storage vesicles containing the GLUT4 transporters move from the cytoplasm to the plasma membrane. This is known as GLUT4 translocation. The storage vesicles then fuse with the plasma membrane thus enabling glucose to enter the cell. Once the glucose levels decrease and are back within the normal range, the receptors are no longer occupied by insulin and the GLUT4 transporters are recycled back into the cytoplasm in the storage vesicles (Watson and Pessin, 2001, Bryant *et al.,* 2002, Watson *et al.,* 2004).

#### 5.1.3.2. Insulin stimulates glycogenesis

At times when blood glucose concentrations are raised, insulin promotes the addition of glucose molecules to glycogen in the liver ready for storage. This process is known as glycogenesis.

#### 5.1.3.3. Insulin stimulates lipogenesis and inhibits lipolysis

When the liver can no longer store the glucose that has been converted to glycogen the glucose is converted into lipids and stored in adipose tissue until it is required when blood glucose levels fall. This process is known as lipogenesis. Insulin also prevents the breakdown of lipids (lipolysis) that are stored in adipose tissue into fatty acids and glycerol (Kahn and Flier, 2000).

### 5.1.4. The role of insulin in cell differentiation

3T3-L1 cells were first isolated by Green and Kehinde and when confluent they are capable of differentiating into adipocytes (Chang and Polakis, 1978). This differentiation is also known as adipogenesis and involves the conversion of the 3T3-L1 cells from their undifferentiated fibroblast-like preadipocyte form into adipocytes that are round in shape and are filled with triglycerides as well as expressing adipose-associated genes (Reed *et al.,* 1977, Hausman *et al.,* 2001, Reusch *et al.,* 2000). The induction of adipogenesis depends on the cell culture model used due to their ability to respond to certain agents (Gregoire, 2001). When the 3T3-L1 cells were maintained in cell culture medium supplemented with foetal calf serum (FCS) they can spontaneously differentiate into adipocytes over a number of weeks. However, these cells will not express the adipocyte phenotype until confluency has been reached and cell division has stopped (Gregoire *et al.,* 1998, Reed *et al.,* 1977). The expression of the adipocyte phenotype by these cells at confluency can be controlled by specific agents or hormones that are known to have an effect on lipogenesis or lipolysis (Reed *et al.,* 1977). The standard adipogenic cocktail used for the accelerated induction of maximal differentiation at confluence contains supraphysiological concentrations of insulin, dexamethasone (DEX) and isobutylmethylxanthine (IBMX). DEX is a synthetic glucocorticoid agonist that is used for the activation of the glucocorticoid receptor pathway and IBMX is a cAMP-phosphodiesterase inhibitor that is used for the activation of the cAMP-dependent protein kinase pathway (Gregoire, 2001, Reed *et al.,* 1977, Gregoire *et al.,* 1998, Ntambi and Young-Cheul, 2000, Schmidt *et al.,* 1990). The requirement of these two compounds for the acceleration of the differentiation process suggests the involvement of insulin, the glucocorticoid receptor pathway and the cAMP-dependent protein kinase pathway in adipogenesis (Gregoire, 2001). DEX plays a role in the induction of 3T3-L1 cell differentiation whereas IBMX has been predicted to potentiate the effects of the glucocorticoids (e.g. DEX) (Schmidt *et al.,* 1990).

### 5.1.5. Overall aim, specific aims and experimental strategy

#### 5.1.5.1. Overall aim

Insulin is known to be important for the accelerated differentiation of cells. The initial aim of this chapter was to characterise the differentiation of 3T3-L1 cells from their fibroblastic form to the adipocytic form.

The next aim was to demonstrate the importance of insulin for cell differentiation and to investigate the effect of MeG on cell differentiation.

#### 5.1.5.2. Specific aims

- The initial aim of this chapter was to demonstrate the differentiation of 3T3-L1 cells induced by the differentiation cocktail containing insulin
- To confirm the importance of insulin in the differentiation process by comparing 3T3-L1 differentiation induced by the differentiation cocktail in the presence and absence of insulin
- To demonstrate that the addition of relevant channel blockers to the differentiation cocktail can result in the inhibition of 3T3-L1 cell differentiation
- To investigate the effect of covalently modified insulin on the differentiating ability of these cells

#### 5.1.5.3. Experimental strategy

To set up an adipogenesis assay, using an adipogenic cocktail supplemented with insulin to induce 3T3-L1 differentiation from the fibroblastic phenotype to the adipogenic phenotype. To use the assay to investigate the effects of relevant channel blockers and MeG on cell differentiation.

## 5.2. Materials and methods

### 5.2.1. Materials

7F2 (mouse osteoblast progenitor cell line) cells and 3T3-L1 (mouse embryonic fibroblast-adipose like cell-line) cells were donated from Dr Bronwen Evans, Department of Child Health, University Hospital of Wales, Heath Park Campus, Cardiff. All cell culture media ingredients, unless otherwise stated, were obtained from Gibco®, Invitrogen Ltd, Paisley, UK. D-glucose, insulin, adipogenesis assay reagents as well as all the reagents used for RNA extraction, PCR and electrophoresis were purchased from Sigma-Aldrich.

### 5.2.2. Cell culture

The cells used for the determination of cell differentiation were 3T3-L1 (mouse embryonic fibroblast-adipose like cell line). This particular cell line was chosen because they have the ability to differentiate into adipocytes. For 3T3-L1 cell culture and cell husbandry see section 2.3.

#### 5.2.2.1. Adipogenesis assay cell culture medium

The nature of the induction of adipogenesis depends on the specific cell culture model used because the responsiveness to inducing agents varies considerably between preadipose cell lines and primary preadipocytes. Overall, in serum-containing medium, the standard adipogenic cocktail for maximal differentiation contains, supraphysiological concentrations of insulin, dexamethasone (DEX) which is a synthetic glucocorticoid agonist traditionally used to stimulate the glucocorticoid receptor pathway and isobutylmethylxanthine (IBMX) which is a cAMP-phosphodiesterase inhibitor traditionally used to stimulate the cAMP-dependent protein kinase pathway (Gregoire, 2001, Gregoire *et al.,* 1998, Ntambi and Young-Cheul, 2000).

| | **Control cell culture medium (50 ml)** | **Adipogenic cell culture medium (50 ml)** | **Post-adipogenic cell culture medium (50 ml)** |
|---|---|---|---|
| **DMEM (ml)** | 44.988 | 43.488 | 43.488 |
| **10 % FBS (ml)** | 5 | 5 | 5 |
| **1 % pen/strep (ml)** | 0.5 | 0.5 | 0.5 |
| **1 mg/ml insulin (ml)** | - | 0.5 | 0.5 |
| **1 mM dexamethasone (ml)** | - | 0.0125 | - |
| **50 mM IBMX (ml)** | - | 0.5 | - |
| **Ethanol (ml)** | 0.512 | - | 0.512 |

**Table 5.1. The volumes of reagents required to make 50 ml of control, adipogenic and post-adipogenic cell culture medium for 3T3-L1 cells.**

### 5.2.3. Adipogenesis assays and adipocyte formation

3T3-L1 cells, a cloned subline of 3T3-mouse embryo fibroblasts, undergo differentiation in culture, gaining both morphological and biochemical characteristics of adipocytes. Several days after reaching confluence, 3T3-L1 cells lose their fibroblastic morphology, round up, and deposit large amounts of cytoplasmic triglyceride (Student *et al.,* 1980).

#### 5.2.3.1. Adipogenesis assay

Cells were seeded into 12-well plates at a density of 30,000/well. Figure 5.2 shows the differentiation process that occurred once the cells reached confluency. Once confluent, the cells were left for a further 48 hours in 3T3-L1 cell culture medium to begin spontaneous differentiation.

To accelerate the differentiation process, the cell culture medium was aspirated from 2-day post-confluent cells and was replaced with the adipogenic cocktail containing 10 % FBS-DMEM, 1 µg/ml insulin, 0.25 µM dexamethasone and 0.5 mM IBMX. Forty-eight hours later, the adipogenic cocktail was aspirated and replaced with the post-adipogenic medium containing 10 % FBS-DMEM containing 1 µg/ml insulin. A further 48 hours later, the medium was aspirated and replaced with 10 % FBS-DMEM. Thereafter, the 10 % FBS-DMEM medium was changed every 2 days until completion of the assay at day 10 (Tafuri, 1996).

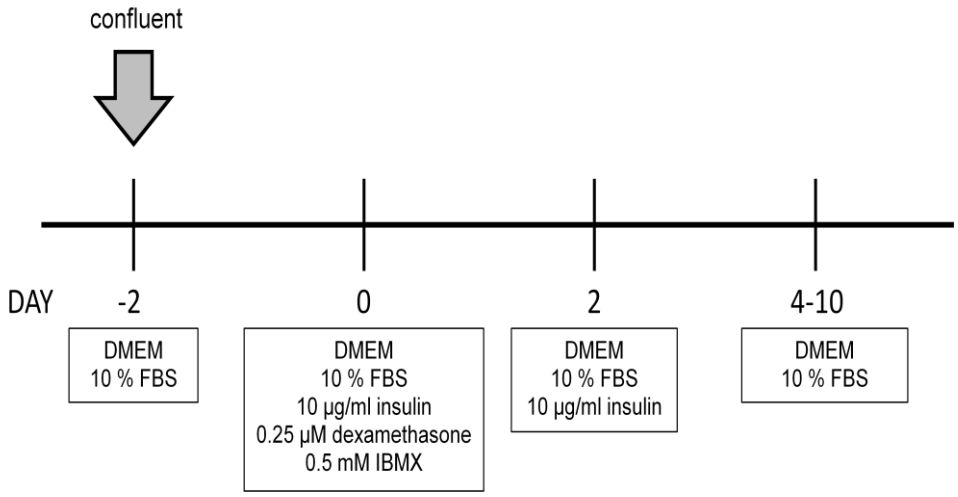


**Figure 5.2. Scheme showing the 3T3-L1 cell differentiation process**

#### 5.2.3.2. Oil red O staining for lipids

Oil red O is a lysochrome (fat-soluble dye) diazo dye used for the staining of neutral triglycerides and lipids and was therefore used to distinguish between preadipocytes and adipocytes.

A 0.5 % (w/v) stock solution of stain was prepared by dissolving oil red O (purchased from Sigma-Aldrich) in isopropanol and filtered to remove any grit. An oil red O working solution was prepared by mixing 6 ml of the 0.5 % (w/v) stock solution with 4 ml distilled water. The staining procedure was as follows: the 10 % FBS-DMEM medium was aspirated from the wells and the cell monolayer was washed with 1x D-PBS and the cells were then fixed with formal saline (10 % formaldehyde in PBS) for 15 minutes. Cells were then washed twice with distilled water. Stain was applied to each well and incubated for 15 minutes. The stain was aspirated and the cells were washed with 60 % isopropanol to remove any excess stain, followed by several washes with 1x D-PBS until all the background stain was removed. Cells were stored in 1x D-PBS and photographed under the microscope. Lipid droplets were stained red.

#### 5.2.3.3. Quantification of lipid formation

The distilled water that was left for the photographing was aspirated and the cells were left to dry. Once dry, 100 % isopropanol was added to each well to break down the cell membrane and extract the dye. The 12-well plate was placed on a plate rocker for 15-30 minutes. Then 100 µl from each well was transferred into the wells of a 96-well plate and the absorbance was measured at 490 nm using an ELISA plate reader.

### 5.2.4. Glucose uptake and GLUT4 expression

The following techniques were studied and carried out to investigate the importance of insulin and to determine the effects of MeG on the biological actions of insulin.

Glucose uptake by rat hemi-diaphragm and 7F2 can be determined using a glucose oxidase/peroxidase assay kit (Sigma). The assay kit contained glucose oxidase/peroxidase reagent, o-dianisidine reagent, assay reagent and a glucose standard.

The initial step in the determination of glucose uptake was to construct a standard curve. Into the first well of a 96-well plate, 40 µl of the blank was added, this was followed by the addition of 40 µl of each standard into their allocated wells. Each concentration was measured in duplicate. At time zero, the reaction was started with the addition of 80 µl of assay reagent into the two wells containing the blanks. Sixty second intervals were allowed between the additions of the assay reagent to the subsequent wells. The plate was wrapped in aluminium (Al) foil and placed in the incubator at 37 $^{o}$C (5% $CO_2$ and 95% air) for 30 minutes. After the 30 minute incubation period, the reaction was stopped with the addition of 80 µl of 12 N $H_2SO_4$ again at 60 second intervals. The absorbance of each well was measured against the reagent blank at 540 nm.

#### 5.2.4.1. Glucose uptake by the rat hemi-diaphragm in the presence and absence of insulin

The diaphragm was removed from Sprague-Dawley rats by dissection and placed in Krebs-Ringer HEPES buffer. The diaphragm was cut into two equal pieces and blot dried to remove any excess buffer. Each half was weighed and the weight was recorded. Each half was placed in a universal tube containing 2 ml of testing solution. The universal tubes were placed on a rocker for 5 hours at 37 $^{o}$C (5% $CO_2$ and 95% air). Immediately after the tissue was added to the testing solution, a 40 µl sample was taken and transferred to a microtitre plate. Samples of the same volume were then taken every hour for the duration of the experiment. At each time point, triplicate readings were taken. At the end of the experiment, the tissue was removed from each of the universal tubes and blot dried, weighed and the weight was recorded. Once all the samples had been collected, glucose uptake could then be determined using the glucose oxidase/peroxidase assay.

When all the samples were collected either from the rat hemi-diaphragm or 7F2 cells the glucose oxidase/peroxidase assay was carried out. The assay was started by adding 80 µl of glucose oxidase/peroxidase assay reagent to the first three wells on the plate representing time zero. The assay reagent was the subsequently added to the remaining wells at 60 second intervals. The plate was wrapped in Al-foil and placed in the incubator at 37 $^{o}$C (5% $CO_2$ and 95% air) for 30 minutes. After the 30 minute incubation period, the reaction was stopped by adding 80 µl of 12 N $H_2SO_4$ to each sample at 60

second intervals. The absorbance was measured against the blank at 540 nm using an ELISA plate reader.

#### 5.2.4.2. Glucose uptake by 7F2 cells in the presence and absence of insulin

Cells were cultured in 75 $cm^2$ flasks as a large number of cells were required for the determination of glucose uptake. The cells were cultured and maintained as previously described in section 2.3. Once the cells covered approximately 80% of the base of the flask, the cells were removed and counted. A cell suspension of 5 x $10^6$ cells was placed into each Eppendorf. The Eppendorfs were centrifuged at 1000 rpm for 3 minutes. Pellets of cells had formed at the bottom of each tube. The supernatant was removed and discarded. The pellet of cells was resuspended in 1 ml testing solution. At time zero, 40 µl samples were taken from each tube and transferred into a 96-well plate and stored on dry ice. The microtitre plate was stored on dry ice so that the samples were frozen down immediately to prevent the cells from further utilising the glucose present. Samples were taken in triplicate every hour for 5-6 hours. Once all the samples had been collected, glucose uptake could then be determined using glucose oxidase/peroxidase assay.

When all the samples were collected either from the rat hemi-diaphragm or 7F2 cells the glucose oxidase/peroxidase assay was carried out. The assay was started by adding 80 µl of glucose oxidase/peroxidase assay reagent to the first three wells on the plate representing time zero. The assay reagent was the subsequently added to the remaining wells at 60 second intervals. The plate was wrapped in Al-foil and placed in the incubator at 37 $^oC$ (5% $CO_2$ and 95% air) for 30 minutes. After the 30 minute incubation period, the reaction was stopped by adding 80 µl of 12 N $H_2SO_4$ to each sample at 60 second intervals. The absorbance was measured against the blank at 540 nm using an ELISA plate reader.

### 5.2.5. Molecular biology

The aim of these experiments was to determine GLUT4 expression in mouse adipose tissue as well as undifferentiated and differentiated 3T3-L1 cells.

### 5.2.5.1. RNA extraction

#### RNA extraction from mouse adipose tissue

The RNA was kindly extracted from mouse adipose tissue and supplied by Dr Riffat Naseem.

#### RNA extraction from 3T3-L1 cells

The medium was aspirated from a confluent 25 $cm^2$ flask of cells and the cell monolayer was washed with 1 ml PBS. Then 2.5 ml of Trizol (1 ml per 10 $cm^2$) was added and spread over the base of the flask. The cell lysate was pipetted several times and transferred into two Eppendorfs. To the Eppendorfs, 0.2 ml of chloroform ($CHCl_3$) was added. The tubes were shaken to mix. The tubes were left at room temperature for 2-3 minutes. The Eppendorfs were centrifuged at 12,000 rpm for 10 minutes. The supernatant was removed carefully to ensure that the colourless aqueous phase was not disturbed and discarded. The remaining colourless aqueous phase containing the RNA was transferred into Eppendorfs.

### 5.2.5.2. Polymerase Chain Reaction

Amplification of the cDNA took place in 12.5 µl reactions using primers purchased from Invitrogen, Ltd. Table 5.1 Contains primer information.

| Primer: | Sequence: |
|---|---|
| β-actin | F: AGAGGGAAATCGTGCGTGACAT<br>R: AGGAAGGCTGGAAAAGAGCC |
| GLUT4 | F: CCGCGGCCTCCTATGAGATACT<br>R: AGCCACCCCGAAGATGAGT |

**Table 5.2. Oligonucleotide primer details for the GLUT4 transporter**

Polymerase chain reaction (PCR) was carried out using the GoTaq® Flexi DNA Polymerase kit (purchased from Promega) and control reactions were carried out using either sterile nuclease-free water rather than cDNA. The standard composition of PCR reactions and the reaction conditions used are shown in Tables 5.2 and 5.3, respectively. The PCR amplification products were analysed by gel electrophoresis and stained with ethidium bromide, in 1x TAE buffer and visualised under UV light.

| Components | Final concentrations | Volumes |
|---|---|---|
| 5x Green GoTaq® Flexi buffer | 1x | 2.5 µl |
| $MgCl_2$, 25 mM | 1.5 mM | 0.75 µl |
| PCR nucleotide (dNTP) mixture | 200 µM each dNTP | 1.25 µl |
| Forward primer | 0.4 µM | 0.5 µl |
| Reverse primer | 0.4 µM | 0.5 µl |
| GoTaq® DNA polymerase (5u $\mu l^{-1}$) | 0.3125 u | 0.0625 µl |
| cDNA (or nuclease-free $H_2O$) | - | 0.5 µl |
| Nuclease-free $H_2O$ | - | To 12.5 µl |

**Table 5.3. The composition of 12.5 µl PCR reactions**

| Step | Temperature ($^oC$) | Time | Number of cycles |
|---|---|---|---|
| Initial denaturation | 95 | 10 min | 1 |
| Denaturation | 95 | 30 s | - |
| Annealing | 55 | 45 s | 30 |
| Extension | 72 | 1 min | - |
| Final extension | 72 | 10 min | 1 |
| soak | 4 | indefinate | - |

**Table 5.4. PCR reaction conditions**

### 5.2.5.3. Electrophoresis

A 1 % agarose gel was made by adding 0.7 g of agarose to 70 ml TAE buffer. This was then placed in the microwave for three 10 second cycles to dissolve. The glass beaker holding the gel was placed in water and allowed to cool to a temperature of approximately 60 $^oC$. Once cooled, 2.1 µl of ethidium bromide was added and mixed. The combs were placed in position and the gel was poured into the tank. If there were any bubbles present these were either carefully pushed to the side or removed from the gel. Once the gel had solidified it was covered with 1 % TAE buffer. The ladder (5 µl) and the sample (10 µl) were loaded on to the gel. The gel was then left to run for 50 minutes (100 mV and 200 mA). Once the gel had finished running, it was carefully removed from the tank and a picture of the gel was taken using a UV light.

### 5.2.6. Statistical analysis

One way analysis of variance (one-way ANOVA) was used to analyse the data produced. Results were considered to be significant if they were at the 95 % confidence level where $p < 0.05$.

## 5.3. Results

3T3-L1 cells, a cloned subline of 3T3 mouse embryo fibroblasts, undergo differentiation in culture, acquiring both morphological and biochemical characteristics of adipocytes. Several days after reaching confluence, 3T3-L1 cells lose their fibroblastic morphology, become spherical in shape and large amounts of cytoplasmic triglyceride are deposited within the cell (Student *et al.,* 1980). Adipogenesis can be quantified using oil red O stain. Oil red O stain is a lysochrome (fat-soluble dye) diazo dye that stains neutral triglycerides and lipids.

The results that follow show that 3T3-L1 cells can be converted from the fibroblastic form into adipocytes (fig. 5.3 and fig 5.4) and shows that certain agents can have an effect on cell differentiation (fig. 5.5 – fig. 5.8).

### 5.3.1. The differentiation of 3T3-L1 cells induced by insulin

In order to demonstrate the importance of insulin in 3T3-L1 cell differentiation it was first necessary to develop an adipogenesis assay that could be used to determine 3T3-L1 cell differentiation. Cell differentiation significantly increased when 3T3-L1 cells were treated with the adipogenic cocktail over a period of 10 days (fig. 5.3 and fig. 5.4). The treatment of cells with the adipogenic cocktail resulted in a 2-fold ($p < 0.05$) and 8-fold ($p < 0.01$) increase in differentiation when compared to cells that were treated with cell maintenance media for the same duration.

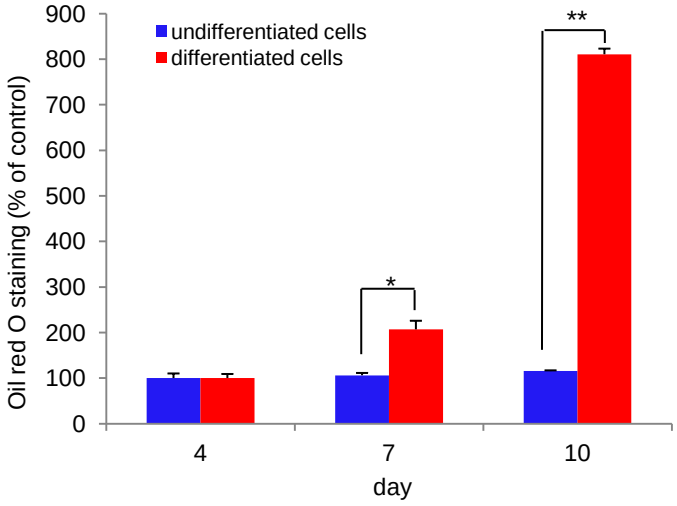


**Figure 5.3. The determination of 3T3-L1 cell differentiation on days 4, 7 and 10 in the presence and absence of adipogenic cocktail containing insulin, DEX and IBMX.** Cells were seeded into a 12-well plate at a density of 30,000/well. Cells were left to reach confluency. Once confluent, cells were left for a further 48 hours in normal cell maintenance medium to begin spontaneous differentiation. The cell medium was aspirated from the 2-day post-confluent cells and was replaced with the adipogenic cocktail containing 10 % FBS-DMEM, 1 µg/ml insulin, 0.25 µM DEX and 0.5 mM IBMX to accelerate the differentiation process. 48 hours later, the adipogenic cocktail was replaced with the post-adipogenic medium containing 10 % FBS-DMEM and 1 µg/ml insulin. 2 days later, the post-adipogenic medium was replaced with 10 % FBS-DMEM. This medium was changed every 2 days thereafter until completion of the assay at day 10. The cells were fixed with formal saline (10 % formaldehyde in PBS) and differentiation was quantified using oil red O stain. Error bars represent the mean +/- SE of three observations. Asterisks indicates significant difference where * represents $p < 0.05$ and ** represents $p < 0.01$ when compared with the corresponding bars for day 4.

In order to distinguish between preadipocytes and adipocytes, oil red O staining was used as it stains neutral triglycerides and lipids red. The images that follow compare 3T3-L1 cells that were treated with cell maintenance medium (fig. 5.4 A-C) with those that were treated with the adipogenic cocktail (fig. 5.4 D-F) and these were then stained with oil red O to quantify cell differentiation. Cells that were treated with cell maintenance medium still appeared to have their fibroblastic morphology, did not appear round and staining did not show the presence of any triglycerides (fig. 5.4 A-C), therefore

suggesting that the cells were not differentiated into adipocytes. Cells that were treated with the adipogenic cocktail did appear round in shape and were stained red due to the presence of triglycerides (fig. 5.4 D-F). On day 4 only a few cells appeared to be round in shape and stained red (fig. 5.4D). Approximately 50 % of the cells stained on day 7 appeared round and are red due to the presence of triglycerides (fig. 5.4E) whereas nearly all the cells stained on day 10 appeared to have taken the adipocyte form (fig. 5.4F).

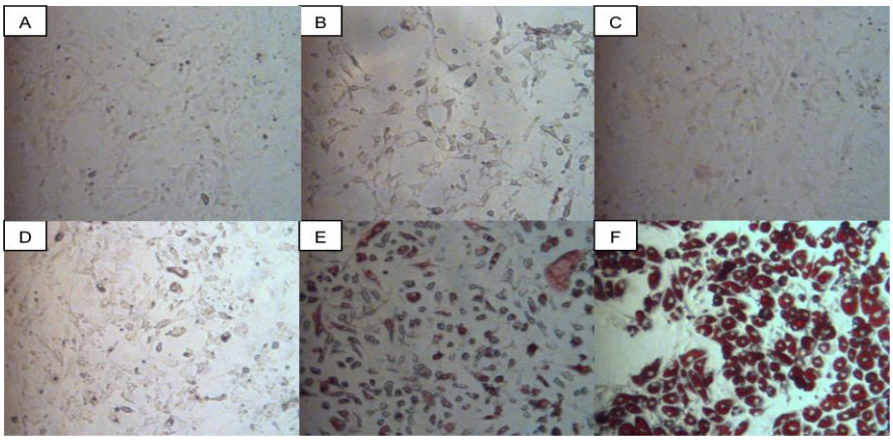


**Figure 5.4. Images showing adipocyte formation quantified using oil red O stain over a period of 10 days.** Images A-C show 3T3-L1 cells treated with cell culture maintenance medium and stained with oil red O solution on: A) day 4; B) day 7 and C) day 10. Images D-F show 3T3-L1 cells treated with the adipogenic cocktail and stained with oil red O solution on: D) day 4; E) day 7 and F) day 10.

### 5.3.2. The effect of insulin and other compounds on 3T3-L1 cell differentiation

The results that follow show the effects of insulin and other compounds on 3T3-L1 differentiation. Insulin is important for cell growth and differentiation. The initial aim was to demonstrate the importance of insulin in 3T3-L1 cell differentiation (fig. 5.5). Adipocytes were observed on all three days despite being treated with the general cell maintenance medium. 3T3-L1 cells were treated with the adipogenic cocktail with and without insulin to investigate the effect of the protein on differentiation. Cells that were treated with the adipogenic cocktail without insulin were still able to differentiate however the

addition of insulin to the adipogenic cocktail did appear to significantly accelerate cell differentiation on day 10 ($p < 0.05$).

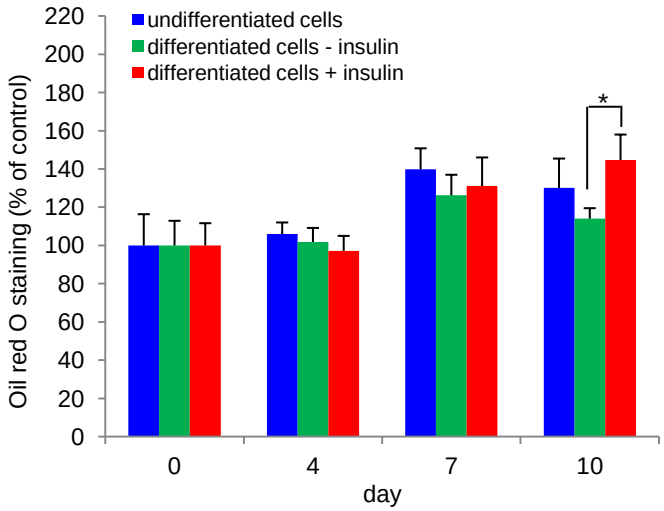


**Figure 5.5. The effect of insulin on 3T3-L1 cell differentiation over a period of 10 days.** Cells were seeded into a 12-well plate at a density of 30,000/well. Once confluent, cells were left for a further 48 hours in normal cell maintenance medium to begin spontaneous differentiation. The cell medium was aspirated from the 2-day post-confluent cells and was replaced with the adipogenic medium containing 10 % FBS-DMEM, 1 µg/ml insulin, 0.25 µM DEX and 0.5 mM IBMX or the adipogenic medium containing 10 % FBS-DMEM, 0.25 µM DEX and 0.5 mM IBMX. 48 hours later, the adipogenic medium +/- insulin was replaced with the post-adipogenic medium containing 10 % FBS-DMEM +/- 1 µg/ml insulin. 2 days later, the post-adipogenic medium was replaced with 10 % FBS-DMEM. This medium was changed every 2 days thereafter until completion of the assay at day 10. The cells were fixed with formal saline (10 % formaldehyde in PBS) and differentiation was quantified using oil red O stain. Error bars represent the mean +/- SE of three observations. Asterisk indicates a significant difference where $p < 0.05$ when the differentiation observed in the presence of insulin was compared with that in the absence of insulin on the same day.

Calcium channels play a role in cell proliferation and differentiation. In order to investigate if these channels were involved in 3T3-L1 cell proliferation and differentiation, the calcium channel blocker, tetrandrine was added to the adipogenic cocktail (fig. 5.6). Cells that were maintained in general cell culture medium showed reduced adipogenesis on days 7 and 10 however, this could

not be the case. Adipogenesis was enhanced in cells that were exposed to the adipogenic cocktail. Adipogenesis increased by approximately 15 and 50 % on days 7 and 10, respectively. The addition of 3 μM tetrandrine to both the general cell culture medium and the adipogenic cocktail had no significant effect on adipogenesis.

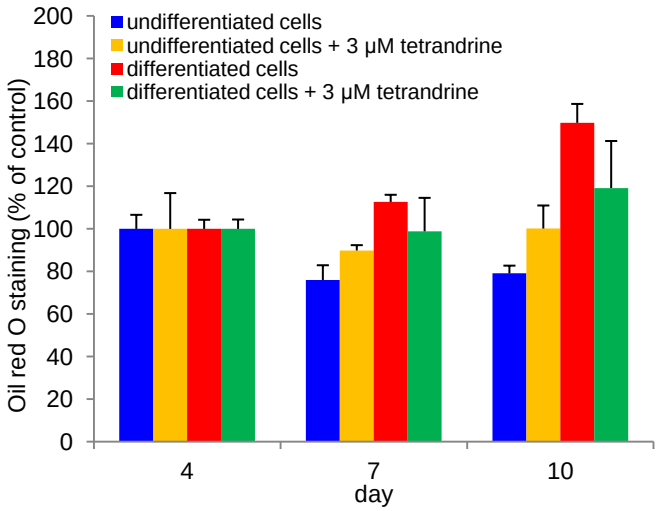


**Figure 5.6. The effect of tetrandrine on 3T3-L1 cell differentiation over a period of 10 days.** Cells were seeded into a 12-well plate at a density of 30,000/well. Once confluent, cells were left for a further 48 hours in normal cell culture maintenance medium to begin spontaneous differentiation. The cell medium was aspirated from the 2-day post-confluent cells and was replaced with the adipogenic cocktail containing 10 % FBS-DMEM, 1 μg/ml insulin, 0.25 μM DEX and 0.5 mM IBMX or the adipogenic cocktail supplemented with 3 μM tetrandrine. 48 hours later, the adipogenic cocktail +/- 3 μM tetrandrine was replaced with the post adipogenic medium containing 10 % FBS-DMEM and 1 μg/ml insulin. 2 days later, the post-adipogenic medium was replaced with 10 % FBS-DMEM. This medium was changed every 2 days thereafter until completion of the assay at day 10. The cells were fixed with formal saline (10 % formaldehyde in PBS) and differentiation was quantified using oil red O stain. Error bars represent the mean +/- SE of three observations.

Potassium channels are crucial for cell proliferation and differentiation. In order to investigate if these channels were involved in 3T3-L1 cell proliferation and differentiation, the BK potassium channel blocker, tetraethylammonium (TEA) was added to the adipogenic cocktail (fig. 5.7). Cells that were

maintained in cell maintenance medium for the duration of the experiment showed no significant increases in adipogenesis. Adipogenesis was enhanced in cells that were exposed to the adipogenic cocktail. In the presence of the adipogenic cocktail, adipogenesis increased by approximately 10 and 30 % on days 7 and 10, respectively. The addition of 10 mM TEA to the adipogenic cocktail, inhibited adipogenesis by approximately 30 and 50 % on days 7 and 10, respectively. The inhibition of adipogenesis by TEA was only significant on day 10 ($p < 0.05$).

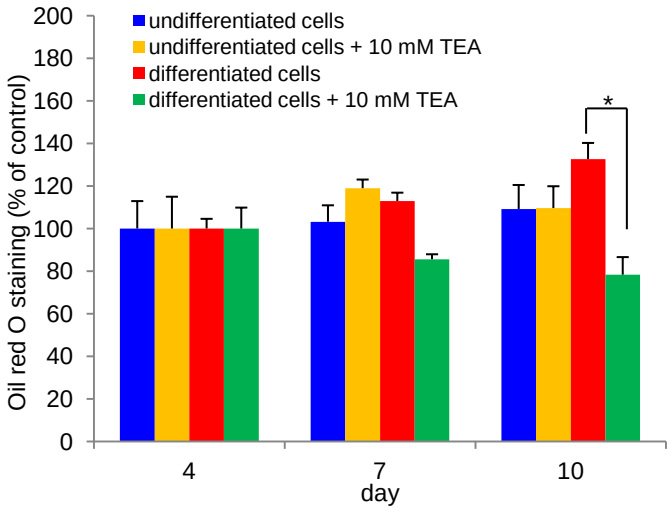


**Figure 5.7. The effect of tetraethylammonium (TEA) on 3T3-L1 cell differentiation over a period of 10 days.** Cells were seeded into a 12-well plate at a density of 30,000/well. Once confluent, cells were left for a further 48 hours in normal cell culture maintenance medium to begin spontaneous differentiation. The cell medium was aspirated from the 2-day post-confluent cells and was replaced with the adipogenic cocktail containing 10 % FBS-DMEM, 1 µg/ml insulin, 0.25 µM DEX and 0.5 mM IBMX or the adipogenic cocktail supplemented with 10 mM TEA. 48 hours later, the adipogenic medium +/- 10 mM TEA was replaced with the post adipogenic medium containing 10 % FBS-DMEM and 1 µg/ml insulin. 2 days later, the post-adipogenic medium was replaced with 10 % FBS-DMEM. This medium was changed every 2 days thereafter until completion of the assay at day 10. The cells were fixed with formal saline (10 % formaldehyde in PBS) and differentiation was quantified using oil red O stain. Error bars represent the mean +/- SE of three observations. Asterisks indicates significant difference where $p < 0.05$ when the differentiation observed in the presence of 10 mM TEA was compared with that in the absence of 10 mM TEA on the same day.

MeG is known to directly inhibit insulin signalling in cultured adipocytes. In order to investigate the effect of MeG on 3T3-L1 cell proliferation and differentiation, MeG was added to the adipogenic cocktail containing insulin (fig. 5.8). Adipogenesis occurred in cells that were exposed to the general maintenance medium. Adipogenesis was enhanced in cells that were exposed to the adipogenic cocktail. In the presence of the adipogenic cocktail, adipogenesis increased by approximately 35, 60 and 100 % on days 4, 7 and 10, respectively. The addition of 10 mM MeG to the adipogenic cocktail, had no significant effect on adipogenesis when compared with the adipogenesis in the absence of MeG observed on the same days.

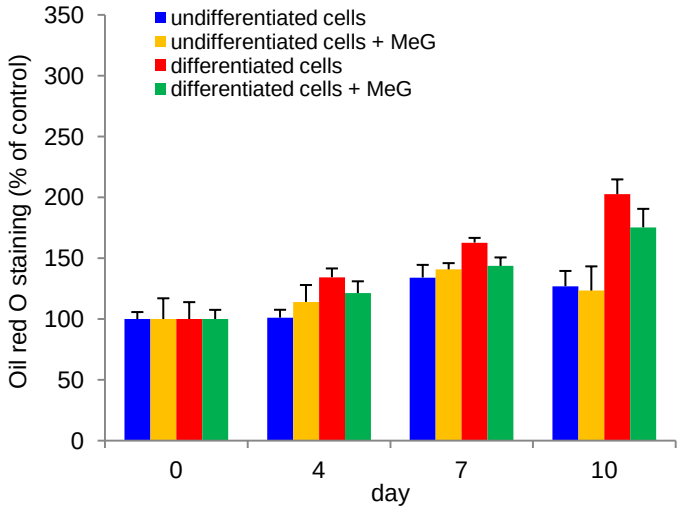


**Figure 5.8. The effect of methylglyoxal (MeG) on 3T3-L1 cell differentiation over a period of 10 days.** Cells were seeded into a 12-well plate at a density of 30,000/well. Once confluent, cells were left for a further 48 hours in normal cell culture maintenance medium to begin spontaneous differentiation. The cell medium was aspirated from the 2-day post-confluent cells and was replaced with the adipogenic cocktail containing 10 % FBS-DMEM, 1 µg/ml insulin, 0.25 µM DEX and 0.5 mM IBMX or the adipogenic medium supplemented with 1 µM MeG. 48 hours later, the adipogenic cocktail +/- 1 µM MeG was replaced with the post adipogenic medium containing 10 % FBS-DMEM and 1 µg/ml insulin. 2 days later, the post-adipogenic medium was replaced with 10 % FBS-DMEM. This medium was changed every 2 days thereafter until completion of the assay at day 10. The cells were fixed with formal saline (10 % formaldehyde in PBS) and differentiation was quantified using oil red O stain. Error bars represent the mean +/- SE of three observations.

### 5.3.3. Glucose uptake by rat hemi-diaphragm and 7F2 cells

In order to investigate the effect of MeG (and other compounds) on insulin action an attempt was made to develop an assay whereby insulin stimulated glucose uptake by both insulin sensitive cells and tissue could be determined. Glucose uptake by the rat hemi-diaphragm and 7F2 cells proved unsuccessful. In experiments using the rat hemi-diaphragm there was no basal glucose uptake and insulin did not stimulate glucose uptake into the tissue (data not shown). In experiments using 7F2 cells no insulin stimulated glucose uptake was observed and in fact the data suggested that insulin actually inhibited glucose uptake (data not shown).

## 5.4. Discussion and conclusions

The results in this chapter have shown that 3T3-L1 cells are capable of differentiating from the fibroblastic form into adipocytes whether it occurs spontaneously or is accelerated *via* the addition of an adipogenic cocktail consisting of supraphysiological concentrations of insulin, DEX and IBMX (fig. 5.3 and fig. 5.4). Insulin is important for 3T3-L1 cell differentiation as the exclusion of the hormone from the adipogenic cocktail significantly inhibited ($p < 0.05$) cell differentiation by approximately 5 and 30 % on days 7 and 10, respectively (fig. 5.5). The inclusion of tetrandrine (a calcium channel blocker) (fig. 5.6) to the adipogenic cocktail had no significant effect on 3T3-L1 cell adipogenesis. The addition of TEA (a BK potassium channel blocker) (fig. 5.7) to the adipogenic cocktail inhibited 3T3-L1 adipogenesis by approximately 30 and 50 % on days 7 and 10, respectively. The inhibition of adipogenesis by TEA was only significant on day 10 ($p < 0.05$). The inhibition in adipogenesis produced by TEA suggested that potassium channels play an important role in the cell differentiation process. The addition of 10 mM MeG (fig. 5.8) to the adipogenic cocktail, had no significant effect on 3T3-L1 adipogenesis.

Although 3T3-L1 differentiation was observed the amount of differentiation was not consistent in all experiments. For example, the initial experiment carried out to develop the adipogenesis assay showed that there was a 700 % increase in adipogenesis on day 10 whereas in other experiments there was only a 50 – 100 % increase in adipogenesis on day 10.

Reasons for the variation in the amount of differentiation might be due to the cells having different passage numbers (e.g. higher passage than others) and/or due to the degree of cell confluence (e.g. over confluent cells). Cells with a high passage number can experience changes in morphology and may not respond to stimuli as well as cells with a lower passage number and this may help explain why adipogenesis varied between individual experiments. Allowing the cells to become over confluent might have resulted in the inhibition of growth or prevented them from differentiating.

The exclusion of insulin from the adipogenic cocktail caused 3T3-L1 cells to remain in the undifferentiated fibroblast-like preadipocyte form. However, when maintained in cell culture medium supplemented with FCS/FBS, the 3T3-L1 fibroblast-like cells can spontaneously differentiate over a period of several weeks. These cells only express the adipocyte phenotype when the cells are confluent and cell division has stopped (Gregoire *et al.,* 1998, Reed *et al.,* 1977). The period of time needed for the confluent cell cultures to adopt the adipocyte phenotype can be altered by specific agents that are known to have an effect on lipogenesis and lipolysis (Reed *et al.,* 1977). The standard adipogenic cocktail used for the accelerated induction of maximal differentiation at confluence contains supraphysiological concentrations of insulin, DEX and IBMX. DEX is a synthetic glucocorticoid agonist that is responsible for the activation of the glucocorticoid receptor pathway and IBMX is a cAMP-phosphodiesterase inhibitor which is used to activate the cAMP-dependent protein kinase pathway (Gregoire, 2001, Reed *et al.,* 1977, Gregoire *et al.,* 1998, Ntambi and Young-Cheul, 2000, Schmidt *et* al., 1990). Both DEX and IBMX are used in conjunction with each other as IBMX can potentiate the effect of glucocorticoid agonists like DEX (Schmidt *et al.,* 1990). The constant exposure of 3T3-L1 cells to these supraphysiological concentrations of insulin once confluent will result in > 75 % of the cells adopting the adipocyte form within 3-4 weeks. Therefore, supraphysiological concentrations of insulin are used to accelerate and maximise adipocyte formation, however, the removal of insulin from the differentiation cocktail will result in < 1 % of the cells adopting the adipocyte form (Reed *et al.,* 1977). This confirms the importance of insulin and glucocorticoids such as DEX in the differentiation process.

Hyperinsulinemia is a common feature in obesity and is associated with weight gain. Hyperinsulinemia can be due to the excessive production of exogenous

insulin or it can occur in those individuals who do not produce enough insulin or the insulin that is produced does not work efficiently and they require intense administration of exogenous insulin. It is possible that endogenous hyperinsulinemia as a result of excessive food consumption can stimulate adipogenesis as well as significantly increasing white adipose tissue (WAT) mass resulting in obesity with insulin resistance but this remains to be proved (Klemm *et al.,* 2001). Insulin degrades rapidly in the 48 hours between medium changes in the adipogenesis process; this may explain why supraphysiological concentrations of insulin are required for cell differentiation. Differentiated cells have been shown to have higher rates of insulin degradation than undifferentiated cells (Reed *et al.,* 1977).

As the 3T3-L1 cells differentiate and become adipocytes the number of insulin receptors present are said to increase. It has been reported that the ability of human adipocytes to bind insulin is significantly greater than the ability of human fibroblasts to bind the hormone. However the mechanisms responsible for the increased number of insulin receptors seen in adipocytes remain unknown.

Potassium channels are important for cell proliferation and cell differentiation. Ramirez-Ponce et al (1990) were the first to study the electrophysiological characteristics of white adipocytes using the whole-cell patch clamp method. They showed that rat white adipocytes contain voltage-dependent potassium ($K^+$) channels of the delayed rectifier type (Hamida *et al.,* 2011, Ramirez-Ponce *et al.,* 1996). Since then, a number of other authors have confirmed this finding in isolated white adipocytes. It is possible that insulin can modulate the $K^+$-channel conductances in adipocytes. It has been predicted that insulin increases the number of voltage-dependent $K^+$-channels in adipocytes and have implicated these channels in the adipogenesis process (Hamida *et al.,* 2011, Ramirez-Ponce *et al.,* 1996).

Potassium currents have been identified in all differentiated cells but only occasionally in preadipocytes. However, the number of $K^+$-channels and thus $K^+$ currents increased in adipocytes in the presence of insulin. Insulin alters the electrical properties of adipocytes and may therefore also modulate $K^+$ conductance in these cells. $K^+$-channels can be blocked by the $K^+$-channel blocker, TEA. This chapter investigated whether $K^+$-channels play a role in

adipogenesis by adding 10 mM TEA to the differentiation cocktail. It has been previously shown by (Henney *et al.,* 2009) that a concentration of 0.3 mM TEA was sufficient enough to block the channel. Ramirez-Ponce et al (2002) also demonstrated that mature white adipocytes that were differentiated in culture can also be blocked by low concentrations of this $K^+$-channel blocker. The data in this chapter suggested that the concentration of TEA used (10 mM) may not inhibit cell proliferation but may in fact inhibit cell differentiation, hence the decrease in adipogenesis observed when the cells were treated with the adipogenic cocktail supplemented with 10 mM TEA compared to the adipogenic cocktail in the absence of TEA. This data suggested that insulin was not the only important factor for adipocyte formation but that the expression of functional $K^+$-channels are also important for adipocyte development in culture.

Ramirez-Ponce et al (1991) also confirmed the presence of voltage-dependent calcium ($Ca^{2+}$) channels in adipocytes. The $Ca_v3.1$ T-type channel is the dominant voltage-dependent $Ca^{2+}$ channel in mouse preadipocytes and is thought to be involved in the regulation of preadipocyte proliferation which is an important step in the development of adipose tissue (Oguri *et al.,* 2010).

Intracellular calcium $[Ca^{2+}]_i$ plays an important role in some of the metabolic disorders that are related to obesity. $[Ca^{2+}]_i$ plays an important regulatory role in adipogenesis and is therefore an important contributor to increased adipose tissue mass. Increasing $[Ca^{2+}]_i$ during the initial stages of the differentiation process will result in the inhibition of adipogenesis, however in contrast, increasing $[Ca^{2+}]_i$ during the latter stages of adipogenesis will stimulate the differentiation process. Therefore, $[Ca^{2+}]_i$ stimulates and accelerates adipogenesis whilst inducing the adipocyte phenotype during the latter stages of the differentiation process. For this to happen, increased $[Ca^{2+}]_i$ levels result in a significant increase in the expression of PPARγ which is essential if the cells are to adopt the adipocyte phenotype (Cammisotto and Bukowiecki, 2004, Shi *et al.,* 2000). Therefore one would expect the addition of tetrandrine, a known $Ca^{2+}$-channel blocker, to the adipogenic cocktail to inhibit $[Ca^{2+}]_i$ resulting in reduced PPARγ expression and decreased adipogenesis, however, this was not the case.

Extensive research has been carried out to determine the role of MeG in the structural and functional changes in human insulin. Jia et al (2006) incubated insulin (1 µg/µl) with MeG (100 µM) for different periods of time. Using mass spectrometry they showed that after an incubation period of 2 hours there were no additional peaks noticed therefore suggesting that there were no changes in the structure or mass of insulin. After an incubation period of 3 days, mass spectrometry identified two additional peaks at *m/z* 5880 and 5934. The peak identified at *m/z* 5880 corresponded with the addition of one MeG molecule (72 Da) to insulin (5808 Da) whereas, the peak identified at *m/z* corresponded with the addition of two molecules of MeG to insulin along with the loss of one water molecule (54 Da) (Jia *et al.,* 2006). This information suggested that the incubation with MeG caused the mass of insulin to increase. It is known that MeG can react readily with the free amino groups of arginine and lysine residues of proteins resulting in the formation of MeG-adducts. Insulin contains one arginine and one lysine residue on the B-chain at positions 22 and 29, respectively. When MeG reacts with the lysine residue at position 29, CEL is formed and it is the formation of this that causes the mass of insulin to increase by 72 Da. However, when MeG reacts with the arginine residue at position 22, a condensation reaction occurs resulting in the formation of a hydroimidazolone. It is the formation of this hydroimidazolone that causes the mass of insulin to increase by 54 Da (Jia *et al.,* 2006).

The same authors have also shown that the formation of MeG-adducts will significantly inhibit glucose uptake by insulin-sensitive cells (e.g. 3T3-L1 cells). To determine the role of MeG in the development of insulin resistance, both insulin and MeG were added directly to the 3T3-L1 cells for a period of 30 minutes prior to the determination of glucose uptake. The authors predicted that for the toxin to interfere with insulin-stimulated glucose uptake it would need to modify the insulin receptor therefore inhibiting the binding of insulin leading to impaired glucose uptake (Jia *et al.,* 2006, Jia and Wu, 2007). Jia et al (2006) showed that the 30 minute exposure of cells to MeG did not significantly affect glucose uptake. They also showed that in the cells exposed to MeG there were no changes in the expression of the IR, IRS-1 and PI3K when compared with the expression observed in cells that were not exposed to the toxin. Although there were no changes in expression observed, they did report however, that there was reduced IRS-1 tyrosine phosphorylation and

PI3K activity (Jia *et al.,* 2006, Jia and Wu, 2007). The reduction in PI3K activity coincided with the inhibition of IRS-1 tyrosine phosphorylation.

The addition of the MeG-scavenger *N*-acetyl-cysteine (NAC) reversed these reductions and therefore suggested that MeG was involved in the inhibition of insulin-stimulated glucose uptake. From this information, the authors concluded that MeG was not affecting the binding affinity or the expression of the insulin receptor but was in fact inhibiting insulin signalling in the insulin-sensitive cells due to decreased IRS-1 tyrosine phosphorylation as well as impaired IRS-1/PI3K association (Riboulet-Chavey *et al.,* 2006, Jia *et al.,* 2006, Jia and Wu, 2007).

Jia et al (2006) also looked at the effect MeG-adduct formation had on the release of insulin from the pancreatic β-cells and on insulin clearance. The cleavage of proinsulin in the β-cells results in the production of insulin and C-peptide. For every molecule of insulin that is released, one molecule of C-peptide is also released. Therefore, it is possible to quantify insulin release from the β-cells by measuring the amount of C-peptide that is released (Jia *et al.,* 2006). The authors showed that as a consequence of MeG-adduct formation, the amount of C-peptide, and therefore insulin, released from the cells decreased. Hyperinsulinemia may also occur due to reduced insulin clearance in the liver as a result of MeG-adduct formation (Jia *et al.,* 2006). Insulin levels in the blood are maintained by a process known as endocytosis. During this process, the insulin receptor with bound insulin is internalised back into the cell where it is stored until it is required. In 3T3-L1 cells, endocytosis results in the breakdown of insulin and the recycling of the receptors back to the plasma membrane. These authors compared insulin levels in the media of cells that were treated with either insulin or MeG-modified insulin. They found that the media of cells treated with insulin contained lower concentrations of insulin than the media of cells treated with MeG-modified insulin. This information suggested that modified insulin was unable to undergo endocytosis but the mechanism involved in this process requires further investigation (Jia *et al.,* 2006).

As MeG was added to the differentiation cocktail containing insulin, it was possible that the insulin was covalent modified and as a result caused changes in insulin signalling and therefore insulin action. It has been shown in this chapter that insulin is important for adipogenesis and if there is impaired

insulin signalling due to MeG-adduct formation this would explain the decreases in adipogenesis observed.

The addition of MeG to the differentiation cocktail may also decrease adipogenesis *via* the inhibition of both PPARγ and C/EBPα (CCAAT/enhancer binding protein-α) as both of these are known to be crucial for cell differentiation to occur.

An attempt to investigate the effect of MeG on insulin action using a glucose uptake assay proved unsuccessful. The 7F2 cells were in their osteoblastic form rather than their differentiated adipocytic form. This may partly explain insulin did not stimulate glucose uptake by these cells. Also whilst still in the osteoblastic form, these cells would not express the GLUT4 transporter that is crucial for insulin-stimulated glucose uptake. However, if they had been differentiated into adipocytes the cells should then express the GLUT4 transporter and insulin-stimulated glucose uptake would be expected. Both the rat hemi-diaphragm tissue and 7F2 cells may also be lacking insulin receptors. Insulin receptors are vital so that insulin can bind. Once insulin binds to its receptor, it stimulates GLUT4 translocation from the intracellular storage sites to the plasma ready for glucose uptake. Therefore, reductions in insulin receptors means less insulin can bind resulting in decreased glucose uptake.

Interestingly, it was found that the undifferentiated 3T3-L1 cells expressed high levels of GLUT4. As 3T3-L1 cells can spontaneously differentiate over a period of time one would therefore expect to see GLUT4 expression. These cells can also express high quantities of the GLUT1 transporter isoform (Olson and Knight, 2003), this may help explain why there might also be reduced GLUT4 expression.

Insulin can rapidly decrease GLUT4 expression in 3T3-L1 adipocytes (Flores-Riveros *et al.,* 1993, Olson and Knight, 2003). If 3T3-L1 cells are continuously exposed to insulin, GLUT4 expression varies *in vivo* and *in vitro*. Animals that have been exposed to intense concentrations of insulin have demonstrated increased GLUT4 expression in their adipose tissue, whereas the intense exposure of 3T3-L1 cells *in vitro* resulted in either no change or a significant decrease in GLUT4 expression. This suggests that the GLUT4 is no longer responding to insulin directly (Olson and Knight, 2003). The incubation of 3T3-L1 adipocytes in media not supplemented with glucose results in reduced GLUT4 expression. GLUT4 expression in such cases reduced 10-fold and

leads to increases in GLUT1 expression (Olson and Knight, 2003). Therefore, further work needs to be carried out to optimise conditions for molecular biology and then to determine both GLUT4 and GLUT1 expression in 3T3-L1 cells.

This chapter has shown that 3T3-L1 cells can differentiate from their fibroblastic form to the adipogenic form whether it occurs spontaneously or is accelerated *via* the addition of a differentiation cocktail. The importance of insulin in the differentiation process has been shown as well as highlighting the role of $K^+$ and $Ca^{2+}$ channels in this process. In view of the lack of effect of insulin on glucose uptake, it is now necessary to look at the antilipolytic effects by determining glycerol release from differentiated cells. Another approach to determine the effect of MeG on insulin action would be to carry out receptor binding assays.

# Chapter 6:

# General discussion & future work

## 6.1. General discussion and conclusions

The overall aim of this thesis was to investigate the potential role of the bacterial metabolic toxin hypothesis in the development of diabetes. In order to do this, the strategy was to identify a property of the two major proteins in the blood (HSA and insulin) that could be measured in order to determine covalent modification. The property chosen was coelenterazine chemiluminescence. The results in this thesis showed that:

- Both albumin and insulin have a mono-oxygenase activity demonstrated by coelenterazine chemiluminescence
- That coelenterazine binds to Sudlow's site I (warfarin site) on HSA
- That the production of the bacterial metabolic toxin, MeG, leads to the covalent modification of both albumin and insulin, thus reducing the biological activities of these proteins.

The data in this thesis demonstrated that both HSA and BSA were able to catalyse coelenterazine chemiluminescence (fig. 3.6). However, BSA was significantly better ($p < 0.001$) than HSA at catalysing coelenterazine chemiluminescence despite having a 78 % sequence similarity. Using this same method, the abilities of three other proteins – insulin, gelatin and haemoglobin at catalysing coelenterazine chemiluminescence were also investigated (fig. 3.7). Insulin was also shown to catalyse coelenterazine chemiluminescence. Interestingly, gelatin and the well known oxygen carrier, haemoglobin, were poor at catalysing the coelenterazine chemiluminescence reaction. It was then necessary to demonstrate if the ability of these proteins at catalysing coelenterazine chemiluminescence was consistent with them having enzymatic activity. To demonstrate this, 4 criteria were used to determine if HSA catalysed coelenterazine chemiluminescence was enzymatic: (1) heat denaturable; (2) exhibits saturable substrate characteristics; (3) inhibition or activation by specific cations that are known to bind to the protein and (4) inhibition by drugs that are known to bind to the protein.

It was shown that HSA catalysed coelenterazine chemiluminescence was heat denaturable (fig. 3.8). Denaturation is defined as the loss of enough structure to make the enzyme inactive. Increasing temperature is factor known to denature proteins. When HSA was exposed to a temperature of 95 $^{o}$C for 15 minutes, it was irreversibly denatured thus preventing it from refolding when cooled, resulting in reduced enzymatic activity and the inhibition of HSA catalysed coelenterazine chemiluminescence. It has since been shown that by increasing the heating period from 15 minutes to 30 minutes, HSA catalysed coelenterazine chemiluminescence was inhibited by > 90 % (Vassel *et al.,* 2012). Under the same conditions, insulin was not denatured (fig. 3.9). Human insulin is a much smaller protein than HSA, thus making it more difficult to denature. It has been shown that insulin can be denatured in Tris-HCl buffer, pH 7.4, containing 0.2 mM cysteine for 6 hours at a temperature of 22 $^{o}$C (Jiang and Chang, 2005).

To determine the maximum velocity of the HSA catalysed coelenterazine chemiluminescence reaction (fig. 3.10), the coelenterazine concentration was increased until a constant rate of product formation was seen. From this, the substrate concentration ($K_m$) at which the rate is half of the $V_{max}$ was determined. It was shown that at a coelenterazine concentration of 40 µM, the protein was saturated. Saturation occurs because as the substrate concentration increased, more of the free-HSA was converted to the coelenterazine-HSA form. The $K_m$ was shown to be approximately 20 µM.

The effect of increasing pH on the ability of HSA and insulin to catalyse coelenterazine chemiluminescence was also investigated. It was shown that HSA (fig. 3.11) and insulin (fig. 3.12) were pH sensitive. As the pH became increasingly alkaline, the coelenterazine chemiluminescence catalysed by both proteins increased. The half maximum for HSA and insulin were at approximately pH 8.2 and pH 7.8, respectively. The large increase in chemiluminescence observed at alkaline pH suggests that there must be at least one basic amino acid residue in the binding region that is important for the catalysis. Therefore, the pH at the half maximum represents the pKa of the amino group in the protein that is important for catalysis.

The entrance to the pocket to which coelenterazine is predicted to bind on HSA consists of two lysine residues (Ly195 and Lys199) and three arginine residues (Arg218, Arg222 and Arg257) (Otagiri, 2005, Sugio *et al.,* 1999). Under acidic conditions, the amino groups of these residues are protonated, therefore making the entrance to the pocket positively charged. This positive charge under these conditions prevents coelenterazine from binding to the protein, hence why no chemiluminescence was observed. As the pH becomes more alkaline, the residues at the entrance lose protons through deprotonation making the entrance uncharged, resulting in chemiluminescence.

Albumin has a negative charge but several cations can bind weakly and reversible to the protein (Varshney *et al.,* 2010). Of the cations tested, $Fe^{2+}$, $Fe^{3+}$ and $Zn^{2+}$ ($p < 0.001$; fig. 3.13 – fig. 3.15 and fig. 3.17) significantly inhibited coelenterazine chemiluminescence catalysed by HSA, however, this was dependent on the concentration and had a potency of $Fe^{2+}/Fe^{3+} > Zn^{2+}$. The addition of $Ca^{2+}$ (fig. 3.16) did not significantly affect the coelenterazine chemiluminescence catalysed by HSA. The presence of the cation and coelenterazine at the same concentration will result in them both competing for the binding site. Which of these will bind depends on their binding affinities for the protein. If the cation had the highest affinity for the protein then it would bind resulting in the inhibition of HSA catalysed coelenterazine chemiluminescence and *vice versa*. When the concentration of the cation increases above the coelenterazine concentration ($> 10^{-5}$ M) the cation will bind to the protein. The cation binds due to its ability to saturate the protein, therefore inhibiting light emission. However, when the concentration of the substrate is higher than that of the cation, coelenterazine will bind to the protein, resulting in enhanced light emission. The cation binding site is unknown and it is possible that the effect produced by these cations may be due to an allosteric effect.

Interestingly, $Zn^{2+}$ produced opposite effects on HSA and human insulin. The addition of $Zn^{2+}$ significantly inhibited HSA catalysed coelenterazine chemiluminescence ($p < 0.001$; fig. 3.17), but significantly enhanced human insulin catalysed coelenterazine chemiluminescence ($p < 0.0001$; fig. 3.18). $Zn^{2+}$ is known to be important for the biosynthesis and storage of insulin and is known to interact with insulin. Enhanced human insulin catalysed coelenterazine chemiluminescence may be due to $Zn^{2+}$ causing the protein to undergo a conformational change, and it is this change that allows

coelenterazine to bind more effectively resulting in increased chemiluminescence.

An advantage of knowing that certain drugs can bind to either Sudlow's site I (e.g. warfarin) or Sudlow's site II (e.g. diazepam) made it possible to predict the coelenterazine binding site on the protein. All of the drugs that are known to bind to Sudlow's site I tested significantly inhibited HSA catalysed coelenterazine chemiluminescence ($p < 0.001$; fig. 4.6 – fig. 4.9). At this site, competition can exist between coelenterazine and the drug when they are present at the same concentration however; the compound with the highest binding affinity for the site will displace the other (Rahman *et al.,* 2005). The concentration of each of the compounds will determine which will become bound to HSA. If the concentration of the drug is lower than the coelenterazine concentration ($< 10^{-5}$ M) there is more of the substrate present and therefore it is the coelenterazine that will bind to HSA, hence why no significant change in HSA catalysed coelenterazine chemiluminescence was observed. As the concentration of the drug rises above the coelenterazine concentration ($> 10^{-5}$ M), there is more drug present and available to bind to HSA, therefore preventing coelenterazine from binding thus inhibiting HSA catalysed coelenterazine chemiluminescence. The addition of the site II drug – diazepam, also significantly inhibited HSA catalysed coelenterazine chemiluminescence ($p < 0.001$; fig. 4.10) but not to the same extent as that observed with the addition of the site I drugs. However, the other site II drugs tested (phenytoin and ibuprofen) did not significantly affect HSA catalysed coelenterazine chemiluminescence (fig. 4.11 and fig. 4.12). From this data, Sudlow's site I was predicted to be the coelenterazine binding site.

Competitive binding experiments can be used to investigate the high affinity binding of drugs to proteins (Kragh-Hansen, 1991). Binding may occur to one site (Brodersen *et al.,* 1977) and it was therefore necessary to investigate the competitive binding properties of warfarin and coelenterazine on HSA catalysed coelenterazine chemiluminescence. Warfarin is known to have a weak fluorescence, but this fluorescence is enhanced when it binds to HSA. The fluorescence observed when warfarin binds to HSA decreases if a second ligand such as coelenterazine competes for the site already occupied by warfarin (Sahoo *et al.,* 2008). However, the inhibition of HSA catalysed coelenterazine chemiluminescence by the addition of warfarin demonstrated characteristics of both competitive and uncompetitive inhibition. As both

competitive and uncompetitive inhibition was observed, this suggests that warfarin is capable of binding with different affinities to either the free enzyme (HSA only) or to the HSA-coelenterazine complex. Therefore, it is possible that warfarin could interfere with substrate binding (increase $K_m$) and reduce catalysis in the HSA-coelenterazine complex (decrease $V_{max}$) (fig. 4.13). From this, it can be concluded that the inhibition observed in the presence of warfarin exhibited mixed inhibition enzyme kinetics. Mixed inhibition is usually the result of an allosteric effect where the inhibitor binds to a different site on the enzyme to that of the substrate. The binding of warfarin to the allosteric site causes the enzyme to undergo a conformational change and causes the substrate to have a decreased affinity for the binding site. In such cases, the binding of the inhibitor will affect the binding of the substrate and the binding of the substrate will affect the binding of the inhibitor.

In the experiment used to determine the type of enzyme inhibition in the presence of warfarin, the concentration of HSA was similar to or higher than the coelenterazine concentration, thus a key condition for the Michaelis-Menten equation is that the enzyme does not significantly reduce the substrate concentration, therefore to a first approximation the equation may not hold. That is why the results state that the approximate $K_m$ was 20 μM as it was not possible to a precise Lineweaver-Burk plot.

Molecular 3D modelling was used to identify the coelenterazine binding site. This method demonstrated the importance of Sudlow's site I as the major catalytic site on HSA (fig. 4.14A), therefore confirming this site as the coelenterazine binding site. It was shown that coelenterazine fit "snugly" into site I, where warfarin is also capable of binding. However, when coelenterazine was placed in the pocket containing site II, it did not fit comfortably and resulted in a number of interactions with the surface of the protein (fig. 4.14B). As well as confirming the coelenterazine binding site, molecular 3D modelling also highlighted five basic amino acid residues – Tyr150, Lys195, Arg222, His242 and Arg257 within the binding site (fig. 4.14A). These residues fit with and support the pH profile of HSA shown in Chapter 3 (fig. 3.11) where an increase in HSA catalysed coelenterazine chemiluminescence at alkaline pH was consistent with at least one basic amino acid being involved in coelenterazine binding and/or catalysis. Interestingly, similar basic amino acid residues have been found in the coelenterazine binding sites of aequorin and obelin. This data suggests that

only a few fundamental amino acid residues at the coelenterazine binding site are enough to catalyse coelenterazine chemiluminescence.

From this, the genetic engineering of Sudlow's site I could significantly enhance HSA catalysed coelenterazine chemiluminescence and can potentially bring it close to or better than the naturally occurring coelenterazine luciferases and photoproteins (Vassel *et al.,* 2012).

The incubation of both albumin and insulin with MeG for a period of one week resulted in the covalent modification of the proteins (fig. 4.15). MeG is known to target arginine and lysine residues of such proteins, but of these, MeG favours arginine residues (Gao and Wang, 2006). MeG can cause the irreversible modification of arginine residues resulting in the formation of hydroimidazolones (Lo *et al.,* 1994, Thornalley, 2008). Hydroimidazolones are the most common adducts found in the plasma. It is the modification of these residues that alters the biological activity of the proteins. The modification of these residues on the insulin molecule can result in changes in biological function. Changes in insulin function that are associated with modification by MeG suggests that the toxin may be involved in the development of insulin resistance and may potentially lead to the progression of diabetes (Jia *et al.,* 2006). Interestingly, the modification of albumin and insulin by $H_2O_2$ significantly enhanced protein catalysed coelenterazine chemiluminescence ($p < 0.01$; fig. 4.16).

In order to investigate the effect of MeG on insulin action an attempt was made to develop an assay whereby insulin stimulated glucose uptake by both insulin sensitive cells (7F2) and tissue (rat hemi-diaphragm) could be determined. Glucose uptake by these proved unsuccessful. The rat hemi-diaphragm demonstrated no basal glucose uptake and the addition of insulin did not stimulate glucose uptake. In experiments using 7F2 cells, no insulin stimulated glucose uptake was observed and in some cases the data suggested that insulin was actually inhibiting glucose uptake.

It was demonstrated that 3T3-L1 cells could be differentiated from the fibroblastic to the adipogenic form by treatment with an adipogenic cocktail containing supraphysiological concentration of insulin as well as IBMX and DEX (fig. 5.3 and fig. 5.4). The importance of insulin in this process was demonstrated as the removal of insulin from the adipogenic cocktail significantly inhibited cell differentiation (fig. 5.5).

The decreases in cell differentiation observed in cells treated with the adipogenic cocktail supplemented with TEA (fig. 5.7) demonstrated the importance of voltage-dependent $K^+$ channels in the cell differentiation process.

To conclude, the results demonstrate for the first time the ability of HSA and BSA to catalyse coelenterazine chemiluminescence. This was consistent with HSA having a mono-oxygenase activity. Insulin was also able to catalyse coelenterazine chemiluminescence. The coelenterazine chemiluminescence catalysed by insulin increased with the addition of $Zn^{2+}$. HSA catalysed coelenterazine chemiluminescence was heat denaturable, saturable by the substrate, inhibited by cations that can bind to the protein and inhibited by drugs that are known to bind to Sudlow's site I on the protein. Molecular 3D modelling confirmed the coelenterazine binding and also identified five basic amino acid residues that may play a crucial role in the binding of coelenterazine and the catalysis of the reaction. These results support the bacterial metabolic toxin hypothesis and have important consequences in diseases such as diabetes, where a mono-oxygenase has the potential of affecting a number of cell surface proteins. The coelenterazine chemiluminescence model used has the potential to be developed into a clinical test where the concentrations of these toxins in the blood of subjects can be measured. It can also be used in the pharmaceutical industry to investigate the pharmacokinetics of new drugs prior to their release on to the market.

### 6.2. Future work

The results in this thesis have demonstrated how the modification of proteins, such as insulin by bacterial metabolic toxins, like MeG, may play an important role in the development of diabetes. However, there is still a considerable amount of work that can be carried out to further investigate this topic as well as a number of experiments that generated negative data requiring further investigation. Further work can be carried out to determine the enzymatic activity of proteins:

- To determine if insulin is a mono-oxygenase as molecular 3D modelling did not identify the binding site. Also, the ability of insulin to oxidise its receptor needs to be investigated

- To investigate the effect of superoxide on protein catalysed coelenterazine chemiluminescence. The addition of superoxide dismutase should convert superoxide to $H_2O_2$ thus reducing the activity of the protein (Lucas and Solano, 1992)
- The conditions used to denature HSA were not sufficient enough to denature human insulin. Therefore it is now necessary establish another technique such as that described by Jiang and Chang (2005) to denature insulin. Then once insulin has been successfully denatured to investigate the effect of denaturation on insulin catalysed coelenterazine chemiluminescence
- It was not possible to determine the approximate $K_m$ of coelenterazine on insulin as an experiment to demonstrate the chemiluminescence in the presence of increasing substrate concentrations was not investigated. It is now necessary to demonstrate whether the effect of insulin on coelenterazine chemiluminescence is saturable in order to determine if it is binding or is it actually generating superoxide which is an established oxidant for coelenterazine (Lucas and Solano, 1992)
- More attention needs to be focused on $Zn^{2+}$ to further determine its role as it may have a significant clinical relevance (e.g. to investigate what is the mechanism of action of $Zn^{2+}$)
- In order to determine the $k_{cat}$ of HSA and insulin, it is necessary to determine the fluorescence of the product, coelenteramide, to quantify the turnover (Shimomura and Teranishi, 2000)
- To construct a Dixon plot to determine the $K_i$ for the HSA-coelenterazine complex
- The genetic engineering of Sudlow's site I could significantly enhance HSA catalysed coelenterazine chemiluminescence thereby bringing it close to or even better than the other naturally occurring coelenterazine luciferases and photoproteins
- To determine if other drugs that are known to bind to albumin (e.g. furosemide) exhibit competitive/mixed enzyme kinetics
- It has been shown that the bacterial metabolic toxin, MeG, can covalently modify both albumin and insulin, therefore further work needs to be carried out to investigate the effect of other metabolites, such as alcohols, diols, aldehydes, ketones and acids on such proteins (Campbell *et al.,* 2010)

- The covalent modification of insulin resulted in reduced mono-oxygenase activity, the consequences of this on diabetes will need to be investigated
- To determine if MeG-adduct formation can be detected in clinical samples and if so, could this be used as a clinical test to predict the development of pathological conditions, such as the complications associated with diabetes (microvascular or macrovascular conditions) in the future
- To determine if protein catalysed coelenterazine chemiluminescence can be developed into a clinical test whereby this method is used to investigate the pharmacokinetics of new drugs to their release on the market

Investigations to determine the effect of MeG on the biological activity were unsuccessful. Therefore, future work to determine the effect of the toxin on the biological activity of insulin will include:

- Now that it has been shown that these proteins can be covalently modified by these putative toxins, the next step would be to investigate the biological activity of the modified proteins in processes such as glucose uptake and cell differentiation. For example, as insulin is known to increase glucose uptake by insulin-sensitive tissues as well as playing an important role in cell differentiation, work can be carried out to compare glucose uptake and cell differentiation in the presence of normal and covalently modified insulin
- To quantify the expression of GLUT1 and GLUT4 in insulin-sensitive tissues (e.g. 3T3-L1 cells and rat hemi-diaphragm)
- PPARγ and C/EBPα are known to be crucial for cell differentiation, therefore it is also necessary to investigate the expression of both of these in undifferentiated and differentiated 3T3-L1 cells
- Lipolysis is a process where triglycerides are hydrolysed into glycerol and free fatty acids. Increased lipolysis has been observed in obese and diabetic subjects. Therefore, lipolysis assays can be carried out on differentiated 3T3-L1 to quantify glycerol release (Green *et al.,* 2004).

# Chapter 7:

# Appendix

## 7.1. Publications relevant to this thesis

1. Campbell, A. K., Matthews, S. B., **Vassel, N**., Cox, C. D., Naseem, R., Chaichi, J., Holland, I. B., Green, J. & Wann, K. T. (2010) Bacterial metabolic 'toxins': a new mechanism for lactose and food intolerance, and irritable bowel syndrome. *Toxicology*, 278, 268-76.

2. **Vassel, N**., Cox, C. D., Naseem, R., Morse, V., Evans, R. T., Power, R. L., Brancale, A., Wann, K. T. & Campbell, A. K. (2012) Enzymatic activity of albumin shown by coelenterazine chemiluminescence. *Luminescence*, 27, 234-41.

## 7.2. Cell culture media formulae

### MINIMAL ESSENTIAL MEDIUM (MEM) ALPHA

| Components | MW | Concentration (mg/L) |
|---|---|---|
| **Amino acids** | | |
| Glycine | 75 | 50 |
| L-Alanine | 89 | 25 |
| L-Arginine | 211 | 105 |
| L-Asparagine-$H_2O$ | 150 | 25 |
| L-Aspartic acid | 133 | 30 |
| L-Cysteine hydrochloride-$H_2O$ | 176 | 100 |
| L-Cysteine | 313 | 31 |
| L-Glutamic acid | 147 | 75 |
| L-Glutamine | 146 | 292 |
| L-Histidine | 155 | 31 |
| L-Isoleucine | 131 | 52.4 |
| L-Leucine | 131 | 52 |
| L-Lysine | 183 | 73 |
| L-Methionine | 149 | 15 |
| L-Phenylalanine | 165 | 32 |
| L-Proline | 115 | 40 |
| L-Serine | 105 | 25 |
| L-Threonine | 119 | 48 |
| L-Tryptophan | 204 | 10 |
| L-Tyrosine | 181 | 36 |
| L-Valine | 117 | 46 |

| | | |
|---|---|---|
| **Vitamins** | | |
| Ascorbic acid | 176 | 50 |
| Biotin | 244 | 0.1 |
| Choline chloride | 140 | 1 |
| D-Calcium pantothenate | 477 | 1 |
| Folic acid | 441 | 1 |
| Niacinamide | 122 | 1 |
| Pyridoxal hydrochloride | 204 | 1 |
| Riboflavin | 376 | 0.1 |
| Thiamine hydrochloride | 337 | 1 |
| Vitamin $B_{12}$ | 1355 | 1.36 |
| i-Inositol | 180 | 2 |
| **Inorganic salts** | | |
| Calcium chloride ($CaCl_2$-$2H_2O$) | 147 | 264 |
| Magnesium sulphate (MgSO4) (anhyd.) | 120 | 97.67 |
| Potassium chloride (KCl) | 75 | 400 |
| Sodium bicarbonate (NaHCO3) | 84 | 2200 |
| Sodium Chloride (NaCl) | 58 | 6800 |
| Sodium phosphate monobasic ($NaH_2PO_4$-$2H_2O$) | 156 | 158 |
| **Other components** | | |
| D-Glucose (Dextrose) | 180 | 1000 |
| Lipoic acid | 206 | 0.2 |
| Phenol red | 376.4 | 10 |
| Sodium pyruvate | 110 | 110 |

## DULBECCO'S MODIFIED EAGLE MEDIUM (D-MEM)

| Components | MW | Concentration (mg/L) |
|---|---|---|
| **Amino acids** | | |
| Glycine | 75 | 30 |
| L-Arginine hydrochloride | 211 | 84 |
| L-Cysteine 2HCl | 313 | 63 |
| L-Glutamine | 146 | 580 |
| L-Histidine hydrochloride-H2O | 210 | 42 |
| L-Isoleucine | 131 | 105 |
| L-Leucine | 131 | 105 |
| L-Lysine hydrochloride | 183 | 146 |
| L-Methionine | 149 | 30 |
| L-Phenylalanine | 165 | 66 |
| L-Serine | 105 | 42 |
| L-Threonine | 119 | 95 |
| L-Tryptophan | 204 | 16 |
| L-Tyrosine | 181 | 72 |
| L-Valine | 117 | 94 |
| **Vitamins** | | |
| Choline chloride | 140 | 4 |
| D-Calcium pantothenate | 477 | 4 |
| Folic acid | 441 | 4 |
| Niacinamide | 122 | 4 |
| Pyridoxine hydrochloride | 204 | 4 |
| Riboflavin | 376 | 0.4 |
| Thiamine hydrochloride | 337 | 4 |

| | | |
|---|---|---|
| i-Inositol | 180 | 7.2 |
| | | |
| **Inorganic salts** | | |
| Calcium chloride ($CaCl_2$-$2H_2O$) | 147 | 264 |
| Ferric nitrate ($Fe(NO_3)_3$-$9H_2O$) | 404 | 0.1 |
| Magnesium sulphate ($MgSO_4$-$7H_2O$) | 246 | 200 |
| Potassium chloride (KCl) | 75 | 400 |
| Sodium bicarbonate ($NaHCO_3$) | 84 | 3700 |
| Sodium chloride (NaCl) | 58 | 6400 |
| Sodium phosphate monobasic ($NaH_2PO_4$-$2H_2O$) | 154 | 141 |
| | | |
| **Other components** | | |
| D-Glucose (Dextrose) | 180 | 4500 |
| Phenol red | 376.4 | 15 |
| Sodium pyruvate | 110 | 110 |

# Chapter 8:

# References

## References

ABOU-ZIED, O. K. & AL-SHIHI, O. I. K. (2008) Characterisation of subdomain IIA binding site of human serum albumin in its native, unfolded, and refolded states using small molecular probes. *Journal of the American Chemical Society,* 130**,** 10793-801.

ACHENBACH, P., BONIFACIO, E., KOCZWARA, K. & ZIEGLER, A. G. (2005) Natural history of type 1 diabetes. *Diabetes,* 54**,** S25-31.

ACKERMAN, R. S., COZZARELLI, N. R. & EPSTEIN, W. (1974) Accumulation of toxic concentrations of methylglyoxal by wild-type *Escherichia coli* K-12. *Journal of Bacteriology,* 119**,** 357-62.

ADAMCZYK, M., JOHNSON, D. D., MATTINGLY, P. G., PAN, Y. & REDDY, R. E. (2001) Synthesis of coelenterazine. *Organic Preparations and Procedures International,* 33**,** 477-85.

AHLQVIST, E., AHLUWALIA, T. S. & GROOP, L. (2011) Genetics of type 2 diabetes. *Clinical Chemistry,* 57**,** 241-54.

AHMED, N. & THORNALLEY, P. J. (2007) Advanced glycation endproducts: what is their relevance to diabetic complications? *Diabetes, Obesity and Metabolism,* 9**,** 233-45.

AHMED, N., DOBLER, D., DEAN, M. & THORNALLEY, P. J. (2005) Peptide mapping identifies hotspot site modification in human serum albumin by methylglyoxal involved in ligand binding and esterase activity. *The Journal of Biological Chemistry,* 280**,** 5724-32.

AIZAWA, T., SATO, Y., ISHIHARA, F., TAGUCHI, N., KOMATSU, M., SUZUKI, N., HASHIZUME, K. & YAMADA, T. (1994) ATP-sensitive $K^+$ channel-independent glucose action in rat pancreatic beta-cell. *The American Journal of Physiology,* 266**,** C622-27.

AKERBOLM, H. K. & KNIP, M. (1998) Putative environmental factors in type 1 diabetes. *Diabetes/metabolism Reviews,* 14**,** 31-67.

AROLA, H. & TAMM, A. (1994) Metabolism of lactose in the human body. *Scandinavian Journal of Gastroenterology. Supplement,* 202**,** 21-5.

ASCENZI, P. & FASANO, M. (2010) Allostery in a monomeric protein: the case of human serum albumin. *Biophysical Chemistry,* 148**,** 16-22.

ATKINSON, M. A. & EISENBARTH, G. S. (2001) Type 1 diabetes: new perspectives on disease pathogenesis and treatment. *Lancet,* 358**,** 221-29.

BARNETT, A. (2006) DPP-4 inhibitors and their potential role in the management of type 2 diabetes. *International Journal of Clinical Practice,* 60**,** 1454-70.

BARONI, S., MATTU, M., VANNINI, A., CIPOLLONE, R., AIME, S., ASCENZI, P. & FASANO, M. (2001) Effect of ibuprofen and warfarin on the allosteric properties of haem-human serum albumin. A spectroscopic study. *European Journal of Biochemistry,* 268.

BASKARAN, S., RAJAN, D. P. & BALASUBRAMANIAN, K. A. (1989) Formation of methylglyoxal by bacteria isolated from human faeces. *Journal of Medical Microbiology* 28**,** 211-5.

BERG, J. M., TYMOCZKO, J. L. & STRYER, L. (2002) *Biochemistry*.

BESSER, G. & THORNER, M. O. (2002) *Comprehensive Clinical Endocrinology*.

BEST, L. & THORNALLEY, P. J. (1999) Trioses and related substances: tools for the study of pancreatic beta-cell function. *Biochemical Pharmacology,* 57.

BEST, L. (2002) Study of a glucose-activated anion-selective channel in rat pancreatic beta-cells. *Pflugers Archiv: European Journal of Physiology,* 445**,** 97-104.

BODEN, G., CHEN, X., RUIZ, J., WHITE, J. V. & ROSSETTI, L. (1994) Mechanisms of fatty-acid induced inhibition of glucose uptake. *The Journal of Clinical Investigation,* 93**,** 2438-2446.

BONORA, E. (2008) Protection of pancreatic beta cells: is it feasible? *Nutrition, metabolism, and Cardiovascular Diseases,* 18**,** 74-83.

BOOTH, I. R., FERGUSON, G. P., MILLER, S., LI, C., GUNASEKERA, B. & KINGHORN, S. (2003) Bacterial production of methylglyoxal: a survival strategy or death by misadventure? *Biochemical Society Transactions,* 31**,** 1406-1408.

BOS, O. J. M., LABRO, J. F. A., FISCHER, M. J. E., WILTING, J. & JANSSEN, L. H. M. (1989) The molecular mechanism of the neutral-to-base transition of human serum albumin. *The Journal of Biological Chemistry,* 264**,** 953-59.

BOS, O. J. M., REMIJN, J. P., FISCHER, M. J. E., WILTING, J. & JANSSEN, L. H. M. (1988) Location and characterization of the warfarin binding site of human serum albumin. A comparative study of two large fragments. *Biochemical Pharmacology,* 37**,** 3905-09.

BRESSON, D. & VON HERRATH, M. (2004) Mechanisms underlying type 1 diabetes. *Drug Discovery Today: Disease Mechanisms,* 1**,** 321-27.

BRODERSEN, R., SJODIN, T. & SJOHOLM, I. (1977) Independent binding of ligands to human serum albumin. *The Journal of Biological Chemistry,* 252**,** 5067-72.

BROWNLEE, M. (2001) Biochemistry and molecular cell biology of diabetic complications. *Nature,* 414**,** 813-20.

BROWNLEE, M. (2005) The pathobiology of diabetic complications: a unifying mechanism. *Diabetes,* 54**,** 1615-25.

BRYANT, N. J., GOVERS, R. & JAMES, D. E. (2002) Regulated transport of the glucose transporter GLUT4. *Nature Reviews. Molecular Cell Biology,* 3.

CABRERA-RODE, E., SARMIENTO, L., MOLINA, G., PEREZ, C., ARRANZ, C., GALVAN, J. A., PRIETO, M., BARRIOS, J., PALOMERA, R., FONSECA, M., MAS, P., DIAZ-DIAZ, O. & DIAZ-HORTA, O. (2005) Islet cell related antibodies and type 1 diabetes associated with echovirus 30 epidemic: a case report. *Journal of Medical Virology,* 76**,** 373-7.

CAMMISOTTO, P. G. & BUKOWIECKI, L. J. (2004) Role of calcium in the secretion of leptin from white adipocytes. *American Journal of Physiology. Regulatory, Integrative and Comparative Physiology,* 287, R1380-86.

CAMPBELL, A. K. & HERRING, P. J. (1990) Imidazolopyrazine bioluminescence in copepods and other marine organisms. *Marine Biology,* 104**,** 219-25.

CAMPBELL, A. K. & MATTHEWS, S. B. (2005) Darwin's illness revealed. *Postgraduate Medical Journal,* 81**,** 248-51.

CAMPBELL, A. K. (Ed.) (1988) *Chemiluminescence,* Chichester, England and VCH Verlagsgesellschaft mbH, Weinheim, Federal Republic of Germany, Ellis Horwood Ltd.

CAMPBELL, A. K., MATTHEWS, S. B., VASSEL, N., COX, C. D., NASEEM, R., CHAICHI, J., HOLLAND, I. B., GREEN, J. & WANN, K. T. (2010) Bacterial metabolic 'toxins': a new mechanism for lactose and food intolerance, and irritable bowel syndrome. *Toxicology,* 278**,** 268-76.

CAMPBELL, A. K., NASEEM, R., HOLLAND, I. B., MATTHEWS, S. B. & WANN, K. T. (2007) Methylglyoxal and other carbohydrate metabolites

induce lanthanum-sensitive $Ca^{2+}$ transients and inhibit growth in *E.coli*. *Archives of Biochemistry and Biophysics,* 468**,** 107-13.

CAMPBELL, A. K., PATEL, A., HOUSTON, W. A., SCOLDING, N. J., FRITH, S., MORGAN, B. P. & COMPSTON, D. A. (1989) Photoproteins as indicators of intracellular free $Ca^{2+}$. *Journal of bioluminescence and chemiluminescence,* 4**,** 463-74.

CAMPBELL, A. K., WANN, K. T. & MATTHEWS, S. B. (2004) Lactose causes heart arrhythmia in the water flea *Daphnia pulex*. *Comparative Biochemistry and Physiology. Part B, Biochemistry and Molecular Biology,* 139**,** 225-34.

CAMPBELL, A. K., WAUD, J. P. & MATTHEWS, S. B. (2005) The molecular basis of lactose intolerance. *Science Progress,* 88**,** 157-202.

CAROLA, R., HARLEY, J. & NOBACK, C. (1990) The pancreas as a digestive organ. *Human Anatomy and Physiology.*

CASH, B. D. & CHEY, W. D. (2004) Irritable bowel syndrome - an evidence based approach to diagnosis. *Alimentary Pharmacology and Therapeutics,* 19**,** 1235-45.

CHAKRAVARTHY, M. V. & SEMENKOVICH, C. F. (2007) The ABCs of beta-cell dysfunction in type 2 diabetes. *Nature Medicine,* 13**,** 241-2.

CHAN, B., DODSWORTH, N., WOODROW, J., TUCKER, A. & HARRIS, R. (1995) Site-specific N-terminal auto-degradation of human serum albumin. *European Journal of Biochemistry,* 227**,** 524-8.

CHANG, T. H. & POLAKIS, S. E. (1978) Differentiation of 3T3-L1 fibroblasts to adipocytes. Effect of insulin and indomethacin on the levels of insulin receptors. *The Journal of Biological Chemistry,* 253, 4693-96.

CHAPLEN, F. W. R. (1998) Incidence and potential implications of the toxic metabolite methylglyoxal in cell culture: a review. *Cytotechnology,* 26**,** 173-83.

CHAUSMER, A. B. (1998) Zinc, insulin and diabetes. *Journal of the American College of Nutrition,* 17**,** 109-15.

CHEN, J., FITOS, I. & HAGE, D. S. (2006) Chromatographic analysis of allosteric effects between ibuprofen and benzodiazepines on human serum albumin. *Chirality,* 18**,** 24-36.

COOK, L. J., DAVIES, J., YATES, A. P., ELLIOTT, A. C., LOVELL, J., JOULE, J. A., PEMBERTON, P., THORNALLEY, P. J. & BEST, L. (1998) Effects of methylglyoxal on rat pancreatic beta-cells. *Biochemical Pharmacology,* 55**,** 1361-7.

CORMIER, M. J., LEE, J. & WAMPLER, J. E. (1975) Bioluminescence: recent advances. *Annual Review of Biochemistry,* 45**,** 255-72.

DAS, U. N. (1999) GLUT-4, tumor necrosis factor, essential fatty acids and daf-genes and their role in insulin resistance and non-insulin dependent diabetes mellitus. *Prostaglandins, Leukotrienes and Essential Fatty Acids,* 60**,** 13-20.

DE MEYTS, P. (2004) Insulin and its receptor: structure, function and evolution. *BioEssays,* 26**,** 1351-62.

DE WERGIFOSSE, B., DUBUISSON, M., MARCHAND-BRYNAERT, J., TROUET, A. & REES, J. F. (2004) Coelenterazine: a two-stage antioxidant in lipid micelles. *Free Radical Biology and Medicine,* 36**,** 278-87.

DEEB, O., ROSALES-HERNANDEZ, M. C., GOMEZ-CASTRO, C., GARDUNO-JUAREZ, R. & CORREA-BASURTO, J. (2009) Exploration of human serum albumin binding sites by docking and molecular dynamics flexible ligand-protein interactions. *Biopolymers,* 93**,** 161-170.

DEREWENDA, U., DEREWENDA, Z., DODSON, G. G., HUBBARD, R. E. & KORBER, F. (1989) Molecular structure of insulin: the insulin monomer and its assembly. *British Medical Bulletin,* 45**,** 4-18.

DHAR, A., DESAI, K., LIU, J. & WU, L. (2009) Methylglyoxal, protein binding and biological samples: are we getting the true measure? *Journal of Chromatography. B, Analytical Technologies in the Biomedical and Life Sciences,* 877**,** 1093-100.

DOCKAL, M., CARTER, D. C. & RUKER, F. (2000) Conformational transitions of the three recombinant domains of human serum albumin depending on pH. *The Journal of Biological Chemistry,* 275**,** 3042-50.

DONATH, M. Y. & EHSES, J. A. (2006) Type 1, type 1.5, and type 2 diabetes: NOD the diabetes we thought it was *Proceedings of the National Academy of Sciences of the United States of America,* 103**,** 12217-8.

DUBUISSON, M., REES, J. F. & MARCHAND-BRYNAERT, J. (2005) Coelenterazine (marine bioluminescent substrate): a source of inspiration for the discovery of novel antioxidants. *Drug Development and Industrial Pharmacy,* 31**,** 827-49.

DUNN, M. F. (2005) Zinc-ligand interactions modulate assembly and stability of the insulin hexamer - a review. *Biometals,* 18**,** 295-303.

ESCHER, J. C., DE KONING, N. D., VAN ENGEN, C. G., ARORA, S., BULLER, H. A., MONTGOMERY, R. K. & GRAND, R., J. (1992) Molecular basis of lactase levels in adult humans. *The Journal of Clinical Investigation,* 89**,** 480-3.

FAIRWEATHER, D. & ROSE, N. R. (2002) Type 1 diabetes: virus infection or autoimmune disease? *Nature Immunology,* 3**,** 338-40.

FASANO, M., CURRY, S., TERRENO, E., GALLIANO, M., FANALI, G., NARCISO, P., NOTARI, S. & ASCENZI, P. (2005) The extraordinary ligand binding properties of human serum albumin. *IUBMB Life,* 57**,** 787-96.

FAURE, P., ROUSSEL, A., COUDRAY, C., RICHARD, M. J., HALIMI, S. & FAVIER, A. (1992) Zinc and insulin sensitivity. *Biological Trace Element Research,* 32**,** 305-10.

FERGUSON, A. (1981) Diagnosis and treatment of lactose intolerance. *British Medical Journal,* 283**,** 1423-4.

FERGUSON, G. P., TOTEMEYER, S., MACLEAN, M. J. & BOOTH, I. R. (1998) Methylglyoxal production in bacteria: suicide or survival? *Archives of Microbiology,* 170**,** 209-18.

FLATT, P. R., ABDEL-WAHAB, Y. H., BOYD, A. C., BARNETT, C. R. & O'HARTE, F. P. (1997) Pancreatic B-cell dysfunction and glucose toxicity in non-insulin-dependent diabetes. *The Proceedings of the Nutrition Society,* 56**,** 243-62.

FRAYN, K. N. (2003) The glucose-fatty acid cycle: a physiological perspective. *Biochemical Society Transactions,* 31**,** 1115-9.

FREEDBERG, W. B., KISTLER, W. S. & LIN, E. C. (1971) Lethal synthesis of methylglyoxal by Escherichia coli during unregulated glycerol metabolism. *Journal of Bacteriology,* 108**,** 137-44.

FRISSORA, C. L. & KOCH, K. L. (2005) Symptom overlap and comorbidity of irritable bowel syndrome with other conditions. *Current Gastroenterology Reports,* 7**,** 264-71.

FUJIMOTO, W. Y. (2000) The importance of insulin resistance in the pathogenesis of type 2 diabetes mellitus. *The American Journal of Medicine,* 108**,** 9-14.

FUJIWARA, S. & AMISAKI, T. (2006) Molecular dynamics study of conformational changes in human serum albumin by binding of fatty acids. *Proteins,* 64**,** 730-9.

GAMMELTOFT, S. & VAN OBBERGHEN, E. (1986) Protein kinase activity of the insulin receptor. *Biochemical Journal,* 235**,** 1-11.

GAO, Y. & WANG, Y. (2006) Site-selective modifications of arginine residues in human haemoglobin induced by methylglyoxal. *Biochemistry,* 45**,** 15654-60.

GARLICK, R. L. & MAZER, J. S. (1983) The principle site of nonenzymatic glycosylation of human serum albumin *in vivo*. *The Journal of Biological Chemistry,* 258**,** 6142-6.

GERICH, J. E. (1999) Is insulin resistance the principle cause of type 2 diabetes? *Diabetes, Obesity and Metabolism,* 1**,** 257-63.

GHUMAN, J., ZUNSZAIN, P. A., PETITPAS, I., BHATTACHARYA, A. A., OTAGIRI, M. & CURRY, S. (2005) Structural basis of the drug-binding specificity of human serum albumin. *Journal of Molecular Biology,* 353**,** 38-52.

GILLESPIE, K. M. (2006) Type 1 diabetes: pathogenesis and prevention. *Canadian Medical Association Journal,* 175**,** 165-70.

GOLDSTEIN, B. J. (2002) Insulin resistance as the core defect in type 2 diabetes mellitus. *The American Journal of Cardiology,* 90**,** 3-10.

GORDON, S. E. (1964) The glucose-fatty acid cycle in this pathogenesis of diabetes mellitus. *Transactions of the American Clinical and Climatological Association,* 76**,** 124-34.

GOULD, G. W. & HOLMAN, G. D. (1993) The glucose transporter family: structure, function and tissue-specific expression. *The Biochemical Journal,* 295 (Pt 2), 329-41.

GREEN, A., RUMBERGER, J. M., STUART, C. A. & RUHOFF, M. S. (2004) Stimulation of lipolysis by tumor necrosis factor-alpha in 3T3-L1 adipocytes is glucose dependent: implications for long-term regulation of lipolysis. *Diabetes,* 53**,** 74-81.

GREENE, P. S. & GREENE, M. T. (2009) Darwin's illness. *Journal of the History of Biology***,** 198-201.

GREGOIRE, F. M. (2001) Adipocyte differentiation: from fibroblast to endocrine cell. *Experimental Biology and Medicine (Maywood, N.J.),* 226, 997-1002.

GREGOIRE, F. M., SMAS, C. M. & SUL, H. S. (1998) Understanding adipocyte differentiation. *Physiological Reviews,* 78, 783-809.

GRILL, V. & BJORKLUND, A. (2000) Dysfunctional insulin secretion in type 2 diabetes: role of metabolic abnormalities. *Cellular and Molecular Life Sciences,* 57**,** 429-40.

GUO, Q., MORI, T., JIANG, Y., HU, C., OSAKI, Y., YONEKI, Y., SUN, Y., HOSOYA, T., KAWAMATA, A., OGAWA, S., NAKAYAMA, M., MIYATA, T. & ITO, S. (2009) Methylglyoxal contributes to the development of insulin resistance and salt sensitivity in Sprague-Dawley rats. *Journal of Hypertension,* 27**,** 1664-71.

GUPTA, D., GHOSHAL, U. C., MISRA, A., CHOUDHURI, G. & SINGH, K. (2007) Lactose intolerance in patients with irritable bowel syndrome from northern India: a case-control study. *Journal of Gastroenterology and hepatology,* 22**,** 2261-5.

HAMIDA, Z. J., COMTOIS, A. S., PORTMANN, M., BOUCHER, J. P. & SAVARD, R. (2011) Effect of electrical stimulation on lipolysis of human white adipocytes. *Applied Physiology, Nutrition, and Metabolism,* 36, 271-75.

HAN, Y., RANDELL, E. W., VASDEV, S. C., GILL, V. D., GADAG, V., NEWHOOK, L. A., GRANT, M. & HAGERTY, D. (2007) Plasma methylglyoxal and glyoxal are elevated and related to early membrane alteration in young, complication-free patients with type 1 diabetes. *Molecular and Cellular Biochemistry,* 305**,** 123-31.

HAN, Y., RANDELL, E., VASDEV, S., GILL, V., CURRAN, M., BOUCHER, J. P. & SAVARD, R. (2009) Plasma advanced glycation end product, methylglyoxal-derived hydroimidazolone is elevated in young, complication-free patients with type 1 diabetes. *Clinical Biochemistry,* 42**,** 562-9.

HASTINGS, J. W. & KRAUSE, K. L. (2005) Luciferases and light-emitting accessory proteins: structural biology. *Encyclopedia of Life Sciences.*

HAUSMAN, D. B., DIGIROLAMO, M., BARTNESS, T. J., HAUSMAN, G. J. & MARTIN, R. J. (2001) The biology of white adipocyte proliferation. *Obesity Reviews: An Official Journal of the International Association for the Study of Obesity,* 2, 239-54.

HAYMAN, J. A. (2009) Darwin's illness revisited. *British Medical Journal,* 339**,** b4968.

HE, X. M. & CARTER, D. C. (1992) Atomic structure and chemistry of human serum albumin. *Nature,* 358**,** 209-15.

HENNEY, N. C., LI, B., ELFORD, C., REVIRIEGO, P., CAMPBELL, A. K., WANN, K. T. & EVANS, B. A. (2009) A large-conductance (BK) potassium channel subtype affects both growth and mineralization of human osteoblasts. *American Journal of Physiology. Cell Physiology,* 297, C1397-408.

HSIEH, M. S. & CHAN, W. H. (2009) Impact of methylglyoxal and high glucose co-treatment on human mononuclear cells. *International Journal of Molecular Sciences,* 10**,** 1445-64.

HUA, Q. & WEISS, M. A. (2004) Mechanism of insulin fibrillation *The Journal of Biological Chemistry,* 279**,** 21449-460.

HUSSAIN, K. & COSGROVE, K. E. (2005) From congenital hyperinsulinism to diabetes mellitus: the role of the pancreatic B-cell $K_{ATP}$ channels. *Pediatric Diabetes,* 6**,** 103-13.

JAN, C. R., CHEN, C. H., WANG, S. C. & KUO, S. Y. (2005) Effect of methylglyoxal on intracellular calcium levels and viability in renal tubular cells. *Cellular Signalling,* 17**,** 847-55.

JIA, X. & WU, L. (2007) Accumulation of endogenous methylglyoxal impaired insulin signaling in adipose tissue of fructose-fed rats. *Molecular and Cellular Biochemistry,* 306**,** 133-39.

JIA, X., OLSON, D. J., ROSS, A. R. & WU, L. (2006) Structural and functional changes in human insulin induced by methylglyoxal. *FASEB Journal: Official publication of the Federation of American Societies for Experimental Biology,* 20**,** 1555-7.

JIANG, C. & CHANG, J. Y. (2005) Unfolding and breakdown of insulin in the presence of endogenous thiols. *FEBS Letters,* 579**,** 3927-31.

JOHNSON, A. O., SEMENYA, J. G., BUCHOWSKI, M. S., ENWONWU, C. O. & SCRIMSHAW, N. S. (1993) Correlation of lactose maldigestion, lactose intolerance, and milk intolerance. *The American Journal of Clinical Nutrition* 57**,** 399-401.

KAHN, C. R. (1985) The molecular mechanism of insulin action. *Annual Review of Medicine,* 36**,** 429-51.

KAHN, C. R. & WHITE, M. F. (1988) The insulin receptor and the molecular mechanism of insulin action. *The Journal of Clinical Investigation,* 82**,** 1151-6.

KAHN, S. E. (2001) Clinical review 135: The importance of beta-cell failure in the development and progression of type 2 diabetes. *The Journal of Clinical Endocrinology and Metabolism,* 86**,** 4047-58.

KAMINSKI, S., CIESLINSKA, A. & KOSTYRA, E. (2007) Polymorphism of bovine beta-casein and its potential effect on human health. *Journal of Applied Genetics,* 48**,** 189-98.

KASUGA, M. (2006) Insulin resistance and pancreatic beta cell failure. *The Journal of Clinical Investigation,* 116**,** 1756-60.

KHAN, A. H. & PESSIN, J. E. (2002) Insulin regulation of glucose uptake: a complex interplay of intracellular signalling pathways. *Diabetologia,* 45, 1475-83.

KLEMM, D. J., LEITNER, J. W., WATSON, P., NESTEROVA, A., REUSCH, J. E., GOALSTONE, M. L. & DRAZNIN, B. (2001) Insulin-induced adipocyte differentiation. Activation of CREB rescues adipogenesis from the arrest caused by inhibition of prenylation. *The Journal of Biological Chemistry,* 276.

KNIP, M., VEIJOLA, R., VIRTANEN, S. M., HYOTY, H., VAARALA, O. & AKERBLOM, H. K. (2005) Environmental triggers and determinants of type 1 diabetes. *Diabetes,* 54**,** S125-36.

KOBER, A., OLSSON, Y. & SJOHOLM, I. (1980) Binding of drugs to human serum albumin. XIV. The theoretical basis for the interaction between phenytoin and valporate. *Molecular Pharmacology,* 18**,** 237-42.

KORB, O., STUTZLE, T. & EXNER, T. E. (2006) PLANTS: application of ant colony optimisation to structure-based design. *Ant colony Optimisation and Swarm Intelligence, 5th International Workshop, ANTS 2006.* Universite Libre de Bruxelles, Brussels, Belgium.

KOSTER, J. C., PERMUTT, M. A. & NICHOLS, C. G. (2005) Diabetes and insulin secretion: the ATP-sensitive K+ channel (K ATP) connection. *Diabetes,* 54**,** 3065-72.

KRAGH-HANSEN, U. (1991) Octanoate binding to the indole- and benzodiazepine-binding region of human serum albumin. *The Biochemical Journal,* 273**,** 641-4.

KRAGH-HANSEN, U., CHUANG, V. & OTAGIRI, M. (2002) Practical aspects of the ligand-binding and enzymatic properties of human serum albumin. *Biological and Pharmaceutical Bulletin,* 25**,** 695-74.

LEE, H. K., SEO, I. A., SUH, D. J., LEE, H. J. & PARK, H. T. (2009) A novel mechanism of methylglyoxal cytotoxicity in neuroglial cells. *Journal of Neurochemistry,* 108**,** 273-84.

LEE, J. (2001) Bioluminescence. *Encyclopedia of Life Sciences.*

LEJON, S., CRAMER, J. F. & NORDBERG, P. (2008) Structural basis for the binding of naproxen to human serum albumin in the presence of fatty acids and the GA module. *Acta Crystallographica. Section F, Structural Biology and Crystallization Communications,* 64**,** 64-9.

LIU, Z. J., VYSOTSKI, E. S., CHEN, C. J., ROSE, J. P., LEE, J. & WANG, B. C. (2000) Structure of the $Ca^{2+}$-regulated photoprotein obelin at 1.7 A resolution determined directly from its sulfur substructure. *Protein Science,* 9**,** 2085-93.

LO, T. W., WESTWOOD, M. E., MCLELLAN, A. C., SELWOOD, T. & THORNALLEY, P. J. (1994) Binding and modification of proteins by methylglyoxal under physiological conditions. A kinetic and mechanistic study with N alpha-acetylarginine, N alpha-acetylcysteine, and N alpha-acetyllysine, and bovine serum albumin. *The Journal of Biological Chemistry,* 269**,** 32299-305.

LU, J., STEWART, A. J., SADLER, P. J., PINHEIRO, T. J. T. & BLINDAUER, C. A. (2008) Albumin as a zinc carrier: properties of its high-affinity zinc-binding site. *Biochemical Society Transactions,* 36**,** 1317-21.

LUCAS, M. & SOLANO, F. (1992) Coelenterazine is a superoxide anion-sensitive chemiluminescent probe: its usefulness in the assay of respiratory burst in neutrophils. *Analytical Biochemistry,* 206**,** 273-7.

MALLEFET, J. & SHIMOMURA, O. (1995) Presence of coelenterazine in mesopleagic fishes from the Strait of Messina. *Marine Biology,* 124**,** 381-85.

MARCHETTI, P., DEL PRATO, S., LUPI, R. & DEL GUERRA, S. (2006) The pancreatic beta-cell in human type 2 diabetes. *Nutrition, Metabolism and Cardiovascular Disease,* 16**,** S3-6.

MASUOKA, J., HEGENAUER, J., VAN DYKE, B. R. & SALTMAN, P. (1993) Intrinsic stoichiometric equilibrium constants for the binding of zinc(II) and copper(II) to the high affinity site of serum albumin. *Journal of Biological Chemistry,* 268**,** 21533-37.

MATTHEWS, S. B. & CAMPBELL, A. K. (2000) When sugar is not so sweet. *Lancet,* 355**,** 1330.

MATTHEWS, S. B., WAUD, J. P., ROBERTS, A. G. & CAMPBELL, A. K. (2005) Systemic lactose intolerance: a new perspective on an old problem. *Postgraduate Medical Journal,* 81**,** 167-73.

MCCARTHY, M. I. & ZEGGINI, E. (2009) Genome-wide association studies in type 2 diabetes. *Current Diabetes Reports,* 9**,** 164-71.

MIKI, T., MINAMI, K., ZHANG, L., MORITA, M., GONOI, T., SHIUCHI, T., MINOKOSHI, Y., RENAUD, J. M. & SEINO, S. (2002) ATP-sensitive potassium channels participate in glucose uptake in skeletal muscle and adipose tissue. *American Journal of Physiology Endocrinology and Metabolism,* 283, 1178-84.

MITRA, R. K., SINHA, S. S. & PAL, S. K. (2007) Hydration in protein folding: thermal unfolding/refolding of human serum albumin. *Langmuir,* 23**,** 10224-29.

MOSTAFA, A. A., RANDELL, E. W., VASDEV, S. C., GILL, V. D., HAN, Y., GADAG, V., RAOUF, A. A. & EL SAID, H. (2007) Plasma protein advanced glycation end products, carboxymethyl cysteine, and carboxyethyl cysteine, are elevated and related to nephropathy in patients with diabetes. *Molecular and Cellular Biochemistry,* 302**,** 35-42.

MUECKLER, M. (1994) Facilitative glucose transporters. *European Journal of Biochemistry,* 219, 713-25.

MUKOHDA, M., YAMAWAKI, H., NOMURA, H., OKADA, M. & HARA, Y. (2009) Methylglyoxal inhibits smooth muscle contraction in isolated blood vessels. *Journal of Pharmacological Sciences,* 109**,** 305-10.

MUZAMMIL, S., KUMAR, Y. & TAYYAB, S. (1999) Molten globule-like state of human serum albumin at low pH *European Journal of Biochemistry,* 266**,** 26-32.

NANDI, A., KITAMURA, Y., KAHN, C. R. & ACCILI, D. (2004) Mouse models of insulin resistance. *Physiological Reviews,* 84**,** 623-47.

NASERKE, H. E., ZIEGLER, A. G., LAMPASONA, V. & BONIFACIO, E. (1998) Early development and spreading of autoantibodies to epitopes of IA-2 and their association with progression to type 1 diabetes. *The Journal of Immunology* 161**,** 6963-9.

NOORMAGI, A., GAVRILOVA, J., SMIRNOVA, J. R., TOUGU, V. & PALUMA, A. (2010) Zinc (II) ions co-secreted with insulin suppress inherent amyloidogenic properties of monomeric insulin. *Biochemical Journal,* 430**,** 511-18.

NOTKINS, A. L. & LERNMARK, A. (2001) Autoimmune type 1 diabetes: resolved and unresolved issues. *The Journal of Clinical Investigation,* 108**,** 1247-52.

NTAMBI, J. M. & YOUNG-CHEUL, K. (2000) Adipocyte differentiation and gene expression. *The Journal of Nutrition,* 130, 3122S-126S.

OBA, Y., TSUDUKI, H., KATO, S., OJIKA, M. & INOUYE, S. (2004) Identification of the luciferin-luciferase system and quantification of coelenterazine by mass spectrometry in the deep-sea luminous ostracod, *Conchoecia pseudodiscophora*. *Chembiochem,* 5**,** 1495-99.

OGURI, A., TANAKA, T., LIDA, H., MEGURO, K., TAKANO, H., OONUMA, H., NISHIMURA, S., MORITA, M., YAMASOBA, T., NAGAI, R. & NAKAJIMA, T. (2010) Involvement of CaV3.1 T-type calcium channels in cell proliferation in mouse preadipocytes. *American Journal of Physiology. Cell Physiology,* 298, C1414-23.

OHMIYA, Y. & HIRANO, T. (1996) Shining the light: the mechanism of the bioluminescence reaction of calcium-binding photoproteins. *Chemistry and Biology,* 3**,** 337-47.

**OLSON 2003**

OLSON, A. L. & PESSIN, J. E. (1996) Structure, function, and regulation of the mammalian facilitative glucose transporter gene family. *Annual Review of Nutrition,* 16, 235-56.

ORREGO, F. & QUINTANA, C. (2007) Darwin's illness: a final diagnosis. *Notes and Records of the Royal Society of London,* 61**,** 23-9.

OTAGIRI, M. (2005) A molecular functional study on the interactions of drugs with plasma proteins. *Drug Metabolism and Pharmacokinetics,* 20**,** 309-23.

OZANNE, S. E. & HALES, C. N. (2002) Early programming of glucose-insulin metabolism. *Trends in Endocrinology and Metabolism,* 13**,** 368-73.

PARONEN, J., KNIP, M., SAVILAHTI, E., VIRTANEN, S. M., ILONEN, J., AKERBLOM, H. K. & VAARALA, O. (2000) Effect of cow's milk exposure and maternal type 1 diabetes on cellular and humoral immunisation to dietry insulin in infants at genetic risk for type 1 diabetes. Finnish trial to reduce IDDM in the genetically at risk study group. *Diabetes,* 49**,** 1657-65.

PEPPA, M., URIBARRI, J. & VLASSARA, H. (2003) Glucose, advanced glycation end products, and diabetes complications: what is new and what works. *Clinical Diabetes,* 21**,** 186-87.

PESSIN, J. E. & SALTIEL, A. R. (2000) Signaling pathways in insulin action: molecular targets of insulin resistance. *The Journal of Clinical Investigation,* 106**,** 165-9.

PETITPAS, I., BHATTACHARYA, A. A., TWINE, S., EAST, M. & CURRY, S. (2001) Crystal structure analysis of warfarin binding to human serum

albumin: anatomy of drug site I. *Journal of Biological Chemistry,* 276**,** 22804-9.

PETRIE, J. R., PEARSON, E. R. & SUTHERLAND, C. (2011) Implications of genome wide association studies for the understanding of type 2 diabetes pathophysiology. *Biochemical Pharmacology,* 81**,** 471-7.

PICKUP, J. C. & WILLIAMS, G. (2003) *Textbook of Diabetes*, Blackwell Publishing.

PIHOKER, C., GILLIAM, L. K., HAMPE, C. S. & LERNMARK, A. (2005) Autoantibodies in diabetes. *Diabetes,* 54**,** S52-61.

POCOCK, G. & RICHARDS, C. D. (2004) The pancreas. *Human Physiology - The Basis of Medicine.* second ed.

QATANANI, M. & LAZAR, M. A. (2007) Mechanisms of obesity-associated insulin resistance: many choices on the menu. *Genes and Development,* 21**,** 1443-55.

QIN, J., RUIQIANG, L., RAES, J., ARUMUGAM, M., BURGDORF, K. S., MANICHANH, C., NIELSEN, T., PONS, N., LEVENEZ, F., YAMADA, T., MENDE, D. R., LI, J., XU, J., LI, S., LI, D., CAO, J., WANG, B., LIANG, H., ZHENG, H., XIE, Y., TAP, J., LEPAGE, P., BERTALAN, M., BATTO, J. M., HANSEN, T., LE PASLIER, D., LINNEBERG, A., NEILSEN, B., PELLETIER, E., RENAULT, P., SICHERITZ-PONTEN, T., TURNER, K., ZHU, H., YU, C., LI, S., JIAN, M., ZHOU, Y., LI, Y., ZHANG, X., LI, S., QIN, N., YANG, H., WANG, J., BRUNAK, S., DORE, J., GUARNER, F., KRISTIANSEN, K., PEDERSEN, O., PARKHILL, J., WEISSENBACH, J., BORK, P., EHRLICH, D. & WANG, J. (2010) A human gut microbial gene catalogue established by metagenomic sequencing. *Nature,* 464**,** 59-65.

QUEISSER, M. A., YAO, D., GEISLER, S., HAMMES, H. P., LOCHNIT, G., SCHLEICHER, E. D., BROWNLEE, M. & PREISSNER, K. T. (2010) Hyperglycaemia impairs proteasome function by methylglyoxal. *Diabetes,* 59**,** 670-8.

RABBANI, N. & THORNALLEY, P. J. (2011) Glyoxalase in diabetes, obesity and related disorders. *Seminars in Cell & Developmental Biology,* 22**,** 309-17.

RAHMAN, M. M., RAHMAN, M. H. & RAHMAN, N. N. (2005) Competitive binding of ibuprofen and naproxen to bovine serum albumin: modified form of drug-drug displacement interaction at the binding site. *Pakistan Journal of Pharmaceutical Sciences,* 18**,** 43-7.

RAMIREZ-PONCE, M. P., ACOSTA, J. & BELLIDO, J. A. (1990) Electrical activity in white adipose tissue of rat. *Revista Espanola de Fisiologia,* 46, 133-38.

RAMIREZ-PONCE, M. P., ACOSTA, J. & BELLIDO, J. A. (1991) Effects of noradrenaline and insulin on electrical activity in white adipose tissue of rat. *Revista Espanola de Fisiologia,* 47, 217-21.

RAMIREZ-PONCE, M. P., MATEOS, J. C. & BELLIDO, J. A. (2002) Insulin increases the density of potassium channels in white adipocytes: possible role in adipogenesis. *The Journal of Endocrinology,* 174, 299-307.

RAMIREZ-PONCE, M. P., MATEOS, J. C., CARRION, N. & BELLIDO, J. A. (1996) Voltage-dependent potassium channels in white adipocytes. *Biochemical and Biophysical Research Communications,* 223, 250-56.

RANDLE, P. J., GARLAND, P. B., HALES, C. N. & NEWSHOLME, E. A. (1963) The glucose fatty-acid cycle. Its role in insulin sensitivity and the metabolic disturbances of diabetes mellitus. *Lancet,* 1**,** 785-9.

REED, B. C., KAUFMANN, S. H., MACKALL, J. C., STUDENT, A. K. & LANE, M. D. (1977) Alterations in insulin binding accompanying differentiation of 3T3-L1 preadipocytes *Proceedings of the National Academy of Sciences,* 74, 4876-80.

REES, J. F., DE WERGIFOSSE, B., NOISET, O., DUBUISSON, M., JANSSENS, B. & THOMPSON, E. M. (1998) The origins of marine bioluminescence: turning oxygen defence mechanisms into deep-sea communication tools. *The Journal of Experimental Biology,* 201**,** 1211-221.

RENSTROM, F., BUREN, J., SVENSSON, M. & ERIKSSON, J. W. (2007) Insulin resistance induced by high glucose and high insulin precedes insulin receptor substrate 1 protein depletion in human adipocytes. *Metabolism,* 56**,** 190-8.

REUSCH, J. E., COLTON, L. A. & KLEMM, D. J. (2000) CREB activation induces adipogenesis in 3T3-L1 cells. *Molecular and Cellular Biology,* 20, 1008-20.

REZAEI TAVIRANI, M., MOGHADDAMNIA, S. H., RANJBAR, B., AMANI, M. & MARASHI, S. A. (2006) Conformational study of human serum albumin in pre-denaturation temperatures by differential scanning calorimetry, circular dichroism and UV spectroscopy. *Journal of Biochemistry and Molecular Biology,* 39**,** 530-6.

RIBOULET-CHAVEY, A., PIERRON, A., DURAND, I., MURDACA, J., GIUDICELLI, J. & VAN OBBERGHEN, E. (2006) Methylglyoxal impairs insulin signaling pathways independently of the formation on intracellular reactive oxygen species. *Diabetes,* 55**,** 1289-99.

RIGNELL-HYDBOM, A., RYLANDER, L. & HAGMAR, L. (2007) Exposure to persistent organochlorine pollutants and type 2 diabetes mellitus. *Human & Experimental Toxicology,* 26**,** 447-52.

ROBERTSON, R. P. & HARMON, J. S. (2006) Diabetes, glucose toxicity, and oxidative stress: A case of double jeopardy for the pancreatic islet beta cell. *Free Radical Biology and Medicine,* 41**,** 177-84.

RORSMAN, P., ELIASSON, L., RENSTROM, E., GROMADA, J., BARG, S. & GOPEL, S. (2000) The cell physiology of biphasic insulin secretion. *News in Physiological Sciences,* 15**,** 72-7.

ROSEN, O. M. (1987) After insulin binds *Science,* 237**,** 1452-8.

SAHOO, B. K., GHOSH, K. S. & DASGUPTA, S. (2008) Molecular interactions of isoxazolcurcumin with human serum albumin: spectroscopic and molecular modelling studies. *Biopolymers,* 91**,** 108-19.

SALTIEL, A. R. & KAHN, C. R. (2001) Insulin signalling and the regulation of glucose and lipid metabolism. *Nature,* 414**,** 799-806.

SARAIVA, M. A., BORGES, C. M. & FLORENCIO, M. H. (2006) Non-enzymatic model glycation reactions--a comprehensive study of the reactivity of a modified arginine with aldehydic and diketonic dicarbonyl compounds by electrospray mass spectrometry. *Journal of Mass Spectrometry,* 41**,** 755-70.

SAVAGE, D. B., PETERSEN, K. F. & SHULMAN, G. I. (2007) Disordered lipid metabolism and the pathogenesis of insulin resistance. *Physiological Reviews,* 87**,** 507-20.

SCHMIDT, W., POLL-JORDAN, G. & LOFFLER, G. (1990) Adipose conversion of 3T3-L1 cells in a serum-free culture system depends on epidermal growth factor, insulin-like growth factor I, corticosterone, and cyclic AMP. *The Journal of Biological Chemistry,* 265, 15489-95.

SHEEHAN, W., MELLER, W. H. & THURBER, S. (2008) More on Darwin's illness: comment on the final diagnosis of Charles Darwin. *Notes and Records of the Royal Society of London,* 62**,** 205-9.

SHI, H., HALVORSEN, Y. D., ELLIS, P. N., WILKISON, W. O. & ZEMEL, M. B. (2000) Role of intracellular calcium in human adipocyte differentiation. *Physiological Genomics,* 3, 75-82.

SHIMOMURA, O. (1979) Structure of the chromophore of *Aequorea* green fluorescent protein. *FEBS Letters,* 104**,** 220-22.

SHIMOMURA, O. (1986) Isolation and properties of various molecular forms of aequorin. *Biochemical Journal,* 234**,** 271-7.

SHIMOMURA, O. (1987) Presence of coelenterazine in non-bioluminescent marine organisms. *Comparative Biochemistry and Physiology Part B: Comparative Biochemistry,* 86B**,** 361-63.

SHIMOMURA, O. & JOHNSON, F. H. (1978) Peroxidized coelenterazine, the active group in the photoprotein aequorin. *Proceedings of the National Academy of Sciences,* 75**,** 2611-15.

SHIMOMURA, O., JOHNSON, F. H. & SAIGA, Y. (1962) Extraction, purification and properties of aequorin, a bioluminescent protein from the luminous hydromedusan, *Aequorea*. *Journal of Cellular and Comparative Physiology,* 59**,** 223-39.

SHIMOMURA, O. & TERANISHI, K. (2000) Light-emitters involved in the luminescence of coelenterazine. *Luminescence,* 15**,** 51-8.

SIDDLE, K., KUMAR, S. & O'RAHILLY, S. (2005) The insulin receptor and downstream signalling. *Insulin resistance: insulin action and its disturbances in disease.* Chichester, UK, John Wiley & Sons, Ltd.

SIDDLE, K., URSO, B., NIELSER, C. A., COPE, D. L., MOLINA, L., SURINYA, K. H. & SOOS, M. A. (2001) Specificity in ligand binding and intracellular signalling by insulin and insulin-like growth factor receptors. *Biochemical Society Transactions,* 29**,** 513-25.

SIMARD, J. R., ZUNSZAIN, P. A., HAMILTON, J. A. & CURRY, S. (2006) Location of high and low affinity fatty acid binding sites on human serum albumin revealed by NMR drug-competition analysis. *Journal of Molecular Biology,* 361**,** 336-51.

SINGH, R., BARDEN, A., MORI, T. & BEILIN, L. (2001) Advanced glycation end-products: a review. *Diabetologia,* 42**,** 129-46.

SLACK, J. M. W. (1995) Developmental biology of the pancreas. *Development,* 121**,** 1569-80.

SOKOLOWSKA, M., PAWLAS, K. & BAL, W. (2010) Effect of common buffers and heterocyclic ligands on the binding of Cu(II) at the multimetal binding site in human serum albumin. *Bioinorganic Chemistry and Applications,* 2010**,** 725153-60.

SORIA, B., ANDREU, E., BERNA, G., FUENTES, E., GIL, A., LEON-QUNITO, T., MARTIN, F., MONTANYA, E., NADAL, A., REIG, J. A., RIPOLL, C.,

ROCHE, E., SANCHEZ-ANDRES, J. V. & SEGURA, J. (2000) Engineering pancreatic islets. *Pflugers Archiv: European Journal of Physiology,* 440**,** 1-18.

STECK, A. K. & REWERS, M. J. (2011) Genetics of type 1 diabetes. *Clinical Chemistry,* 57**,** 176-85.

STEINTHORSDOTTIR, V., THORLEIFSSON, G., REYNISDOTTIR, I., BENEDIKTSSON, R., JONSDOTTIR, T., WALTERS, G. B., STYRKARSDOTTIR, U., GRETARSDOTTIR, S., EMILSSON, V., GHOSH, S., BAKER, A., SNORRADOTTIR, S., BJARNASON, H., NG, M. C., HANSEN, T., BAGGER, Y., WILENSKY, R. L., REILLY, M. P., ADEYEMO, A., CHEN, Y., ZHOU, J., GUDNASON, V., CHEN, G., HUANG, H., LASHLEY, K., DOUMATEY, A., SO, W. Y., MA, R. C., ANDERSEN, G., BORCH-JOHNSEN, K., JORGENSEN, T., VAN VLIET-OSTAPTCHOUK, J. V., HOFKER, M. H., WIJMENGA, C., CHRISTIANSEN, C., RADDER, D. J., ROTIMI, C., GURNEY, M., CHAN, J. C., PEDERSEN, O., SIGURDSSON, G., GULCHER, J. R., THORSTEINSDOTTIR, U., KONG, A. & STEFANSSON, K. (2007) A variant in CDKAL1 influences insulin response and risk of type 2 diabetes. *Nature Genetics,* 39**,** 770-5.

STUDENT, A. K., HSU, R. Y. & LANE, M. D. (1980) Induction of fatty acid synthetase synthesis in differentiating 3T3-L1 preadipocytes. *The Journal of Biological Chemistry,* 255, 4745-50.

STUMVOLL, M., GOLDSTEIN, B. J. & VAN HAEFTEN, T. W. (2005) Type 2 diabetes: principles of pathogenesis and therapy. *Lancet,* 365**,** 1333-46.

SUAREZ, F. L., SAVAIANO, D. A. & LEVITT, M. D. (1995) A comparison of symptoms after the consumption of milk or lactose-hydrolyzed milk by people with self-reported severe lactose intolerance. *The New England Journal of Medicine,* 333**,** 1-4.

SUDLOW, G., BIRKETT, D. J. & WADE, D. N. (1975) The characterisation of two specific drug binding sites on human serum albumin. *Molecular Pharmacology,* 11**,** 824-32.

SUGIO, S., KASHIMA, A., MOCHIZUKI, S., NODA, M. & KOBAYASHI, K. (1999) Crystal structure of human serum albumin at 2.5 A resolution. *Protein Engineering Design and Selection,* 12**,** 439-446.

SWAGERTY, D. L., JR., WALLING, A. D. & KLEIN, R. M. (2002) Lactose intolerance. *American Family Physician,* 65**,** 1845-50.

SWEENE, I. (1992) Pancreatic beta-cell growth and diabetes mellitus. *Diabetologia,* 35**,** 193-201.

TAFURI, S. R. (1996) Troglitazone enhances differentiation, basal glucose uptake, and GLUT1 protein levels in 3T3-L1 adipoytes. *Endocrinology,* 137, 4706-12.

TAJMIR-RIAHI, H. A. (2007) An overview of drug binding to human serum albumin: protein folding and unfolding *Scientia Iranica,* 14**,** 87-95.

TAN, D., WANG, Y., LO, C. Y., SANG, S. & HO, C. T. (2008) Methylglyoxal: its presence in beverages and potential scavengers. *Annals of the New York Academy of Sciences,* 1126**,** 72-5.

TERANISHI, K., ISOBE, M. & YAMADA, T. (1994) Synthesis of silyl peroxide of coelenterazine (*oplophorus luciferin*) analogue for precursor of luminescence. *Tetrahedron Letters,* 35**,** 2565-68.

THOMSON, C. M., HERRING, P. J. & CAMPBELL, A. K. (1997) The widespread occurrence and tissue distribution of the imidazolopyrazine luciferins. *Journal of bioluminescence and chemiluminescence,* 12**,** 87-91.

THORNALLEY, P. J. (1996) Pharmacology of methylglyoxal: formation, modification of proteins and nucleic acids, and enzymatic detoxification--a role in pathogenesis and antiproliferative chemotherapy. *General Pharmacology,* 27**,** 565-73.

THORNALLEY, P. J. (2005) Dicarbonyl intermediates in the maillard reaction. *Annals of the New York Academy of Sciences,* 1043**,** 111-7.

THORNALLEY, P. J. (2008) Protein and nucleotide damage by glyoxal and methylglyoxal in physiological systems--role in ageing and disease *Drug Metabolism and Drug Interactions,* 23**,** 125-50.

THORNALLEY, P. J., LANGBORG, A. & MINHAS, H. S. (1999) Formation of glyoxal, methylglyoxal and 3-deoxyglucosone in the glycation of protein by glucose. *Biochemical Journal,* 344**,** 109-16.

TURK, Z. (2010) Glycotoxines, carbonyl stress and relevance to diabetes and its complications. *Physiological Research,* 59**,** 147-56.

TURKOSKI, B. B. (2006) Diabetes and diabetes medications. *Orthopaedic Nursing,* 25**,** 227-31.

ULRICH, P. & CERAMI, A. (2001) Protein glycation, diabetes and aging. *Recent Progress in Hormone Research,* 56**,** 1-21.

VARSHNEY, A., SEN, P., AHMAD, E., REHAN, M., SUBBARAO, N. & KAHN, R. H. (2010) Ligand binding strategies of human serum albumin: How can the cargo be utilised? *Chirality,* 22**,** 77-87.

VASSEL, N., COX, C. D., NASEEM, R., MORSE, V., EVANS, R. T., POWER, R. L., BRANCALE, A., WANN, K. T. & CAMPBELL, A. K. (2012) Enzymatic activity of albumin shown by coelenterazine chemiluminescence. *The Journal of Biological and Chemical Luminescence,* 27**,** 234-41.

VESA, T. H., MARTEAU, P. & KORPELA, R. (2000) Lactose intolerance. *Journal of the American College of Nutrition,* 19**,** 165S-175S.

VINSON, J. A. & HOWARD, T. B. (1996) Inhibition of protein glycation and advanced glycation end products by ascorbic acid and other vitamins and nutrients. *Journal of Nutritional Biochemistry,* 7**,** 659-63.

VIRKAMAKI, A., UEKI, K. & KAHN, C. R. (1999) Protein-protein interaction in insulin signaling and the molecular mechanisms of insulin resistance. *The Journal of Clinical Investigation,* 103**,** 931-43.

WA, C., CERNY, R. L., CLARKE, W. A. & HAGE, D. S. (2007) Characterization of glycation adducts on human serum albumin by matrix-assisted laser desorption/ionization time-of-flight mass spectrometry. *Clinica Chimica Acta; International Journal of Clinical Chemistry,* 385**,** 48-60.

WANG, H., MENG, Q. H., GORDON, J. R., KHANDWALA, H. & WU, L. (2007) Proinflammatory and proapoptotic effect of methylglyoxal on neutrophils from patients with type 2 diabetes mellitus. *Clinical Biochemistry,* 40**,** 1232-9.

WARNER, M. J. & OZANNE, S. E. (2010) Mechanisms involved in the developmental programming of adulthood disease. *The Biochemical Journal,* 427**,** 333-47.

WASMUTH, H. E. & KOLB, H. (2000) Cow's milk and immune-mediated diabetes. *The Proceedings of the Nutrition Society,* 59**,** 573-9.

WATANABE, H., KRAGH-HANSEN, U., TANASE, S., NAKAJOU, K., MITARAI, M., IWAO, Y., MARUYAMA, T. & OTAGIRI, M. (2001) Conformational stability and warfarin-binding properties of human serum albumin studied by recombinant mutants. *The Biochemical Journal,* 357**,** 269-74.

WATANABE, H., TANASE, S., NAKAJOU, K., MARUYAMA, T., KRAGH-HANSEN, U. & OTAGIRI, M. (2000) Role of arg-410 and tyr-411 in

human serum albumin for ligand binding and esterase-like activity. *Biochemical Journal,* 349**,** 813-19.

WATKINS, P. J. (1998) What is diabetes? *ABC of Diabetes.* fourth ed.

WATSON, R. T., KANZAKI, M. & PESSIN, J. E. (2004) Regulated membrane trafficking of the insulin-responsive glucose transporter 4 in adipocytes. *Endocrine Reviews,* 25, 177-204.

WATSON, R. T. & PESSIN, J. E. (2001) Intracellular organisation of insulin signaling and GLUT4 translocation. *Recent Progress in Hormone Research,* 56, 175-94.

WAUD, J. P., MATTHEWS, S. B. & CAMPBELL, A. K. (2008) Measurement of breath hydrogen and methane, together with lactase genotype, defines the current best practice for investigation of lactose sensitivity. *Annals of Clinical Biochemistry,* 45**,** 50-8.

WEYER, C., BOGARDUS, C., MOTT, D. M. & PRATLEY, R. E. (1999) The natural history of insulin secretory dysfunction and insulin resistance in the pathogenesis of type 2 diabetes mellitus. *The Journal of Clinical Investigation,* 104**,** 787-94.

WHEELER, E. & BARROSO, I. (2011) Genome-wide association studies and type 2 diabetes. *Briefings in Functional Genomics,* 10**,** 52-60.

WHELAN, J. (2007) Double diabetes. *New Scientist,* 196**,** 48-51.

WHO (2006) Definition and diagnosis of diabetes mellitus and intermediate hyperglycaemia.

WILD, S., ROGLIC, G., GREEN, A., SICREE, R. & KING, H. (2004) Global prevalence of diabetes: estimates for the year 2000 and projections for 2030. *Diabetes Care,* 27**,** 1047-53.

WOO, J. & VON ARNIM, A. G. (2008) Mutational optimization of the coelenterazine-dependent luciferase from *Renilla*. *Plant Methods,* 4**,** 23-33.

WOO, J., HOWELL, M. H. & VON ARNIM, A. G. (2008) Structure-function studies on the active site of the coelenterazine-dependent luciferase from Renilla. *Protein Science,* 17**,** 725-35.

WOOD, I. S. & TRAYHURN, P. (2003) Glucose transporters (GLUT and SGLT): expanded families of sugar transport proteins. *The British Journal of Nutrition,* 89, 3-9.

YAMASAKI, K., MARUYAMA, T., KRAGH-HANSEN, U. & OTAGIRI, M. (1996) Characterisation of site I on human serum albumin: concept about the

structure of a drug binding site. *Biochimica et Biophysica Acta,* 1295**,** 147-57.

YANG, F., BIAN, C., ZHU, L., ZHAO, G., HUANG, Z. & HUANG, M. (2007) Effect of human serum albumin on drug metabolism: structural evidence of esterase activity of human serum albumin. *Journal of Structural Biology,* 157.

YIM, M. B., YIM, H. S., LEE, C., KANG, S. O. & CHOCK, P. B. (2001) Protein glycation: creation of catalytic sites for free radical generation. *Annals of the New York Academy of Sciences,* 928**,** 48-53.

YOON, J. W. & JUN, H. S. (2001) Cellular and molecular pathogenic mechanisms of insulin-dependent diabetes mellitus. *Annals of the New York Academy of Sciences,* 928**,** 200-11.

ZHANG, Q., AMES, J. M., SMITH, R. D., BAYNES, J. W. & METZ, T. O. (2009) A perspective on the Maillard reaction and the analysis of protein glycation by mass spectrometry: probing the pathogenesis of chronic disease. *Journal of Proteome Research,* 8**,** 754-69.